

The Pacific oyster, *Crassostrea gigas*, shows negative correlation to naturally elevated carbon dioxide levels: Implications for near-term ocean acidification effects

Alan Barton,^a Burke Hales,^{b,*} George G. Waldbusser,^b Chris Langdon,^c and Richard A. Feely^d

^aPacific Coast Shellfish Grower's Association, Emerald Isle, North Carolina

^bCollege of Oceanic and Atmospheric Sciences, Oregon State University, Corvallis, Oregon

^cDepartment of Fisheries and Wildlife and Coastal Marine Experiment Station, Oregon State University, Newport, Oregon

^dPacific Marine Environmental Laboratory, National Oceanic and Atmospheric Administration, Seattle, Washington

Abstract

We report results from an oyster hatchery on the Oregon coast, where intake waters experienced variable carbonate chemistry (aragonite saturation state < 0.8 to > 3.2; pH < 7.6 to > 8.2) in the early summer of 2009. Both larval production and midstage growth (~ 120 to ~ 150 μm) of the oyster *Crassostrea gigas* were significantly negatively correlated with the aragonite saturation state of waters in which larval oysters were spawned and reared for the first 48 h of life. The effects of the initial spawning conditions did not have a significant effect on early-stage growth (growth from D-hinge stage to ~ 120 μm), suggesting a delayed effect of water chemistry on larval development.

Rising atmospheric carbon dioxide (CO_2) driven by anthropogenic emissions has resulted in the addition of over 140 Pg-C (1 Pg = 10^{15} g) to the ocean (Sabine et al. 2011). The thermodynamics of the reactions between carbon dioxide and water require this addition to cause a decline of ocean pH and carbonate ion concentrations ($[\text{CO}_3^{2-}]$). For the observed change between current-day and preindustrial atmospheric CO_2 , the surface oceans have lost approximately 16% of their $[\text{CO}_3^{2-}]$ and decreased in pH by 0.1 unit, although colder surface waters are likely to have experienced a greater effect (Feely et al. 2009). Projections for the open ocean suggest that wide areas, particularly at high latitudes, could reach low enough $[\text{CO}_3^{2-}]$ levels that dissolution of biogenic carbonate minerals is thermodynamically favored by the end of the century (Feely et al. 2009; Steinacher et al. 2009), with implications for commercially significant higher trophic levels (Aydin et al. 2005).

There is considerable spatial and temporal variability in ocean carbonate chemistry, and there is evidence that these natural variations affect marine biota, with ecological assemblages next to cold-seep high- CO_2 sources having been shown to be distinct from those nearby but less affected by the elevated CO_2 levels (Hall-Spencer et al. 2008). Coastal environments that are subject to upwelling events also experience exposure to elevated CO_2 conditions where deep water enriched by additions of respiratory CO_2 is brought up from depth to the nearshore surface by physical processes. Feely et al. (2008) showed that upwelling on the Pacific coast of central North America markedly increased corrosiveness for calcium carbonate minerals in surface nearshore waters. A small but significant amount of anthropogenic CO_2 present in the upwelled source waters provided enough additional CO_2 to cause widespread corrosiveness on the continental shelves (Feely et al. 2008). Because the source water for upwelling

on the North American Pacific coast takes on the order of decades to transit from the point of subduction to the upwelling locales (Feely et al. 2008), this anthropogenic CO_2 was added to the water under a substantially lower- CO_2 atmosphere than today's, and water already en route to this location is likely carrying an increasing burden of anthropogenic CO_2 . Understanding the effects of natural variations in CO_2 in these waters on the local fauna is critical for anticipating how more persistently corrosive conditions will affect marine ecosystems.

The responses of organisms to rising CO_2 are potentially numerous and include negative effects on respiration, motility, and fertility (Portner 2008). From a geochemical perspective, however, the easiest process to understand conceptually is that of solid calcium carbonate ($\text{CaCO}_{3,s}$) mineral formation. In nearly all ocean surface waters, formation of $\text{CaCO}_{3,s}$ is thermodynamically favored by the abundance of the reactants, dissolved calcium ($[\text{Ca}^{2+}]$), and carbonate ($[\text{CO}_3^{2-}]$) ions. While oceanic $[\text{Ca}^{2+}]$ is relatively constant at high levels that are well described by conservative relationships with salinity, ocean $[\text{CO}_3^{2-}]$ decreases as atmospheric CO_2 rises, lowering the energetic favorability of $\text{CaCO}_{3,s}$ formation. This energetic favorability is proportional to the saturation state, Ω , defined by

$$\Omega_f = \frac{[\text{CO}_3^{2-}][\text{Ca}^{2+}]}{K_{\text{sp},f}}$$

where the subscript f refers to the phase of the mineral being formed and $K_{\text{sp},f}$ is the apparent thermodynamic solubility product of that phase. Precipitation is thermodynamically possible for $\Omega_f > 1$, and greater values of Ω_f correspond to greater energetic favorability for precipitation. Calcium carbonate exists in a variety of phases distinguished by crystal structure and associated contributions of contaminating elements. The most common phases are the low-magnesium phases calcite and aragonite and high-magnesium calcite. Aragonite is about twice as

* Corresponding author: bhales@coas.oregonstate.edu

soluble as calcite, and the solubility of high-Mg calcites increases with increased magnesium in the crystal lattice (Morse and Mackenzie 1990). Aragonite, in particular, plays an important role in the calcareous structures produced by corals, pteropods, and early life stages of larval oysters.

The CaCO_3 shell-forming bivalves, including oysters (Gazeau et al. 2007; Miller et al. 2009; Waldbusser et al. 2011), mussels (Gazeau et al. 2007; Thomsen et al. 2010), and clams (Green et al. 2009; Talmage and Gobler 2009; Waldbusser et al. 2010), show negative responses to lowered Ω values, even when those perturbations occur above the $\Omega = 1$ thermodynamic threshold for the minerals in question. Larval oysters appear to be particularly susceptible to the influences of ambient seawater chemistry, as they form their larval shell material out of the more soluble aragonite (Stenzel 1964) and only deposit less soluble calcite following settlement. Additionally, some studies indicate amorphous calcium carbonate (ACC) as an even more soluble mineral precursor (Weiss et al. 2002) during early stages of calcification, although other studies question the ubiquity of this finding (Mount et al. 2004; Kudo et al. 2010).

Regardless of exact calcification mechanisms, previous studies have shown that oyster larvae respond negatively to more acidic conditions. Kurihara et al. (2007) found a reduction in development success when *Crassostrea gigas* larvae were exposed to acidified conditions (pH = 7.4). Watson et al. (2009) exposed D-hinge (1-d-old) larvae of the Sydney rock oyster (*Saccostrea glomerata*) to a range of pH conditions (7.6–8.1) over a period of 10 d and showed a significant decline in the survival and growth of young larvae at lower pH. In a study starting with 5-d-old larvae, Miller et al. (2009) also showed a significant decrease in growth rate of *C. virginica* when exposed to lower pH conditions but relatively little effect on survival. Reduced larval growth of *C. virginica* in response to reduced pH was also found by Talmage and Gobler (2009), with negative effects on survival and metamorphosis also observed. Studies on adult bivalves have shown that net calcification was possible under more acidified conditions (Gazeau et al. 2007), and the ability to overcome dissolution increased with postlarval size (Waldbusser et al. 2010). Mineral polymorph, high energetic costs of early life history development, and the generally high mortality rates in larvae (Rumrill 1990) all suggest larvae will be the most susceptible developmental stage of marine bivalves.

On the North American Pacific coast, native populations of the oyster *Ostrea lurida* were unable to sustain extensive harvesting (White et al. 2009), and the commercial oyster industry there is supported primarily by cultivation of the nonnative *C. gigas*, which was introduced near the beginning of the 20th century but has limited naturally sustaining populations (Ruesink et al. 2005) because of cold in situ temperatures limiting reproduction of this species and low residence times of water and, consequently, planktonic larvae in many local estuaries (Banas et al. 2007). Therefore, the commercial oyster industry is dependent on hatcheries that rear larvae to settlement size before distributing them to the growers. In recent years,

natural and hatchery larval production have been severely depressed in the Pacific Northwest, and a lack of sufficient “seed” has threatened an industry with a total economic value estimated at US\$278 million as of 2009 (Pacific Coast Shellfish Growers Association 2010). Hatchery problems started in 2006, when high concentrations of the pathogenic bacterium *Vibrio tubiashii* were observed, perhaps associated with high-nutrient, low- O_2 coastal upwelled waters (Grantham et al. 2004; Chan et al. 2008) mixing with warm late-summer bay waters (Elston et al. 2008). The Whiskey Creek Shellfish Hatchery in Netarts Bay on the northern Oregon coast ($\sim 45.4^\circ\text{N}$, 123.9°W) experienced high concentrations of *V. tubiashii* and difficulties in seed production (Elston et al. 2008). However, by the summer of 2008, bacterial monitoring indicated that pronounced mortality events often occurred in the absence of detectable *V. tubiashii*. On the other hand, these larval mortality events often coincided with strong coastal upwelling and the presence of seawater thermodynamically unstable with respect to aragonite in Netarts Bay.

Although the effects of ocean acidification have been forecast for nearly 30 yr (Feely and Chen 1982), the issue has only recently received community-wide interest with workshops (Fabry et al. 2009) and strategy documents (e.g., National Research Council 2010) completed in the last few years, along with development of large-scale international integrated projects (<http://www.epoca-project.eu>) and locally integrated observation networks (<http://c-can.msi.ucsb.edu>). As a result, the chemical signature and ecological effects of acidification have been under way long before adequate scientific monitoring and classical experimentation could sufficiently be put in place to resolve either the baseline or the mechanisms of ecosystem responses. Because of this known information deficiency, workshop reports (Fabry et al. 2009) have strongly recommended that the scientific community engage affected stakeholders and attempt to mine nontraditional data sources for relevant information.

In this study, we follow this recommendation by augmenting existing monitoring measurements with state-of-the-art carbonate chemistry validation to evaluate the response of *C. gigas* larvae, grown under otherwise optimal conditions at an affected commercial hatchery on the Oregon coast, to natural changes in carbonate chemistry associated with periodic seasonal upwelling during the summer of 2009.

Methods

Whiskey Creek Hatchery (WCH), a commercial shellfish hatchery and largest independent producer of oyster seed in the Pacific Northwest, is located in Netarts Bay, a small bay on the northern Oregon coast (Fig. 1). Netarts Bay is a lagoon-type estuary dominated by water inputs from the adjacent North Pacific Ocean, with equivalent mean depth and tidal amplitude (~ 2 m) and only minimal freshwater inputs via two small creeks that enter the east and south edges of the bay. The hatchery is situated on the eastern edge of the bay, about halfway between its northern and southern extents. Seawater for larval rearing is drawn

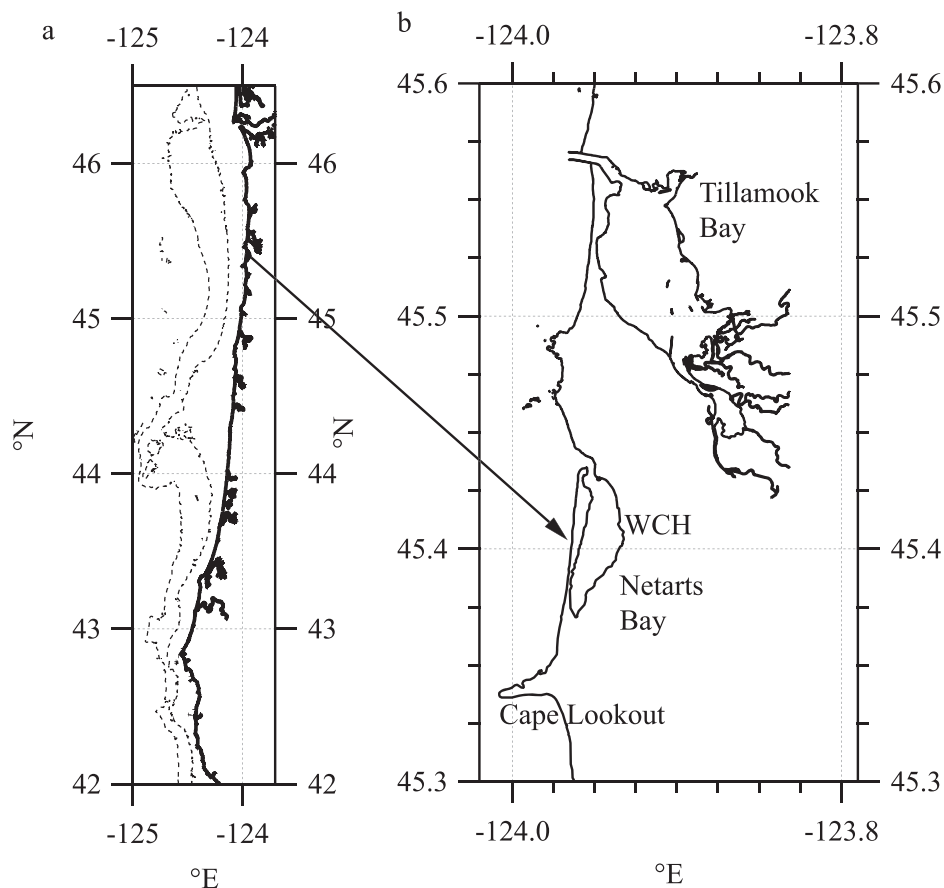


Fig. 1. (a) Map of Oregon coast from California border to the mouth of the Columbia River. Dotted contours offshore show the position of the 100- and 200-m isobaths. (b) Expanded view of Netarts Bay, where "WCH" denotes the position of the Whiskey Creek Hatchery.

directly from the bay through a submerged intake pipe about 0.5 m above the bottom at an average water depth of about 2 m. Temperature is maintained at either $\sim 18^{\circ}\text{C}$ (for broodstock) or $\sim 25^{\circ}\text{C}$ (for fertilization and larval rearing) within the hatchery, while salinity varies with natural fluctuations, in this case over a range of ~ 28 – 33 .

The oyster production cycle within the hatchery follows general procedures for oyster hatchery production. Broodstock are obtained from sustaining native populations in Willapa Bay, Washington, oyster reserve or from the Molluscan Broodstock Program (<http://hmssc.oregonstate.edu/projects/mbp/index.html>) throughout the production cycle. After they are brought to the hatchery, they are kept in tanks flushed with ambient Netarts Bay seawater maintained at 18°C and fed with an excess supply of algae (produced in the hatchery) for a minimum of 2 wk to maximize fitness and fecundity while preventing natural spawning by not allowing temperatures to rise above 18°C . Oysters are strip spawned by sacrificing several individual males and females that are visually confirmed to be in peak fitness and fertility. Spawns are performed two to four times each week throughout the growing season, producing cohorts of 2×10^8 – 2×10^9 larvae per spawn.

Harvested eggs are screened to remove debris and thoroughly rinsed on a $20\text{-}\mu\text{m}$ screen. Clean eggs are

resuspended in 0.1-m^3 tanks of filtered seawater, typically at concentrations of 10^{10} m^{-3} , then fertilized with a sperm suspension. Within 30–60 min, eggs are examined microscopically to insure proper fertilization and then placed into 22-m^3 tanks of seawater at concentrations not exceeding $2 \times 10^7\text{ m}^{-3}$. This represents one cohort of oyster larvae.

After 48 h, D-hinge larvae are collected during tank water change and transferred to 22-m^3 tanks of new seawater pumped from the bay; larvae are stocked initially at a concentration of $5 \times 10^7\text{ m}^{-3}$. Small larvae are fed a diet of the haptophyte *Isochrysis galbani* at cell densities of $\sim 5 \times 10^{10}\text{ m}^{-3}$ until 7–10 days after fertilization. For the next few weeks, larvae are fed a mixed diet of diatoms (primarily *Chaetoceros gracilis* and *Thalassiosira* sp. fed at cell densities of $\sim 7 \times 10^{10}\text{ m}^{-3}$), and water in the holding tanks is replaced completely every 48 h. Larvae are typically large enough to be retained on $100\text{-}\mu\text{m}$ sieves (nominally 140 – $150\text{ }\mu\text{m}$ in long-axis shell length) within 1–2 wk after fertilization.

Although we do not discuss later development here, the hatchery produces and rears larvae until roughly 12–24 h before settlement, when they are packaged and shipped to commercial oyster growers across the Pacific Northwest. Rearing of successful cohorts continues for an additional 7–14 d beyond the times described above, at which point

larvae are harvested on 236- μm sieves (310–330- μm shell length) and distributed to growers. Low-production cohorts are not maintained beyond the 150- μm size threshold.

Hatchery operators have found that certain optimal ratios of biomass per volume are ideal for growth and feeding in various settings. In order to balance production rates and expenses associated with heating and maintain water, the hatchery maintains a near-constant tank-specific biomass by condensing or dividing cohorts into or across tanks as required. The hatchery uses a volumetric cone to estimate tank biomass and adjust the number of tanks as needed at each tank change. We can therefore utilize the data collected on the total number of tanks per cohort as a measure of larval biomass production. The change in the number of tanks is thus a proxy for the net production of a cohort of larvae. Relative larval production, P , was calculated from the relative change in the number of tanks between the initial number of tanks at the postfertilization D-hinge stage to the number of tanks when larvae are retained on 100- μm screens, that is, $P = (T_{100} - T_D)/T_D$, where T_{100} and T_D are the numbers of tanks at the 100- μm screen and D-hinge stages of production, respectively. A value of 0 in this case would imply no larval biomass production and could be attained by either limited growth and high survival or high growth and low survival, while a value of 1 would imply a doubling of larval biomass, and a value of -1 would imply complete mortality.

Hatchery personnel estimate larval development and growth by various metrics. Early development is tracked by estimating the number of fertilized eggs that develop to healthy D-hinged larvae as the ratio of healthy D-hinged larvae over successfully fertilized eggs. Growth is tracked by logging the number of days it takes for components of a cohort to reach benchmark sizes based on direct observations and sieves used to capture larvae during regular tank changes. Specifically, the number of days until the first observation of 120- μm larvae and the number of days until all surviving larvae reach 150 μm are cataloged. We utilized these records to estimate early-stage growth and midstage growth related to important transitions in larval feeding and development stages. Early-stage growth was defined as the time required until the first observation of individuals in a cohort reaching a shell length of 120 μm . Up to this size stage, sizes are obtained by microscopic analyses of subsamples from the cohort. Importantly, this metric potentially captures the dynamics of the fittest individuals in the cohort; however, the D-hinge developed integrates the entire early development. We defined midstage growth by calculating the time between first observation of larvae at 120- μm shell length and the time at which all surviving larvae are retained on a 100- μm screen (nominally 150- μm shell length). Larval nutrition in early-stage growth is reported to be mixotrophic with larvae depending on both egg reserves and limited ingestion of microalgae (Rico-Villa et al. 2009; Kheder et al. 2010a,b). In midstage growth, larvae become more dependent on exogenous food sources, and changes in diet or food availability have more pronounced effects on growth (Rico-Villa et al. 2009; Kheder et al. 2010a,b).

Water samples were collected from the hatchery seawater system weekly in the morning (\sim 08:00 h local time) and

afternoon (14:00 h) in addition to a few other times selected by the hatchery personnel. This sampling point was separated from the bay by a flow transit time of a few seconds and coincides with the location in the hatchery where the tanks are filled. Samples for analysis of seawater CO_2 partial pressure (P_{CO_2}) and total dissolved CO_2 (T_{CO_2}) were collected in 350-mL amber glass bottles with minimal headspace and poisoned with 300 μL of saturated HgCl_2 solution before being sealed with urethane-lined crimp-seal metal caps. We have shown in previous research (Hales et al. 2005; Bandstra et al. 2006) that samples collected in this manner are stable for several months or more for CO_2 analyses. Samples were analyzed for T_{CO_2} following the method developed in Hales's lab by Bandstra et al. (2006) and for P_{CO_2} by recirculating headspace air through the sample and a nondispersive infrared detector using a small air pump and a fritted bubbling stone. Results were corrected for the pressure of analysis headspace and for the temperature difference between analytical and in situ conditions to yield P_{CO_2} values in dekapascals rather than the nearly numerically equivalent and more widely used μatm unit at in situ temperature (T) and T_{CO_2} values in $\mu\text{mol kg}^{-1}$. Uncertainty for the T_{CO_2} analyses is expected to be less than 0.2% (accuracy and precision), based on the results of Bandstra et al. (2006), and less than 5% for the P_{CO_2} analyses, based on comparison between archived samples and measurements made in situ by a variety of methods (membrane and showerhead equilibration of flowing sample streams and moored measurement of P_{CO_2} using absorbance-based sensors; Evans et al. 2011).

Inlet water aragonite saturation state (Ω_A) was calculated from the T , salinity (S), and P_{CO_2} and T_{CO_2} data at in situ conditions using a program written by the authors that accounts for the equilibrium interactions between the carbonic acid species at in situ conditions, using the carbonic acid dissociation constants of Mehrbach et al. (1973) as refit by Lueker et al. (2000), the boric acid constants as defined by Dickson (1990), and the aragonite solubility as defined by Mucci (1983). This choice of constants is appropriate for freshwater and salinities above 20 but is unverified for the range 0–20 and should be used with caution in lower salinity ranges where verification is insufficient. Calcium concentrations were calculated assuming conservative dependence on salinity with a freshwater end member of 1 mmol kg^{-1} , appropriate for local riverine inputs. From these measurements and choice of equilibrium constants, we can calculate pH on the total hydrogen ion scale, hereafter referred to as pH_T . Propagation of analytical uncertainty in the measured P_{CO_2} and T_{CO_2} data (stated above) dominates the uncertainty in calculated Ω_A , which is about 5%, while calculated pH_T is uncertain by about ± 0.02 . We do not consider inaccuracy in the thermodynamic constants used in our calculations. The most significant of these is the inaccuracy of the solubility of aragonite, which, as reported in the literature is uncertain by about $\pm 10\%$. Absolute values of Ω_A and pH_T will suffer additional accuracy uncertainty if the equilibrium constants are considered, but relative changes in either term are known to within the above-stated propagation of analytical precision. Comparison of these

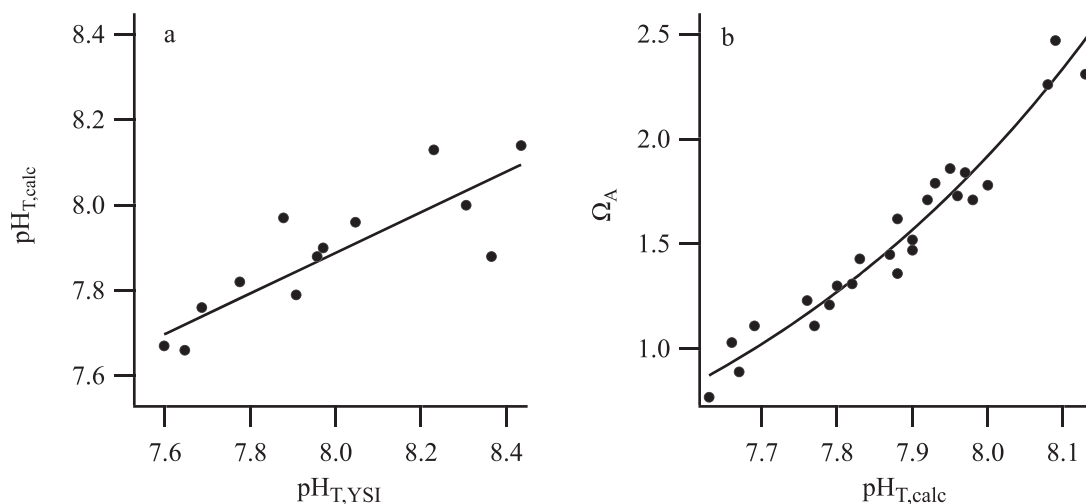


Fig. 2. (a) Correlation between $\text{pH}_{T,\text{calc}}$ calculated from P_{CO_2} and T_{CO_2} measured on discrete samples and $\text{pH}_{T,\text{YSI}}$, corrected to the total hydrogen ion scale from the NBS-scale pH measured with the YSI 6000 EDS sonde, for those samples with good T, S agreement. $\text{pH}_T = 0.45\text{pH}_{T,\text{YSI}} + 4.22$, $F_{1,12} = 26.80$, $p = 0.0002$, $R^2 = 0.70$. (b) Relationship between aragonite saturation state (Ω_A) and $\text{pH}_{T,\text{calc}}$ for all discrete samples ($\Omega_A = -0.288 + 0.9274e^{(1.7345\Delta\text{pH}_T)}$, $F_{2,23} = 248.84$, pseudo- $R^2 = 0.96$, $p < 0.0001$, where $\Delta\text{pH}_T = \text{pH}_T - 7.5$ and pseudo- $R^2 = 1 - [\text{residual sums of squares} / \text{the total corrected sums of squares}]$, appropriate for nonlinear regressions).

results with those of other studies will require careful examination of acid dissociation and mineral solubility assumptions.

It is important to note that the data presented here are for the conditions at the hatchery inlet sampling point. We maintain this for two reasons. Part of our objective is quantification of the natural variation in conditions in ambient bay waters, and direct measurements were not made in the water after heating. Treatment of the water approximates isochemical heating, in which alkalinity and T_{CO_2} do not change because of the quiescent conditions and short time scale of the heating and the slow response of CO_2 to gas exchange. If waters were only warmed, calculated Ω_A values would be about 0.2 higher in warmed waters than at the intake at in situ T, and thus the responses we report would take place at more stable mineral solubility conditions. The most likely chemical change would be relaxation of the warmed waters to P_{CO_2} values in equilibrium with the atmosphere while alkalinity remained constant. This would have two consequences. Warmed waters would mostly lose CO_2 to the atmosphere, resulting in potentially higher mean Ω_A values, and moving toward a common P_{CO_2} would tend to reduce the dynamic range in Ω_A . Therefore, our measurements, if anything, underestimate the mean Ω_A and overestimate its dynamic range in fertilization and rearing waters. We believe that this choice of Ω_A values is the most conservative in implicating ocean acidification effects on larval oysters.

The high variability of the bay-water chemistry and the frequency of the spawning operations made the approximately weekly discrete samples alone insufficient for capturing the conditions experienced during spawning operations, and we were forced to use these discrete samples to ground-truth a continuous record of pH being recorded by an in situ Yellow Springs Instruments (YSI) 6000 EDS sonde, located in the bay at the inlet of the

hatchery intake pipe, starting in late May 2009. Along with pH, the sonde also recorded temperature and salinity at 30-s intervals. The sonde was recovered monthly for cleaning and calibrated for pH using Oakton buffers (<http://www.4oakton.com>) at pH 7 and 10 on the National Bureau of Standards (NBS) scale. One calibration operation occurred in the middle of the presented record on 01 July 2009 and two others preceding and following the sampling interval. No drift was obvious during these calibrations, and no drift correction was applied.

As there can be decoupling between pH and mineral saturation state, pH is an imperfect variable for assessing corrosivity of ocean water to calcium carbonate biominerals. This is especially true in a complicated matrix like seawater where ionic strength effects can lead to large uncertainties in the determination of pH itself. We made two corrections to the in situ pH record. We first corrected the NBS-scale YSI measurements to the total hydrogen ion scale using the nonlinear empirical relationship between the total hydrogen ion activity coefficient and temperature and salinity given by Millero et al. (1988). The corrections made to adjust to the pH_T scale were on the order of 0.13 unit, with dependence on the T and S of the sample water. We then synchronized our discrete measurements with the continuous in situ record and used our calculated pH_T values to verify the accuracy of the in situ measurements. We limited our analyses only to times when the measured discrete sample T and S agreed with the synchronized in situ observations to within $\pm 0.5^\circ\text{C}$ and 0.75, respectively, to ensure comparisons of common water types. The discrete and in situ T and S measurements were quite closely correlated ($R^2 > 0.98$ for both parameters), but periodic deviations occurred, as expected in a dynamic setting such as this. The linear relationship between in situ and discrete-sample calculated pH (Fig. 2a) was used to convert the continuous in situ record into one that was

internally consistent with our CO_2 chemical analyses ($\text{pH}_{\text{T,calc}} = 0.45\text{pH}_{\text{T,YSI}} + 4.22$, $F_{1,12} = 26.80$, $p = 0.0002$, $R^2 = 0.70$). This correction is large, with slope < 1 and offset > 0 . This is not unexpected, as the YSI electrode is advertised to produce accuracy of only ± 0.2 unit, although precision is 0.01 unit (<http://www.ysi.com/productsdetail.php?6600V2-1>). If this inaccuracy exists as nonlinearity in relatively narrow pH ranges (~ 0.6 in this case) or as function of T and/or S fluctuations, none of which are specified by the manufacturer, it could account for the majority of this disagreement. However, the average residual difference between predicted pH_{T} from our regression analysis and measured pH_{T} is 0.06 (± 0.06 , 1 SD), with a maximum residual value of 0.19; thus, for our purposes, this is adequate.

As stated, pH is not expected to be a perfect predictor for mineral saturation state, but the correlation between pH_{T} and Ω_{A} from our discrete samples (Fig. 2b) was strong enough to give good predictive power ($\Omega_{\text{A}} = -0.288 + 0.927e^{(1.735\Delta\text{pHt})}$, $F_{2,23} = 248.84$, pseudo- $R^2 = 0.96$, $p < 0.0001$, where $\Delta\text{pH}_{\text{T}} = \text{pH}_{\text{T}} - 7.5$ and pseudo- $R^2 = 1 - [\text{residual sums of squares divided by the total corrected sums of squares}]$, appropriate for nonlinear regressions). After correcting the in situ pH with the relationship shown in Fig. 2a, we then converted that record to a continuous time series of Ω_{A} with the relationship shown in Fig. 2b. Conditions for individual spawns were determined by averaging the Ω_{A} record between 0:800 h and 12:00 h local time on the day of the spawn, corresponding to the interval in which spawn tanks were filled.

A simple linear regression analysis was used to quantify the effect of aragonite saturation state at time of spawn on the proportion of healthy D-hinge, relative production value (both described above), the early-stage growth rate (up to 120- μm shell length), and the midstage growth rate (120–150- μm shell length). The proportional D-hinge data were arcsin square-root transformed because of the problems associated with parametric analysis of proportional data. Assumptions of heteroscedasticity and normality of residuals were checked with visual examination of residuals and by the Shapiro–Wilk statistic, and these assumptions were met. We additionally checked for overly influential data points by examining Studentized residuals and Cook's distance and found one observation that corresponded to an overly influential data point in two of the three regressions. We censored each point and repeated the statistical analyses but have included the point on subsequent graphs. The exclusion of this point did not change the inferences from either analysis. All analyses were run in SAS v9.1, using Proc Reg for linear regressions and Proc Nlin for the nonlinear regression.

Results

Netarts Bay carbonate chemistry—Water sampling and continuous analysis for the period 01 June–03 August 2009 (Figs. 3, 4) show that the bay is subjected to two major forcings that affect its carbonate chemistry. The first is the upwelling state of the adjacent coastal ocean. During upwelling, evidenced by high atmospheric pressure and

strong north winds (Fig. 3a), colder, saltier (Fig. 3b), low-pH (Fig. 3c) aragonite-undersaturated (Fig. 3d) deep-origin upwelled water is brought to the surface very near the coast (Hales et al. 2005; Feely et al. 2008), and this water spills over the sill at the bay mouth into the bay. During reduced upwelling or relaxation events, low- CO_2 photo-synthetically modified (high pH, high Ω_{A}) surface waters are forced back onshore and enter the bay. The time scale of this forcing ranges from several days, corresponding to the frequency of relaxation events during the upwelling season, to several months, corresponding to the seasonal shift between winter downwelling- and summer upwelling-favorable winds. During the record of interest in 2009, there were periods of strong upwelling from about year-day 161–186 (10 June–05 July) and again from about year-day 195–212 (14–31 July), punctuated by periods of weak variable to south winds from year-day 153–161 (02–10 June), 187–194 (06–13 July), and 213–217 (01–05 August).

The second forcing factor is diurnal metabolic variability within the bay. This is visible as the high-frequency patterns superimposed on the smoothed records of Fig. 3, and one part of the record is examined in more detail in Fig. 4. The bay contains broad shallows populated by extensive eelgrass beds and benthic microalgae, and on high-insolation days, photosynthetic uptake of CO_2 from bay waters is high. In contrast, nighttime respiration produces abundant CO_2 . This results in a clear pattern of high P_{CO_2} and T_{CO_2} in the morning discrete samples, with greatly reduced levels in the afternoon samples (Fig. 4), that drives the diurnal signal in pH_{T} and Ω_{A} (e.g., increasing values during the day and decreasing values through the night). Note that thermal forcing alone would predict higher afternoon P_{CO_2} , opposite of what is seen. This effect occurs independent of tidal forcing and is apparent in both upwelling and relaxation (or reversal) oceanic conditions. Unlike the upwelling-modulated changes, the bay's carbonate chemistry is decoupled from its temperature and salinity in these intervals.

Oyster larval performance—Larval performance was assessed by four measures derived from hatchery records: early development to D-hinge, the relative production, early-stage growth when larvae depend on mixotrophic nutrition, and midstage when larvae transition to exogenous food sources. Successful development from fertilized egg to D-hinge is measured by the proportion of fertilized eggs that make it to D-hinge in ~ 24 h. The relative production term provides a proxy for cohort biomass, with positive numbers indicating growth in cohort biomass and negative numbers indicating mortality. Our early- and midstage growth metrics estimate the time required to reach and exceed a benchmark size. Aragonite saturation state at the time of spawning did not have significant effects on D-hinge development ($F_{1,14} = 3.97$, $p = 0.0663$, adjusted $R^2 = 0.17$; Fig. 5a) and early-stage growth ($F_{1,15} = 0.00$, $p = 0.9845$, adjusted $R^2 < 0$; Fig. 5b). However significant effects of carbonate conditions at time of spawn were found on midstage growth ($F_{1,14} = 13.87$, $p = 0.0025$, adjusted $R^2 = 0.47$; Fig. 5c) and relative production ($F_{1,15} = 17.93$, $p = 0.0008$, adjusted $R^2 = 0.53$; Fig. 5d). Differing numbers of

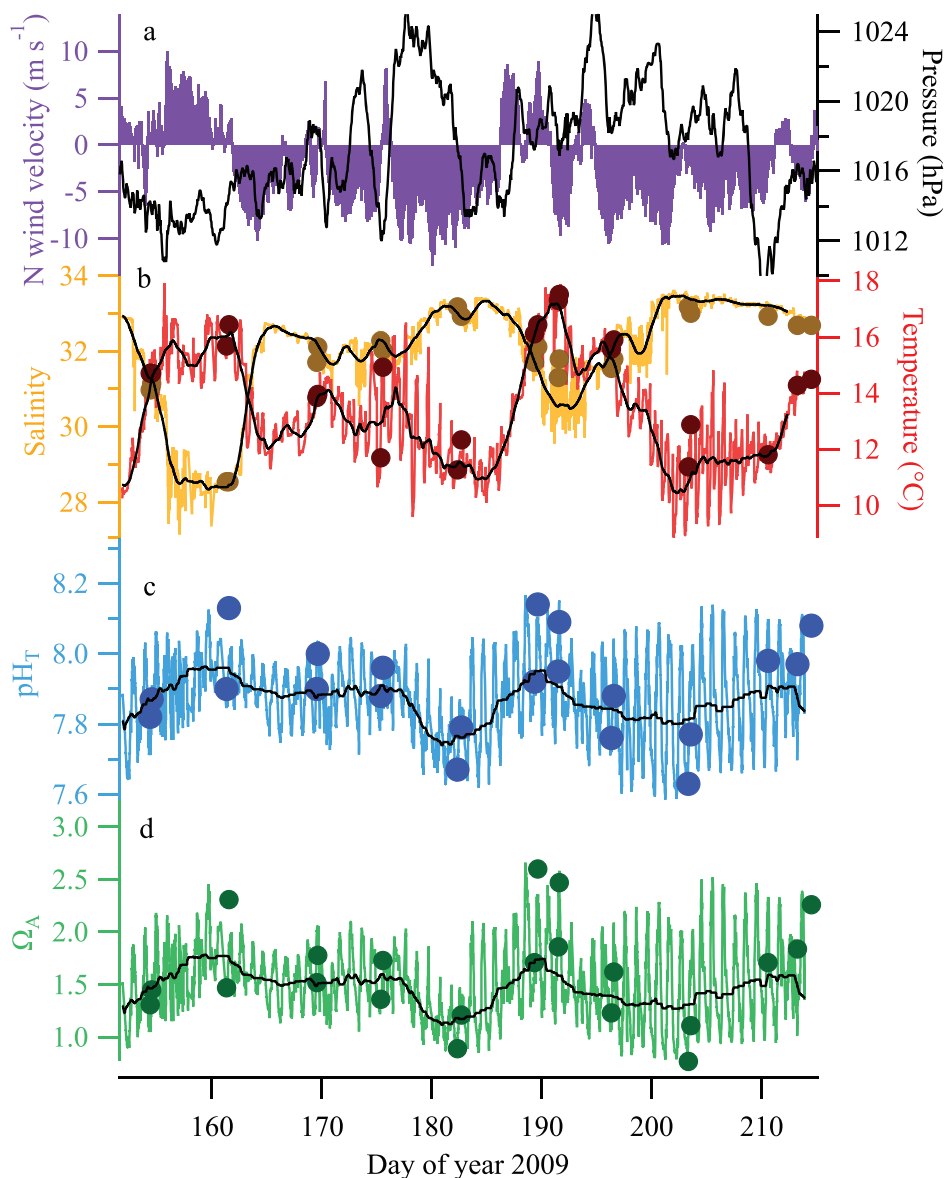


Fig. 3. Variability in environmental conditions in Netarts Bay, 01 June–03 August 2009. (a) Record of north wind velocity (left axis) and atmospheric pressure (right axis), showing the atmospheric conditions driving upwelling variability over the period of interest. (b) Record of salinity (left axis) and temperature (right axis) at the hatchery intake. Black lines are 3-day running-median smoothed representations of each record, distinguishing the upwelling forcing from the diurnal forcing. Similarly colored circles are corrected discrete measurements of each parameter, corresponding to the discrete samples analyzed for CO_2 chemistry. (c) pH_T from the corrected in situ measurements made by the YSI sonde at the hatchery intake (blue line) and calculated from the discrete samples analyzed for P_{CO_2} and T_{CO_2} (blue circles). Black line is the 3-day filtered pH_T record, as for T and S, above. (d) Aragonite saturation (Ω_A), calculated from the corrected YSI pH_T data and the regression of Fig. 2b (green line) and from the discrete measurements of P_{CO_2} and T_{CO_2} (green circles).

degrees of freedom result from either missing data points or one data point in each of the midgrowth and relative production regressions having been censored due to the finding that each point was overly influential by Studentized residuals, Cook's distance, and DFFITS diagnostics. These censored data points have, however, been included in the plots of Fig. 5 as filled circles.

Discussion

This work differs from previous studies of calcifying organism responses to changing acid-base chemistry in several key ways. First, we utilized hatchery records of larval performance under naturally fluctuating ambient-water CO_2 chemistry of Oregon's coastal upwelling system

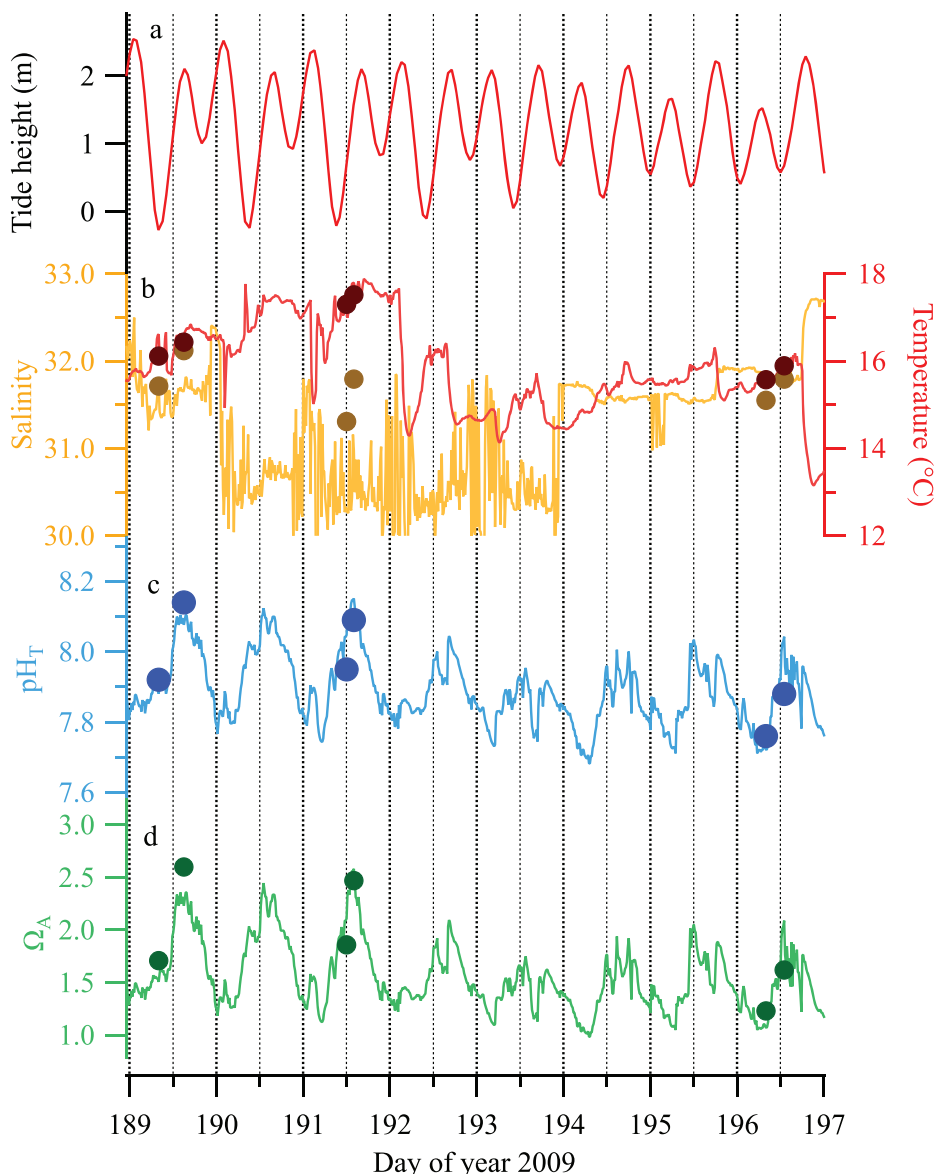


Fig. 4. Demonstration of effect of diurnal variability on Netarts Bay carbonate chemistry for a subset of the data presented in Fig. 3, 08–17 July 2009. (a) Tidal stage is largely uncorrelated with (b) in-bay T and S or (c) pH or (d) aragonite saturation. Bay carbonate chemistry shows regular diurnal variability, with maximum pH_T and Ω_A at or shortly after local noon and minima in early morning. Vertical dashed lines represent local midnight (major ticks) and noon (minor ticks).

with *C. gigas*, a nonnative study organism that has been resident in these waters for nearly a century. No artificial manipulations of water chemistry outside of those occurring naturally were conducted. Second, we have focused on the larval stages of several cohorts grown under commercial hatchery conditions and protocols. Finally, we have resolved the vagaries of in situ pH electrode time-series data with discrete measures of seawater carbonate chemistry analyzed with state-of-the-art methodology. With this novel approach, we have observed significant relationships between aragonite saturation states at the time of spawning and subsequent growth and production of larvae over the

size range of ~ 120 to $\sim 150\text{-}\mu\text{m}$ shell length (Fig. 5) but not on early growth and development.

Recent work by A. Hettinger (unpubl.) on the native *O. lurida* showed carryover effects of water chemistry experienced at early stage (larvae) to the later postlarval juvenile stage. The carryover effect was evident after 1 mo of growth when juveniles exposed to acidified conditions in their larval stages failed to attain the same size as juveniles derived from larvae exposed to less acidic conditions. Our findings and those of A. Hettinger (unpubl.) illustrate important concepts of how variable acidification may affect coastal and estuarine ecosystems. The timing of spawning

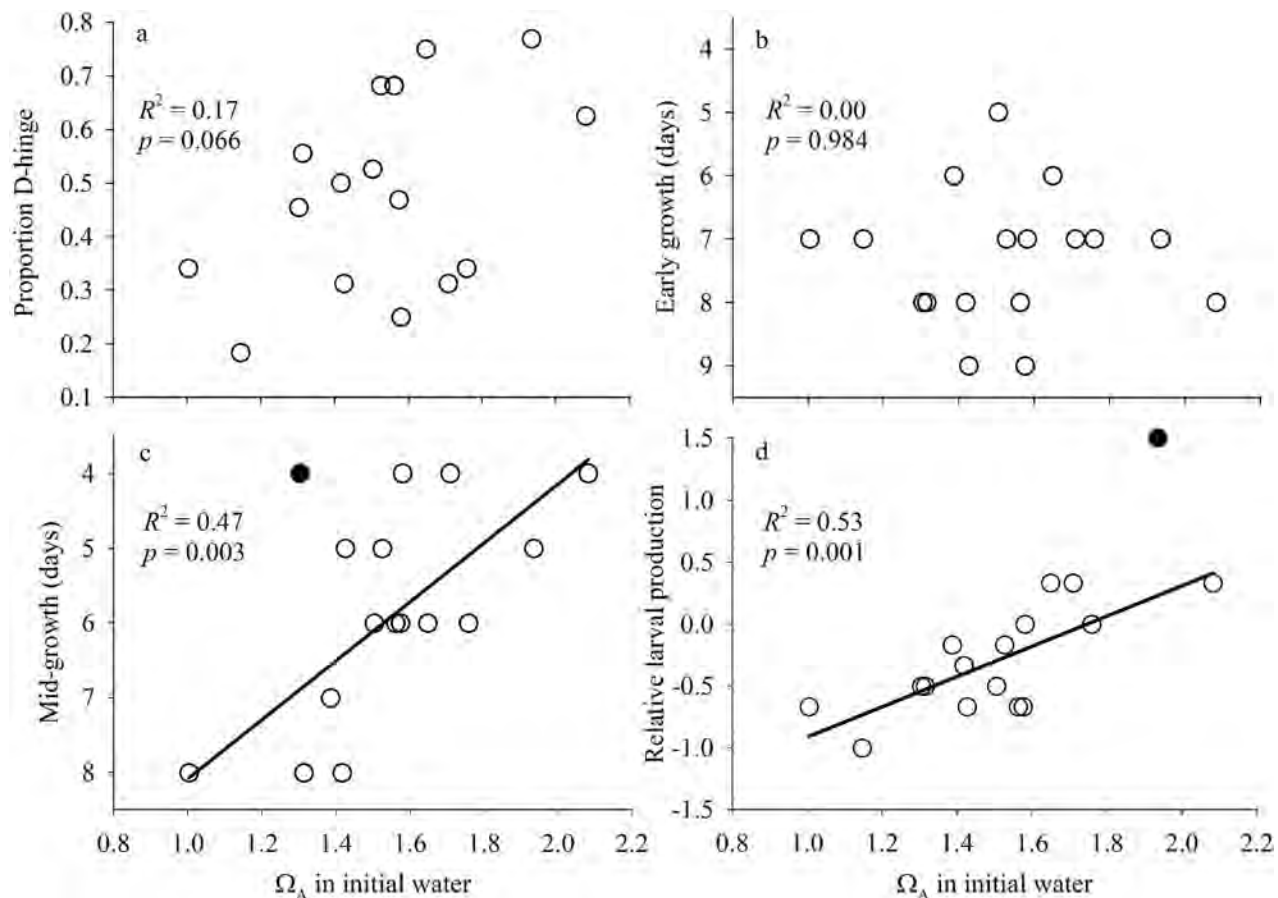


Fig. 5. Relationship between saturation state of aragonite and (a) proportion of larvae developing to D-hinge stage, (b) number of days for larvae to reach a nominal 120- μ m size, (c) number of days for larvae to grow from 120- to 150- μ m nominal size, and (d) overall relative production of each cohort. As described in the Methods section, relative production does not include the changes in the cohort prior to D-hinge; relative production captures only the changes from the D-hinge stage up to competent to settle. Data points in black on graphs 5c and 5d are statistical outliers and were excluded from regression analysis. Reduced R^2 values and p -values of linear regression analyses are shown in the figure. Other statistics for significant relationships are (c) midstage, growth slope = -3.95 ± 1.05 days, intercept = 12.02 ± 1.67 days and (d) relative production, slope = 1.22 ± 0.29 days, intercept = -2.13 ± 0.44 days.

and release of gametes into the water column are critical in light of variable local conditions occurring on top of a shifting CO_2 chemistry baseline (Waldbusser et al. 2010, 2011). Others have demonstrated the importance of environmental conditions related to climate and weather patterns in controlling interannual oyster recruitment (Kimmel and Newell 2007). Our results further highlight the ecological significance of windows of opportunity for successful recruitment that may be likened to match-mismatch theory (Cushing 1990). However, it is important to note that in the current study, we have evaluated hatchery production and therefore minimized the typically extreme mortality of larval oysters in the wild by growing them under otherwise ideal conditions.

Long-term records of recruitment of Pacific oysters in Willapa Bay, Washington, have previously shown multiple year failures in recruitment (Dumbauld et al. 2011). Recent Pacific Northwest failures in natural recruitment have also corresponded with diminished oyster seed production at WCH (S. Cudd pers. comm.). Within a hatchery setting, oysters are spawned frequently (every few days at WCH

over several months) and cohorts distinct, whereas natural populations typically have fewer cohorts per season that are often variable in timing and generally result in an integrated cohort over the spawning season. Within the hatchery, temperature and food concentrations are all held at near-constant and optimal levels, and broodstock are optimized for reproduction, while these conditions vary significantly in natural waters during the spawning season. Additionally, Rumrill (1990) noted that fertilization failure, adverse hydrography, substrate limitation, and predation are the most important determinants of the success of natural populations of meroplankton, such as larval oysters. Recent biochemical studies of oyster larvae indicate the importance of food quality and quantity in conjunction with sensitivity to fluctuating salinity and temperature (Hofmann et al. 2004). Increased food availability and quality generally improved tolerance of *C. gigas* larvae to salinity and temperature variability in these modeling studies. If we view the less favorable aragonite formation energetics associated with high- CO_2 upwelling conditions as sublethal acute stress and recognize

that early development is energetically expensive, as is shell construction (Palmer 1992), then the moderate acidification we measured can be considered a stress that requires additional energy to overcome (Portner 2008).

Many marine bivalve species share similar developmental stages from egg fertilization to metamorphosed juveniles, although the timing and typical sizes at which these stages occur will vary both within and among species. Recent studies suggest that early *C. gigas* larvae up to about 120 microns in shell length are mixotrophic, with egg yolk reserves providing a major source of nutrition (Rico-Villa et al. 2009; Kheder et al. 2010a,b). In our analyses of production and growth, there was no significant Ω_A effect (over the natural range of conditions) during early egg development on growth through this early stage (Fig. 5a,b); however, production was ultimately affected (Fig. 5d). This finding suggests that within-cohort variability may allow some individuals to continue to grow without incident while reaching our initial early-growth benchmark (Fig. 5b), while others cannot survive, leading to increased mortality and ultimately decreased cohort production (Fig. 5d). It is important to note that the relative production term uses the change in number of tanks from the D-hinge stage to competent to settle and therefore does not overlap with the proportion of D-hinge value. Growth was, however, significantly affected for midstage larvae that depend primarily on exogenous food sources (Fig. 5c). These findings suggest that the effects of acidification during egg development may have carried over (A. Hettinger unpubl.) to affect the growth and survival of midstage larvae. The nature of this putative carryover effect is unclear but could be due to the cumulative effects of stress on later larval development, metabolism or feeding physiology. Further research on the effects of ocean acidification on larval development and physiology is needed.

The fact that the bay itself experiences large fluctuations in carbonate chemistry driven by primarily natural mechanisms provides an opportunity for adaptive strategies to be implemented by resource managers such as hatchery operators. In the case of Netarts Bay, WCH operators have already implemented a strategy to avoid early morning tank-filling operations during strong upwelling conditions and as a result have restored a significant amount of lost production. Nevertheless, climatic shifts that are likely to move the mean state toward higher- CO_2 , more corrosive conditions are a cause for concern (Feely et al. 2009; Rykaczewski and Dunne 2010). Feely et al. (2008) estimated that the most recent exposure of upwelled source waters off the US west coast was a few decades ago, yet the waters were still influenced by addition of anthropogenic CO_2 from a 1960s-vintage atmosphere. If correct, this means that waters already in transit to the upwelling locations have been exposed to more recent, higher- CO_2 atmospheres, and increasingly corrosive upwelled water is inevitable in coming years. Likewise, the intensity and persistence of upwelling that has accompanied hypoxic events (Grantham et al. 2004; Chan et al. 2008) off the Oregon coast has been hypothesized as a recurring feature of a warming climate (Barth et al. 2007; McGregor et al. 2007). Enhanced upwelling will carry

increased corrosivity of shelf waters, much as it drives increased hypoxia. In each case, the fluctuations in local CO_2 chemistry will be superimposed on a trend of increasing corrosivity, meaning that the conditions favorable for larval oyster production will have lower frequency of occurrence and shorter persistence. Even if commercial shellfish producers are able to predict favorable conditions, the windows of opportunity for these adaptive strategies to be implemented will be diminished.

Two significant shortcomings exist with regard to understanding acidification effects on natural populations of organisms in variable coastal and estuarine habitats: prediction of how carbonate conditions will vary in coastal and estuarine environments with increasing atmospheric CO_2 and a better understanding of the fundamental biology underlying the responses of multicellular organisms to acidification. The first of these will be addressed by development of better predictive capability (Juranek et al. 2009) such that stakeholders may be able to plan production operations for the most favorable conditions. Our limited experience suggests that the multitude of forcing time scales still requires high-resolution monitoring of water CO_2 chemistry before we are fully capable of developing predictive models.

The second can be addressed only by more focused experimental work on physiological mechanisms of early larval response in conditions with tightly controlled carbonate chemistry. Our findings in the hatchery setting corroborate the laboratory-based experiments of Kurihara et al. (2007) illustrating the sensitivity of the very early developmental stages to ambient chemistry, although the hatchery larvae in this study experienced a much narrower range of carbonate chemistry. The descriptive biology of oyster larvae has been well documented; however, the dynamic responses of initial shell formation to environmental signals is still poorly understood. Initial shell is thought to be formed between the periostracum and the shell gland and thus “protected” from ambient conditions. How protected this initial shell material is, the energetics of this initial shell formation, and physiological plasticity are still poorly constrained. Numerous studies have now illustrated a pattern of negative response to acidification for many marine species, including bivalves (Kurihara et al. 2007; Miller et al. 2009; Watson et al. 2009), and many more will likely follow. In almost all cases, it has been shown that mollusks tend to respond negatively to increasing corrosiveness of water. However, only a handful of studies have addressed the underlying physiological and ecological mechanisms of these responses to develop a clear and well-founded argument for how other related organisms will respond (Wood et al. 2008; Thomsen et al. 2010; Ries 2011). Although shell mineralogy is a possible first-order explanation for the responses of calcifying organisms to acidification (Cooley and Doney 2009), it is clear that many other factors will determine susceptibility of biogenic minerals to dissolution (e.g., Glover and Kidwell 1993), and calcifying organisms may respond in less predictable ways (Ries et al. 2009). Although the history of studies of biomineralization spans several decades, aspects of the mechanisms of shell formation are still poorly understood, in particular during the very early life stages of mollusks. Some

recent work questions our current understanding of biomineralization (Mount et al. 2004), and we are far from understanding the processes underlying the patterns of response.

The fact that multiple parameters in the CO₂ chemistry system (pH, P_{CO2}, Ω_A, and so on) all change in response to perturbations complicates this understanding, as there are very likely differential effects of these variables on different physiological processes. Experimental methods that can elucidate these mechanisms will be important. Finally, the ability to predict the acute and chronic sensitivities of organisms to high-CO₂ waters should be a goal of future research. There has been some suggestion that larval and juvenile organisms need to reach critical development states where they can compensate for the deleterious effects of elevated CO₂ levels (Green et al. 2009; Waldbusser et al. 2010), and it may be that *C. gigas* larvae are especially sensitive to chemical conditions at the time of spawning. This may require development of acute and chronic threshold definitions, assessment of the sensitivity of organisms to the persistence of conditions, and stage-based models of organism responses.

The current study illustrates the value of monitoring efforts, which, if applied with stakeholder interests at hand, can provide valuable economic feedback (as is the case with WCH). Our study, relying on hatchery records and utilizing their production model, does potentially suffer from the lack of strict control as found in other more constrained experimental systems. We therefore acknowledge the correlative and suggestive nature of this study; however, it highlights the significance of current-day variable carbonate chemistry effects on commercially important species (and reliant regional economy) in surface waters and validates previous laboratory-based acidification experiments in which carbonate chemistry was manipulated. The significant effects on hatchery-based oyster production indicates that local and regional acidification effects are already on us, and responses of these coupled natural human systems to increasing CO₂ are likely unfavorable.

Acknowledgments

We thank Sue Cudd and Mark Wiegert, owners and operators of the Whiskey Creek Hatchery, for their assistance with developing a sampling program at the hatchery and for sharing their operational and production data with us. This work was supported by the Pacific Shellfish Institute, through efforts led by Andrew Suhrbier, and the Pacific Coast Shellfish Growers Association, through efforts led by Robin Downey. Conversations with Alan Trimble were greatly instructive in building our understanding of the local shellfish environment and ecology. National Science Foundation grant OCE-1041267 supported G.G.W., and the National Oceanic and Atmospheric Administration Ocean Acidification Program supported R.A.F. in preparation of this manuscript. Pacific Marine Environmental Laboratory contribution number 3720. Two anonymous reviewers provided thoughtful comments that greatly improved the final manuscript.

References

AYDIN, K. Y., G. A. MCFARLANE, J. R. KING, B. A. MEGREYA, AND K. W. MYERS. 2005. Linking oceanic food webs to coastal production and growth rates of Pacific salmon (*Oncorhynchus* spp.), using models on three scales. *Deep-Sea Res. II* **52**: 757–780, doi:10.1016/j.dsr2.2004.12.017

BANAS, N. S., B. M. HICKEY, J. A. NEWTON, AND J. L. RUESINK. 2007. Tidal exchange, bivalve grazing, and patterns of primary production in Willapa Bay, Washington, USA. *Mar. Ecol. Prog. Ser.* **341**: 123–129, doi:10.3354/meps341123

BANDSTRA, L., B. HALES, AND T. TAKAHASHI. 2006. High-frequency measurement of seawater total carbon dioxide. *Mar. Chem.* **100**: 24–38, doi:10.1016/j.marchem.2005.10.009

BARTH, J. A., AND OTHERS. 2007. Delayed upwelling alters nearshore coastal ocean ecosystems in the northern California current. *Proc. Natl. Acad. Sci.* **10**: 3719–3724, doi:10.1073/pnas.0700462104

CHAN, F., J. A. BARTH, J. LUBCHENCO, A. KIRINCICH, H. WEEKS, W. T. PETERSON, AND B. A. MENGE. 2008. Emergence of anoxia in the California current large marine ecosystem. *Science* **319**: 920, doi:10.1126/science.1149016

COOLEY, S. R., AND S. C. DONEY. 2009. Anticipating ocean acidification's economic consequences for commercial fisheries. *Environ. Res. Lett.* **4**: 024007, doi:10.1088/1748-9326/4/2/024007

CUSHING, D. H. 1990. Plankton production and year-class strength in fish populations—an update of the match-mismatch hypothesis. *Adv. Mar. Biol.* **26**: 249–293, doi:10.1016/S0065-2881(08)60202-3

DICKSON, A. G. 1990. Thermodynamics of the dissociation of boric acid in synthetic seawater from 273.15 to 298.15 K. *Deep-Sea Res.* **37**: 755–766.

DUMBAULD, B. R., B. E. KAUFFMAN, A. TRIMBLE, AND J. L. RUESINK. 2011. The Willapa Bay oyster reserves in Washington state: Fishery collapse, creating a sustainable replacement, and the potential for habitat conservation and restoration. *J. Shellfish Res.* **30**: 71–83, doi:10.2983/035.030.0111

ELSTON, R. A., H. HASEGAWA, K. L. HUMPHREY, I. K. POLYAK, AND C. C. HASE. 2008. Re-emergence of *Vibrio tubiashii* in bivalve shellfish aquaculture: Severity, environmental drivers, geographic extent and management. *Dis. Aquat. Org.* **82**: 119–134, doi:10.3354/dao01982

EVANS, W., B. HALES, AND P. STRUTTON. 2011. The seasonal cycle of surface ocean pCO₂ on the Oregon shelf. *J. Geophys. Res. Oceans* **116**: C05012, doi:10.1029/2010JC006625

FABRY, V. J., AND OTHERS. 2009. Present and future impacts of ocean acidification on marine ecosystems and biogeochemical cycles. Report of the Ocean Carbon and Biogeochemistry Scoping Workshop on Ocean Acidification Research (UCSD, Scripps Institution of Oceanography; 9–11 October 2007).

FEELY, R. A., AND C.-T. A. CHEN. 1982. The effect of excess CO₂ on the calculated calcite and aragonite saturation horizons in the northeast Pacific Ocean. *Geophys. Res. Lett.* **9**: 1294–1297, doi:10.1029/GL009i011p01294

———, S. C. DONEY, AND S. R. COOLEY. 2009. Ocean acidification: Present conditions and future changes in a high-CO₂ world. *Oceanography* **22**: 36–47, doi:10.5670/oceanog.2009.95

———, C. L. SABINE, J. M. HERNANDEZ-AYON, D. IANSON, AND B. HALES. 2008. Evidence for upwelling of corrosive “acidified” water onto the continental shelf. *Science* **320**: 1490–1492, doi:10.1126/science.1155676

GAZEAU, F., C. QUIBLIER, J. M. JANSEN, J. P. GATTUSO, J. J. MIDDELBURG, AND C. H. R. HEIP. 2007. Impact of elevated CO₂ on shellfish calcification. *Geophys. Res. Lett.* **34**: L07603, doi:10.1029/2006GL028554

GLOVER, C. P., AND S. M. KIDWELL. 1993. Influence of organic matrix on the postmortem destruction of molluscan shells. *J. Geol.* **101**: 729–747, doi:10.1086/648271

GRANTHAM, B. A., AND OTHERS. 2004. Upwelling-driven nearshore hypoxia signals ecosystem and oceanographic changes in the northeast Pacific. *Nature* **429**: 749–754, doi:10.1038/nature02605

- GREEN, M. A., G. G. WALDBUSSER, S. L. REILLY, K. EMERSON, AND S. O'DONNELL. 2009. Death by dissolution: Sediment saturation state as a mortality factor for juvenile bivalves. *Limnol. Oceanogr.* **54**: 1037–1047, doi:10.4319/lo.2009.54.4.1037
- HALES, B., T. TAKAHASHI, AND L. BANDSTRA. 2005. Atmospheric CO₂ uptake by a coastal upwelling system. *Glob. Biogeochem. Cycles* **19**: GB1009, doi:10.1029/2004GB002295
- HALL-SPENCER, J. M., AND OTHERS. 2008. Volcanic carbon dioxide vents show ecosystem effects of ocean acidification. *Nature* **454**: 96–99, doi:10.1038/nature07051
- HOFMANN, E. E., E. N. POWELL, E. A. BOCHENEK, AND J. A. KLINCK. 2004. A modelling study of the influence of environment and food supply on survival of *Crassostrea gigas* larvae. *ICES J. Mar. Sci.* **61**: 596–616, doi:10.1016/j.icesjms.2004.03.029
- JURANEK, L. W., AND OTHERS. 2009. A novel method for determination of aragonite saturation state on the continental shelf of central Oregon using multi-parameter relationships with hydrographic data. *Geophys. Res. Lett.* **37**: L01601, doi:10.1029/2009GL040423
- KHEDER, R. B., C. QUERE, J. MOAL, AND R. ROBERT. 2010a. Effect of nutrition on *Crassostrea gigas* larval development and the evolution of physiological indices. Part A: Quantitative and qualitative diet effects. *Aquaculture* **305**: 165–173, doi:10.1016/j.aquaculture.2010.04.022
- , ———, ———, AND ———. 2010b. Effect of nutrition on *Crassostrea gigas* larval development and the evolution of physiological indices. Part B: Effects of temporary food deprivation. *Aquaculture* **308**: 174–182, doi:10.1016/j.aquaculture.2010.08.030
- KIMMEL, D. G., AND R. I. E. NEWELL. 2007. The influence of climate variation on eastern oyster (*Crassostrea virginica*) juvenile abundance in Chesapeake Bay. *Limnol. Oceanogr.* **52**: 959–965, doi:10.4319/lo.2007.52.3.0959
- KUDO, M., J. KAMEDA, K. SARUWATARI, N. OZAKI, K. OKANO, H. NAGASAWA, AND T. KOGURE. 2010. Microtexture of larval shell of oyster, *Crassostrea nippona*: A FIB-TEM study. *J. Struct. Biol.* **169**: 1–5, doi:10.1016/j.jsb.2009.07.014
- KURIHARA, H., S. KATO, AND A. ISHIMATSU. 2007. Effects of increased seawater pCO₂ on early development of the oyster *Crassostrea gigas*. *Aquat. Biol.* **1**: 91–98, doi:10.3354/ab00009
- LUEKER, T. J., A. G. DICKSON, AND C. D. KEELING. 2000. Ocean pCO₂ calculated from dissolved inorganic carbon, alkalinity, and equations for K₁ and K₂: Validation based on laboratory measurements of CO₂ in gas and seawater at equilibrium. *Mar. Chem.* **70**: 105–119, doi:10.1016/S0304-4203(00)00022-0
- MCGREGOR, H. V., M. DIMA, H. W. FISCHER, AND S. MULITZA. 2007. Rapid 20th-century increase in coastal upwelling off northwest Africa. *Science* **315**: 637–639, doi:10.1126/science.1134839
- MEHRBACH, C., C. H. CULBERSON, J. E. HAWLEY, AND R. M. PYTKOWICZ. 1973. Measurement of the apparent dissociation constants of carbonic acid in seawater at atmospheric pressure. *Limnol. Oceanogr.* **18**: 897–907, doi:10.4319/lo.1973.18.6.0897
- MILLER, A. W., A. C. REYNOLDS, C. SOBRINO, AND G. F. RIEDEL. 2009. Shellfish face uncertain future in high CO₂ world: Influence of acidification on oyster larvae calcification and growth in estuaries. *PLoS ONE* **4**: e5661, doi:10.1371/journal.pone.0005661
- MILLERO, F. J., T. PLESE, AND M. FERNANDEZ. 1988. The dissociation of hydrogen sulfide in seawater. *Limnol. Oceanogr.* **33**: 269–274, doi:10.4319/lo.1988.33.2.0269
- MORSE, J. W., AND F. T. MACKENZIE. 1990. Geochemistry of sedimentary carbonates. *Developments in Sedimentology* 48. Elsevier.
- MOUNT, A. S., A. P. WHEELER, R. P. PARADKAR, AND D. SNIDER. 2004. Hemocyte-mediated shell mineralization in the eastern oyster. *Science* **304**: 297–300, doi:10.1126/science.1090506
- MUCCI, A. 1983. The solubility of calcite and aragonite in seawater at various salinities, temperatures, and 1 atmosphere total pressure. *Am. J. Sci.* **238**: 780–799, doi:10.2475/ajs.283.7.780
- NATIONAL RESEARCH COUNCIL. 2010. Ocean acidification: A national strategy to meet the challenges of a changing ocean. National Academies Press.
- PACIFIC COAST SHELLFISH GROWERS ASSOCIATION. 2010. Shellfish production on the west coast. Available from http://www.pcsga.org/pub/farming/production_stats.pdf
- PALMER, A. R. 1992. Calcification in marine mollusks—how costly is it? *Proc. Natl. Acad. Sci.* **89**: 1379–1382, doi:10.1073/pnas.89.4.1379
- PORTNER, H. O. 2008. Ecosystem effects of ocean acidification in times of ocean warming: A physiologist's view. *Mar. Ecol. Prog. Ser.* **373**: 203–217, doi:10.3354/meps07768
- RICO-VILLA, B., S. POUVREAU, AND R. ROBERT. 2009. Influence of food density and temperature on ingestion, growth and settlement of Pacific oyster larvae, *Crassostrea gigas*. *Aquaculture* **287**: 395–401, doi:10.1016/j.aquaculture.2008.10.054
- RIES, J. B. 2011. A physiochemical framework for interpreting the biological calcification response to CO₂-induced ocean acidification. *Geochim. Cosmochim. Acta* **14**: 4053–4064, doi:10.1016/j.gca.2011.04.025
- , A. L. COHEN, AND D. C. MCCORKLE. 2009. Marine calcifiers exhibit mixed responses to CO₂-induced ocean acidification. *Geology* **37**: 1131–1134, doi:10.1130/G30210A.1
- RUESINK, J. L., H. S. LENIHAN, A. C. TRIMBLE, K. W. HEIMAN, F. MICHELI, J. E. BYERS, AND M. C. KAY. 2005. Introduction of non-native oysters: Ecosystem effects and restoration implications. *Annu. Rev. Ecol. Syst.* **36**: 643–689, doi:10.1146/annurev.ecolsys.36.102003.152638
- RUMRILL, S. S. 1990. Natural mortality of marine invertebrate larvae. *Ophelia* **32**: 163–198.
- RYKACZEWSKI, R. R., AND J. P. DUNNE. 2010. A measured look at ocean chlorophyll trends. *Nature* **472**: E5–E6, doi:10.1038/nature09952
- SABINE, C. L., R. A. FEELY, R. WANNINKHOF, T. TAKAHASHI, S. KHATIWALA, AND G.-H. PARK. 2011. The global ocean carbon cycle. p. S100–S108. *In* State of the Climate in 2010, 3. *Glob. Oceans. Bull. Am. Meteorol. Soc.* **92**: S100–S108, doi:10.1175/1520-0477-92.6.S1
- STEINACHER, M., F. JOOS, T. L. FROLICHER, G. K. PLATTNER, AND S. C. DONEY. 2009. Imminent ocean acidification in the Arctic projected with the NCAR global coupled carbon cycle-climate model. *Biogeosciences* **6**: 515–533, doi:10.5194/bg-6-515-2009
- STENZEL, H. B. 1964. Oysters: Composition of the larval shell. *Science* **145**: 155–156, doi:10.1126/science.145.3628.155
- TALMAGE, S. C., AND C. J. GOBLER. 2009. The effects of elevated carbon dioxide concentrations on the metamorphosis, size, and survival of larval hard clams (*Mercenaria mercenaria*), bay scallops (*Argopecten irradians*), and eastern oysters (*Crassostrea virginica*). *Limnol. Oceanogr.* **54**: 2072–2080, doi:10.4319/lo.2009.54.6.2072
- THOMSEN, J., AND OTHERS. 2010. Calcifying invertebrates succeed in a naturally CO₂-rich coastal habitat but are threatened by high levels of future acidification. *Biogeosciences* **7**: 3879–3891, doi:10.5194/bg-7-3879-2010
- WALDBUSSER, G. G., H. BERGSCHNEIDER, AND M. A. GREEN. 2010. Size-dependent pH effect on calcification in post-larval hard clam *Mercenaria* spp. *Mar. Ecol. Prog. Ser.* **417**: 171–182, doi:10.3354/meps08809

- , E. P. VOIGT, H. BERGSCHNEIDER, M. A. GREEN, AND R. I. E. NEWELL. 2011. Biocalcification in the eastern oyster (*Crassostrea virginica*) in relation to long-term trends in Chesapeake Bay pH. *Estuar. Coasts* **34**: 221–231, doi:[10.1007/s12237-010-9307-0](https://doi.org/10.1007/s12237-010-9307-0)
- WATSON, S.-A., P. C. SOUTHGATE, P. A. TYLER, AND L. S. PECK. 2009. Early larval development of the Sydney rock oyster *Saccostrea glomerata* under near-future predictions of CO₂-driven ocean acidification. *J. Shellfish Res.* **28**: 431–437, doi:[10.2983/035.028.0302](https://doi.org/10.2983/035.028.0302)
- WEISS, I. M., N. TUROSS, L. ADDADI, AND S. WEINER. 2002. Mollusc larval shell formation: Amorphous calcium carbonate is a precursor phase for aragonite. *J. Exp. Zool.* **293**: 478–491, doi:[10.1002/jez.90004](https://doi.org/10.1002/jez.90004)
- WHITE, J., J. L. RUESINK, AND A. C. TRIMBLE. 2009. The nearly forgotten oyster: *Ostrea lurida* Carpenter 1864 (Olympia oyster) history and management in Washington State. *J. Shellfish Res.* **28**: 43–49, doi:[10.2983/035.028.0109](https://doi.org/10.2983/035.028.0109)
- WOOD, H. L., J. I. SPICER, AND S. WIDDICOMBE. 2008. Ocean acidification may increase calcification rates, but at a cost. *Proc. R. Soc. B Biol. Sci.* **275**: 1767–1773, doi:[10.1098/rspb.2008.0343](https://doi.org/10.1098/rspb.2008.0343)

Associate Editor: John Albert Raven

Received: 17 May 2011
Accepted: 16 January 2012
Amended: 27 January 2012

Update on Hatchery Research and Use of State Funds to improve Larval Performance at Whiskey Creek Shellfish Hatchery

Alan Barton, Sue Cudd, and Mark Weigardt

In early 2008, the problems experienced at Whiskey Creek Shellfish Hatchery were thought to be attributable to the presence of *vibrio tubiashii*, a common marine bacteria that was found in unusually high concentrations in Netarts Bay during 2006 and 2007. Much of the early research and systems development at the hatchery were therefore targeted at reducing the concentration of *vibrio* and its toxins present in incoming seawater. However, further research in 2008 and 2009 has revealed that although *vibrio tubiashii* is a significant stress factor for shellfish larvae, it is not the underlying cause of the catastrophic mortality events that have brought production at Whiskey Creek to a standstill. Therefore, beginning in July 2008, the emphasis of research in the hatchery shifted toward understanding the fundamental changes in seawater chemistry that are influencing marine life in our coastal waters. The results of this research and our progress toward developing a solution will be detailed in the following sections.

Impacts of upwelling on shellfish larvae

In July 2008, a huge mortality event resulted in the loss of several billion bivalve larvae at Whiskey Creek, and brought production to a halt. While devastating for the hatchery, this event led us to perhaps our only clear revelation in 2008- *upwelling of nutrient rich, deep ocean water onto the continental shelf results in a sharp decline in the performance of bivalve larvae.*

When persistent winds blow from the North (for 24-48 hours or more), surface water near the coast is pushed offshore, and is replaced by cold, deep water masses. This upwelled water is characterized by very low pH (measured as low as 7.55-7.6 in 2008 and 2009). When this acidified water is observed in the hatchery, mass mortality events have followed in 24-48 hours. In these very extreme conditions, larvae of all sizes and species (Pacific oysters, Kumamoto oysters, Manila clams, and Mediterranean mussels) are dramatically affected. Although production was slow throughout the 2008 season, the sudden, catastrophic mortality events observed in July were clearly associated with this strong upwelling event.

An isolated example from this year can perhaps illustrate our sense of how upwelling/downwelling events are affecting the growth of shellfish larvae in our hatchery. To preface this, we should mention that larval production in the early months of the 2009 season has been quite good, with small larvae growing at normal rates for the first time since mid 2007. However, in mid-April 2009, winds began to blow from the north, and were sufficiently strong and sustained to produce an early upwelling event, which brought acidified seawater (pH=7.55) into Netarts Bay. Although this event was brief, significant mortality was observed over the next two weeks, particularly among small oyster larvae (both Pacific and Kumamoto).

A number of pH measurements were recorded during this following this recent upwelling event, and can provide some important insights into understanding Netarts bay. The following table shows the minimum daily pH measurements (recorded early each morning) on several days at the end of April.

4/21/2009	4/23/2009	4/24/2009	4/28/09	4/29/09
7.58	7.67	7.70	7.73	7.92

Admittedly, trying to determine trends in pH data is somewhat suspect- pH is affected by biology, and using it as a marker of upwelled water masses is therefore questionable. However, the data shown above gives a good general sense of the changes that follow an upwelling event. The minimum daily pH rises slowly in the 7-10 days after North winds relaxed, which suggests that upwelled water is slowly mixing with surrounding seawater on the continental shelf, or that biology (algae, etc) is slowly raising the pH by consuming excess CO₂ in the upwelled water. Which explanation, or combination of the two, makes the most sense is a question for the oceanographic community- however, the point for our purposes is plain: even though the upwelling has relaxed, the 'bad' properties of the seawater in Netarts Bay do not immediately vanish. During the entire period described in the table, slow growth and mortality of small larvae continued to plague the hatchery.

In fact, slow growth of small larvae continued through the first week of May, when minimum pH values continued to drop to 7.9-8.0 each day. Starting on May 1, winds began to blow from the South, and some fairly large storms passed through during the first week of the month, with strong sustained winds and gusts as high as 50 MPH. These winds presumably started a strong downwelling event and pushed the remaining 'bad' water offshore to reset the system. Following this storm, an immediate change was observed in the hatchery, and the growth of small larvae has been normal ever since.

This fairly isolated event greatly improves our confidence that upwelling of deeper ocean water is directly linked to poor performance of larvae in the hatchery. Unlike 2008, when poor performance throughout the season clouded our observations, production in 2009 was quite good both before and after this brief cycle of upwelling and downwelling, which provided a clear signal that larval mortality was directly related to this incoming water mass.

Related research- ocean acidification and potential effects on shellfish larvae

The presence of acidified seawater on the Oregon continental shelf has been well documented by recent oceanographic studies. Feely et al (2008) recorded upwelling events in July 2007, and recorded water masses acidic enough to be considered corrosive to shellfish. Shellfish build their shells from calcium carbonate (CaCO₃), which has several different crystal forms. Many shellfish, as well as most corals in the ocean, form their shells from a type of calcium carbonate called aragonite, which is fairly easy to dissolve. Feely's measurements showed upwelled water that was corrosive enough to dissolve aragonite and literally eat away at the shells of many animals on the continental shelf.

It turns out that adult oysters form their shells from a type of calcium carbonate called calcite, which is much more difficult to dissolve, and they therefore are somewhat more protected than other animals. Adult mussels, for example, form their shells from aragonite. Recent studies have shown that under slightly acidified conditions, the growth of adult mussels is dramatically slowed, while the reduction in growth of adult oysters is only slightly reduced (Gazeau, et al 2007). Although this was a lab study, recent studies have shown that ocean acidification may be beginning to damage coral and shellfish in their natural environment (Langdon, et al (2003) and Cutlip, K (2008)).

Oyster *larvae*, however, are a different story altogether. A surprising amount of research has been conducted to determine what makes up the shell of oyster larvae (Weiss, et al 2002, Lee et al 2004, etc), and shows that the shells of oyster larvae are composed of aragonite, which makes them very susceptible to the acidified water observed on the Oregon continental shelf in 2007. Moreover, these studies also conclude that the shells of small oyster larvae (1-3 days old) are formed partially from amorphous calcium carbonate (ACC), which is EXTREMELY easy to dissolve. In fact, animals have to expend a lot of energy to form ACC even in normal conditions.

Adult Oyster Shell	Calcite	Harder to dissolve
Adult Mussel Shell, Older Oyster Larvae	Aragonite	Easier to dissolve
Young Oyster Larvae	Amorphous Calcium Carbonate (ACC)	<u>Really</u> easy to dissolve

This research was very enlightening, and seems to explain many of the problems we have observed in the hatchery. Most of the ongoing problems experienced in 2007 and 2008 involved the growth of young larvae. In many cases, once they reached the umboe stage (typically after 7-10 days), larvae had a much easier time growing to setting size. In even slightly acidified seawater, young larvae need to expend a great deal of energy to form shell, since it is composed partially of ACC. Under these same conditions, older larvae would have an easier time forming aragonite shell, but their overall growth should also be somewhat slower than in normal conditions.

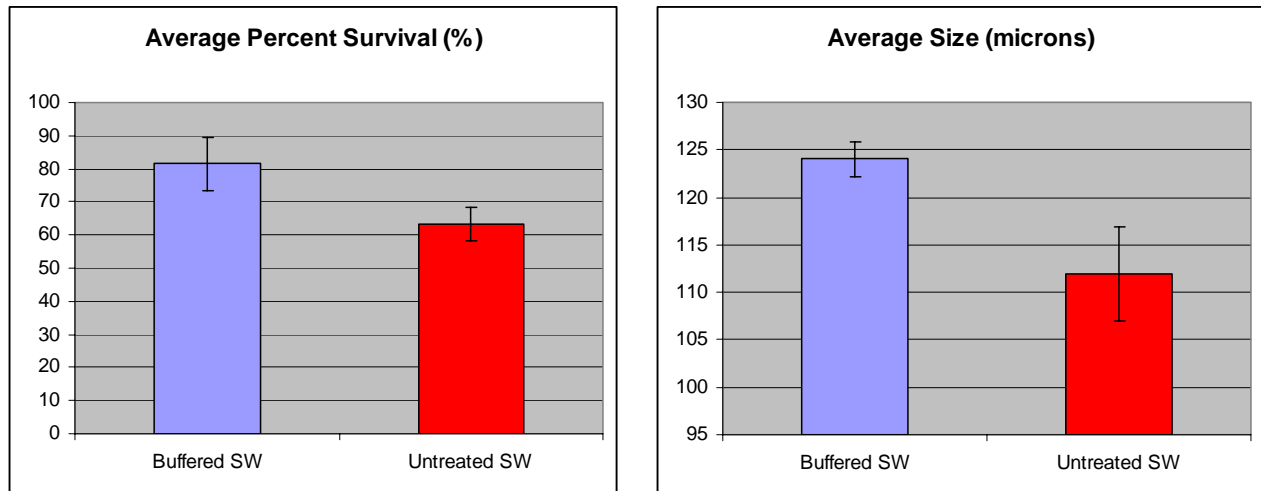
The experiment of Gazeau et al (2007) mentioned above supports this idea- in their example, we're considering the top two forms of calcium carbonate shown in the table above, calcite and aragonite. Even in only slightly acidified conditions, their study showed that the growth rate of animals was reduced. The growth of adult oysters (which form their shell from calcite) slowed slightly in acidified water, but not as much as adult mussels (which form their shells from aragonite). It seems plausible to apply this reasoning to growth of larvae in the hatchery. In the case of oyster larvae, we are now considering the bottom two carbonate forms in the table above. Under slightly acidified conditions, older larvae, which form their shells of aragonite, should show a slight reduction in growth. Younger larvae, however, which form their shells (partially) from ACC, would experience a much greater reduction in growth under the same conditions. Current research is directly investigating the effects of acidified water on oyster larvae, and supports the idea that young larvae are most at risk (Kurihara et al, 2007 and unpublished work currently under investigation by Whitman Miller of the Smithsonian Research Institute- referenced in Cutlip, K (2008)).

This line of reasoning also seems to explain the massive mortality events observed during periods of strong upwelling. During these periods, when the pH drops to 7.6 or lower, seawater is directly corrosive to aragonite, and both young and old larvae will experience a great deal of stress. In these periods, larvae throughout the hatchery may feel the direct effects of acidification, or simply expend so much energy building shell that they are weakened, and can more easily succumb to normal stressors like bacteria blooms in larval tanks.

Hatchery experiments- Fall 2008

In late summer 2008, experiments began in the hatchery to test the effects of low pH on oyster larvae. Conveniently, the ocean provided all the low pH water necessary for these experiments, which acted as our low pH control. Carbonate buffers were used to artificially raise the pH in some tanks, and early results were quite promising. The graphs on the following page show the results of a buffering experiment conducted in small (10 L) buckets- untreated seawater in these experiments ranged from 7.7-7.8 during the 9 day experimental period, and treated seawater was buffered to an approximately constant pH of 8.3. A marked increase in both larval survival and growth can be seen in the buffered seawater tanks.

pH Bioassay- Day 9 (August 15, 2008)



In the hatchery itself, early attempts to buffer seawater in large tanks (6000-20000 gallons) also met with some success, and the performance of older larvae (especially mussels and clams) was dramatically improved, especially during conditions when incoming seawater was extremely low (minimum pH of 7.6). However, the results in large tanks were less impressive with younger larvae, and in general, buffering alone did not solve all of our problems. As is becoming the trend in this battle, however, our failure to fix the hatchery did lead to an important further insight.

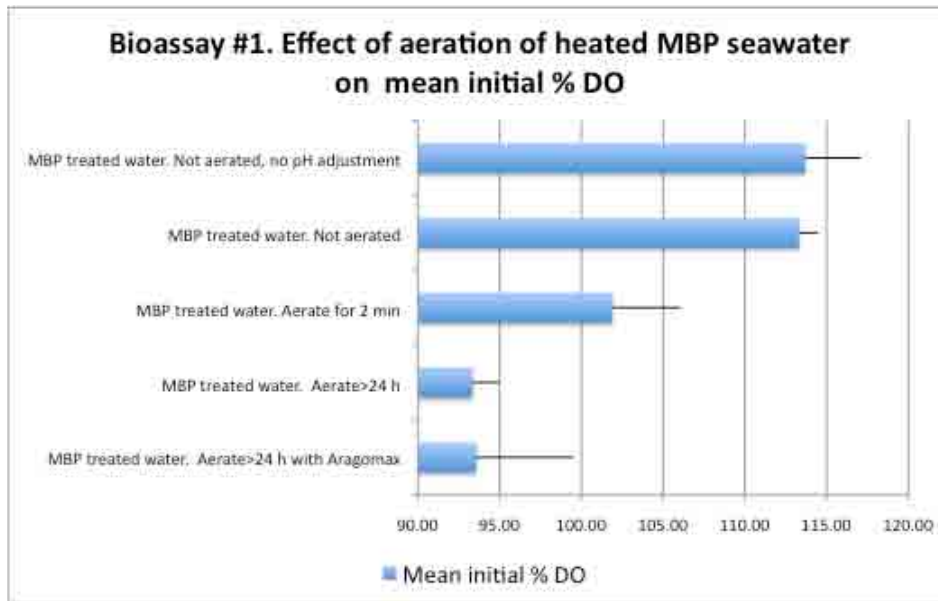
From these concurrent experiments, it became clear that what happens in a 10L bucket is quite different than what happens in a 6000 gallon tank. Whatever changes take place in a small container of buffered seawater appear to happen very quickly, while the same processes appear to be much slower in a large volume of water. Seawater chemistry involves a very complex set of interacting reactions- it is likely that although the 'quick fix' of adding buffers to a large volume of water improves conditions to a degree, buffering alone cannot address the underlying problems which force this system out of balance.

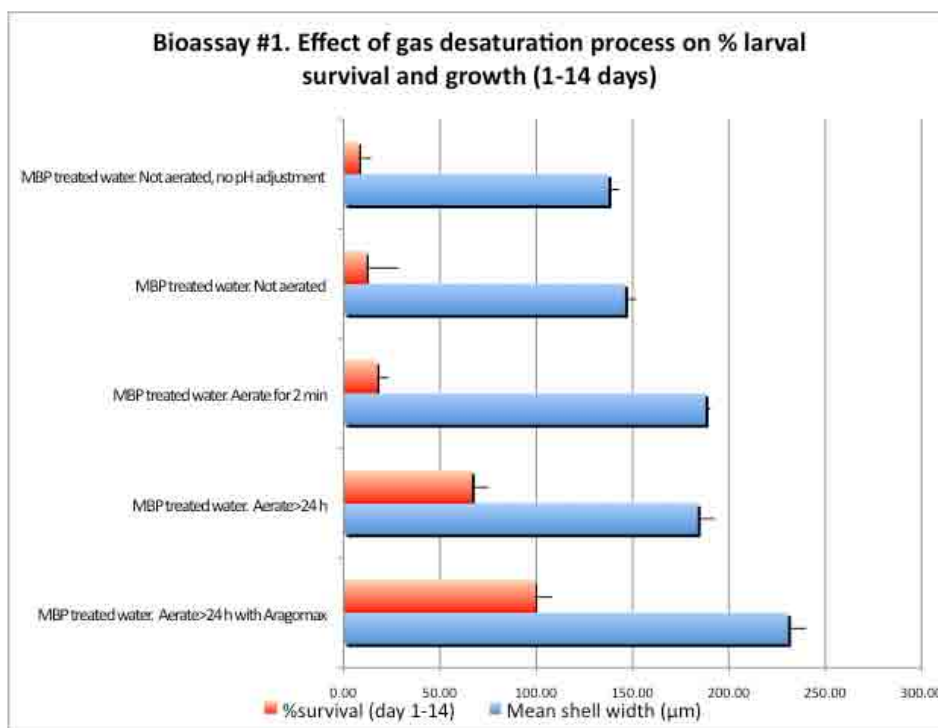
Feely et al (2007) states that the real culprit in this caper is atmospheric CO₂, derived from human inputs. In their opinion, high CO₂ in the air has increased the pCO₂ (partial pressure of CO₂) in seawater, which is ultimately forcing down the pH of the ocean. In addition to human influences, the pCO₂ of seawater can be influenced by biology- respiration of animals in seawater can greatly increase the pCO₂ of seawater in coastal areas. It is likely that biology in our bay, especially during the dead zone events of the past several years, contributed to high pCO₂ along our coast, and has helped to push this system further out of balance.

Unlike most gases, CO₂ is fairly difficult to remove from seawater, even with vigorous aeration. As a result, it can take several hours to significantly reduce CO₂ concentrations in a large volume of seawater. This idea may help to explain the differences observed in small containers of buffered seawater, where the high surface to volume ratio could allow CO₂ to escape quickly.

Degassing experiments

Unfortunately, until quite recently (this week, actually) we haven't had the tools available to assess $p\text{CO}_2$ concentrations directly. However, Chris Langdon at MBP has conducted some relevant work using O_2 saturation as a proxy for the saturation of other gases in seawater. In addition to elevated $p\text{CO}_2$, Chris' work also considers the direct effects of other gases such as nitrogen and methane, which can be directly toxic to shellfish larvae in supersaturated conditions. Some of Chris' work with degassing is summarized in the graphs below and shows a dramatic increase in the survival and growth of larvae after vigorous aeration and storage for a 24 hour period.





Whether the changes produced by degassing are related to high nitrogen, methane, or increased $p\text{CO}_2$, it is clear that some measurable changes take place when tanks of seawater are vigorously aerated. It is also clear that these changes can result in improved performance of larvae.

Based on these results, we began to measure O_2 saturation in tanks at Whiskey Creek. The following table shows $\% \text{O}_2$ measurements from several locations in the hatchery. The probe used to collect these measurements may be slightly inaccurate, but the measurements are reliable and repeatable. Therefore, the relative differences between readings can be used to gain valuable insights about gas saturation.

<u>Source</u>	<u>% O_2 (3/29)</u>	<u>% O_2 (4/1)</u>
Cold Seawater (12 degC)	105%	88.5%
Heated Seawater (25 deg C)	113%	98%
Heated Seawater in tank immediately after filling	94%	
Heated Seawater in tank after 1 hour	86%	
Heated Seawater in tank filled overnight	84%	
Treated Seawater from existing seawater treatment system (heated)	84%	84%

To begin a discussion of this data, we should state that whenever cold seawater is heated in a heat exchanger, the water *has* to become supersaturated. Cold water holds more dissolved gases than warm water, so rapid heating means that there will temporarily be too much gas in the heated water when it comes out of the pipe. With that said, there are some interesting points to be made about the measurements shown above.

The equilibrium $\% \text{O}_2$ in these measurements seems to be 84%. When a tank is filled slowly overnight and allowed to sit (with gentle aeration), it eventually settles in at 84% saturation and stays at 84% over the next 48 hours. Over the past year, we have observed improved performance of larvae in tanks filled

overnight, when compared to tanks filled during the day. The differences in %O₂ seen above may help explain these differences in performance, and illustrate how residence time remains an important factor in adjusting seawater chemistry. If it takes over one hour to reduce O₂ concentrations to equilibrium in a large tank, then it should take significantly longer to drive off stubborn gases like CO₂.

The data above also shows that treated seawater (passed through the existing treatment system) seems to be effectively degassed, and exits the system at 84% saturation. Vigorous aeration is an integral component of the treatment system (by happy accident), since the treatment system contains both a protein skimmer (with a venturi air injector) and a fluidized bioreactor powered by a tremendous amount of aeration. In addition, the system is designed to maximize residence time in the tanks, which seems to be a critical component of the degassing process.

Developing a comprehensive approach to the 2009 growing season

Although our understanding of water quality problems is admittedly imperfect, our investigation into ocean acidification research and early experiments with buffering and degassing of upwelled water provided us with some valuable insights, and provided some direction for continued research in 2009. In short, our strategy was to take a comprehensive approach to the problem, and modify the existing treatment system to address any potential stressors that could arise in the 2009 season.

*Reducing the prevalence of *Vibrio tubiashii* in the hatchery*

It is important to note that although *vibrio tubiashii* is no longer the primary focus of our research efforts, it is a significant stressor for oyster larvae. It was therefore critical that we take steps to reduce bacterial contamination in the hatchery, both to improve the overall health of larvae and to remove an additional variable that could further complicate our continued research efforts. Therefore, a significant portion of the funds received from the state of Oregon was used to improve the cleanliness of the hatchery and limit the prevalence of vibrios in our seawater systems.

The first step in this process was simply to shut down completely and dry out the facility for a period of six weeks, to eliminate any lingering sources of contamination from the previous season. During this period, much of the plumbing throughout the hatchery was replaced, and systems were modified to improve the process of disinfecting seawater lines. All media in the external sand filters was also replaced. Finally, all algae stocks from 2008 were discarded and replaced with fresh cultures from outside sources. The rigorous maintenance conducted in the winter months allowed us to enter the 2009 with a clean slate, and minimize the effects of an additional stressor that could potentially confound our continued research efforts.

In my mind, continued work to better identify and understand vibrio outbreaks is a critical component of our continued research efforts. My own understanding of vibrio improved when I began to think of the high prevalence of vibrio in the bay a *symptom* of water quality problems, rather than the cause. *Vibrio tubiashii* is a fast-growing, opportunistic bacterium which primarily acts as part of the ocean's 'clean up crew'. Its role in the environment is to break down organic matter, and when there is a lot of decaying organic matter in the ocean, we can expect there to be a lot of vibrio around to clean up the mess. Therefore, it is hoped that vibrio research will continue in earnest, with the goal of understanding the environmental factors that contribute to vibrio blooms in our coastal waters. If we can better understand the chemical cues that produce vibrio outbreaks in coastal bays, we may better understand the underlying changes in seawater chemistry that contribute to larval mortality.

Increased use of selected broodstock

During the 2008 season, MBP selected broodstock was used for commercial spawns on a number of occasions. In several instances, we observed that MBP groups fared better than larvae spawned from 'wild' broodstock. Certainly, use of MBP broodstock was not a magic bullet- during periods of extremely poor water quality, MBP larvae also experienced significant mortality. Nevertheless, using selected broodstock seemed to confer a definite advantage to larvae, and increased use of MBP broodstock has become a primary goal for the 2009 season. A large number of MBP larvae have already been produced this season, and early reports from growers have been very positive.

In a concerted effort to identify resistant MBP families, Chris Langdon and Mark Camara have planned and carried out a commercial spawn at Whiskey Creek, using a large pool of crosses derived from MBP broodstock. This pool of MBP crosses is currently in production at Whiskey Creek in large 6000 gallon, and is being treated as a normal group of larvae in our production cycle. In this way, they hope to expose the larvae to the stresses typically encountered at the hatchery during periods of poor water quality. At harvest, Mark Camara will use genetic techniques to identify specific crosses that harvest quickly and show high survival. This technique will allow for the rapid detection of resistant crosses, and within 2-3 months could identify a subset of 'super-crosses' which show elevated performance in the larval stage.

Strategy for use of the seawater treatment system in 2009

Limited use at the beginning of the season- In 2008, it was very difficult to make progress toward improving the seawater treatment system because it was impractical to continuously run side by side comparisons of treated and untreated seawater. Because of the extreme variability observed in our incoming seawater, we often missed the start of poor water quality events in commercial scale bioassays. Therefore, we decided to set up a redundant set of plumbing in part of the hatchery (where small larvae are typically grown), so that side by side experiments could be conducted with small larvae in more controlled conditions. These experiments (treatment vs. control) will be run continuously throughout the 2009 season. Over time, individual variations in water masses will average out, and provide a clear picture of the benefits conferred by seawater treatment.

Individual tests of additional treatments- A number of potential additions to the treatment process were discussed over the winter, some of which had shown positive results in late 2008. However, before adding them wholesale to the treatment system, each component was tested individually to understand its potential impacts on seawater quality, and the results are discussed in the following section. Essentially, our goal in these experiments was to ensure that each additional treatment was not *harmful* to larvae. As stated before, water quality in Netarts Bay is extremely variable, and discarding a treatment because it didn't help *this week* could eliminate treatments that could potentially be very important later in the season. This 'kitchen sink' approach to seawater treatment should provide our best defense against a variety of stressors, and the individual trials of each component will insure that these additions do not negatively impact the overall performance of the system.

Improvements to the treatment system

Installation of a pH control system- Low pH of seawater remains a relevant concern for the hatchery, particularly during extreme upwelling events, and buffering experiments in 2008 met with some limited success. Therefore, we took steps this spring to automate the process of buffering incoming seawater. Bill Robertson designed an efficient and effective system for the hatchery, which is currently in use at the front end of our seawater treatment system. Thus far, the system has functioned flawlessly, and insures that treated seawater never drops below a pH of 7.9.

Pre-heating seawater prior to treatment- In 2008, cold seawater was passed through the treatment system, then heated afterward. However, because of concerns about gas saturation, the process was reversed over the winter, and seawater is now heated prior to entering the treatment system. This change should help in our efforts to drive off gasses, since gasses are much less soluble at high temperature. As the data presented earlier shows, the treatment system now seems to function as an effective degasser (at least for volatile gases like oxygen, nitrogen, and methane), and reduces O₂ saturation to equilibrium concentrations.

CO₂ scrubbers- As was mentioned earlier, offgassing of CO₂ can take much longer than many other gases. In further efforts to reduce the pCO₂ of treated seawater, all air entering the treatment system through the protein skimmers and the bioreactors is passed through air scrubbers. These scrubbers reduce the concentration of CO₂ in air to near zero. This increases the concentration gradient between air and water, and should speed up the removal CO₂ from the incoming seawater. CO₂ scrubbers have also been tested on the air supply to individual tanks in the hatchery, and the preliminary results have been quite promising. The following data shows the size of larvae in 6000 gallon tanks after eight days, and shows a marked improvement in the size of larvae when continuously aerated with CO₂-free air.

<u>Treatment</u>	<u>Size range</u>	<u>% on 100um screen</u>
Untreated Seawater	110-130 microns	trace
Untreated Seawater, w/ CO ₂ air scrubber	120-150 microns	~30%

In a subsequent bioassay, however, no improvement was observed with use of the CO₂ scrubber, and both groups of larvae were identical in size after eight days. Potentially, the water masses were quite different in the second experiment, and rendered the treatment unnecessary. For our purposes, that's okay. The treatment shows promising results in some conditions, and does not produce negative effects in others, so we will continue to proceed cautiously with the use of CO₂ scrubbers in seawater treatment.

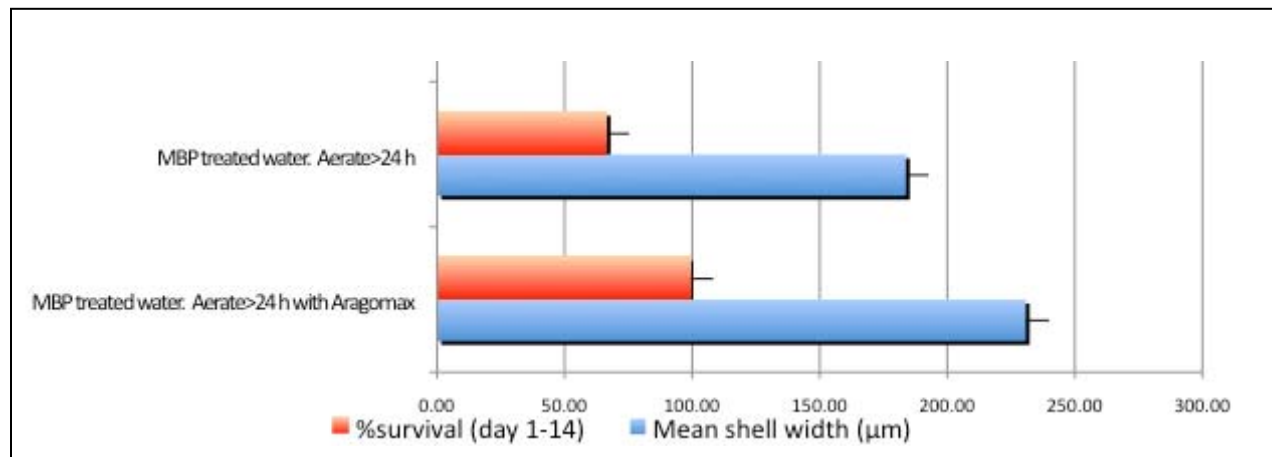
Venturis- In many commercial locations (fish farms, dams, etc), degassing of water is an important process, and a number of simple technologies exist to remove gasses from seawater. We have adapted one such technology for filling individual tanks in the hatchery, and measurements of %O₂ saturation show an improvement over tanks filled without the venturis.

<u>Source</u>	<u>% O₂ (3/29)</u>
Heated Seawater (25 deg C)	113%
Heated Seawater in tank immediately after filling	94%
Heated Seawater in tank immediately after filling w/ Venturi	89%
Heated Seawater in tank filled overnight	84%

These venturis are currently being used to fill most tanks in the hatchery, and certainly show no adverse effects on larvae. Although treated seawater %O₂ saturations are already reduced to equilibrium levels, venturis are also being used when tanks are filled with treated seawater. The technology is simple and

cheap, and has been shown not to harm larvae, so we are including it in our comprehensive set of treatment options.

Coral sand- Another treatment that has shown great promise in both small scale and large scale bioassays is passing seawater through coral sand as it enters the tank. Large scale experiments in fall of 2008 showed a marked improvement in larval growth, and follow up experiments at MBP supported this assertion in replicated bucket trials, the results of which are shown below.



Large scale experiments in 2009 also show the positive effects of coral- the table below shows size measurements of larvae after ten days, and shows a big improvement in the growth of larvae when seawater is passed through coral (and a venturi).

<u>Treatment</u>	<u>Size range</u>	<u>% on 100um screen</u>
Untreated Seawater	100-130 microns	trace
Untreated Seawater, w/ venturi and coral	110-150 microns	~40%

A second bioassay in 2009 showed no improvement with the addition of a venturi and coral to untreated seawater, and larvae in both the treatment and control were identical in size after 10 days. However, no negative effect was observed, and repeated experiments in the past year (five trials with positive results in 2008 and 2009) give us confidence that the addition of coral to the treatment system can significantly improve larval growth and survival.

‘Why’ adding coral helps is unclear, but there are at least two plausible explanations. First, the coral may simply be helping in the degassing process, by further agitating water as it falls in the tank. Second, some evidence suggests that larvae need small crystals of aragonite to be present in seawater, to aid in shell formation. During acidified conditions, these normally-occurring particles may have dissolved, and need to be replaced in our larval tanks. These particles could either be used directly in shell formation, or serve as seed crystals for non-biogenic precipitation of calcium carbonate, and make it much easier for larvae to build their shells. Regardless of the reasons, repeated bioassays show that coral helps, and it has therefore been included as a final step in our seawater treatment process.

Moving forward with the modified treatment system

The set of changes detailed above have resulted in a much more comprehensive approach to seawater treatment. The system, as best we are able, addresses the four major stressors we feel are affecting shellfish larvae: *vibrio tubiashii*, direct effects of low pH, indirect effects of elevated pCO₂ on shell formation, and degassing of gases such as carbon dioxide, methane, and nitrogen. To be sure, some additional tweaking of the system will follow in the coming months, but we are now essentially at the end of the list of available treatment options. We will continue limited use of the treatment system in side by side comparisons with untreated seawater throughout the growing season. If seawater conditions deteriorate in the coming months, we will switch over full production to treated seawater whenever it becomes necessary. Certainly, we do not have complete confidence that the new treatment system will solve all of our water quality problems, but by address a number of potential stress factors we may provide enough advantage to significantly improve production in the hatchery.

In the meantime, we will continue to improve our understanding of seawater chemistry, and build on collaborations recently established with researchers around the country.

Seawater Monitoring Program

By the end of 2008, we came to understand that our knowledge of our coastal bays and estuaries is at best imperfect. It also became clear that the difficulties we are facing are part of a big, global problem, from conversations with hatchery managers as far away as Australia, England, and Chile, and from current research showing the decline in growth of corals and shellfish around the world. Most of all, it became clear that we need to build collaborations with a diverse set of researchers if we hope to fully understand and correct these water quality problems.

To that end, the PCSGA seed supply committee developed and secured funding for a comprehensive monitoring program in both Netarts Bay and Willapa Bay, which will be managed by Dan Cheney and researchers at the Pacific Shellfish Institute (PSI). Data loggers deployed in each location will record hourly measurements of pH, temperature, salinity, dissolved oxygen, carbon dioxide, and oxidation/reduction potential. Each week, water samples will also be sent to Burke Hales, a chemical oceanographer at OSU who specializes in ocean acidification research. Burke will provide redundancy to check the accuracy of our data loggers, and will also obtain accurate measurements of pCO₂, dissolved inorganic carbon (DIC), and total alkalinity, as well as total nutrient concentrations. These samples will take the guesswork out of our efforts to define water quality problems, and Burke's lab will provide the expertise required to pinpoint exactly what is wrong with seawater in our coastal bays.

In addition, weekly samples of treated seawater from the hatchery will be sent to Burke's lab, and will allow us to understand whether our treatments are sufficient to return water quality to 'normal'. By correlating Burke's measurements with the performance of larvae in both treated and untreated seawater, we should gain valuable insight into which parameters are of most concern to shellfish larvae.

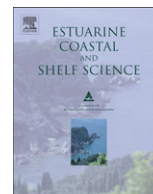
This monitoring program will also include sending weekly water samples to Ralph Elston, in a continued effort to monitor outbreaks of *vibrio tubiashii*, and to monitor total bacteria counts in the bay. Hopefully, comparing these results to detailed measurements of seawater chemistry can determine the environmental factors that trigger *vibrio* blooms and the production of toxins that cause mortality in shellfish larvae.

In addition, this program will include the work already being conducted by Alan Trimble, which includes routine plankton samples in Willapa Bay. It is hoped that comparison of this data with Burke and Ralph's measurements will help identify which environmental factors are of greatest concern for shellfish larvae in the natural environment.

We now have a lot of heads together on this issue, and the collaborations fostered by the seed supply committee have brought together researchers with a wide range in areas of expertise. By combining their talents and overlaying oceanographic measurements, bacteria monitoring, plankton sampling, and larval performance data from the hatchery, we hope to obtain a clear picture of the changes affecting our coastal bays and estuaries, and take great strides to mitigate their effects on the Pacific Northwest shellfish industry.

References

- Catlip, K. Rising Acidity of Estuary Waters May Spell Trouble for Oysters and Other Shellfish. *Inside Smithsonian Research*, spring (2008).
- Feely, R.A., Sabine, C.L., Hernandez-Ayon, J.M., Iansun, P., and Hales, B. Evidence for Upwelling of Corrosive “Acidified” Water onto the Continental Shelf. *Science*, 320, 1490 (2008).
- Gazeau, F., Quiblier, C., Jansen, J., Gattuso, J.P., Middleburg, J.J., and Heip, C.H.R. Impact of Elevated CO₂ on Shellfish Calcification. *Geophysical Research Letters*, 34: L07603 (2007).
- Kurihara, H., Kato, S., Ishimatsu, A. Effects of Increased pCO₂ on Early Development of the Oyster *Crassostrea gigas*. *Aquatic Biology*, 1: 91-98 (2008).
- Langdon, C., Broecker, W.S., Hammond, D.E., Glenn, E., Fitzsimmons, K., Nelson, S.G., Peng, T.H., Hajdas, I., and Bonani, G. Effects of Elevated CO₂ on the Community Metabolism of an Experimental Coral Reef. *Global Biogeochemical Cycles*, 17, no. 1011 (2003).
- Lee, S.W., Hong, S.M., and Choi, C.S. Characteristics of Calcification Processes in Embryos and Larvae of the Pacific Oyster *Crassostrea gigas*. *Bulletin of Marine Science*, 78(2): 309-317 (2006).
- Weiss, I.M., Tucoss, N. Addadi, L., and Weiner, S. Mollusc Larval Shell Formation Amorphous Calcium Carbonate is a Precursor Phase for Aragonite. *Journal of Experimental Zoology*, 293: 478-491 (2002).



The combined effects of ocean acidification, mixing, and respiration on pH and carbonate saturation in an urbanized estuary

Richard A. Feely^{a,*}, Simone R. Alin^a, Jan Newton^b, Christopher L. Sabine^a, Mark Warner^c, Allan Devol^c, Christopher Krembs^d, Carol Maloy^d

^a Pacific Marine Environmental Laboratory/NOAA, 7600 Sand Point Way NE, Seattle, WA 98115, USA

^b Applied Physics Laboratory, University of Washington, Box 355640, Seattle, WA 98105, USA

^c School of Oceanography, University of Washington, Box 355351, Seattle, WA 98195, USA

^d Washington State Department of Ecology, PO Box 47710, Olympia, WA 98504-7710, USA

ARTICLE INFO

Article history:

Received 18 October 2009

Accepted 7 May 2010

Available online 15 May 2010

Keywords:

acidification

pH

estuary

saturation

carbonate minerals

respiration

ABSTRACT

Puget Sound is a large estuary complex in the U.S. Pacific Northwest that is home to a diverse and economically important ecosystem threatened by anthropogenic impacts associated with climate change, urbanization, and ocean acidification. While ocean acidification has been studied in oceanic waters, little is known regarding its status in estuaries. Anthropogenically acidified coastal waters upwelling along the western North American continental margin can enter Puget Sound through the Strait of Juan de Fuca. In order to study the combined effects of ocean acidification and other natural and anthropogenic processes on Puget Sound waters, we made the first inorganic carbon measurements in this estuary on two survey cruises in February and August of 2008. Observed pH and aragonite saturation state values in surface and subsurface waters were substantially lower in parts of Puget Sound than would be expected from anthropogenic carbon dioxide (CO₂) uptake alone. We estimate that ocean acidification can account for 24–49% of the pH decrease in the deep waters of the Hood Canal sub-basin of Puget Sound relative to estimated pre-industrial values. The remaining change in pH between when seawater enters the sound and when it reaches this deep basin results from remineralization of organic matter due to natural or anthropogenically stimulated respiration processes within Puget Sound. Over time, however, the relative impact of ocean acidification could increase significantly, accounting for 49–82% of the pH decrease in subsurface waters for a doubling of atmospheric CO₂. These changes may have profound impacts on the Puget Sound ecosystem over the next several decades. These estimates suggest that the role ocean acidification will play in estuaries may be different from the open ocean.

Published by Elsevier Ltd.

1. Introduction

Over the past two-and-a-half centuries, fossil fuel burning and land-use changes associated with human activities have caused the atmospheric CO₂ concentrations to rise from 280 ppm to about 387 ppm (Le Quéré et al., 2009). Over the same time interval, the surface oceans have absorbed more than 550 billion tons of carbon dioxide from the atmosphere, or approximately 30% of the total anthropogenic carbon dioxide emissions (Canadell et al., 2007). This absorption of CO₂ from the atmosphere has benefitted

humankind significantly by reducing the greenhouse gas levels in the atmosphere (IPCC, 2007; Sabine and Feely, 2007). However, when anthropogenic CO₂ is absorbed by seawater, chemical reactions occur that reduce seawater pH, concentration of carbonate ion ([CO₃²⁻]), and the saturation states of the biominerals aragonite (Ω_{arg}) and calcite (Ω_{cal}) in a process commonly referred to as ocean acidification. The in situ degree of saturation of seawater with respect to aragonite and calcite is the product of the concentrations of calcium and carbonate ions, at the in situ temperature, salinity, and pressure, divided by the apparent stoichiometric solubility product (K_{sp}) for those conditions:

* Corresponding author.

E-mail addresses: richard.a.feely@noaa.gov (R.A. Feely), simone.r.alin@noaa.gov (S.R. Alin), newton@apl.washington.edu (J. Newton), chris.sabine@noaa.gov (C.L. Sabine), warner@u.washington.edu (M. Warner), devol@u.washington.edu (A. Devol), ckre461@ecy.wa.gov (C. Krembs), cfal461@ecy.wa.gov (C. Maloy).

$$\Omega_{\text{arg}} = [\text{Ca}^{2+}] [\text{CO}_3^{2-}] / K_{\text{sparg}}^* \quad (1)$$

$$\Omega_{\text{cal}} = [\text{Ca}^{2+}] [\text{CO}_3^{2-}] / K_{\text{spcal}}^* \quad (2)$$

where the calcium concentration is estimated from the salinity and the carbonate ion concentration is calculated from the dissolved inorganic carbon (DIC) and total alkalinity (TA) data. Since the calcium to salinity ratio in seawater does not vary by more than a few percent, variations in the ratio of $[\text{CO}_3^{2-}]$ to the stoichiometric solubility product primarily govern the degree of saturation of seawater with respect to these minerals. In general, surface seawater is supersaturated with respect to calcium carbonate minerals (i.e. $\Omega > 1$; see Feely et al., 2009). When carbonate saturation states in seawater drop below saturation ($\Omega = 1$), whether the reason for the decline in saturation is due to ocean acidification or other natural processes, carbonate biominerals in shells and skeletons may begin to dissolve, and we describe the water as “corrosive” for this reason. We reserve the term “acidified” to refer to the oceanic conditions attributable to oceanic uptake of anthropogenic CO_2 and the associated chemical changes.

Since the beginning of the industrial era, the pH of average open-ocean surface waters has decreased by about 0.1, equivalent to an overall increase in the hydrogen ion concentration or “acidity” of about 30%. By the end of this century, surface ocean pH is expected to decline by another 0.3–0.4 pH (Feely et al., 2004, 2009; Orr et al., 2005; Doney et al., 2009; Steinacher et al., 2009). In coastal regions, ocean acidification can interact with other natural and anthropogenic environmental processes to hasten local declines in pH and carbonate mineral saturation states (Feely et al., 2008; Salisbury et al., 2008; Wootton et al., 2008). The coastal region off western North America is strongly influenced by seasonal upwelling, which typically begins in early spring when the Aleutian low-pressure system moves to the northwest and the Pacific High moves northward, causing a strengthening of the northwesterly winds (Hill et al., 1998; Pennington and Chavez, 2000; Hickey and Banas, 2003). These winds drive surface waters offshore via Ekman transport, which induces the upwelling of CO_2 -rich, offshore intermediate waters onto the continental shelf from April through November (Feely et al., 2008). These acidified, oxygen-depleted waters have the potential for entering Puget Sound via the Juan de Fuca submarine canyon in the summer and fall months (Masson, 2002, 2006; Masson and Cummins, 2007; Moore et al., 2008a).

Puget Sound is a deep, fjord-type, semi-enclosed estuary in northwest Washington State that is connected to the Pacific Ocean at its northern end by the Strait of Juan de Fuca (Fig. 1). Exchange of

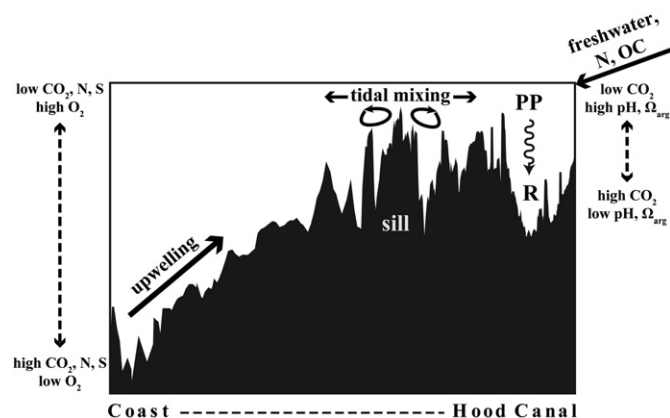


Fig. 2. Conceptual diagram illustrating processes contributing to the formation of corrosive conditions within the greater Puget Sound ecosystem. Along the coast, spring–summer upwelling brings water rich in CO_2 and nutrients (N in figure), high in salinity (S in figure), and low in O_2 close to the ocean surface and into the Strait of Juan de Fuca. Tidal mixing through the strait causes strong vertical mixing over the sills at Admiralty Inlet, where marine water flows into the Puget Sound and Hood Canal basins. Large inputs of freshwater, nutrients, and organic carbon (OC) characterize the inland portion of Puget Sound. Nutrient input stimulates primary production (PP) in surface waters. Upon sinking and decay of phytoplankton, remineralization (R) oxidizes the OC to CO_2 , which in turn lowers pH and Ω_{arg} .

waters between the strait and the four interconnected basins of Puget Sound (Whidbey, Main, Hood Canal, and South Sound) is limited by a double sill at Admiralty Inlet (Figs. 1 and 2). In the wintertime, the winds are predominately from the south and stronger than in the summer, when weaker northwesterly winds are dominant. Associated with the seasonal change in wind direction is a corresponding change over the continental shelf from downwelling in winter to upwelling in summer. Although inflow from the strait to the sound occurs episodically throughout the seasonal cycle, the deep-water inflow tends to be warmer but saltier in the summer because of upwelling along the coast (Cannon et al., 1990; Thomson, 1994; Moore et al., 2008b). Tidal currents and vertical mixing are strongest near Admiralty Inlet, where the tidal currents range from approximately 0.5 to 1.0 m s^{-1} (e.g. Geyer and Cannon, 1982).

As an estuary with ~4000 km of shoreline, Puget Sound has an extensive land–water interface, with large fluxes of freshwater, sediments, organic matter, nutrients, and pollutants entering the sound from a variety of natural and urbanized landscapes (Emmett et al., 2000). Within Puget Sound, circulation is sluggish in many of the restricted inlets of Hood Canal and South Sound so that terrestrial inputs may have relatively localized impacts. For instance, localized inputs of nitrogenous nutrients, such as are associated with development and urbanization, have been observed to stimulate enhanced primary production in surface waters in certain parts of Puget Sound with restricted circulation and developing shorelines (Newton and Van Voorhis, 2002; Simonds et al., 2008). As phytoplankton die and sink from euphotic surface waters, the organic matter they contain is remineralized back to carbon dioxide by natural respiration processes, consuming oxygen and leading to both potential hypoxia and lower pH and Ω_{arg} values in the process. Thus, bottom waters in some areas of the sound are predisposed to the occasional formation of hypoxic, corrosive conditions because of natural physical and biological processes. In Hood Canal, for example, strong stratification, slow flushing, and restricted mixing lead to hypoxic conditions (Newton et al., 2002, 2003, 2008). While hypoxia in areas such as Hood Canal is a natural condition that fluctuates with climate forcing (Brandenberger et al., 2008), these conditions may be exacerbated by anthropogenic stressors such as

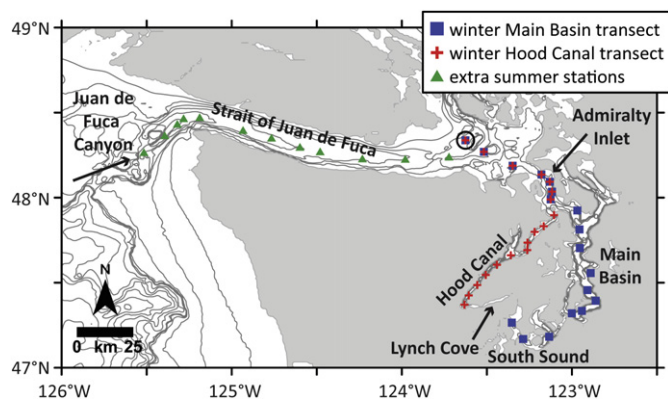


Fig. 1. Map of the study area showing the location of geographic features discussed in the text and stations used in Figs. 3 and 4. Winter 2008 transects are shown in squares and crosses. Summer 2008 transects occupied the same stations, as well as additional stations throughout the Strait of Juan de Fuca and into coastal waters, which appear as triangles. The northernmost winter station (circled in the figure) is not shown in the summer transects.

nutrient enrichment and ocean acidification. In Hood Canal, the late 1990s and early 2000s have seen particularly low oxygen concentrations with fish kill events occurring in three years since 2000, stimulating increased local evaluation of nutrient loading and its role in increased localized hypoxia (Newton et al., 2008). In this paper, we estimate the contribution of ocean acidification to the formation of the low pH subsurface waters undersaturated with respect to aragonite that we observed in Puget Sound.

2. Analytical methods

In February and August 2008, we collected water samples on two University of Washington (UW) Puget Sound Regional Synthesis Model (PRISM) cruises in the Strait of Juan de Fuca and throughout Puget Sound onboard the R/V *Thompson* and Environmental Protection Agency (EPA) Ocean Survey Vessel *Bold*, respectively. Full water column conductivity–temperature–depth rosette stations were occupied at specified locations along two transects, one along Hood Canal and the other through the Main Basin into South Sound (Figs. 1, 3, and 4). Water samples were collected on both cruises in modified Niskin-type bottles and analyzed in the laboratory for DIC, TA, oxygen, and nutrients. DIC was analyzed using coulometric titration (Johnson et al., 1985, 1987; DOE, 1994; Ono et al., 1998). TA was measured by the potentiometric titration method (Millero et al., 1993; DOE, 1994; Ono et al., 1998). Certified Reference Materials were analyzed with both the DIC and TA samples as an independent verification of instrument calibrations (Dickson et al., 2007). The DIC and TA data are accurate to within $\sim 1 \mu\text{mol kg}^{-1}$ and $\sim 2 \mu\text{mol kg}^{-1}$, respectively.

The saturation of seawater with respect to aragonite and seawater pH (on the seawater pH scale) were calculated from the DIC and TA data using the program CO2SYS developed by Lewis and Wallace (1998), using the Mehrbach et al. (1973) carbonate constants as refit by Dickson and Millero (1987). The pressure effect on the solubility is estimated from the equation of Mucci (1983), incorporating the adjustments to the constants recommended by Millero (1995). Based on the uncertainties in the DIC and TA measurements and the thermodynamic constants, the uncertainty in the calculated aragonite saturation state is approximately ± 0.02 .

Oxygen analysis was done by modified Winkler titration (Carpenter, 1965), and nutrients (nitrate, nitrite, ammonium, phosphate, silicate) were analyzed using a Technicon AutoAnalyzer II (UNESCO, 1994) at the University of Washington Marine Chemistry Laboratory.

3. Results

The wintertime (February 2008) distributions of salinity, oxygen, pH, and aragonite saturation in the Strait of Juan de Fuca, Main Basin, South Sound, and Hood Canal are shown in Fig. 3. In the winter, the entire water column of the Main Basin was well mixed with only small, primarily north–south, gradients in pH (7.71–7.75). South Sound was slightly more stratified. The entire water column from the Strait of Juan de Fuca through Main Basin to South Sound was undersaturated with respect to aragonite ($\Omega_{\text{arg}} = 0.79$ –0.95). The entire water column in Hood Canal was also undersaturated with respect to aragonite, but in contrast to the Main Basin was stratified with strong vertical and

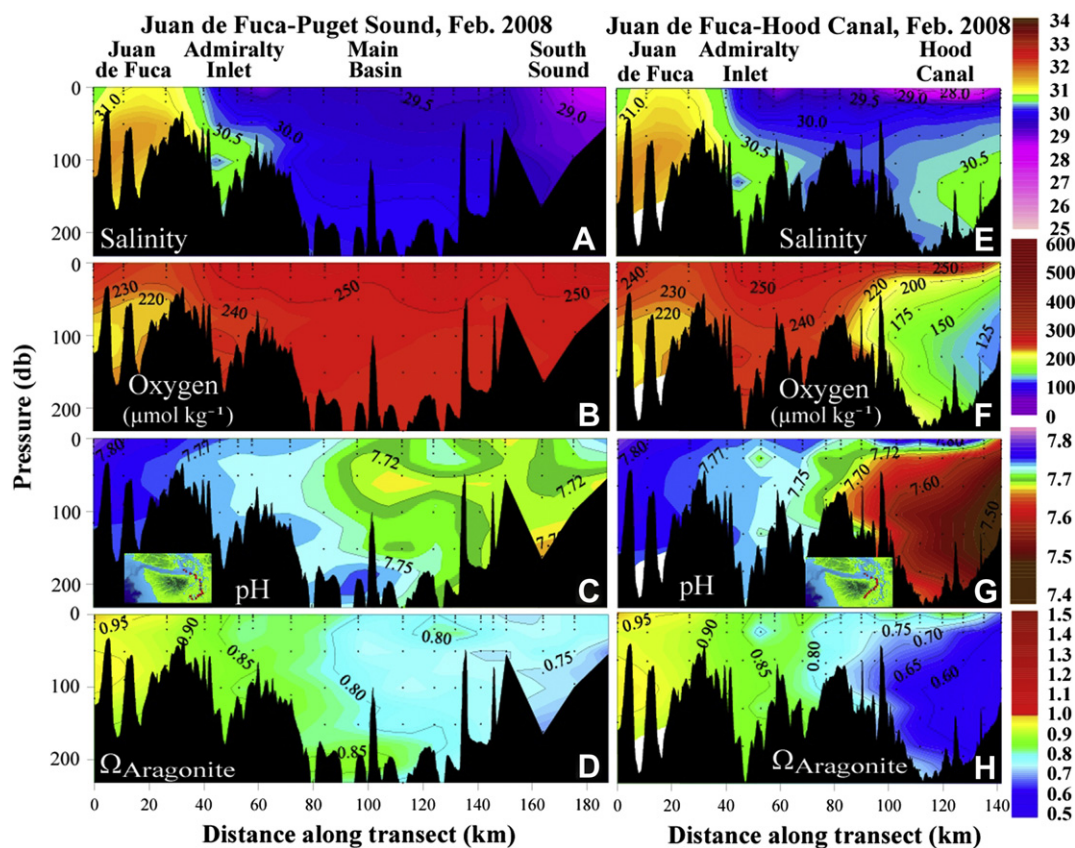


Fig. 3. Distribution of (A) salinity, (B) oxygen, (C) pH, and (D) Ω_{arg} along a transect from the Strait of Juan de Fuca through the Main Basin and into South Sound; and (E) salinity, (F) oxygen, (G) pH, and (H) Ω_{arg} from the Strait of Juan de Fuca to the southern end of Hood Canal during February 2008. Note that color scales for winter cross-sections span smaller ranges for some parameters than summer cross-sections. Black dots represent sampling depths.

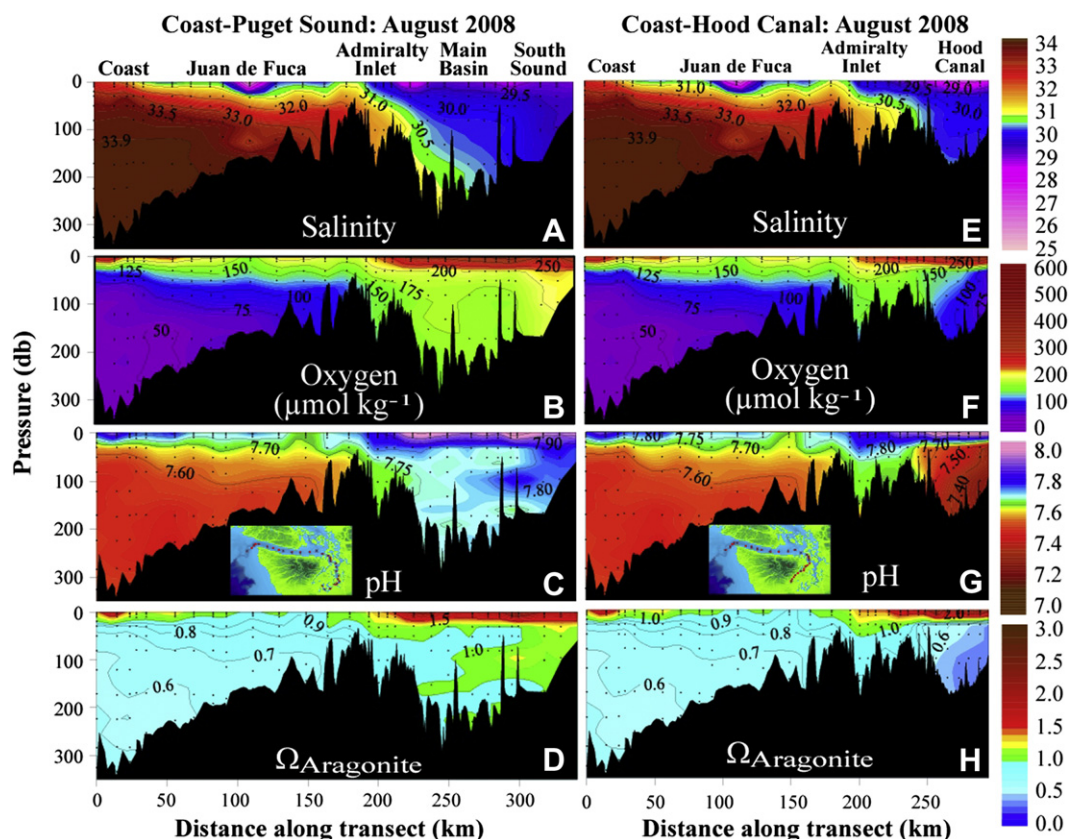


Fig. 4. Distribution of (A) salinity, (B) oxygen, (C) pH, and (D) Ω_{arg} along a transect from the coast through Puget Sound's Main Basin and into South Sound; and (E) salinity, (F) oxygen, (G) pH, and (H) Ω_{arg} on a transect from the coast to the southern end of Hood Canal during August 2008. Note that color scales for summer cross-sections span larger ranges for some parameters than winter cross-sections. Black dots represent sampling depths.

north–south gradients in salinity (27.5–30.5), pH (7.50–7.85), and Ω_{arg} values (0.50–0.85). Oxygen concentrations throughout the Main Basin and South Sound were undersaturated (oxygen saturation at observed water densities of Puget Sound waters is $\sim 280\text{--}321 \mu\text{mol kg}^{-1}$; calculated as in Garcia and Gordon, 1992), but remained substantially above the hypoxic levels ($\sim 62 \mu\text{mol kg}^{-1}$ or about $2 \text{ mg O}_2 \text{ L}^{-1}$; the common definition of hypoxia). Oxygen concentrations in Hood Canal were strongly stratified, ranged from 119 to $279 \mu\text{mol kg}^{-1}$ ($3.8\text{--}8.9 \text{ mg L}^{-1}$), and grew increasingly undersaturated with depth and proximity to the southern end of Hood Canal, where the lowest oxygen concentrations were observed. The conditions observed in winter, when the water column should mix most deeply in all areas, reflect the water column baseline for the seasonal evolution of chemical conditions from spring to fall as rates of biological processes in surface waters increase with the warming and increased stratification of the water column.

The summertime (August 2008) distributions of salinity, oxygen, pH, and aragonite saturation in the Strait of Juan de Fuca, Main Basin, South Sound, and Hood Canal are shown in Fig. 4. Low pH (< 7.75), low aragonite saturation state ($\Omega_{\text{arg}} = \sim 0.9$), high salinity (> 31.0) water undersaturated in oxygen enters the Strait of Juan de Fuca in the deeper waters and flows eastward toward Admiralty Inlet where it mixes upward due to strong tidal mixing (Fig. 2). A portion of this water returns to the mouth of the strait in the outflowing surface water, lowering pH and Ω_{arg} values to near saturation. The remaining fraction flows over the sill at Admiralty Inlet and spills into the deeper basins. The pH values of the deep waters flowing into Puget Sound over the sill range from 7.64 to

7.78, with Ω_{arg} values ranging from 0.77 to 1.05, and oxygen concentrations of $105\text{--}184 \mu\text{mol kg}^{-1}$. Outflowing surface waters at the sill have higher pH values that range from 7.75 to 7.81, with Ω_{arg} values from 0.99 to 1.12, and oxygen concentrations of $168\text{--}192 \mu\text{mol kg}^{-1}$. In the shallow surface waters (depth $< 8 \text{ m}$) of Main Basin, South Sound, and Hood Canal, the pH ranged from 7.77 to 8.25, Ω_{arg} was saturated to supersaturated everywhere (1.01–2.79), and oxygen concentrations ranged from $192 \mu\text{mol kg}^{-1}$ to $385 \mu\text{mol kg}^{-1}$. Below 50 m in the Main Basin and South Sound, the pH values were lower (7.71–7.91), the waters ranged from slightly supersaturated to undersaturated with respect to aragonite ($\Omega_{\text{arg}} = 0.86\text{--}1.35$), and oxygen concentrations ranged from 142 to $217 \mu\text{mol kg}^{-1}$. In contrast, the deep waters of Hood Canal had markedly lower pH and Ω_{arg} values and oxygen concentrations (7.32–7.75, 0.34–0.97, and $57\text{--}175 \mu\text{mol kg}^{-1}$, respectively) than the deep waters of the Main Basin. These highly corrosive waters with pH values < 7.4 and $\Omega_{\text{arg}} < 0.6$ reach as shallow a depth as 50 m in the southern part of the Hood Canal Basin. Within Puget Sound, only the deepest sample from the southernmost station in Hood Canal was hypoxic ($57 \mu\text{mol kg}^{-1} = 1.9 \text{ mg L}^{-1}$), and surface ($< 2 \text{ m}$ depth) nitrate concentrations in this area were between 0.07 and $1.36 \mu\text{mol kg}^{-1}$, indicating strong stratification and nutrient-limited phytoplankton growth. However, we were not able to sample in Lynch Cove, the arm of Hood Canal where the most severe hypoxia has previously been observed (Fig. 1), because the ship was too large to navigate there. Thus, it is possible that more extensive hypoxic conditions were present at the time that may have affected the aragonite saturation values in that arm.

4. Discussion

4.1. The contribution of ocean acidification to the corrosiveness of Puget Sound waters

Since there are no high-quality, long-term, carbon times-series measurements in Puget Sound, it is not possible to directly determine the increase of anthropogenic CO₂ in the region. However, coastal waters, which are the source for the marine waters in the Puget Sound system, carry an anthropogenic CO₂ burden, and a corresponding pH decrease associated with ocean acidification, that can be estimated by extrapolating the open-ocean CO₂ results for the North Pacific to the coastal region (Feely et al., 2008). Sabine et al. (2004) determined that the surface waters of the North Pacific were enriched in DIC by about 55–60 μmol kg⁻¹ due to the uptake of anthropogenic CO₂ since the beginning of the industrial age. This is equivalent to a pH drop of about 0.1 units. Feely et al. (2008) used the WOCE/JGOFS Global CO₂ Survey data to determine that the upwelled corrosive waters along the Pacific Northwest coast contained approximately 31 ± 4 μmol kg⁻¹ anthropogenic CO₂, corresponding to a pH decrease of ~0.05 units. However, Doney et al. (2007) used both data and model results to show that in coastal regions fossil fuel combustion and agricultural practices produce increased atmospheric inputs of strong acids (HNO₃ and H₂SO₄) and bases (NH₃) to the coastal ocean that can further reduce the pH by as much as an additional 50%. Based on these three studies, a reasonable estimate of the range of the present-day pH decrease in the Puget Sound region due to ocean acidification is between 0.05 and 0.15.

Another way to estimate the potential anthropogenic CO₂ impact on Puget Sound is to calculate how much the DIC has increased in Puget Sound, assuming that the partial pressure of CO₂ of the waters (pCO₂) has increased at the same rate as the atmosphere. Takahashi et al. (2009) examined over three million surface CO₂ observations collected over the last 40 years and found that, within the uncertainties of the estimates, surface water pCO₂ values everywhere are increasing at about the same rate as the atmosphere. Atmospheric CO₂ during the February and August 2008

Puget Sound cruises was 106 ppm and 104 ppm higher than the pre-industrial value of 280 ppm, respectively. Rising CO₂ levels do not change the total alkalinity of the waters, so a first-order estimate of the pre-industrial DIC can be made by decreasing the modern pCO₂ values by 106 or 104 ppm and calculating DIC from the TA and adjusted pCO₂ values using the CO2SYS program (Lewis and Wallace, 1998).

The estimated anthropogenic DIC increases from the pre-industrial to the present for Puget Sound surface waters ranged from 13 to 36 μmol kg⁻¹ (Table 1). This is considerably less than the estimated anthropogenic DIC increases in open-ocean waters (55–60 μmol kg⁻¹) because waters in Puget Sound have very high Revelle factors (RF) (Revelle and Suess, 1957). The RF indicates how much change in DIC would be expected with a given change in pCO₂, with high RFs corresponding to smaller changes in DIC. Modern Puget Sound RF values range from 14 to 19 (Table 1), significantly higher than open-ocean RF values, which range from 8 to about 15 (Sabine et al., 2004). RF values are higher in Puget Sound than the open ocean because the DIC to TA ratio is higher (Feely et al., 2009). Although the DIC changes are relatively small, surface water changes in pH estimated using this approach indicate pH decreases of up to 0.11 in Puget Sound since the pre-industrial era. Surface Ω_{arg} values appear to have decreased since the pre-industrial era by 0.09–0.33, with larger decreases in the summer and in the Main Basin (Table 1).

Deep-water anthropogenic DIC increases within Puget Sound from the pre-industrial to the present ranged from 7–18 μmol kg⁻¹ in the summer to 10–14 μmol kg⁻¹ in the winter (Table 1). The corresponding pre-industrial to present decreases in pH and aragonite saturation state are 0.00–0.06 and 0.02–0.09, respectively, with larger decreases in the Main Basin (Table 1). Since deep waters enter Puget Sound through Admiralty Inlet, the net biological respiration signal can be estimated by comparing the average DIC from Admiralty Inlet to the deep DIC values within each basin. Since transit times between Admiralty Inlet and the deep parts of each basin are not known, we used the average Admiralty Inlet value across all depths and both sampling seasons (2008 average DIC_{AI} = 2068 μmol kg⁻¹). Deep DIC values in Hood

Table 1
Average and standard error values for estimated pre-industrial (PI) summer and winter and measured Feb. and Aug. 2008 carbon system conditions at the mouth of the Juan de Fuca Canyon (no Feb. 2008 data or winter PI estimate), Admiralty Inlet, and in Puget Sound's Main Basin and Hood Canal.

Location	pH		Ω_{arg}		DIC (μmol kg ⁻¹)		TA (μmol kg ⁻¹)		Revelle factor	
	Surface (0–20 m)	Deep ^a	Surface (0–20 m)	Deep ^a	Surface (0–20 m)	Deep ^a	Surface (0–20 m)	Deep ^a	Surface (0–20 m)	Deep ^a
Juan de Fuca mouth										
PI – summer	7.87	7.59	1.33	0.68	2064	2254	2171	2268	15.6	18.7
Aug. 2008	7.80 ± 0.10	7.55 ± 0.01	1.19 ± 0.34	0.61 ± 0.02	2085 ± 57	2264 ± 7	2171 ± 31	2268 ± 7	16.5	18.7
Admiralty Inlet										
PI – winter	7.84	7.83	1.03	1.03	2032	2043	2107	2117	17.3	17.3
PI – summer	7.85	7.77	1.23	1.02	2034	2093	2129	2162	16.1	17.4
Feb. 2008	7.78 ± 0.01	7.77 ± 0.01	0.90 ± 0.03	0.89 ± 0.03	2050 ± 11	2061 ± 20	2107 ± 15	2117 ± 23	18.1	18.1
Aug. 2008	7.79 ± 0.02	7.72 ± 0.06	1.07 ± 0.05	0.92 ± 0.13	2053 ± 21	2108 ± 62	2129 ± 15	2162 ± 43	17.1	18.0
Main Basin										
PI – winter	7.71	7.73	0.93	0.89	1985	1987	2041	2044	17.7	17.8
PI – summer	8.05	7.83	1.89	1.16	1884	2022	2052	2111	12.6	16.4
Feb. 2008	7.74 ± 0.02	7.73 ± 0.03	0.79 ± 0.03	0.78 ± 0.04	1998 ± 4	2001 ± 6	2041 ± 6	2044 ± 8	18.2	18.2
Aug. 2008	7.95 ± 0.09	7.77 ± 0.02	1.56 ± 0.32	1.00 ± 0.04	1920 ± 48	2040 ± 8	2052 ± 20	2111 ± 9	14.2	17.3
Hood Canal										
PI – winter	7.77	7.60	0.84	0.66	1966	2076	2018	2095	18.3	18.8
PI – summer	8.01	7.41	1.73	0.42	1881	2115	2032	2080	13.3	17.6
Feb. 2008	7.72 ± 0.07	7.56 ± 0.06	0.75 ± 0.07	0.61 ± 0.06	1981 ± 49	2086 ± 18	2018 ± 38	2095 ± 6	18.9	18.8
Aug. 2008	7.90 ± 0.20	7.39 ± 0.05	1.50 ± 0.66	0.40 ± 0.05	1913 ± 97	2122 ± 18	2032 ± 31	2080 ± 6	14.7	17.3

^a Depth range for “deep” samples is >100 m in Main Basin, >75 m in Hood Canal, and >20 m at Admiralty Inlet. Depth cutoffs were chosen on the basis of relative depth and stratification in each location.

Canal, for example, were $54 \mu\text{mol kg}^{-1}$ higher than the average Admiralty Inlet value on the summer cruise and $18 \mu\text{mol kg}^{-1}$ higher during the winter cruise. This increase is taken to be the net modern respiration signal. If we compare this respiration signal to the total difference between the average pre-industrial Admiralty Inlet (PI average $\text{DIC}_{\text{AI}} = 2051 \mu\text{mol kg}^{-1}$) and modern deep Hood Canal DIC values, we see that ocean acidification accounts for 24% of the total increase in DIC due to the combination of acidification and respiration in summer and 49% in winter.

As CO_2 continues to rise in the atmosphere, the percentage contribution of anthropogenic CO_2 to the development of corrosive conditions in the deep waters of Puget Sound will likely increase with time. For instance, if we do the same calculations for a $2\times\text{CO}_2$ (560 ppm) world, calculating the expected anthropogenic DIC in the deep water of Hood Canal by adding 280 ppm to the pre-industrial pCO_2 values and using 2008 measured TA values, we estimate that $19\text{--}25 \mu\text{mol kg}^{-1}$ of anthropogenic CO_2 would be present in Hood Canal deep waters in summer and winter, respectively. Under this scenario, the estimated percentage contribution of ocean acidification to the corrosiveness forecasted for the southern end of Hood Canal increases to $49\text{--}82\%$. Of course, the uncertainty on this calculation is very high, as other changes that may occur over the intervening time were not taken into account, such as increased water temperature associated with anthropogenic climate change and its effects on biological and physical processes (e.g. Bopp et al., 2002; Hofmann and Todgham, 2010); changes in terrestrial inputs of nutrients, freshwater, and carbon linked to climate or land-use change (e.g. Borges and Gypens, 2010); or changes in marine inputs due to basin-scale changes in ocean circulation (e.g. Rykaczewski and Dunne, 2010). Nonetheless, this estimate illustrates the increased role that ocean acidification may play in a high- CO_2 world in exacerbating local or regional hotspots of corrosive conditions where the impacts of multiple stressors converge.

The calculations presented in Table 1 suggest that in pre-industrial times the waters flowing into Puget Sound at depth through Admiralty Inlet were above saturation with respect to aragonite, whereas today they are undersaturated. The deep waters of the Main Basin also experienced supersaturated waters that were not observed in the modern data. While the deep waters of Hood Canal were likely undersaturated during the pre-industrial era, the degree of undersaturation is greater today than it would have been then. However, it is difficult to estimate the uncertainty in these calculations. Coastal regions are likely to have experienced additional anthropogenic stressors compared to the open ocean, so the calculations presented here represent conservative estimates (e.g. Doney et al., 2007).

It is clear that additional measurements of the Puget Sound biogeochemistry and ecosystems are needed to document and monitor for further changes as atmospheric CO_2 continues to rise in the future. Further work is also needed to assess the role of anthropogenic nutrient inputs to generating corrosive and hypoxic conditions in Puget Sound, as previous work suggests that the effects of nutrient inputs on biological processes may be quite localized and not a significant contributor to basin-wide conditions, but that changes in the timing of inputs may be an important consideration (e.g. Simonds et al., 2008; Steinberg et al., in preparation). Previous work on the comparative effects of nutrient enrichment, eutrophication, and ocean acidification in estuaries and coastal oceans has focused on the chemical and biological effects of these processes in surface waters in regions with more significant anthropogenic nutrient loading, such as Chesapeake Bay and the Belgian coastal zone (Borges and Gypens, 2010; Waldbusser et al., in press). This study highlights the importance of considering the synergistic effects of the processes

leading to hypoxia (i.e. biological and physical processes, whether natural or anthropogenically enhanced) and ocean acidification (i.e. ocean CO_2 uptake and consequent chemical transformations) in benthic waters of estuaries and coastal oceans.

4.2. Potential impacts on marine organisms in the Puget Sound region

At the present time, a lack of biologically meaningful, field-based information from the Puget Sound region limits our understanding of how varying exposure to waters undersaturated with respect to aragonite might affect the development and survival of larval, juvenile, and adult stages of organisms that live there. Laboratory and mesocosm experiments suggest that pH and saturation state values of the observed magnitude may impair overall calcification rates for many species of marine calcifiers, including cold water corals, coccolithophorids, foraminifera, sea urchins and pteropods (Spero et al., 1997; Riebesell et al., 2000; Engel et al., 2005; Orr et al., 2005; Guinotte et al., 2006; Kleypas et al., 2006; Fabry et al., 2008; Guinotte and Fabry, 2008; Doney et al., 2009; Ries et al., 2009). Similar decreases in calcification rates would be expected for edible mussels, clams, and oysters (Green et al., 2004; Gazeau et al., 2007; Hettinger et al., 2010). Other studies suggest that some species of juvenile fish and shellfish of economic importance to coastal regions are highly sensitive to higher-than-normal CO_2 concentrations with high mortality rates at higher CO_2 concentrations (Ishimatsu et al., 2004; Gazeau et al., 2007). Over the last four years, some oyster hatcheries in the Pacific Northwest region have experienced mass mortalities of oyster larvae in association with a combination of circumstances including unusually saline surface waters and the upwelling of cold, CO_2 - and nutrient-rich waters, which contained high concentrations of the pathogenic bacteria, *Vibrio tubiashii* (Elston et al., 2008), and would also have low pH and Ω_{arg} values (e.g. Feely et al., 2008). Finally, some species of diatoms associated with harmful algal blooms are known to increase in abundance in warm, CO_2 -rich coastal waters, including diatoms from the genus *Pseudonitzschia* (Moore et al., 2008c).

In Puget Sound, as may be the case for other coastal embayments and estuaries of the Pacific Northwest and elsewhere, the impacts of lowered seawater pH and hypoxia may have a synergistic or compounding impact on organisms. Locations optimal for low oxygen levels that occur normally due to natural respiration and circulation processes in subsurface waters are also where lowered seawater pH occurs. These stressful conditions may be exacerbated by combined impacts from global, regional, and local anthropogenic processes including ocean acidification, land-use change, and nutrient enrichment. The additional pH, Ω_{arg} , and O_2 decreases associated with these anthropogenic stressors may cross critical thresholds for organisms living near the edge of their physiological tolerances and may thus appear as abrupt and major changes in the health of an ecosystem (cf. Grantham et al., 2004; Chan et al., 2008). For example, the recent rapid pH decline observed by Wootton et al. (2008) at Tatoosh Island over an 8-year period in Northwest Washington State is probably explained by a combination of factors including enhanced upwelling of waters off the Washington coast resulting from changes in regional ocean circulation as well as a smaller contribution from ocean acidification. Enhanced upwelling would cause more CO_2 -enriched and O_2 -depleted waters to be mixed upward at Admiralty Inlet and flow into the deep basins of Puget Sound as well as to be transported at the surface back out through the Strait of Juan de Fuca to Tatoosh Island (e.g. Fig. 2). The rapid decline of the large mussel populations at Tatoosh Island and the mass mortalities of oyster

larvae in the Pacific Northwest oyster hatcheries may be early indications of the kind of ecosystem changes caused by the combined effects of multiple processes and stressors interacting in a high-CO₂ world.

Estuaries face a unique status with respect to ocean acidification. The natural and anthropogenic enrichment of nutrients in estuaries may enhance the production and subsequent remineralization of organic matter leading to hypoxia and low pH waters. The input of “acidified” low pH upwelled water from the ocean combines with this process to produce very low pH conditions. Because naturally low carbonate saturation and pH levels in the North Pacific predispose the Pacific Northwest coast in general, and Puget Sound in particular, to the development of corrosive, hypoxic marine conditions, we suggest that this part of the world ocean is an important natural laboratory for studying the interactions of natural biological and physical processes with regional- to global-scale anthropogenic stressors such as urbanization and ocean acidification, respectively.

5. Conclusions

The patterns of low pH and aragonite saturation states observed in the Puget Sound estuary complex are largely the result of natural mixing, circulation, and biological processes at the present time. Ocean acidification currently plays a smaller but important role in further lowering the natural pH levels by 0.05–0.15 units, with decreases in aragonite saturation state on the order of 0.02–0.33. By the end of this century, ocean acidification may become the dominant process reducing the pH and saturation state of this large, economically important estuary. However, it may be possible to mitigate the continued development and impacts of corrosive conditions by addressing and reducing the regional-scale anthropogenic stressors that contribute to their formation, such as additional nutrient inputs associated with development and urbanization (e.g. Bricker et al., 2007; Simonds et al., 2008). While field data on the impacts of CO₂ on the local marine ecosystems of Puget Sound do not exist, laboratory and field experiments with related species of calcifying organisms suggest that there is a real cause for concern for the health of this economically important marine ecosystem. Similar processes may be causing decreases of pH and aragonite saturation states in other coastal estuaries and embayments of the Pacific Northwest and elsewhere. Further study of ocean acidification in estuaries is thus warranted because natural factors including acidic river inputs and restricted circulation can predispose these ecologically and economically important habitats toward corrosive, hypoxic conditions, and anthropogenic stressors such as nutrient enrichment may compound them.

Acknowledgments

This work was co-sponsored by the National Oceanic and Atmospheric Administration's Pacific Marine Environmental Laboratory, the University of Washington including the Puget Sound Regional Synthesis Model (PRISM), and the Washington State Department of Ecology. Work in Hood Canal was partially funded through the Hood Canal Dissolved Oxygen Program via Naval Sea Systems Command Contract #N00024-02-D-6602 Task 50. The authors wish to thank the officers and crew of the R/V *Thompson* and EPA Ocean Survey Vessel *Bold* for their assistance during the cruises and Cynthia Peacock, Geoff Lebon, Cathy Cosca, Corinne Bassin, Jill Coyle, Dana Greeley, Julia Bos, Kathy Kroglund, Amanda Gray, Megan Black, Sylvia Musielewicz, and Jennifer Nomura for their shipboard and laboratory support of this research effort. This is PMEL contribution number 3455.

References

- Bopp, L., Le Quéré, C., Heimann, M., Manning, A.C., Monfray, P., 2002. Climate-induced oceanic oxygen fluxes: implications for the contemporary carbon budget. *Global Biogeochemical Cycles* 16. doi:10.1029/2001GB001445.
- Borges, A.V., Gypens, N., 2010. Carbonate chemistry in the coastal zone responds more strongly to eutrophication than to ocean acidification. *Limnology and Oceanography* 55, 346–353.
- Brandenberger, J.M., Creclius, E.A., Louchouart, P., 2008. Historical inputs and natural recovery rates for heavy metals and organic biomarkers in Puget Sound during the 20th century. *Environmental Science & Technology* 42, 6786–6790.
- Bricker, S., Longstaff, B., Dennison, W., Jones, A., Boicourt, K., Wicks, C., Woerner, J., 2007. Effects of Nutrient Enrichment in the Nation's Estuaries: A Decade of Change. In: NOAA Coastal Ocean Program Decision Analysis, Silver Spring, MD, 328 pp.
- Canadell, J.G., Le Quere, C., Raupach, M.R., Field, C.B., Buitenhuis, E.T., Ciais, P., Conway, T.J., Gillett, N.P., Houghton, R.A., Marland, G., 2007. Contributions to accelerating atmospheric CO₂ growth from economic activity, carbon intensity, and efficiency of natural sinks. *Proceedings of the National Academy of Sciences of the United States of America* 104, 18866–18870.
- Cannon, G.A., Holbrook, J.R., Pashinski, D.J., 1990. Variations in the onset of bottom-water intrusions of the entrance sill of a fjord. *Estuaries* 13, 31–42.
- Carpenter, J.H., 1965. The Chesapeake Bay Institute technique for the Winkler dissolved oxygen method. *Limnology and Oceanography*, 141–143.
- Chan, F., Barth, J.A., Lubchenco, J., Kirincich, A., Weeks, H., Peterson, W.T., Menge, B.A., 2008. Emergence of anoxia in the California current large marine ecosystem. *Science* 319, 920.
- Dickson, A.G., Millero, F.J., 1987. A comparison of the equilibrium constants for the dissociation of carbonic acid in seawater media. *Deep-Sea Research Part A: Oceanographic Research Papers* 34, 1733–1743.
- Dickson, A.G., Sabine, C.L., Christian, J.R., 2007. Guide to Best Practices for Ocean CO₂ Measurements. In: PICES Special Publication, 3, 191 pp.
- DOE, 1994. Handbook of Methods for the Analysis of the Various Parameters of the Carbon Dioxide System in Sea Water (Version 2), ORNL/CDIAC-74.
- Doney, S.C., Fabry, V.J., Feely, R.A., Kleypas, J.A., 2009. Ocean acidification: the other CO₂ problem. *Annual Review of Marine Science* 1, 169–192.
- Doney, S.C., Mahowald, N., Lima, I., Feely, R.A., Mackenzie, F.T., Lamarque, J.F., Rasch, P.J., 2007. Impact of anthropogenic atmospheric nitrogen and sulfur deposition on ocean acidification and the inorganic carbon system. *Proceedings of the National Academy of Sciences of the United States of America* 104, 14580–14585.
- Elston, R.A., Hasegawa, H., Humphrey, K.L., Polyak, I.K., Hase, C.C., 2008. Re-emergence of *Vibrio tubiashii* in bivalve shellfish aquaculture: severity, environmental drivers, geographic extent and management. *Diseases of Aquatic Organisms* 82, 119–134.
- Emmett, R., Llansó, R., Newton, J., Thom, R., Morgan, C., Levings, C., Copping, A., Fishman, P., 2000. Geographical signatures of North American West Coast estuaries. *Estuaries* 23, 765–792.
- Engel, A., Zondervan, I., Aerts, K., Beaufort, L., Benthien, A., Chou, L., Delille, B., Gattuso, J.P., Harlay, J., Heemann, C., Hoffmann, L., Jacquet, S., Nejstgaard, J., Pizay, M.D., Rochelle-Newall, E., Schneider, U., Terbruggen, A., Riebesell, U., 2005. Testing the direct effect of CO₂ concentration on a bloom of the coccolithophorid *Emiliania huxleyi* in mesocosm experiments. *Limnology and Oceanography* 50, 493–507.
- Fabry, V.J., Seibel, B.A., Feely, R.A., Orr, J.C., 2008. Impacts of ocean acidification on marine fauna and ecosystem processes. *ICES Journal of Marine Science* 65, 414–432.
- Feely, R.A., Doney, S.C., Cooley, S.R., 2009. Ocean acidification: present conditions and future changes in a high-CO₂ world. *Oceanography* 22 (4), 36–47.
- Feely, R.A., Sabine, C.L., Hernandez-Ayon, J.M., Ianson, D., Hales, B., 2008. Evidence for upwelling of corrosive “acidified” water onto the continental shelf. *Science* 320, 1490–1492.
- Feely, R.A., Sabine, C.L., Lee, K., Berelson, W., Kleypas, J., Fabry, V.J., Millero, F.J., 2004. Impact of anthropogenic CO₂ on the CaCO₃ system in the oceans. *Science* 305, 362–366.
- Garcia, H.E., Gordon, L.I., 1992. Oxygen solubility in seawater: better fitting equations. *Limnology and Oceanography* 37, 1307–1312.
- Gazeau, F., Quiblier, C., Jansen, J.M., Gattuso, J.P., Middelburg, J.J., Heip, C.H.R., 2007. Impact of elevated CO₂ on shellfish calcification. *Geophysical Research Letters* 34.
- Geyer, W.R., Cannon, G.A., 1982. Sill processes related to deep water renewal in a fjord. *Journal of Geophysical Research* 87 (C10), 7985–7996.
- Grantham, B.A., Chan, F., Nielsen, K.J., Fox, D.S., Barth, J.A., Huyer, A., Lubchenco, J., Menge, B.A., 2004. Upwelling-driven nearshore hypoxia signals ecosystem and oceanographic changes in the northeast Pacific. *Nature* 429, 749–754.
- Green, M.A., Jones, M.E., Boudreau, C.L., Moore, R.L., Westman, B.A., 2004. Dissolution mortality of juvenile bivalves in coastal marine deposits. *Limnology and Oceanography* 49, 727–734.
- Guinotte, J.M., Fabry, V.J., 2008. Ocean acidification and its potential effects on marine ecosystems. *Year in Ecology and Conservation Biology* 2008. *Annals of the New York Academy of Sciences*, 320–342.
- Guinotte, J.M., Orr, J., Cairns, S., Freiwald, A., Morgan, L., George, R., 2006. Will human-induced changes in seawater chemistry alter the distribution of deep-sea scleractinian corals? *Frontiers in Ecology and the Environment* 4, 141–146.

- Hettinger, A., Sanford, E., Gaylord, B., Hill, T.M., Russell, A.D., Forsch, M., Page, H.N., Sato, K., 2010. Ocean acidification reduces larval and juvenile growth in the Olympia oyster (*Ostrea lurida*). EOS Transactions AGU 91 (26), Ocean Sciences Meeting Supplement, Abstract B051A-06.
- Hickey, B.M., Banas, N.S., 2003. Oceanography of the US Pacific Northwest Coastal Ocean and estuaries with application to coastal ecology. *Estuaries* 26, 1010–1031.
- Hill, E.D., Hickey, B.M., Shillington, F.A., Strub, P.T., Barton, E.D., Brink, K., 1998. Eastern boundary current systems of the world. In: Brink, K.H., Robinson, A.R. (Eds.), *The Sea*. Wiley and Sons, pp. 21–62.
- Hofmann, G.E., Todgham, A.E., 2010. Living in the now: physiological mechanisms to tolerate a rapidly changing environment. *Annual Review of Physiology* 72, 127–145.
- IPCC, 2007. Climate Change 2007: The Physical Science Basis: Contribution of Working Group I to the Fourth Assessment Report of the Intergovernmental Panel on Climate Change. Cambridge University Press, Cambridge, United Kingdom.
- Ishimatsu, A., Kikkawa, T., Hayashi, M., Lee, K.S., Kita, J., 2004. Effects of CO₂ on marine fish: larvae and adults. *Journal of Oceanography* 60, 731–741.
- Johnson, K.M., King, A.E., Sieburth, J.M., 1985. Coulometric DIC analyses for marine studies: an introduction. *Marine Chemistry*, 61–82.
- Johnson, K.M., Sieburth, J.M., Williams, P.J.L., Brandstrom, L., 1987. Coulometric total carbon-dioxide analysis for marine studies – automation and calibration. *Marine Chemistry* 21, 117–133.
- Kluydas, J.A., Feely, R.A., Fabry, V.J., Langdon, C., Sabine, C.L., Robbins, L.L., 2006. Impacts of Increasing Ocean Acidification on Coral Reefs and Other Marine Calcifiers: A Guide for Future Research. Report of a Workshop Held 18–20 April 2005, St. Petersburg, FL. Sponsored by NSF, NOAA, and the U.S. Geological Survey, 90 pp.
- Le Quéré, C., Raupach, M.R., Canadell, J.G., Marland, G., Bopp, L., Ciais, P., Conway, T.J., Doney, S.C., Feely, R.A., Foster, P., Friedlingstein, P., Gurney, K., Houghton, R.A., House, J.I., Huntingford, C., Levy, P.E., Lomas, M.R., Majkut, J., Metzl, N., Ometto, J.P., Peters, G.P., Prentice, I.C., Randerson, J.T., Running, S.W., Sarmiento, J.L., Schuster, U., Sitch, S., Takahashi, T., Viovy, N., van der Werf, G.R., Woodward, F.I., 2009. Trends in the sources and sinks of carbon dioxide. *Nature Geoscience* 2, 831–836. doi:10.1038/ngeo689.
- Lewis, E., Wallace, D.W.R., 1998. Program Developed for CO₂ System Calculations. ORNL/CDIAC-105. Carbon Dioxide Information Analysis Center, Oak Ridge National Laboratory, U.S. Department of Energy, Oak Ridge, Tennessee.
- Masson, D., 2002. Deep water renewal in the Strait of Georgia. *Estuarine, Coastal and Shelf Science* 54, 115–126.
- Masson, D., 2006. Seasonal water mass analysis for the Straits of Juan de Fuca and Georgia. *Atmosphere-Ocean* 44, 1–15.
- Masson, D., Cummins, P.F., 2007. Temperature trends and interannual variability in the Strait of Georgia, British Columbia. *Continental Shelf Research* 27, 634–649.
- Mehrbach, C., Culbertson, C.H., Hawley, J.E., Pytkowicz, R.M., 1973. Measurement of apparent dissociation constants of carbonic acid in seawater at atmospheric pressure. *Limnology and Oceanography* 18, 897–907.
- Millero, F.J., 1995. Thermodynamics of the carbon-dioxide system in the oceans. *Geochimica et Cosmochimica Acta* 59, 661–677.
- Millero, F.J., Zhang, J.Z., Lee, K., Campbell, D.M., 1993. Titration alkalinity of seawater. *Marine Chemistry* 44, 153–165.
- Moore, S.K., Mantua, N.J., Kellogg, J.P., Newton, J.A., 2008a. Local and large-scale climate forcing of Puget Sound oceanographic properties on seasonal to inter-decadal timescales. *Limnology and Oceanography* 53, 1746–1758.
- Moore, S.K., Mantua, N.J., Newton, J.A., Kawase, M., Warner, M.J., Kellogg, J.R., 2008b. A descriptive analysis of temporal and spatial patterns of variability in Puget Sound oceanographic properties. *Estuarine, Coastal and Shelf Science* 80, 545–554.
- Moore, S.K., Trainer, V.L., Mantua, N.J., Parker, M.S., Laws, E.A., Backer, L.C., Fleming, L.E., 2008c. Impacts of climate variability and future climate change on harmful algal blooms and human health. *Environmental Health* 7.
- Mucci, A., 1983. The solubility of calcite and aragonite in seawater at various salinities, temperatures, and one atmosphere total pressure. *American Journal of Science* 283, 780–799.
- Newton, J., Van Voorhis, K., 2002. Seasonal Patterns and Controlling Factors of Primary Production in Puget Sound's Central Basin and Possession Sound. Publication #02-03-059. Washington State Department of Ecology, Environmental Assessment Program, Olympia, Washington.
- Newton, J., Bassin, C., Devol, A., Kawase, M., Ruef, W., Warner, M., Hannafous, D., Rose, R., 2008. Hypoxia in Hood Canal: an overview of status and contributing factors. In: Proceedings of the 2007 Georgia Basin Puget Sound Research Conference.
- Newton, J.A., Siegel, E., Albertson, S.L., 2003. Oceanographic changes in Puget Sound and the Strait of Juan de Fuca during the 2000–01 drought. *Canadian Water Resources Journal* 28, 715–728.
- Newton, J.A., Albertson, S.L., Van Voorhis, K., Maloy, C., Siegel, E., 2002. Washington State Marine Water Quality in 1998 Through 2000. Publication #02-03-056. Washington State Department of Ecology, Environmental Assessment Program, Olympia, Washington.
- Ono, T., Watanabe, S., Okuda, K., Fukasawa, M., 1998. Distribution of total carbonate and related properties in the North Pacific along 30°N. *Journal of Geophysical Research – Oceans* 103, 30873–30883.
- Orr, J.C., Fabry, V.J., Aumont, O., Bopp, L., Doney, S.C., Feely, R.A., Gnanadesikan, A., Gruber, N., Ishida, A., Joos, F., Key, R.M., Lindsay, K., Maier-Reimer, E., Matear, R., Monfray, P., Mouchet, A., Najjar, R.G., Plattner, G.K., Rodgers, K.B., Sabine, C.L., Sarmiento, J.L., Schlitzer, R., Slater, R.D., Totterdell, I.J., Weirig, M.F., Yamanaka, Y., Yool, A., 2005. Anthropogenic ocean acidification over the twenty-first century and its impact on calcifying organisms. *Nature* 437, 681–686.
- Pennington, J.T., Chavez, F.P., 2000. Seasonal fluctuations of temperature, salinity, nitrate, chlorophyll and primary production at station H3/M1 over 1989–1996 in Monterey Bay, California. Deep-Sea Research Part II: Topical Studies in Oceanography 47, 947–973.
- Revelle, R., Suess, H.E., 1957. Carbon dioxide exchange between atmosphere and ocean and the question of an increase of atmospheric CO₂ during the past decades. *Tellus* 9, 18–27.
- Riebesell, U., Zondervan, I., Rost, B., Tortell, P.D., Zeebe, R.E., Morel, F.M.M., 2000. Reduced calcification of marine plankton in response to increased atmospheric CO₂. *Nature* 407, 364–367.
- Ries, J.B., Cohen, A.L., McCorkle, D.C., 2009. Marine calcifiers exhibit mixed responses to CO₂-induced ocean acidification. *Geology* 37, 1131–1134.
- Rykaczewski, R.R., Dunne, J.P., 2010. Variation in the relationship among temperature, nutrient concentration, and productivity with climate change in the California Current ecosystem. EOS Transactions AGU 91 (26), Ocean Sciences Meeting Supplement, Abstract IT41B-04.
- Sabine, C.L., Feely, R.A., 2007. The oceanic sink for carbon dioxide. In: Reay, D., Hewitt, N., Grace, J., Smith, K. (Eds.), *Greenhouse Gas Sinks*. CABI Publishing, Oxfordshire, UK, pp. 31–49.
- Sabine, C.L., Feely, R.A., Gruber, N., Key, R.M., Lee, K., Bullister, J.L., Wanninkhof, R., Wong, C.S., Wallace, D.W.R., Tilbrook, B., Millero, F.J., Peng, T.H., Kozyr, A., Ono, T., Rios, A.F., 2004. The oceanic sink for anthropogenic CO₂. *Science* 305, 367–371.
- Salisbury, J., Green, M., Hunt, C., Campbell, J., 2008. Coastal acidification by rivers: a threat to shellfish? *EOS* 89, 513–528.
- Simonds, F.W., Swarzenski, P.W., Rosenberry, D.O., Reich, C.D., Paulson, A.J., 2008. Estimates of Nutrient Loading by Ground-water Discharge into the Lynch Cove Area of Hood Canal, Washington, 2008-5078.
- Spero, H.J., Bijma, J., Lea, D.W., Bemis, B.E., 1997. Effect of seawater carbonate concentration on foraminiferal carbon and oxygen isotopes. *Nature* 390, 497–500.
- Steinacher, M., Joos, F., Frolicher, T.L., Plattner, G.-K., Doney, S.C., 2009. Imminent ocean acidification in the Arctic projected with the NCAR global coupled carbon cycle-climate model. *Biogeosciences* 6, 515–533.
- Steinberg, P.D., Brett, M.T., Bechtold, J.S., Richey, J.E., McGeoch, L.E., Osborne, S.N. The influence of watershed characteristics on nitrogen export to and marine fate in Hood Canal, Washington, USA. *Biogeochemistry*, in preparation.
- Takahashi, T., Sutherland, S.C., Wanninkhof, R., Sweeney, C., Feely, R.A., Chipman, D.W., Hales, B., Friederich, G., Chavez, F., Sabine, C., Watson, A., Bakker, D.C.E., Schuster, U., Metzl, N., Yoshikawa-Inoue, H., Ishii, M., Midorikawa, T., Nojiri, Y., Körtinger, A., Steinhoff, T., Hoppema, M., Olafsson, J., Arnarson, T.S., Tilbrook, B., Johannessen, T., Olsen, A., Bellerby, R., Wong, C.S., Delille, B., Bates, N.R., de Baar, H.J.W., 2009. Climatological mean and decadal change in surface ocean pCO₂, and net sea–air CO₂ flux over the global oceans. Deep-Sea Research Part II: Topical Studies in Oceanography 56, 554–577.
- Thomson, R.E., 1994. Physical oceanography of the Strait of Georgia–Puget Sound–Juan de Fuca Strait system. In: Wilson, R., Beamish, R., Aitkens, F., Bell, J. (Eds.), *Proceedings of the BC/Washington Symposium on the Marine Environment*. Review of the Marine Environment and Biota of Strait of Georgia, Puget Sound and Juan de Fuca Strait.
- UNESCO, 1994. Protocols for the Joint Global Ocean Flux Study (JGOFS) Core Measurements. United Nations Educational, Scientific, and Cultural Organization.
- Waldbusser, G.G., Voigt, E.P., Bergschneider, H., Green, M.A., Newell, R.I.E. Long-term trends in Chesapeake Bay pH and effects on biocalcification in the Eastern Oyster *Crassostrea virginica*. *Estuaries and Coasts*, in press.
- Wootton, J.T., Pfister, C.A., Forester, J.D., 2008. Dynamic patterns and ecological impacts of declining ocean pH in a high-resolution multi-year dataset. *Proceedings of the National Academy of Sciences of the United States of America* 105, 18848–18853.

Evidence for Upwelling of Corrosive “Acidified” Water onto the Continental Shelf

Richard A. Feely,^{1*} Christopher L. Sabine,¹ J. Martin Hernandez-Ayon,² Debby Ianson,³ Burke Hales⁴

The absorption of atmospheric carbon dioxide (CO₂) into the ocean lowers the pH of the waters. This so-called ocean acidification could have important consequences for marine ecosystems. To better understand the extent of this ocean acidification in coastal waters, we conducted hydrographic surveys along the continental shelf of western North America from central Canada to northern Mexico. We observed seawater that is undersaturated with respect to aragonite upwelling onto large portions of the continental shelf, reaching depths of ~40 to 120 meters along most transect lines and all the way to the surface on one transect off northern California. Although seasonal upwelling of the undersaturated waters onto the shelf is a natural phenomenon in this region, the ocean uptake of anthropogenic CO₂ has increased the areal extent of the affected area.

Over the past 250 years, the release of carbon dioxide (CO₂) from industrial and agricultural activities has resulted in atmospheric CO₂ concentrations that have increased by about 100 parts per million (ppm). The atmospheric concentration of CO₂ is now higher than it has been for at least the past 650,000 years, and is expected to continue to rise at an increasing rate, leading to pronounced changes in our climate by the end of this century (1). Since the beginning of the industrial era, the oceans have absorbed ~127 ± 18 billion metric tons of carbon as CO₂ from the atmosphere, or about one-third of the anthropogenic carbon emissions released (2). This process of absorption of anthropogenic CO₂ has benefited humankind by substantially reducing the greenhouse gas concentrations in the atmosphere and minimizing some of the impacts of global warming. However, the ocean's daily uptake of 22 million metric tons of CO₂ has a sizable impact on its chemistry and biology. Recent hydrographic surveys and modeling studies have confirmed that the uptake of anthropogenic CO₂ by the oceans has resulted in a lowering of seawater pH by about 0.1 since the beginning of the industrial revolution (3–7). In the coming decades, this phenomenon, called “ocean acidification,” could affect some of the most fundamental biological and geochemical processes of the sea and seriously alter the fundamental structure of pelagic and benthic ecosystems (8).

Estimates of future atmospheric and oceanic CO₂ concentrations, based on the Intergovernmental Panel on Climate Change (IPCC) CO₂ emission scenarios and general circulation models, indicate

that atmospheric CO₂ concentrations could exceed 500 ppm by the middle of this century, and 800 ppm near the end of the century. This increase would

result in a decrease in surface-water pH of ~0.4 by the end of the century, and a corresponding 50% decrease in carbonate ion concentration (5, 9). Such rapid changes are likely to negatively affect marine ecosystems, seriously jeopardizing the multifaceted economies that currently depend on them (10).

The reaction of CO₂ with seawater reduces the availability of carbonate ions that are necessary for calcium carbonate (CaCO₃) skeleton and shell formation for marine organisms such as corals, marine plankton, and shellfish. The extent to which the organisms are affected depends largely on the CaCO₃ saturation state (Ω), which is the product of the concentrations of Ca²⁺ and CO₃²⁻ divided by the apparent stoichiometric solubility product for either aragonite or calcite:

$$\Omega_{\text{arag}} = [\text{Ca}^{2+}][\text{CO}_3^{2-}]/K'_{\text{sp,arag}} \quad (1)$$

$$\Omega_{\text{cal}} = [\text{Ca}^{2+}][\text{CO}_3^{2-}]/K'_{\text{sp,cal}} \quad (2)$$

where the calcium concentration is estimated from the salinity, and the carbonate ion con-

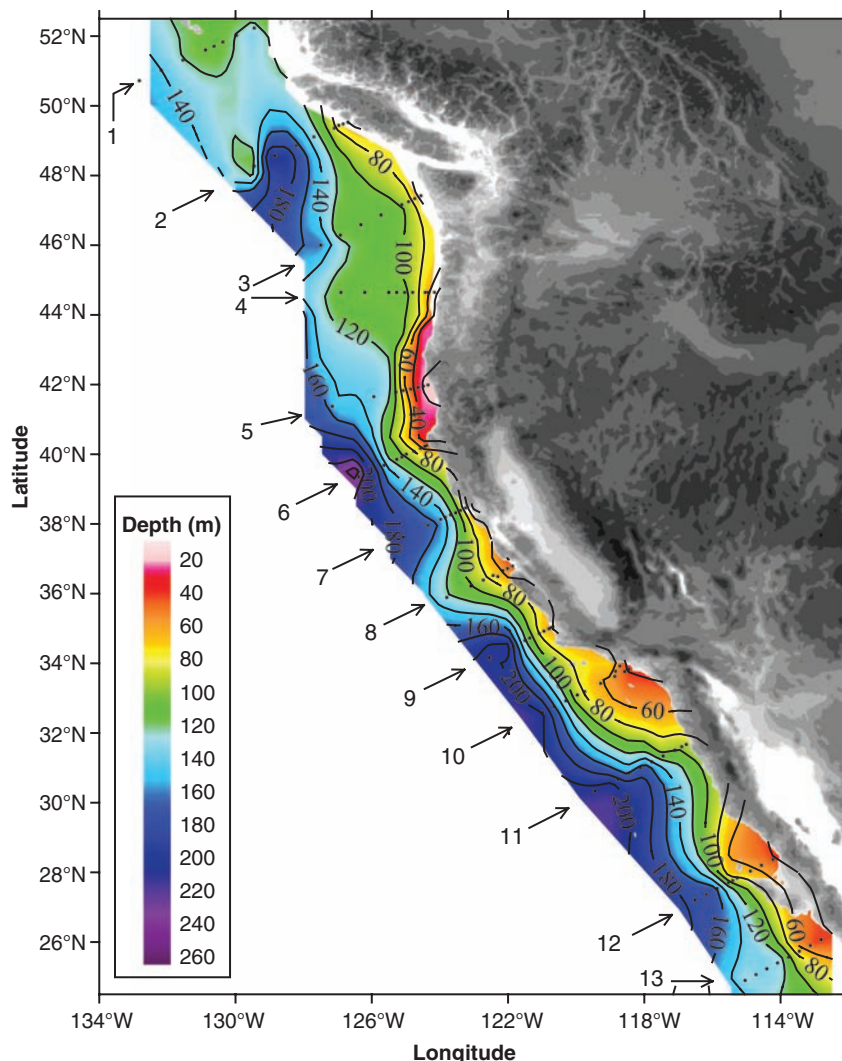


Fig. 1. Distribution of the depths of the undersaturated water (aragonite saturation < 1.0; pH < 7.75) on the continental shelf of western North America from Queen Charlotte Sound, Canada, to San Gregorio Baja California Sur, Mexico. On transect line 5, the corrosive water reaches all the way to the surface in the inshore waters near the coast. The black dots represent station locations.

¹Pacific Marine Environmental Laboratory/National Oceanic and Atmospheric Administration, 7600 Sand Point Way NE, Seattle, WA 98115–6349, USA. ²Instituto de Investigaciones Oceanológicas, Universidad Autónoma de Baja California, Km. 103 Carr. Tijuana-Ensenada, Ensenada, Baja California, Mexico. ³Fisheries and Oceans Canada, Institute of Ocean Science, Post Office Box 6000, Sidney, BC V8L 4B2, Canada. ⁴College of Oceanic and Atmospheric Sciences, Oregon State University, 104 Ocean Administration Building, Corvallis, OR 97331–5503, USA.

*To whom correspondence should be addressed. E-mail: richard.a.feely@noaa.gov

centration is calculated from the dissolved inorganic carbon (DIC) and total alkalinity (TA) measurements (11). In regions where Ω_{arag} or Ω_{cal} is > 1.0 , the formation of shells and skeletons is favored. Below a value of 1.0, the water is corrosive and dissolution of pure aragonite and unprotected aragonite shells will begin to occur (12). Recent studies have shown that in many regions of the ocean, the aragonite saturation horizon shoaled as much as 40 to 200 m as a direct consequence of the uptake of anthropogenic CO_2 (3, 5, 6). It is shallowest in the northeastern Pacific Ocean, only 100 to 300 m from the ocean

surface, allowing for the transport of under-saturated waters onto the continental shelf during periods of upwelling.

In May and June 2007, we conducted the North American Carbon Program (NACP) West Coast Cruise on the Research Ship *Wecoma* along the continental shelf of western North America, completing a series of 13 cross-shelf transects from Queen Charlotte Sound, Canada, to San Gregorio Baja California Sur, Mexico (Fig. 1). Full water column conductivity-temperature-depth rosette stations were occupied at specified locations along each transect (Fig. 1). Water samples were

collected in modified Niskin-type bottles and analyzed for DIC, TA, oxygen, nutrients, and dissolved and particulate organic carbon. Aragonite and calcite saturation, seawater pH (pH_{SW}), and partial pressure of CO_2 ($p\text{CO}_2$) were calculated from the DIC and TA data (11).

The central and southern coastal region off western North America is strongly influenced by seasonal upwelling, which typically begins in early spring when the Aleutian low-pressure system moves to the northwest and the Pacific High moves northward, resulting in a strengthening of the northwesterly winds (13, 14). These winds drive net surface-water Ekman transport offshore, which induces the upwelling of CO_2 -rich, intermediate-depth (100 to 200 m) offshore waters onto the continental shelf. The upwelling lasts until late summer or fall, when winter storms return.

During the cruise, various stages and strengths of upwelling were observed from line 2 off central Vancouver Island to line 11 off Baja California, Mexico. We observed recent upwelling on lines 5 and 6 near the Oregon-California border. Coincident with the upwelled waters, we found evidence for undersaturated, low-pH seawater in the bottom waters as depicted by Ω_{arag} values < 1.0 and pH values < 7.75 . The corrosive waters reached mid-shelf depths of ~ 40 to 120 m along lines 2 to 4 and lines 7 to 13 (Fig. 1). In the region of the strongest upwelling (line 5), the isolines of $\Omega_{\text{arag}} = 1.0$, DIC = 2190, and pH = 7.75 closely followed the 26.2 potential density surface (Fig. 2). This density surface shoaled from a depth of ~ 150 m in the offshore waters and breached the surface over the shelf near the 100-m bottom contour, ~ 40 km from the coast. This shoaling of the density surfaces and CO_2 -rich waters as one approaches land is typical of strong coastal upwelling conditions (15–18). The surface-water $p\text{CO}_2$ on the 26.2 potential density surface was about 850 μatm near the shelfbreak and higher inshore (Fig. 2), possibly enhanced by respiration processes on the shelf (17). These results indicate that the upwelling process caused the entire water column shoreward of the 50-m bottom contour to become undersaturated with respect to aragonite, a condition that was not predicted to occur in open-ocean surface waters until 2050 (5). On line 6, the next transect south, the undersaturated water was close to the surface at ~ 22 km from the coast. The lowest Ω_{arag} values (< 0.60) observed in the near-bottom waters of the continental shelf corresponded with pH values close to 7.6. Because the calcite saturation horizon is located between 225 and 400 m in this part of the northeastern Pacific (19), it is still too deep to shoal onto the continental shelf. Nevertheless, the calcite saturations values drop in the core of the upwelled water ($\Omega_{\text{cal}} < 1.3$).

As noted, the North Pacific aragonite saturation horizons are among the shallowest in the global ocean (3). The uptake of anthropogenic CO_2 has caused these horizons to shoal by 50 to 100 m since preindustrial times so that they are within the density layers that are currently being upwelled along the west coast of North America.

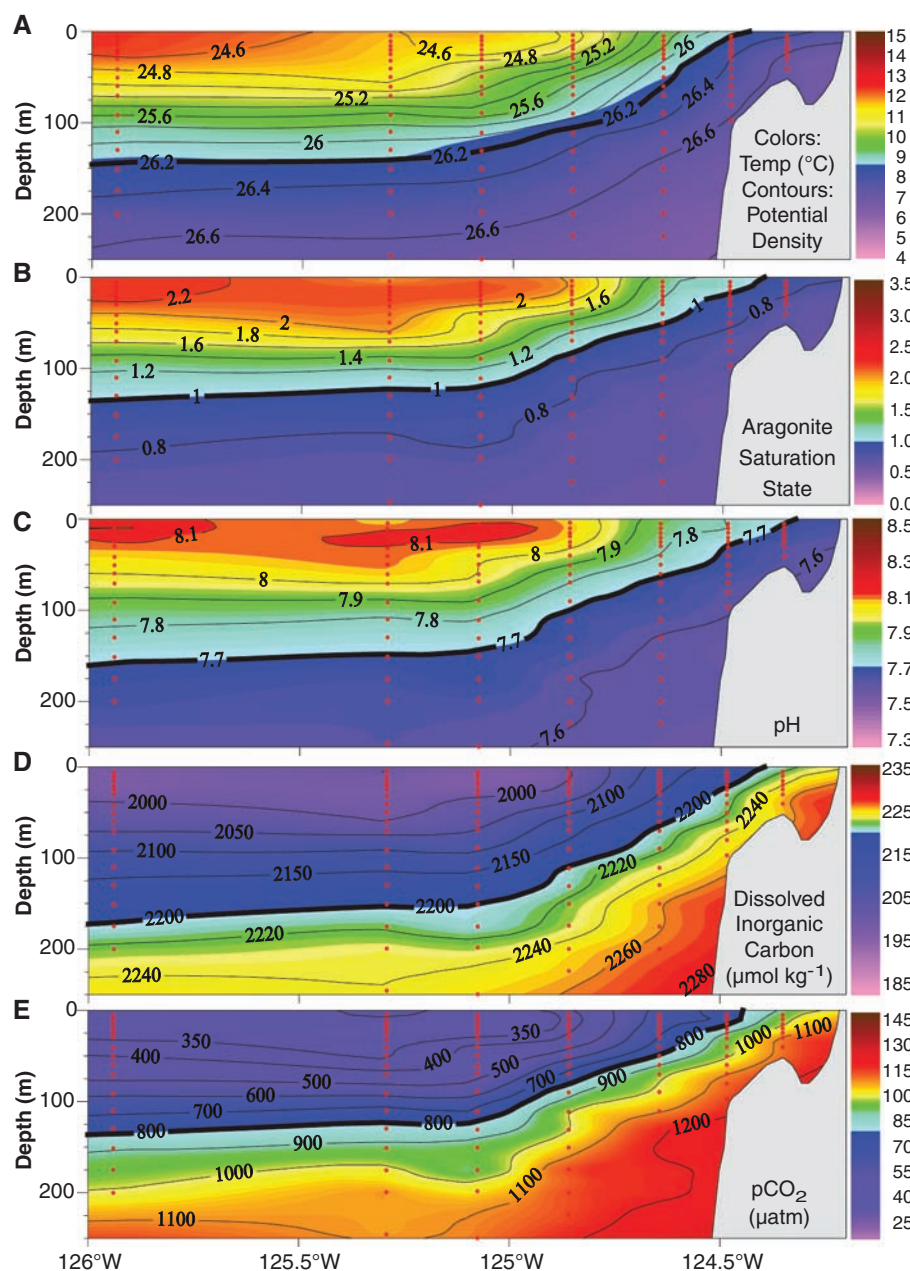


Fig. 2. Vertical sections of (A) temperature, (B) aragonite saturation, (C) pH, (D) DIC, and (E) $p\text{CO}_2$ on transect line 5 off Pt. St. George, California. The potential density surfaces are superimposed on the temperature section. The 26.2 potential density surface delineates the location of the first instance in which the undersaturated water is upwelled from depths of 150 to 200 m onto the shelf and outcropping at the surface near the coast. The red dots represent sample locations.

Although much of the corrosive character of these waters is the natural result of respiration processes at intermediate depths below the euphotic zone, this region continues to accumulate more anthropogenic CO₂ and, therefore, the upwelling processes will expose coastal organisms living in the water column or at the sea floor to less saturated waters, exacerbating the biological impacts of ocean acidification.

On the basis of our observed O₂ values and estimated O₂ consumption rates on the same density surfaces (18–20), the upwelled water off northern California (line 5) was last at the surface about 50 years ago, when atmospheric CO₂ was about 65 ppm lower than it is today. The open-ocean anthropogenic CO₂ distributions in the Pacific have been estimated previously (4, 19, 21). By determining the density dependence of anthropogenic CO₂ distributions in the eastern-most North Pacific stations of the Sabine *et al.* (21) data set, we estimate that these upwelled waters contain $\sim 31 \pm 4 \mu\text{mol kg}^{-1}$ anthropogenic CO₂ (fig. S2). Removing this signal from the DIC increases the aragonite saturation state of the waters by about 0.2 units. Thus, without the anthropogenic signal, the equilibrium aragonite saturation level ($\Omega_{\text{arag}} = 1$) would be deeper by about 50 m across the shelf, and no undersaturated waters would reach the surface. Water already in transit to upwelling centers carries increasing anthropogenic CO₂ and more corrosive conditions to the coastal oceans of the future. Thus, the undersaturated waters, which were mostly a problem for benthic communities in the deeper waters near the shelf break in the preindustrial era, have shoaled closer to the surface and near the coast because of the additional inputs of anthropogenic CO₂.

These observations clearly show that seasonal upwelling processes enhance the advancement of the corrosive deep water into broad regions of the North American western continental shelf. Because the region experiences seasonal periods of enhanced aragonite undersaturation, it is important to understand how the indigenous organisms deal with this exposure and whether future increases in the range and intensity of the corrosiveness will affect their survivorship. Presently, little is known about how this intermittent exposure to corrosive water might affect the development of larval, juvenile, and adult stages of aragonitic calcifying organisms or finfish that populate the neritic and benthic environments in this region and fuel a thriving economy. Laboratory and mesocosm experiments show that these changes in saturation state may cause substantial changes in overall calcification rates for many species of marine calcifiers including corals, coccolithophores, foraminifera, and pteropods, which are a major food source for local juvenile salmon (8, 22–30). Similar decreases in calcification rates would be expected for edible mussels, clams, and oysters (22, 31). Other research indicates that many species of juvenile fish and shellfish of economic importance to coastal regions are highly sensitive to higher-than-normal CO₂ concentrations such that high rates of mortality are directly correlated with the higher CO₂ concentrations (31, 32). Although comprehensive field studies of organisms and their response to sporadic

increases in CO₂ along the western North American coast are lacking, current studies suggest that further research under field conditions is warranted. Our results show that a large section of the North American continental shelf is affected by ocean acidification. Other continental shelf regions may also be affected where anthropogenic CO₂-enriched water is being upwelled onto the shelf.

References and Notes

- U. Siegenthaler *et al.*, *Science* **310**, 1313 (2005).
- C. L. Sabine, R. A. Feely, in *Greenhouse Gas Sinks*, D. Reay, N. Hewitt, J. Grace, K. Smith, Eds. (CABI, Oxfordshire, UK, 2007).
- R. A. Feely *et al.*, *Science* **305**, 362 (2004).
- C. L. Sabine *et al.*, *Science* **305**, 367 (2004).
- J. C. Orr *et al.*, *Nature* **437**, 681 (2005).
- K. Caldeira, M. E. Wickett, *J. Geophys. Res. Oceans* **110**, 365 (2005).
- R. A. Feely *et al.*, *PICES Press* **16**, 22 (2008).
- J. A. Kleypas *et al.*, "Impacts of Increasing Ocean Acidification on Coral Reefs and Other Marine Calcifiers: A Guide for Future Research," report of a workshop held 18 to 20 April 2005, St. Petersburg, FL, sponsored by NSF, NOAA, and the U.S. Geological Survey (2006).
- S. Solomon *et al.*, Eds, in *Contribution of Working Group I to the Fourth Assessment Report of the Intergovernmental Panel on Climate Change* (Cambridge Univ. Press, Cambridge and New York, 2007).
- J. Raven *et al.*, "Ocean acidification due to increasing atmospheric carbon dioxide," policy document 12/05 (The Royal Society, London, 2005).
- The details of the analytical methods and calculations for the carbonate system and anthropogenic CO₂ are given in the supporting online material.
- R. A. Feely *et al.*, *Mar. Chem.* **25**, 227 (1988).
- B. Hickey, in *The Sea*, A. R. Robinson, K. H. Brink, Eds. (Wiley, New York, 1998), vol. 2.
- J. Timothy Pennington, F. P. Chavez, *Deep Sea Res. Part II Top. Stud. Oceanogr.* **47**, 947 (2000).
- A. van Geen *et al.*, *Deep Sea Res. Part II Top. Stud. Oceanogr.* **47**, 975 (2000).
- G. E. Friederich, P. M. Walz, M. G. Burczynski, F. P. Chavez, *Prog. Oceanogr.* **54**, 185 (2002).
- D. Ianson *et al.*, *Deep Sea Res. Part I Oceanogr. Res. Pap.* **50**, 1023 (2003).
- B. Hales *et al.*, *Global Biogeochem. Cycles* **19**, 10.1029/2004GB002295 (2005).
- R. A. Feely *et al.*, *Global Biogeochem. Cycles* **16**, 1144 (2002).
- R. A. Feely *et al.*, *J. Oceanogr.* **60**, 45 (2004).
- C. L. Sabine *et al.*, *Global Biogeochem. Cycles* **16**, 1083 (2002).
- M. A. Green, M. E. Jones, C. L. Boudreau, R. L. Moore, B. A. Westman, *Limnol. Oceanogr.* **49**, 727 (2004).
- J. M. Guinotte *et al.*, *Coral Reefs* **22**, 551 (2003).
- C. Langdon, M. J. Atkinson, *J. Geophys. Res. Oceans* **110**, C09S07 (2005).
- H. J. Spero *et al.*, *Nature* **390**, 497 (1997).
- U. Riebesell *et al.*, *Nature* **407**, 364 (2000).
- I. Zondervan *et al.*, *Global Biogeochem. Cycles* **15**, 507 (2001).
- B. A. Seibel, V. J. Fabry, *Adv. Appl. Biodivers. Sci.* **4**, 59 (2003).
- B. Delille *et al.*, *Global Biogeochem. Cycles* **19**, GB2023 (2005).
- A. Engel *et al.*, *Limnol. Oceanogr.* **50**, 493 (2005).
- F. Gazeau *et al.*, *Geophys. Res. Lett.* **34**, L07603 (2007).
- A. Ishimatsu *et al.*, *J. Oceanogr.* **60**, 731 (2004).
- We thank Captain Richard Verlini and the crew of the *R/V Wecoma* for logistics support. We also thank D. Greeley, D. Wisegarver, P. Covert, and S. Barry for the DIC and TA measurements. Financial support for this work was provided by the National Oceanic and Atmospheric Administration's Global Carbon Cycle Program and the National Aeronautical and Space Administration Ocean Biology and Biogeochemistry Program.

Supporting Online Material

www.sciencemag.org/cgi/content/full/1155676/DC1
Materials and Methods
Figs. S1 and S2
References

25 January 2008; accepted 13 May 2008

Published online 22 May 2008;

10.1126/science.1155676

Include this information when citing this paper.

Regulation of Hepatic Lipogenesis by the Transcription Factor XBP1

Ann-Hwee Lee,^{1*} Erez F. Scapa,^{2,3} David E. Cohen,^{2,3} Laurie H. Glimcher^{1,2*}

Dietary carbohydrates regulate hepatic lipogenesis by controlling the expression of critical enzymes in glycolytic and lipogenic pathways. We found that the transcription factor XBP1, a key regulator of the unfolded protein response, is required for the unrelated function of normal fatty acid synthesis in the liver. XBP1 protein expression in mice was elevated after feeding carbohydrates and corresponded with the induction of critical genes involved in fatty acid synthesis. Inducible, selective deletion of XBP1 in the liver resulted in marked hypocholesterolemia and hypotriglyceridemia, secondary to a decreased production of lipids from the liver. This phenotype was not accompanied by hepatic steatosis or compromise in protein secretory function. The identification of XBP1 as a regulator of lipogenesis has important implications for human dyslipidemias.

Hepatic lipid synthesis increases upon ingestion of excess carbohydrates, which are converted into triglyceride (TG) in the liver and transported to adipose tissue for energy storage. Dysregulation of hepatic lipid metabolism is closely related to the development of metabolic syndrome, a condition characterized by central obesity, dyslipidemia, elevated blood glucose, and hypertension (1). In mammals, hepatic lipid metabolism is controlled by transcription factors, such as liver X receptor (LXR), sterol

regulatory element-binding proteins (SREBPs), and carbohydrate response element-binding protein (ChREBP), that regulate the expression of

¹Department of Immunology and Infectious Diseases, Harvard School of Public Health, Boston, MA 02115, USA. ²Department of Medicine, Harvard Medical School, Boston, MA 02115, USA. ³Division of Gastroenterology, Brigham and Women's Hospital, Boston, MA 02115, USA.

*To whom correspondence should be addressed. E-mail: lglimche@hsph.harvard.edu (L.H.G.); ahlee@hsph.harvard.edu (A.-H.L.)



Supporting Online Material for

Evidence for Upwelling of Corrosive “Acidified” Water onto the Continental Shelf

Richard A. Feely,^{*} Christopher L. Sabine, J. Martin Hernandez-Ayon, Debby Ianson, Burke Hales

^{*}To whom correspondence should be addressed. E-mail: richard.a.feely@noaa.gov

Published 22 May 2008 on *Science Express*
DOI: 10.1126/science.1155676

This PDF file includes:

Materials and Methods
Figs. S1 and S2
References

Correction: The originally posted supporting online material contained a misstatement about the quality assurance procedure for assessing the alkalinity data. The fifth sentence of the second paragraph should read: The replicate samples were interspersed throughout the station analysis for quality assurance.

Science Supporting Online Material

Evidence for Upwelling of Corrosive ‘Acidified’ Water onto the Continental Shelf

Richard A. Feely, Christopher L. Sabine, J. Martin Hernandez-Ayon, Debby Ianson, and Burke Hales

Sampling and Analytical Methods

For the NACP West Coast Cruise, samples were collected and analyzed for dissolved inorganic carbon (DIC), total alkalinity (TA), and hydrographic data along 13 cross-shelf transects from Queen Charlotte Sound, Canada to San Gregorio Baja California Sur, Mexico. Dissolved inorganic carbon (DIC) and total alkalinity (TA) were measured on all the samples and pH_{SW} (pH is reported using the seawater scale) and pCO_2 were calculated from the resulting data utilizing the program of Lewis and Wallace (*S1*). Samples were drawn from the Niskin-type bottles into cleaned, precombusted 300-mL Pyrex bottles using Tygon tubing with silicone ends. DIC was determined by gas extraction and coulometry using a modified Single-Operator Multi-Metabolic Analyzer (SOMMA) system (*S2-S5*). The precision for DIC was $\pm 1.5 \mu\text{mol kg}^{-1}$.

Seawater TA was measured by acidimetric titration, employing the open cell method described by Dickson et al (*S6, S7*). This method involves first acidifying the sample to reduce the sample pH to less than 3.6 followed by bubbling CO_2 -free air through the sample to facilitate removal of the CO_2 evolved by the acid addition. After removal of the carbonate species from solution, the titration proceeds until a pH of less than 3.0 is attained. The precision for TA was $\pm 2.0 \mu\text{mol kg}^{-1}$. Replicate samples were typically taken from the two samples out of each station. The replicate samples were interspersed

throughout the station analysis for quality assurance. No systematic differences between the replicates were observed. The data quality was confirmed by daily analyses of Certified Reference Materials (S8).

Aragonite and calcite saturation levels were calculated using the program developed by Lewis and Wallace (S1) that included the carbonic acid dissociation constants of Merzbach (S9) as refit by Dickson and Millero (S10). The *in-situ* degree of saturation of seawater with respect to aragonite and calcite is the ion product of the concentrations of calcium and carbonate ions, at the in situ temperature, salinity and pressure, divided by the apparent stoichiometric solubility product for those conditions, where the Ca^{+2} concentrations are estimated from the salinity and the carbonate ion concentration is calculated from the DIC and total alkalinity TA data. The pressure affect on the solubility is estimated from the equation of Mucci (S11) that includes the adjustments to the constants recommended by Millero (S12).

Anthropogenic CO₂ in the Northeastern Pacific

The anthropogenic CO₂ of the coastal waters was determined one of two ways. The higher density waters ($\sigma_\theta > 25.0$) were presumed to be consistent with open ocean waters. The large-scale open ocean anthropogenic CO₂ distributions were evaluated by Sabine et al. (S13) for the entire Pacific using the ΔC^* method. These estimates require a water mass age tracer, such as chlorofluorocarbons, which were not available for the coastal waters. Therefore, we took a subset of the stations used by Sabine et al. (S13) that were between 21 - 60°N and 140-109°W (Fig. S1) and fit the estimated anthropogenic CO₂ concentrations as a function of potential density (Fig. S2).

$$\text{Anthropogenic CO}_2 = -2742 + 225.31 (\sigma_\theta) - 4.5604 (\sigma_\theta)^2 \quad (S1)$$

The data were limited to the upper 250 m of the water column since that is the maximum depth of the coastal sections presented here. The anthropogenic CO₂ of the coastal waters was then calculated from potential density using equation *S1*. The highest densities were comparable between the open ocean and the coastal waters.

The lower density waters ($\sigma_\theta < 25.0$) are generally found very near the surface or represent coastal waters with river influences. Either way, these waters are not as strongly connected with the subsurface open-ocean waters and are much more likely to be tracking the current atmospheric CO₂ concentrations. To estimate the pre-industrial DIC concentration of these waters, the measured DIC and TA were used to calculate pCO₂. The calculated pCO₂ was then decreased by the change in atmospheric CO₂ between 1800 and 2007. This revised pCO₂ was then used together with the TA to calculate a pre-industrial DIC. The difference between the measured DIC and the estimated pre-industrial DIC is taken as the anthropogenic CO₂ of these waters. This is the same approach used by Sabine et al. (*S13*) and others for determining surface water anthropogenic CO₂ concentrations.

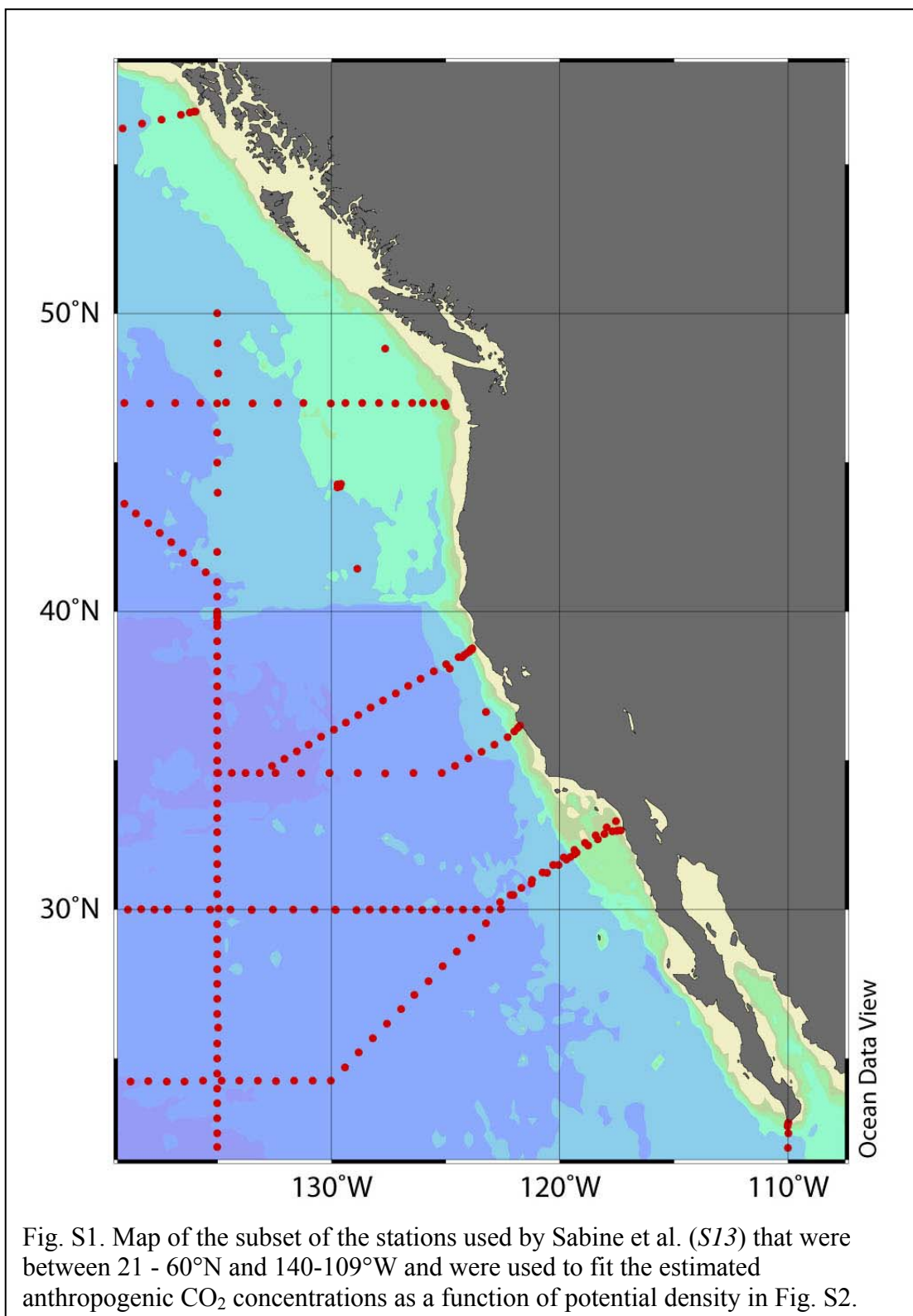
The boundary between these two methods was chosen to be $\sigma_\theta = 25.0$ because the potential density versus anthropogenic CO₂ function showed much larger scatter at $\sigma_\theta < 25.0$. Also, a σ_θ of 25.0 represents the highest density of surface waters from the open-ocean data set, thus cutting all waters with densities lighter than 25.0 eliminated the variable surface waters from the fit.

There are many sources of uncertainty with these crude calculations. The open-ocean ΔC^* calculations for this region yields a calculated RMS error for anthropogenic CO₂ of $\pm 4 \mu\text{mol kg}^{-1}$. There are many other sources of uncertainty here including the quality of

the density versus anthropogenic CO₂ fit, the similarity between coastal and open ocean waters, and the temporal stability of parameters such as the total alkalinity in the coastal region. On the other hand, it is not likely that there is zero anthropogenic CO₂ in the coastal waters and it is not likely that the anthropogenic CO₂ has increased significantly faster than the growth rate of CO₂ in the atmosphere. Based on these considerations, we believe that these estimates are good to within $\pm 50\%$.

References and Notes

- S1. E. Lewis and D. W. R. Wallace, Program developed for CO₂ system calculations, Report 105, Oak Ridge National Laboratory, 33 pp. (Also available currently at: <http://cdiac.esd.ornl.gov/oceans/co2rprt.html>). (1998).
- S2. K. M. Johnson *et al.*, *Marine Chemistry* (16), 61-82 (1985).
- S3. K. M. Johnson *et al.*, *Marine Chemistry*, 21(2), 117-133 (1987).
- S4. K. M. Johnson and D.W.R. Wallace. DOE Research Summary No. 19, Carbon Dioxide Information Analysis Center, Oak Ridge National Laboratory (1992).
- S5. DOE Handbook of methods for the analysis of the various parameters of the carbon dioxide system in sea water. Version 2, A.G. Dickson and C. Goyet, eds., ORNL/CDIAC-74. (1994).
- S6. A. G. Dickson *Oceanography*, 14(4), 21-22. (2001).
- S7. A.G. Dickson *et al.*, *Guide to Best Practices for Ocean CO₂ Measurements*, PICES Special Publication No. 3, 191 pp.
- S8. A. G. Dickson *et al.*, *Marine Chemistry*, 80, 185-197 (2003).
- S9. C. Mehrbach *et al.*, *Limnol. Oceanogr.*, 18, 897–907. (1973).
- S10. A. G. Dickson and F. J. Millero *Deep-Sea Res.*, 34, 1733–1743. (1987).
- S11. A. Mucci *Am. J. Sci.*, **238**, 780–799, 1983.
- S12. F. J. Millero *Geochim. Cosmochim. Acta*, 59(4), 661–677. (1995).
- S13. C. L. Sabine *et al.*, *Global Biogeochem. Cycles*, 16(4), 1083, doi: 10.1029/2001GB001639. (2002).



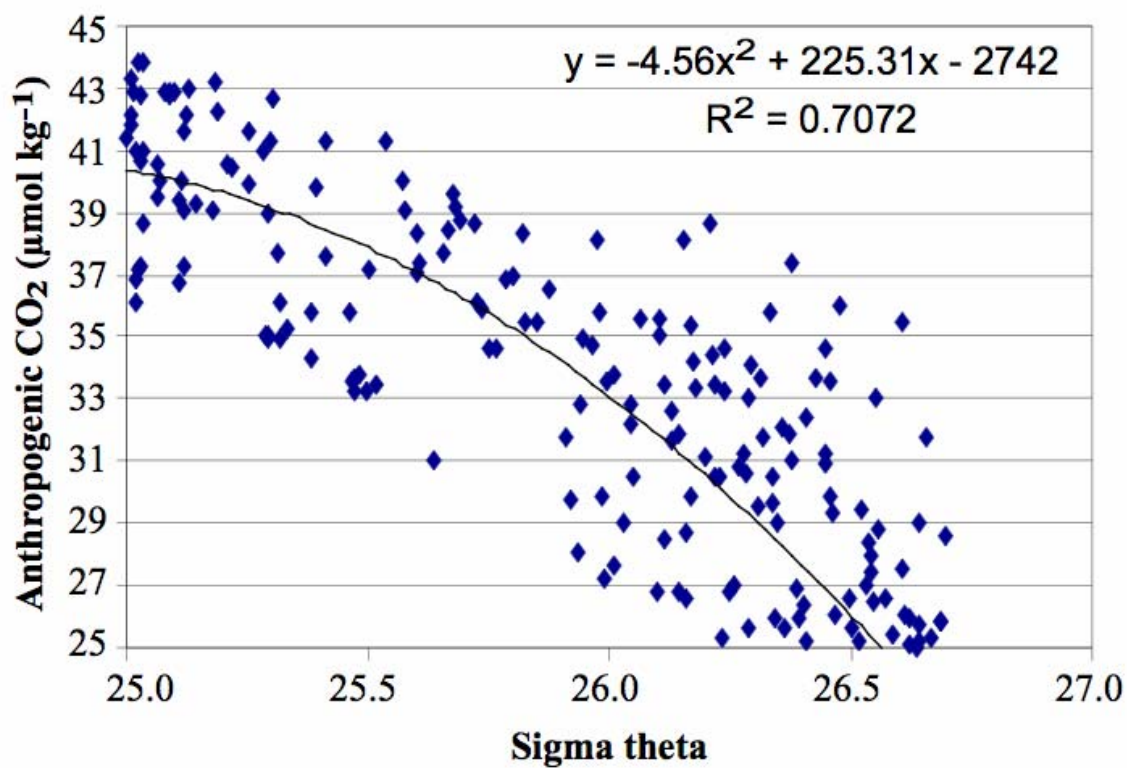


Fig. S2. Plot of the distribution of anthropogenic CO₂ in $\mu\text{mol kg}^{-1}$ as a function of potential density for stations from the northeastern Pacific as shown in Fig. S1 above.

Detecting regional anthropogenic trends in ocean acidification against natural variability

T. Friedrich¹*, A. Timmermann¹*, A. Abe-Ouchi², N. R. Bates³, M. O. Chikamoto², M. J. Church⁴, J. E. Dore⁵, D. K. Gledhill⁶, M. González-Dávila⁷, M. Heinemann¹, T. Ilyina⁸, J. H. Jungclauss⁸, E. McLeod⁹, A. Mouchet¹⁰ and J. M. Santana-Casiano⁷

Since the beginning of the Industrial Revolution humans have released ~500 billion metric tons of carbon to the atmosphere through fossil-fuel burning, cement production and land-use changes^{1,2}. About 30% has been taken up by the oceans³. The oceanic uptake of carbon dioxide leads to changes in marine carbonate chemistry resulting in a decrease of seawater pH and carbonate ion concentration, commonly referred to as ocean acidification. Ocean acidification is considered a major threat to calcifying organisms^{4–6}. Detecting its magnitude and impacts on regional scales requires accurate knowledge of the level of natural variability of surface ocean carbonate ion concentrations on seasonal to annual timescales and beyond. Ocean observations are severely limited with respect to providing reliable estimates of the signal-to-noise ratio of human-induced trends in carbonate chemistry against natural factors. Using three Earth system models we show that the current anthropogenic trend in ocean acidification already exceeds the level of natural variability by up to 30 times on regional scales. Furthermore, it is demonstrated that the current rates of ocean acidification at monitoring sites in the Atlantic and Pacific oceans exceed those experienced during the last glacial termination by two orders of magnitude.

Skeletons and shells of marine calcifiers are made of different crystalline forms of calcium carbonate, such as calcite or aragonite. A decrease in the saturation state of calcium carbonate can result in decreased calcification and increased dissolution of calcium carbonate^{5,7,8}. As aragonite is the more soluble form, its saturation state (Ω_{Ar} , see Supplementary Information for details) can be regarded as a measure for ocean acidification.

Here we present results from a model simulation over 1,300 years (800–2099 AD) that was conducted with a state-of-the-art coupled carbon cycle–climate model (MPI-ESM, see Supplementary Information for details) forced by the most recent reconstructions of solar and volcanic radiative perturbations, land-use changes, aerosols and orbital variations. The model is also subject to historical CO₂ emissions and the A1B greenhouse-gas emission scenario (Fig. 1a,b; ref. 9). The knowledge of the pre-industrial, natural variability (defined here by the years 800 AD to 1750 AD) of the surface aragonite saturation state (Ω_{Ar}^{surf}) will permit a robust determination

of regional signal-to-noise ratios using recent observed and future projected anthropogenic negative trends in Ω_{Ar}^{surf} . Furthermore, we present simulations of the Last Glacial Maximum (LGM) conducted with the models LOVECLIM and MIROC (see Supplementary Information for details) to quantify the impact of the reconstructed ~90 ppmv increase in atmospheric CO₂ between the LGM and pre-industrial times on Ω_{Ar}^{surf} . This will allow us to put recent anthropogenic trends in ocean acidification into the context of the most recent natural event of carbon cycle–climate reorganization.

According to the MPI-ESM simulation of the pre-industrial surface waters, local marine ecosystems have been exposed to a diverse range of natural variability in both the amplitude of the annual cycle and the interannual variability of Ω_{Ar}^{surf} (Supplementary Fig. S1). For example, the Galápagos Islands are located in the centre of upwelling-driven variability, whereas reefs in the Caribbean are only exposed to small interannual changes in carbonate ion concentration. This spatial heterogeneity in natural variability, together with the local equilibration timescale of surface waters to increasing atmospheric pCO_2 and the net air–sea flux of CO₂ are likely to affect the regional impacts of ocean acidification on calcifying marine ecosystems.

Figure 1c,d shows the simulated spatially averaged Ω_{Ar}^{surf} for the main coral reef locations in the Pacific, the Southern Indian Ocean and the Caribbean (see Fig. 1e, dashed blue lines for the averaging regions). Our results reveal that current levels of Ω_{Ar}^{surf} are already considerably lower than the long-term pre-industrial mean. In a recent study⁸ a linear relationship was proposed between Ω_{Ar}^{surf} and coral calcification rates. Using this estimate, our model results suggest that calcification rates at coral reef locations in the western tropical Pacific and the Caribbean may have already dropped by ~15% with respect to their pre-industrial values. This result extends the findings of a previous study¹⁰ that used present-day Ω_{Ar}^{surf} as a reference. Using historical CO₂ emissions and the A1B greenhouse-gas emission scenario (Fig. 1a,b), a drop to about 60% in coral reef calcification is projected for the end of the twenty-first century. It is important to note that carbonate chemistry is only one factor controlling coral calcification rates. Other factors include the effects of light, nutrients and temperature. The synergistic or combined effects are as yet poorly understood.

¹International Pacific Research Center (IPRC), SOEST, University of Hawai'i, Honolulu, Hawaii 96822, USA, ²Research Institute for Global Change, Japan Agency for Marine Science and Technology, Yokohama 236-0001, Japan, ³Bermuda Institute of Ocean Sciences, St George's, GE 01, Bermuda,

⁴Department of Oceanography, University of Hawai'i, Honolulu, Hawaii 96822, USA, ⁵Department of Land Resources and Environmental Sciences, Montana State University, Bozeman, Montana 59717, USA, ⁶NOAA AOML, Cooperative Institute of Marine and Atmospheric Studies, Rosenstiel School of Marine and Atmospheric Science, University of Miami, Miami, Florida 33149, USA, ⁷Departamento de Química, Facultad de Ciencias del Mar, Universidad de Las Palmas de Gran Canaria, Las Palmas de Gran Canaria 35.017, Spain, ⁸Max Planck Institute for Meteorology, Hamburg 20146, Germany, ⁹The Nature Conservancy, Hawai'i Field Office, Honolulu, Hawaii 96817, USA, ¹⁰Département Astrophysique, Géophysique et Océanographie, Université de Liège, Liège B-4000, Belgium. *e-mail: tobiasf@hawaii.edu; axel@hawaii.edu.

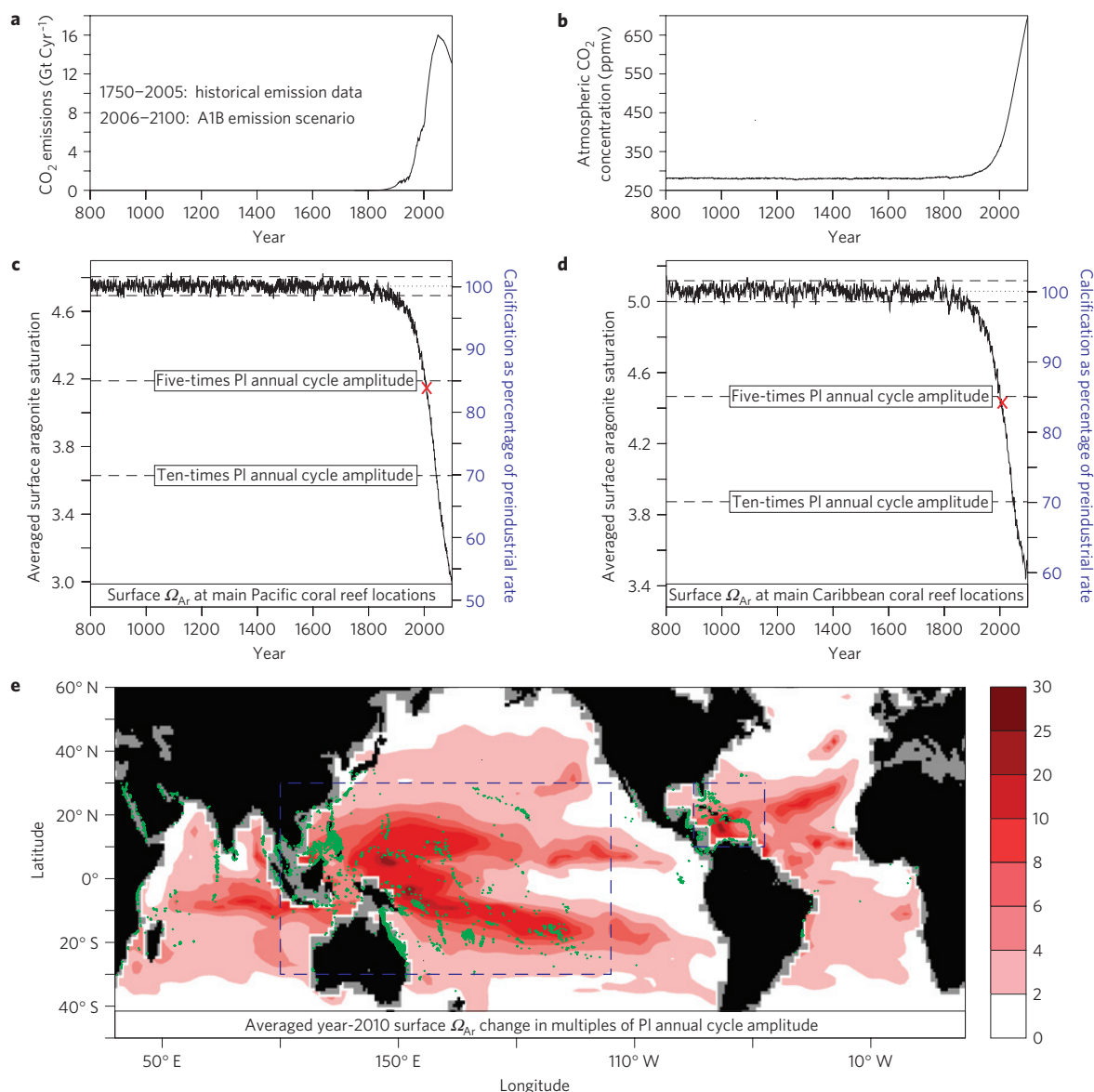


Figure 1 | Regional signal-to-noise ratio of Ω_{Ar}^{surf} . **a**, Carbon dioxide (CO_2) emissions ($Gt\ C\ yr^{-1}$) used as forcing of the MPI-ESM. **b**, Atmospheric CO_2 concentration (ppmv) simulated by the MPI-ESM. **c**, Simulated annual-mean Ω_{Ar}^{surf} averaged over the main Pacific coral reef locations (green dots in the blue rectangle in **e**). Dotted line: pre-industrial (PI) average of simulated Ω_{Ar}^{surf} . Dashed lines: simulated amplitude of mean pre-industrial annual cycle of Ω_{Ar}^{surf} . Right axis: calcification rate with respect to pre-industrial level using ref. 8. Red cross indicates year 2010. **d**, Same as **c** for the main Caribbean coral reef regions (green dots in the blue rectangle in **e**). **e**, Simulated year-2010 change in Ω_{Ar}^{surf} with respect to the simulated pre-industrial average in multiples of simulated pre-industrial amplitude of the annual cycle.

The uncertainty of the ecological response to these projected changes is considerable at present.

The pre-industrial amplitude of the local annual cycle in Ω_{Ar}^{surf} can be regarded as a metric of natural variability to which aragonite-calcifying organisms have been exposed to over a long time and to which they have successfully adapted. Any reduction of Ω_{Ar}^{surf} below the minima given by the range of the unperturbed annual cycle will be interpreted here as a stress to these organisms and their associated ecosystems. Past anthropogenic CO_2 emissions have already pushed the aragonite saturation state of seawater far outside the range of natural variability (Fig. 1c,d). The difference between current and pre-industrial Ω_{Ar}^{surf} exceeds the natural annual cycle range already by a factor of five for the Pacific and Atlantic warm pool reefs (Fig. 1c,d).

Overall, the simulated ratio between the anthropogenic change ($\Omega_{Ar}^{surf}(2010) - \Omega_{Ar}^{surf}(\text{pre-industrial})$) and the natural variability

(expressed in terms of the local, pre-industrial annual cycle range) differs substantially on a regional scale (Fig. 1e). As a result of large natural variability induced by annual to interannual changes in upwelling, equatorial Pacific coral reefs from Galápagos to western Kiribati are projected to experience the most moderate relative decline of the aragonite saturation state due to anthropogenic CO_2 emissions. However, a recent study¹¹ confirmed a decline in some coral species occurring also in the eastern equatorial Pacific. Further to the west, and in off-equatorial regions of Micronesia, Polynesia and Melanesia, a smaller natural variability in Ω_{Ar}^{surf} (Supplementary Fig. S1) leads to a larger anthropogenic signal-to-noise ratio, attaining values of 6–30. It should be noted here that the western equatorial Pacific is the only region in our simulation in which the pre-industrial interannual variability of Ω_{Ar}^{surf} is slightly larger than its annual cycle (Supplementary Fig. S1). However, even when assuming that the pre-industrial interannual variability is a measure

for the corals' 'comfort' zone, present-day values of Ω_{Ar}^{surf} are already exceeding this threshold by a factor of between two and ten.

A large amplitude in the annual cycle corresponds to a smaller signal-to-noise ratio, as documented for higher latitudes in Fig. 1e. However, the combination of a large annual cycle range on top of the anthropogenic signal can lead, in fact, to an earlier undersaturation. On the basis of empirical estimates for the seasonal cycle of carbonate chemistry parameters, it was concluded¹² that undersaturation with respect to aragonite will occur at the surface of the Southern Ocean roughly by the year 2030. Our simulation can confirm this prediction, and it further documents that values of $\Omega_{Ar}^{surf} < 1$ will be found in 30–50% of the ocean poleward of 40° S by the year 2100.

Ocean acidification is anticipated to affect marine ecosystems well beyond the coral reef realm^{13–17}. Laboratory and mesocosm experiments show diverse impacts of ocean acidification on different groups of organisms, or even individual species within the same group. Recent studies using open ocean samples indicate that individual coccolithophores mass¹⁸ and foraminifera shell weight¹⁴ decline as CO₂ concentrations increase.

Observations in the North Pacific¹⁹ reported a -0.06 change in surface ocean pH between 1991 and 2006 in the upper 500 m, of which 52% can be attributed to natural variability. Given the irregular sampling of chemical parameters in most parts of the ocean, a detection of ocean acidification and the determination of its local magnitude can be challenging. Our model-based estimates of anthropogenic change in Ω_{Ar}^{surf} reveal that since the mid-twentieth century the anthropogenic signals have exceeded the pre-industrial interannual variability by at least a factor of two in vast areas of the global oceans (Fig. 2). Applying an exceedance factor of two as a detection limit it becomes apparent that the anthropogenic impact on Ω_{Ar}^{surf} is detectable in almost the entire ocean by year 2010, except for the tropical eastern Pacific and the frontal regions near the subpolar gyres. In the Caribbean, a region with very high signal-to-noise ratio, the detection limit was already exceeded at the beginning of the twentieth century. By around 1980, the anthropogenic signal exceeded the natural range in this region by a factor of ten, in accordance with previous observational estimates²⁰ (Supplementary Fig. S2). According to our modelling results, a robust detection of the anthropogenic signal in Ω_{Ar}^{surf} in the eastern equatorial Pacific against the background variability has been possible for the past 10–20 years. By year 2020–2060, the anthropogenic signal in this region will exceed the natural variability range in aragonite saturation state by at least a factor of five.

In our effort to compare the twentieth century trends of Ω_{Ar}^{surf} with other geochemical trends from the Late Quaternary, we select another benchmark period: the last glacial termination. The concomitant change in atmospheric pCO₂ from ~190 ppmv to ~280 ppmv between 17,000 and 11,000 years BP (ref. 21) represents the most recent increase of such magnitude preceding the industrial revolution. Here we study the effect of the deglacial CO₂ rise on the surface aragonite saturation using two different Earth system models: LOVECLIM and MIROC (see Supplementary Information for details). Switching from LGM to pre-industrial equilibrium conditions generates a decrease of the surface aragonite saturation state of 0.88 (0.64) units in LOVECLIM (MIROC), which is in good agreement with reconstructions¹⁸ (Supplementary Fig. S4). These simulated changes (Fig. 3a), although being somewhat larger even than the change from pre-industrial to present-day conditions simulated by the MPI-ESM (Fig. 3f), occurred over a time period that was two orders of magnitude longer than the industrial period.

To compare the simulated Ω_{Ar}^{surf} changes and their rate of change with previous observations, we focus on continuous records of Ω_{Ar}^{surf} from several monitoring sites in the Pacific²² and the Atlantic^{20,23,24} covering the last two to three decades (Fig. 3b–e). The observed decadal changes are dominated by a trend signal, a pronounced

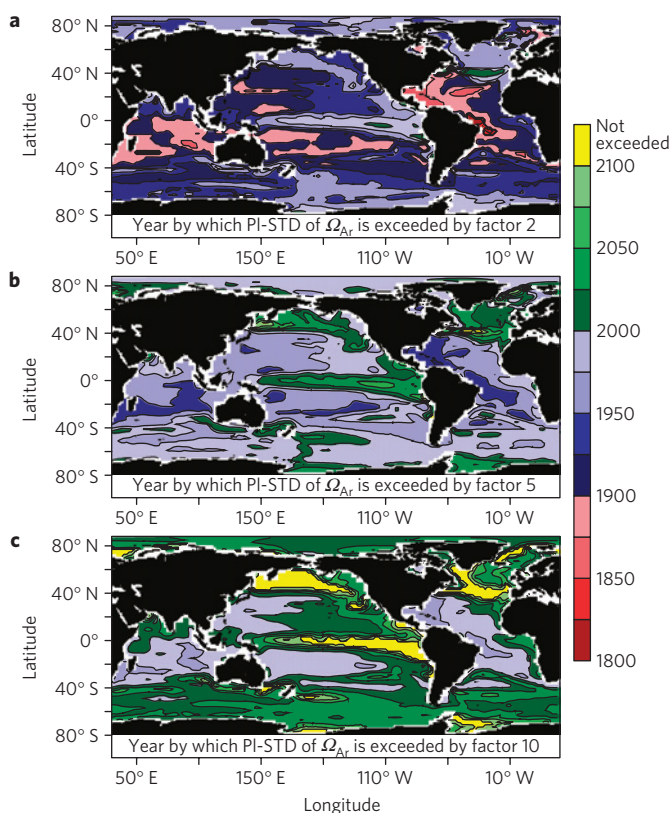


Figure 2 | First year of detectability of anthropogenic Ω_{Ar}^{surf} trend. **a**, Year by which simulated changes in Ω_{Ar}^{surf} (with respect to the pre-industrial mean) exceed simulated pre-industrial (800–1750 AD) standard deviation (PI-STD, based on annual-mean values, see also Supplementary Fig. S1) by a factor of two. **b, c** same as **a** for factors of five and ten respectively. Areas with yellow shading indicate regions where the pre-industrial standard deviation is not exceeded by the respective factor during the course of the model simulation.

annual cycle and interannual variability (Supplementary Fig. S2). The observed trends off the Canary Islands, Bermuda, Hawaii, and in the Caribbean amount to about -0.09 , -0.04 , -0.08 , -0.09 units per decade respectively (Fig. 3i–l). These values are higher than the simulated globally averaged trends over the entire twentieth century, but close to the simulated global values for the twenty-first century (Fig. 3m,n).

The observed present-day, anthropogenic rate of change in Ω_{Ar}^{surf} is one to two orders of magnitude larger than estimated for the last glacial termination (Fig. 3h–l). Already, the weakest observed rate of change in Bermuda exceeds the glacial–interglacial trend by a factor of 32(56) over the LOVECLIM (MIROC) estimates for the last glacial termination. In the Caribbean, where the largest regional trends are reported, the Ω_{Ar}^{surf} decrease over the past ~20 years reaches 78(136) times the glacial–interglacial rate of change documented by LOVECLIM (MIROC).

Summarizing, we conclude that it is virtually certain that anthropogenic trends already exceed the natural variability on regional scales and are hence detectable in many areas of the world's ocean. However, the eastern tropical Pacific is an exception and exhibits the weakest signal-to-noise ratio owing to high ENSO-related natural variability in carbonate chemistry.

An unresolved question to address in future studies is how the detectability of anthropogenic Ω_{Ar}^{surf} trends translates into the detectability of the anthropogenic influence on the functionality of marine ecosystems. Marine organisms are exposed to a multitude of other anthropogenic stress factors. Corals, for instance, experience

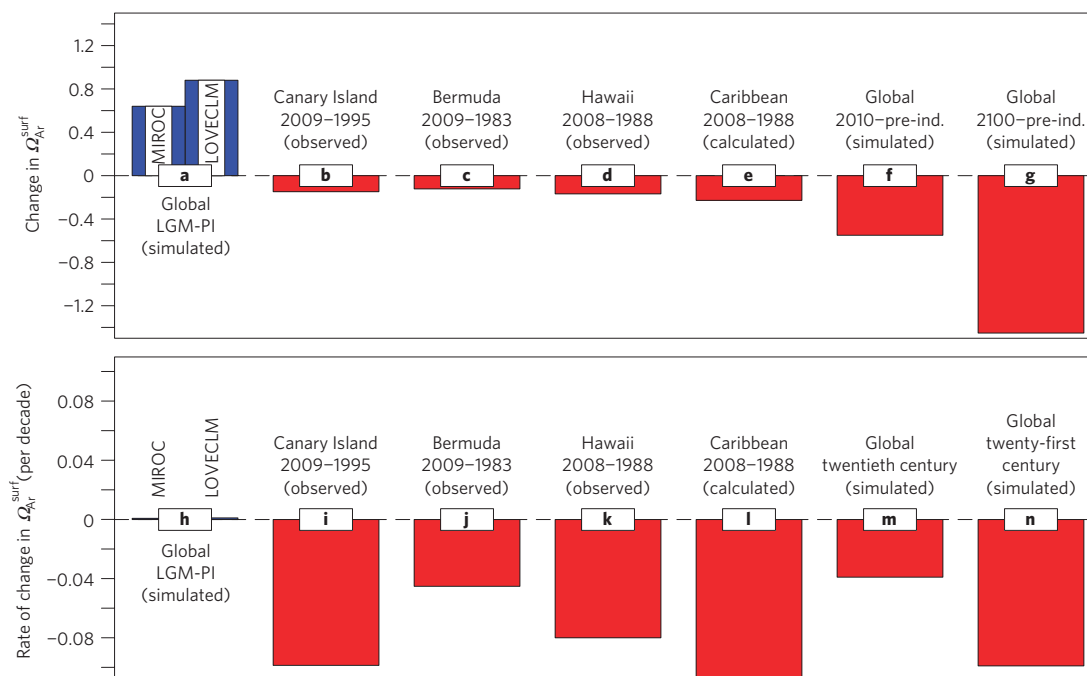


Figure 3 | Current Ω_{Ar}^{surf} trends in the context of the Last Glacial Termination. **a**, Globally averaged change in Ω_{Ar}^{surf} between pre-industrial (PI) times and the Last Glacial Maximum as simulated by the LOVECLIM and the MIROC model respectively. **b–e**, Trends in Ω_{Ar}^{surf} for the European Station for Time series in the Ocean (1995–2009) (**b**), the Bermuda Atlantic Time-series Study (1983–2009) (**c**), Station ALOHA (1988–2008) (**d**) and the Caribbean region (1988–2008; ref. 20) (**e**). **f,g**, Globally averaged change in Ω_{Ar}^{surf} as simulated by the MPI-ESM for the years 2100 (**f**) and 2100 (**g**) respectively (with respect to the pre-industrial average). **h–n**, Rates of change in Ω_{Ar}^{surf} (per decade) for glacial-interglacial as in **a** (**h**), observations as in **b–e** (**i–l**) and the twentieth (**m**) and twenty-first century (**n**), respectively.

increasing stress from ocean acidification, surface warming²⁵ and coastal pollution²⁶. These stress factors probably do not simply add up, but combine in a species-dependent manner²⁷. Tropical surface temperatures are projected to increase at a rate that would lead to massive coral bleaching and mortality in the next three to five decades²⁸. Combined with a detectable change due to reduced ocean aragonite saturation and the corresponding estimated drop in carbonate accretion of ~15% since the industrial revolution (Fig. 1c,d), severe reductions are likely to occur in coral reef diversity, structural complexity and resilience by the middle of this century.

Received 29 September 11; accepted 8 December 2011; published online 22 January 2012

References

- Houghton, R. Revised estimates of the annual net flux of carbon to the atmosphere from changes in land use and land management 1850–2000. *Tellus B* **55**, 378390 (2003).
- Boden, T., Marland, G. & Andres, R. *Global, Regional, and National Fossil-Fuel CO₂ Emissions* Tech. Rep. <http://dx.doi.org/10.3334/CDIAC/00001V2010> (Carbon Dioxide Information Analysis Center, Oak Ridge National Laboratory, US Department of Energy, 2010).
- Canadell, J. *et al.* Contributions to accelerating atmospheric CO₂ growth from economic activity, carbon intensity, and efficiency of natural sinks. *Proc. Natl Acad. Sci. USA* **104**, 18866–18870 (2007).
- Raven, J. *et al.* *Ocean Acidification Due to Increasing Atmospheric Carbon Dioxide* 60, Tech. Rep. (The Royal Society, 2005).
- Kleypas, J. A. *et al.* *Impacts of Ocean Acidification on Coral Reefs and Other Marine Calcifiers: A Guide for Future Research*. Tech. Rep. (NSF, NOAA, and the US Geological Survey, 2006).
- National Research Council Report *Ocean Acidification: A National Strategy to Meet the Challenges of a Changing Ocean* 152 (National Academy of Science, 2010).
- Riebesell, U. *et al.* Reduced calcification of marine plankton in response to increased atmospheric CO₂. *Nature* **407**, 364–367 (2000).
- Langdon, C. & Atkinson, M. J. Effect of elevated pCO₂ on photosynthesis and calcification of corals and interactions with seasonal change in temperature/irradiance and nutrient enrichment. *J. Geophys. Res.* **110**, C09S07 (2005).
- Jungclauss, J. H. *et al.* Climate and carbon-cycle variability over the last millennium. *Clim. Past* **6**, 723–737 (2010).
- Cooley, S. R., Lucey, N., Kite-Powell, H. & Doney, S. C. Nutrition and income from molluscs today imply vulnerability to ocean acidification tomorrow. *Fish Fish.* <http://dx.doi.org/10.1111/j.1467-2979.2011.00424.x> (2011).
- Manzello, D. P. Coral growth with thermal stress and ocean acidification: lessons from the eastern tropical Pacific. *Coral Reefs* **29**, 749–758 (2010).
- McNeil, B. & Matear, R. Southern Ocean acidification: A tipping point at 450-ppm atmospheric CO₂. *Proc. Natl Acad. Sci. USA* **105**, 18860–18864 (2008).
- Feely, R. A., Sabine, C., Hernandez-Ayon, J. M., Ianson, D. & Hales, B. Evidence for upwelling of corrosive acidified water onto the continental shelf. *Science* **320**, 1490–1492 (2008).
- Moy, A. D., Howard, W. R., Bray, S. G. & Trull, T. W. Reduced calcification in modern Southern Ocean planktonic foraminifera. *Nature Geosci.* **2**, 276–280 (2009).
- Yamamoto-Kawai, M., McLaughlin, F. A., Carmack, E. C., Nishino, S. & Shimada, K. Aragonite undersaturation in the Arctic Ocean: Effects of ocean acidification and sea ice melt. *Science* **326**, 1098–1100 (2009).
- Ilyina, T. *et al.* Early detection of ocean acidification effects on marine calcification. *Glob. Biogeochem. Cycles* **23**, GB1008 (2009).
- Atzesu-Scott, K. *et al.* Calcium carbonate saturation states in the waters of the Canadian Arctic Archipelago and the Labrador Sea. *J. Geophys. Res.* **115**, C11021 (2010).
- Beaufort, L. *et al.* Sensitivity of coccolithophores to carbonate chemistry and ocean acidification. *Nature* **476**, 80–83 (2011).
- Byrne, R. H., Mecking, S., Feely, R. A. & Liu, X. Direct observations of basin-wide acidification of the North Pacific Ocean. *Geophys. Res. Lett.* **37**, L02601 (2010).
- Gledhill, D. K., Wanninkhof, R., Millero, F. J. & Eakin, M. Ocean acidification of the Greater Caribbean Region 1996–2006. *J. Geophys. Res.* **113**, C10031 (2008).
- Lüthi, D. *et al.* High-resolution carbon dioxide concentration record 650,000–800,000 years before present. *Nature* **453**, 379–382 (2008).
- Dore, J. E., Lukas, R., Sadler, D. W., Church, M. J. & Karl, D. M. Physical and biogeochemical modulation of ocean acidification in the central North Pacific. *Proc. Natl Acad. Sci. USA* **106**, 12235–12240 (2009).
- Bates, N. R. Interannual variability of the oceanic CO₂ sink in the subtropical gyre of the North Atlantic Ocean over the last two decades. *J. Geophys. Res.* **112**, C09013 (2007).

24. Santana-Casiano, J. M., González-Dávila, M., Rueda, M.-J., Llinás, O. & González-Dávila, E. F. The interannual variability of oceanic CO₂ parameters in the northeast Atlantic subtropical gyre at the ESTOC site. *Glob. Biogeochem. Cycles* **21**, GB1015 (2007).
25. Hoegh-Guldberg, O. Coral bleaching, Climate Change and the future of the worlds coral reefs. *Rev. Mar. Freshwat. Res.* **50**, 839–866 (1999).
26. Doney, S. C. The growing human footprint on coastal and open-ocean biogeochemistry. *Science* **328**, 1512–1516 (2010).
27. Fabricius, K. *et al.* Losers and winners in coral reefs acclimatized to elevated carbon dioxide concentrations. *Nature Clim. Change* **1**, 165–169 (2011).
28. McLeod, E. *et al.* Warming seas in the coral triangle: Coral reef vulnerability and management implications. *Coast. Manag.* **38**, 518–539 (2010).

Acknowledgements

This study was funded by The Nature Conservancy (www.nature.org) and National Science Foundation (NSF) grant #0902133. AT is supported by the Japan Agency for Marine-Earth Science and Technology (JAMSTEC) through its sponsorship of the

International Pacific Research Center and NSF grant #0902551. We thank S. Lorenz for conducting the MPI-ESM experiments. This is International Pacific Research Center contribution number 829.

Author contributions

The paper was written by T.F. and A.T. Data analysis and interpretation were carried out by T.F., A.T., M.H., D.K.G., N.R.B., M.J.C., J.E.D., M.G-D., J.M.S-C., T.I., J.H.J., M.O.C., E.M. and A.M. Observational data were provided by N.R.B., M.J.C., J.E.D., M.G-D. and J.M.S-C. Data for the Caribbean region were calculated by D.K.G. Last Glacial Maximum modelling data were provided by T.F., M.O.C., A.A-O. and A.M.

Additional information

The authors declare no competing financial interests. Supplementary information accompanies this paper on www.nature.com/natureclimatechange. Reprints and permissions information is available online at <http://www.nature.com/reprints>. Correspondence and requests for materials should be addressed to T.F. or A.T.

Effect of Carbonate Chemistry Alteration on the Early Embryonic Development of the Pacific Oyster (*Crassostrea gigas*)

Frédéric Gazeau^{1,2*}, Jean-Pierre Gattuso^{1,2}, Mervyn Greaves³, Henry Elderfield³, Jan Peene⁴, Carlo H. R. Heip^{4,5}, Jack J. Middelburg^{4,6}

1 Centre National de la Recherche Scientifique-Institut National des Sciences de l'Univers, Laboratoire d'Océanographie de Villefranche, Villefranche-sur-Mer, France, **2** Université Pierre et Marie Curie-Paris 6, Observatoire Océanologique de Villefranche, Villefranche-sur-Mer, France, **3** Department of Earth Sciences, University of Cambridge, Cambridge, England, **4** Centre for Estuarine and Marine Ecology, Netherlands Institute of Ecology, Yerseke, The Netherlands, **5** Department of Marine Organic Biogeochemistry, Royal Netherlands Institute for Sea Research, Den Burg, The Netherlands, **6** Faculty of Geosciences, Utrecht University, Utrecht, The Netherlands

Abstract

Ocean acidification, due to anthropogenic CO₂ absorption by the ocean, may have profound impacts on marine biota. Calcareous organisms are expected to be particularly sensitive due to the decreasing availability of carbonate ions driven by decreasing pH levels. Recently, some studies focused on the early life stages of mollusks that are supposedly more sensitive to environmental disturbances than adult stages. Although these studies have shown decreased growth rates and increased proportions of abnormal development under low pH conditions, they did not allow attribution to pH induced changes in physiology or changes due to a decrease in aragonite saturation state. This study aims to assess the impact of several carbonate-system perturbations on the growth of Pacific oyster (*Crassostrea gigas*) larvae during the first 3 days of development (until shelled D-veliger larvae). Seawater with five different chemistries was obtained by separately manipulating pH, total alkalinity and aragonite saturation state (calcium addition). Results showed that the developmental success and growth rates were not directly affected by changes in pH or aragonite saturation state but were highly correlated with the availability of carbonate ions. In contrast to previous studies, both developmental success into viable D-shaped larvae and growth rates were not significantly altered as long as carbonate ion concentrations were above aragonite saturation levels, but they strongly decreased below saturation levels. These results suggest that the mechanisms used by these organisms to regulate calcification rates are not efficient enough to compensate for the low availability of carbonate ions under corrosive conditions.

Citation: Gazeau F, Gattuso J-P, Greaves M, Elderfield H, Peene J, et al. (2011) Effect of Carbonate Chemistry Alteration on the Early Embryonic Development of the Pacific Oyster (*Crassostrea gigas*). PLoS ONE 6(8): e23010. doi:10.1371/journal.pone.0023010

Editor: John Murray Roberts, Heriot-Watt University, United Kingdom

Received: January 10, 2011; **Accepted:** July 11, 2011; **Published:** August 10, 2011

Copyright: © 2011 Gazeau et al. This is an open-access article distributed under the terms of the Creative Commons Attribution License, which permits unrestricted use, distribution, and reproduction in any medium, provided the original author and source are credited.

Funding: This research has received support from the Netherlands Organization of Scientific Research and is a contribution to the "European Project on Ocean Acidification" (EPOCA) which received funding from the European Community's Seventh Framework Programme (FP7/2007-2013) under grant agreement n° 211384. The funders had no role in study design, data collection and analysis, decision to publish, or preparation of the manuscript.

Competing Interests: The authors have declared that no competing interests exist.

* E-mail: f.gazeau@obs-vlfr.fr

Introduction

Due to the absorption of anthropogenic CO₂ by the ocean, seawater pH has already declined by 0.1 unit compared with pre-industrial values [1] and is projected to decrease by another 0.35 unit by the end of the century [2]. This process, known as ocean acidification, will most likely have profound impacts on marine biota. Besides the direct effect of decreasing pH on the physiology and metabolism of marine organisms through a disruption of inter-cellular transport mechanisms [3], calcareous organisms are particularly sensitive due to the decreasing availability of carbonate ions (CO₃²⁻) driven by increasing pCO₂. The calcium carbonate saturation state (Ω) is defined as:

$$\Omega = \frac{[CO_3^{2-}][Ca^{2+}]}{K'_{sp}} \quad (1)$$

where K'_{sp} is the stoichiometric solubility product, a function of temperature, salinity, pressure and the mineral phase considered

(calcite, aragonite or high-magnesian calcite), and, as a consequence of ocean acidification, will significantly decrease in the coming decades. It must be stressed that carbonate saturation states depend not only on pH but also on total alkalinity levels. Total alkalinity measures the ability of a solution to neutralize acids to the equivalence point of carbonate or bicarbonate, acting as a natural buffer to the incorporation of anthropogenic CO₂ in the ocean. As the addition (or removal) of CO₂ to a solution does not change its alkalinity and since the dissolution of calcium carbonate minerals in the water column and in the sediments, as well as alkalinity inputs from continental rock weathering, are very slow processes, they are not expected to significantly buffer ocean acidification in the coming decades [4].

Several experimental studies have investigated the effect of a pCO₂ increase on the growth of calcifying organisms [5]. Species that produce aragonite, less soluble than low-magnesian calcite in seawater, will be especially at risk. As amorphous calcium carbonate and aragonite have been identified as the main CaCO₃ minerals in larval stages of benthic mollusks [6], there is a strong

need to carefully assess the effects of ocean acidification and the associated alteration of the carbonate chemistry on their development. Small changes in the abundance and developmental success of these larval stages control the size and viability of the benthic populations [7] and therefore could induce significant changes in the functioning of coastal ecosystems. Indeed, shellfish are ecosystem engineers governing energy and nutrient flows in coastal ecosystems, provide habitats for many benthic organisms and form an important food source for birds [8,9]. Moreover, global shellfish aquaculture production reached 13.1 million tons in 2008 (27% of the global aquaculture yield), corresponding to a commercial value of US\$13.1 billion. The Pacific Oyster (*Crassostrea gigas*) was the most cultivated species in 2008 with a volume of 6.5 million tons or 9.5% of the total world aquaculture production (FISHSTAT Plus, Universal software for fishery statistical time series, Version 2.3, Food and Agriculture Organization of the United Nations, Fisheries Department, Data and Statistics Unit., 2000).

Several recent studies have focused on the effect of ocean acidification on the early development of molluscan species [10,11,12,13,14,15,16,17,18] and most of them have reported negative impacts of decreasing pH levels on the growth and development of these organisms. Kurihara et al. [12,13], Parker et al. [15] and Gazeau et al. [11] have investigated the effects of decreasing pH on the early embryonic (from fertilization to the D-veliger stage) development of commercially important bivalve species. This developmental period is of the utmost importance since the onset of shell mineralization occurs during the trochophore larval stage and shells are fully mineralized when larvae reach the D-veliger stage, at the second or third day after fertilization [19]. Studies of Kurihara et al. [12,13] on *Crassostrea gigas* and *Mytilus galloprovincialis* showed a strong decrease of developmental success into viable D-shaped larvae and growth rates with increased $p\text{CO}_2$. However, a pH (on the National Bureau of Standards scale, hereafter referred to as pH_{NBS}) of ~ 7.4 was used (0.7 unit lower than control values), a value lower than that projected to occur at the end of this century. Moreover, due to low ambient total alkalinity levels, seawater was highly undersaturated with respect to aragonite in the low pH conditions in these two studies (Ω_a of 0.68 and 0.49, respectively). Parker et al. [15] studied the early embryonic development of the Sydney rock oyster *Saccostrea glomerata* at ambient (375 μatm), 600, 750 and 1000 μatm $p\text{CO}_2$ levels. This experiment showed a general decrease in the percentage and size of D-veliger with increasing $p\text{CO}_2$. However, manipulation of the carbonate chemistry was performed by addition of a strong acid (HCl) to reduce pH, a technique that is not recommended as acid addition also decreases total alkalinity, which is not anticipated to occur in the coming decades. Moreover, as values of total alkalinity and CaCO_3 saturation state were not provided, comparisons with similar studies are not straightforward. Gazeau et al. [11] reported on the impacts of decreasing pH levels on the first 2 d development of blue mussel (*Mytilus edulis*) larvae. They showed that a decrease of pH_{NBS} to ~ 7.8 (control: ~ 8.1), associated with a supersaturation with respect to aragonite ($\Omega_a \sim 1.4$), had no effect on the percentage of embryos developing to viable D-veliger larvae. The effect on average final shell length was limited ($\sim -5 \pm 1\%$). Their results show that a decrease of pH_{NBS} to ~ 7.6 , associated with a slight undersaturation with respect to aragonite, had significant effects on the percentage of embryos that developed to D-veliger larvae normally and more pronounced effects on average final D-veliger shell lengths ($\sim -13 \pm 1\%$). However, this study did not allow the discrimination between the physiological effect of pH decrease, via a disruption of inter-cellular transport

mechanisms, and the effect of the aragonite saturation state, on the larval development of this species.

The objectives of the present study are to investigate the effect of various carbonate chemistry alterations, performed by manipulating pH, total alkalinity and the saturation state with respect to calcium carbonate separately on the survival and growth of Pacific oyster (*Crassostrea gigas*) larvae during the first 3 days of their development.

Materials and Methods

Experimental set-up

A batch of one million embryos of the Japanese oyster (*Crassostrea gigas*) was provided by the commercial hatchery *Roem van Yerseke* (Yerseke, The Netherlands) on 3 June 2009. This batch was transported within 15 min to a temperature-regulated room (19°C) at the *Netherlands Institute of Ecology* (Yerseke, The Netherlands) and evenly distributed into 15 beakers of 4.5 l (larval concentration of ~ 15 ind. ml^{-1}), containing filtered ($0.2 \mu\text{m}$) seawater from the Oosterschelde, the nearby tidal inlet. Five treatments were considered, each of them in triplicate (see Fig. 1 for the experimental setup). One treatment served as a control i.e. beakers were gently bubbled with external ambient air. Two beakers were bubbled with air at 1000 and 2000 μatm of CO_2 (T2 and T3, respectively). The fourth treatment (T4) was bubbled with external ambient air, after total alkalinity (A_T) was decreased to $\sim 1000 \mu\text{mol kg}^{-1}$ by adding 14 ml of HCl 0.1 N and 10.6 g of $\text{CaCl}_2 \cdot 2\text{H}_2\text{O}$ in order to reach saturation states with respect to aragonite and calcite of 1.4 and 2.2, respectively. The last group of beakers (T5) was bubbled with 4000 μatm CO_2 and A_T was increased by adding 1.6 g of NaHCO_3 . Gas cylinders with certified CO_2 concentrations (1000, 2000 and 4000 μatm) were supplied by Westfalen. Embryos were allowed to develop, without additional feeding, until larvae reached the shelled D-veliger stage, i.e. 72 h.

Carbonate chemistry measurements

Seawater pH (on the total scale, hereafter referred to as pH_T) and temperature were measured twice a day in the beakers. pH_T was measured using a pH meter (Metrohm, 826 pH mobile) with a glass electrode (Metrohm, electrode plus) calibrated on the total scale using Tris/HCl and 2-aminopyridine/HCl buffer solutions with a salinity of 35.0 [20]. Samples for salinity and A_T were taken at the start and at the end of the experiment. Samples for A_T were filtered on GF/F filters, poisoned with HgCl_2 and stored in the dark pending measurement (within few days). Salinity was measured using a conductimeter (Radiometer CDM230). Triplicate potentiometric measurements of A_T were performed using a Metrohm titrator and a glass electrode (Metrohm, electrode plus). Measurements were carried out on 50 ml samples at 25°C and A_T was calculated using a Gran function. Titrations of A_T from standard seawater provided by A. G. Dickson (batch 82, $n = 10$) were on average within $0.46 \mu\text{mol kg}^{-1}$ of the nominal value. All parameters of the carbonate chemistry were determined from pH_T , A_T , temperature and salinity using the R package seacarb [21].

Sampling and measurements

At the end of the incubation period, the beakers were emptied. Two liters were passed through a $30 \mu\text{m}$ sieve and concentrated in 50 ml that was fixed in a 5% neutralized-formalin seawater solution to determine developmental success (% of D-veliger larvae) and D-veliger shell length and area. The developmental success into viable D-shaped larvae was defined as the percentage

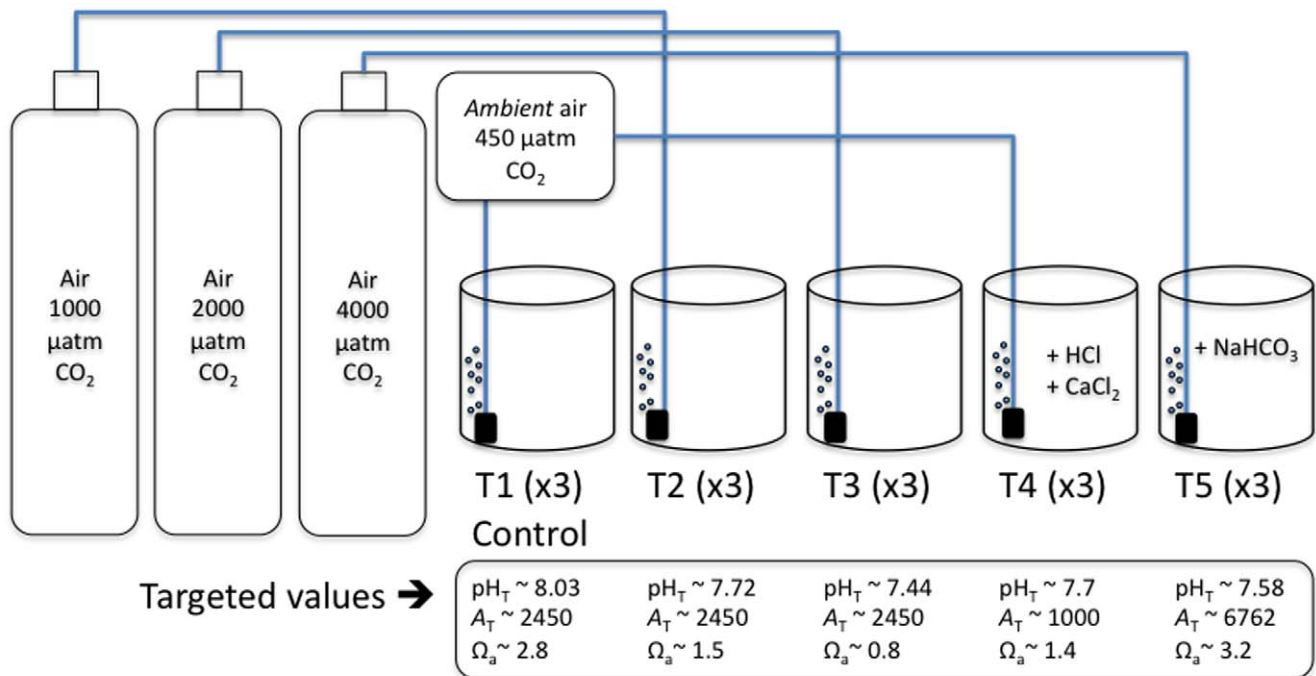


Figure 1. Experimental set-up. For each treatment (in triplicate; $T = 18.9 \pm 0.1^\circ\text{C}$), the target A_T (total alkalinity in $\mu\text{mol kg}^{-1}$), pH_T and Ω_a (saturation state of the seawater with respect to aragonite) are indicated. pH_T was controlled by bubbling ambient or high- CO_2 air. A_T was decreased in T4 by HCl addition and increased in T5 by NaHCO_3 addition. In T4, calcium concentrations have been increased above ambient levels by CaCl_2 addition. See text for more details.

doi:10.1371/journal.pone.0023010.g001

of “normal” D-shape larvae following the criteria proposed by His et al. [22], after observation of at least 500 larvae per replicated culture. D-veliger larvae shell length (anterior to posterior dimension of the shell parallel to the hinge) and area were measured on 100 larvae per replicate based on pictures taken under a microscope ($20\times$; $0.01\ \mu\text{m}$ precision in length measurement), using the software Leica Qwin Pro version 2.4. At the end of the experimental period, 2 l of the cultures were filtered onto GF/F

filters for subsequent analyses of calcium (Ca^{2+}) concentrations. Larvae-free seawater was filtered onto GF/F filters ($4\times$) and served as blanks for Ca^{2+} measurements. Ca^{2+} concentrations were determined by inductively coupled plasma emission spectrophotometry (ICP-OES) after multiple rinses with deionised water to remove seawater Ca^{2+} . In addition to Ca^{2+} from the larvae, Ca^{2+} retained on the filters may come from residual sea salts, from the GF/F filters themselves and/or from the analytical blank of the procedure. To

Table 1. Environmental parameters and carbonate chemistry for the five different treatments during the course of the experiment (mean \pm SD).

	T1 (control)	T2	T3	T4	T5
Measured parameters					
Temperature ($^\circ\text{C}$)	18.9 ± 0.1				
Salinity	34.0 ± 0.1	34.1 ± 0.1	34.1 ± 0.1	35.4 ± 0.1	34.3 ± 0.0
pH_T	8.03 ± 0.01	7.72 ± 0.03	7.41 ± 0.03	7.67 ± 0.03	7.62 ± 0.12
A_T ($\mu\text{mol kg}^{-1}$)	2452.7 ± 6.6	2446.2 ± 8.2	2443.1 ± 3.1	1093.8 ± 4.0	6726.6 ± 37.6
Computed parameters					
pCO_2 (μatm)	448.7 ± 15.6	1019.9 ± 79.9	2170.5 ± 156.9	493.5 ± 42.7	3730.4 ± 946.5
C_T ($\mu\text{mol kg}^{-1}$)	2207.0 ± 10.1	2340.8 ± 12.3	2443.4 ± 10.6	1029.4 ± 8.9	6589.3 ± 133.9
$[\text{HCO}_3^-]$	2010.0 ± 13.0	2209.4 ± 15.1	2320.3 ± 8.6	972.9 ± 9.8	6238.0 ± 161.9
$[\text{CO}_3^{2-}]$	181.9 ± 4.2	97.3 ± 6.3	50.4 ± 3.3	40.0 ± 2.4	226.5 ± 60.3
Ω_a	2.8 ± 0.1	1.5 ± 0.1	0.8 ± 0.1	$1.6 \pm 0.0^*$	3.5 ± 0.9
Ω_c	4.4 ± 0.1	2.3 ± 0.2	1.2 ± 0.1	$2.4 \pm 0.1^*$	5.4 ± 1.4

The partial pressure of CO_2 (pCO_2), dissolved inorganic carbon concentration (C_T) as well as the saturation state of seawater with respect to aragonite and calcite (Ω_a and Ω_c respectively) were computed from pH_T and total alkalinity (A_T).

*: Ω_a and Ω_c were increased by addition of calcium ($\text{CaCl}_2 \cdot 2\text{H}_2\text{O}$; $\times 2.6$ in situ Ca^{2+} concentrations).

doi:10.1371/journal.pone.0023010.t001

separate the contribution to total Ca^{2+} from these components, the filters were rinsed by soaking three times in 30 ml deionised water, increasing the duration each time, with approximately 10 sec allowed for the first rinse, 25 min for the second and an hour for the third. The water from each rinse was analyzed for Ca^{2+} and Na^+ to determine the seawater contribution, then acidified to ~ 0.1 M with nitric acid and reanalysed to determine the water insoluble component removed from the filters during rinsing. After the third rinse, remaining calcium was dissolved from the filters by immersing in 30 ml 0.1 M nitric acid for 30 minutes and the concentrations determined by ICP-OES. Ca^{2+} concentrations were then corrected for the concentration of Ca^{2+} observed on the blank filters following the same procedure and the total acid soluble Ca was calculated. As only one filter per treatment was analysed, the standard deviations associated with these measurements presented in the next section correspond to those for the blank filters. Calcium concentrations were normalized by the amount of eggs inoculated into the beakers at the start of the experiment, assuming that the distribution of the original batch has been performed homogeneously.

Statistics

Since normality and homoscedasticity tests could not be used due to the small number of replicates (3), differences in percentage of viable D-shaped larvae, final shell lengths and areas as well as in the amount of calcium incorporated between the different treatments were tested by means of Kruskal-Wallis tests and post-hoc Dunn's multiple comparison tests (Graphpad Instat software). For all tests, differences were considered significant at $p < 0.05$. In the following section, data are presented as means \pm SD. In order to relate the different measured parameters to the carbonate chemistry parameters at which the organisms were exposed during the incubations, linear and non-linear regressions were performed and the significance of these relationships was tested using student's t-tests.

Results and Discussion

The environmental (temperature and salinity) and carbonate chemistry parameters are shown in Table 1 for each treatment.

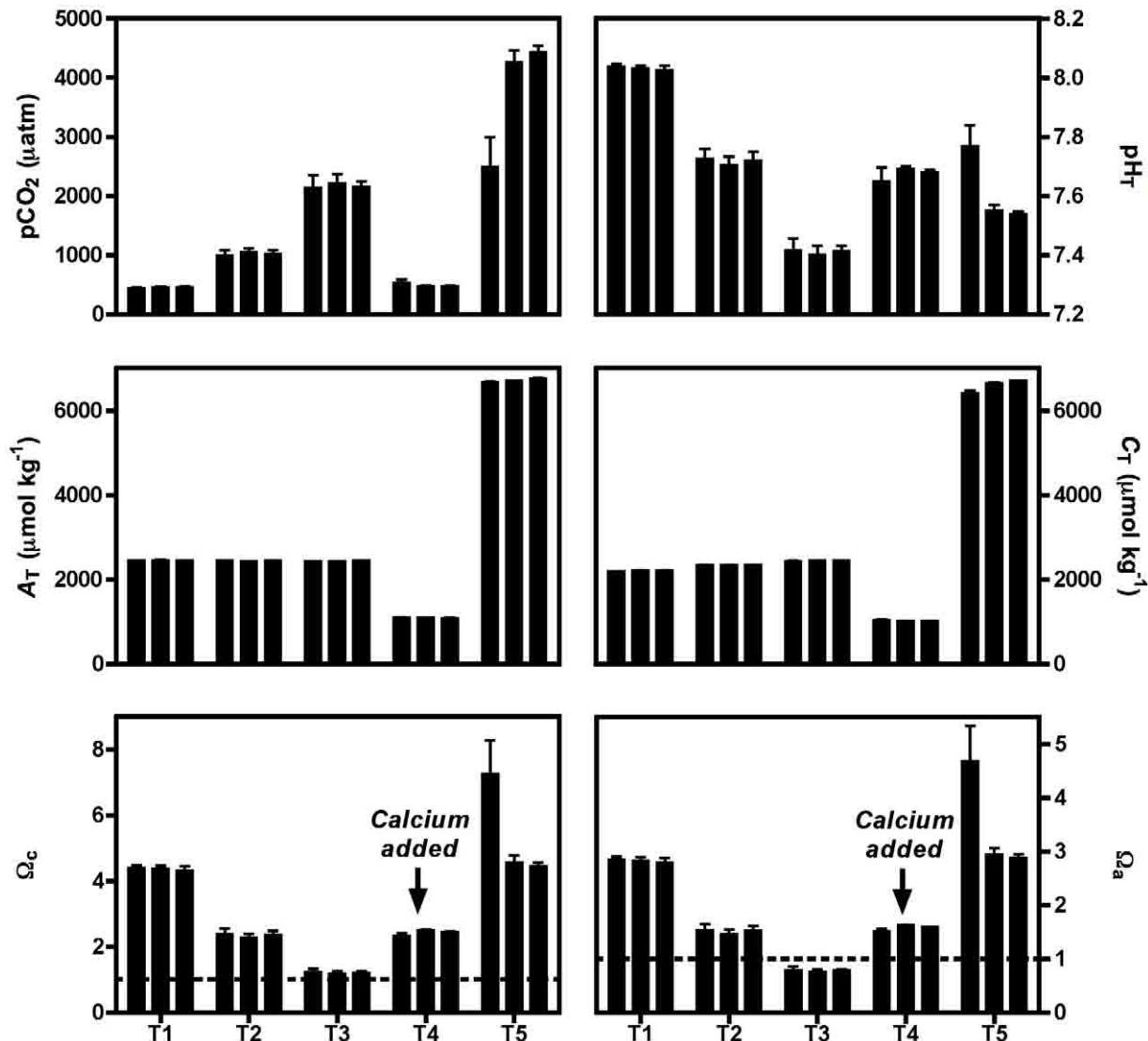


Figure 2. Carbonate chemistry conditions during the experimental period. pCO_2 : partial pressure of CO_2 , pH_T : pH on the total scale, A_T : total alkalinity, C_T : dissolved inorganic carbon, Ω_a and Ω_c : saturation state of the seawater with respect to, respectively, aragonite and calcite. doi:10.1371/journal.pone.0023010.g002

Parameters of the carbonate chemistry are also presented in Fig. 2 for each experimental beaker. Temperature was constant in the beakers at $18.9 \pm 0.1^\circ\text{C}$. Salinity was 34 ± 0.1 in the first three treatments while it was slightly higher in T5 (34.3 ± 0.0) due to the addition of NaHCO_3 and more than 1 unit higher in T4 due to CaCl_2 addition (35.4 ± 0.1). pCO_2 values were close to target values in most cases, except for one experimental beaker of T5 in which bubbling was not optimal and pCO_2 was much lower than the expected value (2502 vs. 4000 μatm). pH_T varied from 8.03 ± 0.01 in the control treatment (T1) to 7.41 ± 0.03 in the beakers that were bubbled with 2000 μatm CO_2 enriched air (T3). A_T was similar in the first 3 treatments while it has been successfully decreased to $\sim 1000 \mu\text{mol kg}^{-1}$ in T4 and increased to $\sim 6800 \mu\text{mol kg}^{-1}$ in T5. Total dissolved inorganic carbon (C_T) concentrations were the lowest in T4 ($1029 \pm 9 \mu\text{mol kg}^{-1}$) and the highest in T5 ($6589 \pm 134 \mu\text{mol kg}^{-1}$) with variable levels within the beakers due to the non-optimal CO_2 equilibration. Seawater was supersaturated with respect to calcite in all treatments with the lowest value for T3 (1.2 ± 0.1). Undersaturation with respect to aragonite was observed in T3 (0.8 ± 0.1) while the other 4 treatments showed Ω_arag values over 1, with a level of 1.6 ± 0.0 in T4 due to addition of CaCl_2 .

Developmental success into viable D-shaped larvae, average D-veliger shell length and area as well as the amount of Ca^{2+} incorporated per egg inoculated, for the five different treatments, are shown in Fig. 3. Percentages of viable D-shaped larvae were 90% in the control treatment and not significantly different between T1, T2, T3 and T5, while significantly lower values were observed for T4 beakers (average of $19 \pm 1\%$). Final D-veliger shell

length and area data showed the same pattern, with no significantly different values between T1, T2, T3 and T5 and significantly lower values in T4 as compared to the control treatment. Final D-veliger shell length and area were respectively $11 \pm 1\%$ and $20 \pm 2\%$ smaller in T4 as compared to control values. Significantly less Ca^{2+} was incorporated by the population in T4 than in the other treatments with a decrease of $45 \pm 14\%$ with respect to control values. Final D-veliger shell length and area as well as the amount of Ca^{2+} incorporated are plotted against pH_T and Ω_a in Fig. 4. None of these parameters were correlated with pH_T or Ω_a . Although seawater pH_T values in T4, T2 and T5 were similar at ~ 7.65 , the larvae were smaller in T4. Increasing the saturation state with respect to aragonite by adding Ca^{2+} (T4) did not positively affect the larval development since D-veliger shell length and area as well as the amount of Ca^{2+} incorporated were lower in T4 than in T2 which had similar Ω_a levels (i.e. ~ 1.5). On one hand, no significant linear and/or non-linear relationships were found between all these parameters and pH or Ω_a . On the other hand, these parameters were significantly correlated with the concentration of CO_3^{2-} ions. Michaelis-Menten functions were used to fit the data (shell length: $r^2 = 0.90$; shell area: $r^2 = 0.90$; calcium incorporated: $r^2 = 0.74$). Carbonate ion concentrations at the aragonite saturation level were estimated for each treatment (average of $64.4 \pm 0.2 \mu\text{mol kg}^{-1}$) and plotted as a dotted line on Fig. 4. Above the CO_3^{2-} saturation level, the effects of decreasing CO_3^{2-} concentrations on shell growth and Ca^{2+} incorporation as well as on the percentage of viable D-shaped larvae during these first 72 h of development were not significant (Fig. 4). Below the saturation level, decreasing CO_3^{2-} concentrations resulted in

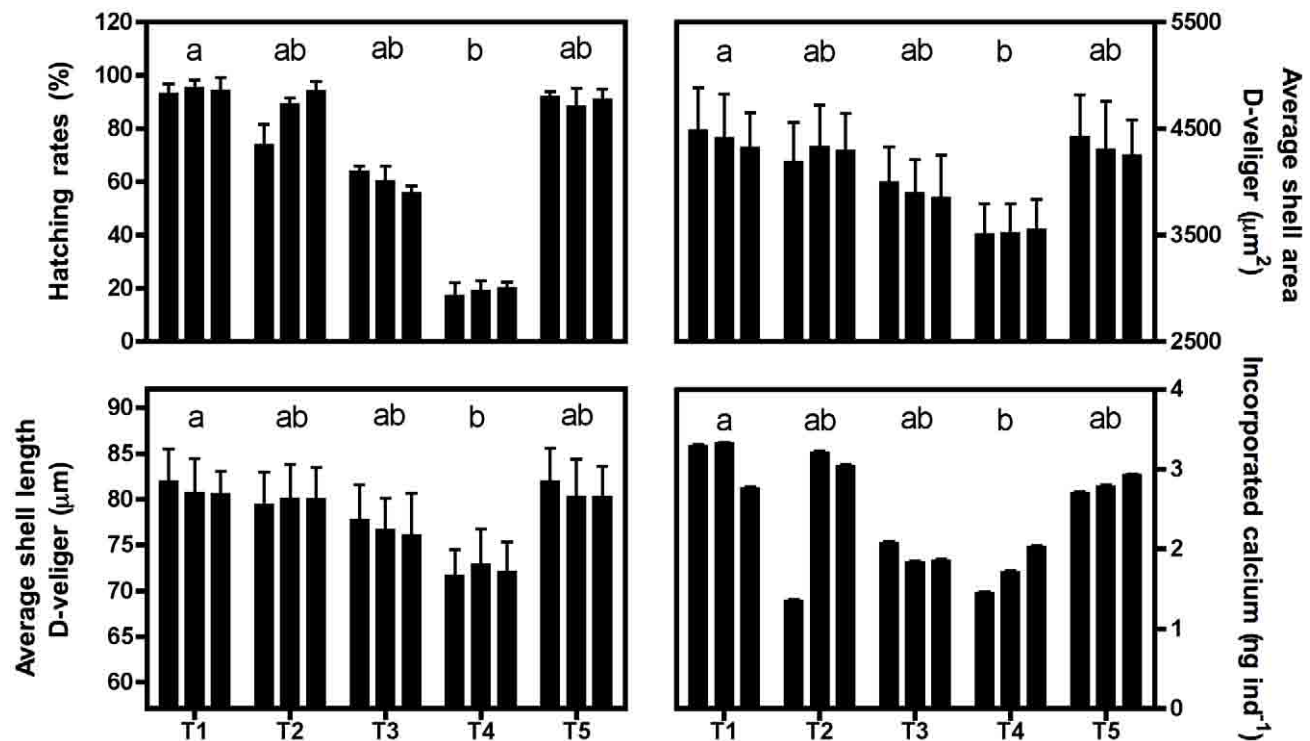


Figure 3. Larval developmental parameters at the end of the incubation period in the five treatments (72 h; T1 to T5). Proportion of embryos that developed to viable D-veliger ($\pm\text{SD}$; upper left plot), average shell area and length of D-veliger larvae ($\pm\text{SD}$; upper right and lower left plot, respectively) as well as the amount of calcium incorporated ($\pm\text{SE}$; lower right plot) are shown. Different letters on bars indicate significant differences in the median values (Kruskal-Wallis and post-hoc Dunn's multiple comparison tests, $p < 0.05$). doi:10.1371/journal.pone.0023010.g003

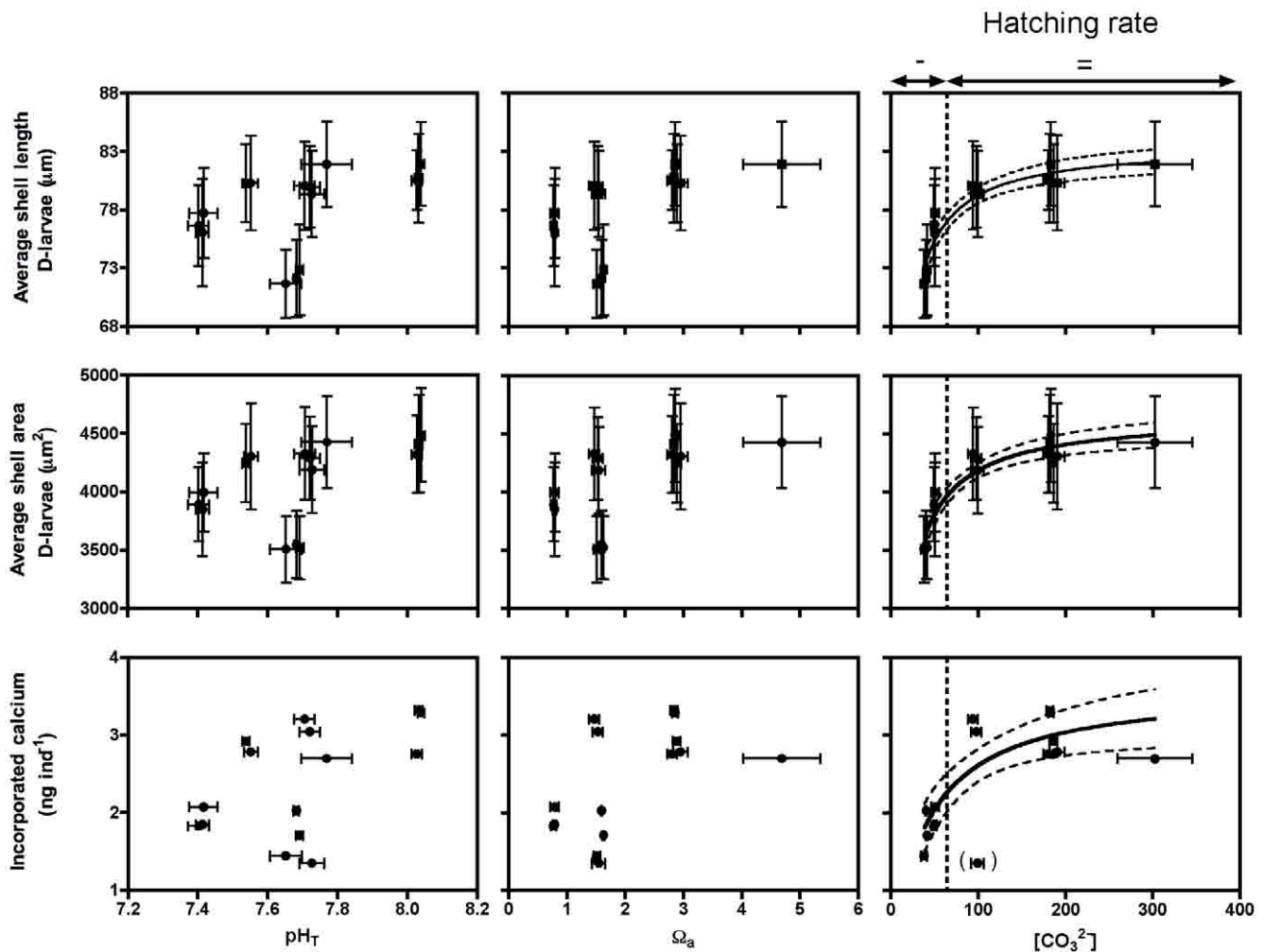


Figure 4. Relationships between larval developmental parameters and conditions of the carbonate chemistry in the five treatments. Relationships between the average (\pm SD) shell length and area of D-veliger larvae as well as the amount of calcium incorporated at the end of the 72 h incubation period, and the average (\pm SD) conditions of the carbonate chemistry in the five treatments are shown; pH_T: pH on the total scale (left plots), Ω_a : saturation state with respect to aragonite (middle plots) and [CO₃²⁻]: carbonate ion concentration (right plots). On the right plots, the dotted lines refer to the carbonate ion concentration at the aragonite saturation level (see text for details). doi:10.1371/journal.pone.0023010.g004

smaller larvae, less Ca²⁺ incorporation in the shells and much lower developmental success (decrease in percentage of viable D-veliger larvae).

The present study is, to the best of our knowledge, one of the first to investigate the effects of carbonate chemistry modifications on the growth of a marine calcifier by separately assessing the effects of decreases in pH, carbonate ion availability and seawater saturation state with respect to calcium carbonate. Separating these potential factors is crucial as total alkalinity levels are not constant in the ocean and a similar decrease in pH does not lead to similar decline in calcium carbonate saturation state. A similar study has been performed recently by Jury et al. [23], based on manipulations of the seawater carbonate chemistry, to determine which parameter controls coral calcification. They showed that the calcification rate of *Madracis auretenra* is mainly governed by the bicarbonate ions concentration and not, as expected, by the aragonite saturation state. In contrast, in the present study, the bicarbonate ion concentration as well as C_T concentration are not correlated with any of the physiological processes measured (data not shown). Moreover, the present study shows that pH is not the main driver of the observed decreases in developmental success

and growth rates. For instance, a decrease of pH_T to ~7.6 (T5; below the projected levels for the end of the present century) had no significant effect on these larvae with similar developmental success and growth rates as compared to control conditions. It must be stressed that, for this treatment, A_T was artificially increased in order to maintain a seawater saturation state with respect to aragonite above 1. This saturation state depends on the availability of both Ca²⁺ and CO₃²⁻ ions. Increasing Ca²⁺ concentrations in order to artificially maintain Ω_a above 1 (T4) had no beneficial effect on the larval development of oysters. As Ca²⁺ concentrations are not limiting in seawater (~10 mmol kg⁻¹), the main factor governing the growth of oyster larvae in our study was CO₃²⁻ ion concentration. Several studies have already shown limited effects of calcium addition above 10 mmol kg⁻¹ with coral calcification rates reaching a plateau at these concentrations [24,25]. The relationship between measured parameters (developmental success, shell length and area and incorporated calcium) and the availability of CO₃²⁻ showed that decreasing CO₃²⁻ levels only had significant effects on the larval development below CO₃²⁻ levels corresponding to aragonite saturation. On one hand, this is in contrast with results from Gazeau et al. [11] that showed that

D-veliger shells of the blue mussel (*Mytilus edulis*) were $5 \pm 1\%$ smaller following a 0.25–0.34 pH unit decrease corresponding to super-saturated conditions with respect to aragonite. On the other hand, Gazeau et al. [11] showed that developmental rates into viable D-shaped larvae at this pH level were not significantly altered, a finding which is consistent with present results. Accordingly, oyster larvae appear more resistant than blue mussel larvae to a decrease of pH as long as CO_3^{2-} concentrations remain above the aragonite saturation level. Further decreasing CO_3^{2-} concentrations below CO_3^{2-} values corresponding to aragonite saturation has dramatic consequences as only $\sim 60\%$ and $\sim 20\%$ of the embryos had developed to viable larvae at CO_3^{2-} concentrations of 50.4 ± 3.3 and $40.0 \pm 2.4 \mu\text{mol kg}^{-1}$, respectively, as compared to more than 90% in the treatments exposed to CO_3^{2-} supersaturated conditions. In the field, the different pressures exerted by the environment and predators result in considerable mortality rates, during the free-swimming larval period, possibly approaching 99% [26]. An additional decrease in developmental success as observed in the present study, under CO_3^{2-} concentrations below aragonite saturated conditions, could therefore compromise the survival of the populations.

Most calcifying species, including mollusks, are able to concentrate Ca^{2+} and CO_3^{2-} ions at the site of calcification [27] and should therefore be able to regulate calcification rates under suboptimal concentrations of Ca^{2+} and CO_3^{2-} . The fact that, even under CO_3^{2-} concentrations below aragonite saturated conditions (T3 and T4, assuming calcium addition has no effect in T4), some larvae were able to produce a shell highlights the efficiency of regulatory mechanisms. However, the percentage of embryos developing to viable D-veliger larvae and the shell sizes of these viable D-veliger larvae were smaller, suggesting that the regulation is not efficient enough to compensate for the low CO_3^{2-} ion availability below aragonite saturated conditions. Nevertheless, many molluscan species are adapted to and able to survive under low alkalinity conditions such as those in freshwater ecosystems. In the marine environment, bivalve growth has been reported by Tunnicliffe et al. [17] under extremely undersaturated

conditions prevailing close to deep hydrothermal sites, although shell growth rates were significantly lower than in non-acidified areas. Recently, Thomsen et al. [28] have shown that blue mussels are actively growing in a bay of the Western Baltic Sea naturally enriched with high CO_2 water, and also juvenile recruitment occurs in summer time coinciding with low pH levels and aragonite undersaturated conditions. In the Oosterschelde tidal inlet (1998–2006, monthly measurements, 5 stations), surface pH_{NBS} varied annually between 8.00 and 8.24, while A_T varied between 2334 and $2567 \mu\text{mol kg}^{-1}$ (data not shown). The organisms inhabiting this ecosystem are therefore never exposed to corrosive waters and are even used to relatively high calcium carbonate saturation levels, especially in spring at the time of recruitment. Whether the organisms inhabiting environments with relatively high calcium carbonate saturation levels will be able to adapt to the anticipated decreases in pH and saturation levels in the coming decades remains an open question. According to the present results, the effects of ocean acidification on larvae of *Crassostrea gigas* from the Oosterschelde estuary during the first 3 days of development are not significant as long as CO_3^{2-} concentrations remains above aragonite saturated conditions. Due to relatively high levels of total alkalinity in this area, it is not expected that seawater will become corrosive for aragonite following a decrease of 0.3 to 0.4 pH unit. However, the present study only focused on the developmental period between embryos and D-veliger larvae, there is still a need to perform experiments on the full larval development of this species and to investigate the response of other crucial physiological processes that have not been considered in the present study such as respiration and excretion.

Author Contributions

Conceived and designed the experiments: FG J-PG JP CHRH JJM. Performed the experiments: FG. Analyzed the data: FG J-PG MG HE CHRH JJM. Contributed reagents/materials/analysis tools: FG J-PG MG HE JP CHRH JJM. Wrote the paper: FG J-PG MG JJM.

References

- Orr JC, Fabry VJ, Aumont O, Bopp L, Doney SC, et al. (2005) Anthropogenic ocean acidification over the twenty-first century and its impact on calcifying organisms. *Nature* 437: 681–686.
- Caldeira K, Wickett ME (2003) Anthropogenic carbon and ocean pH. *Nature* 425: 365–365.
- Pörtner HO, Langenbuch M, Reipschläger A (2004) Biological impact of elevated ocean CO_2 concentrations: Lessons from animal physiology and earth history. *Journal of Oceanography* 60: 705–718.
- Caldeira K, Archer D, Barry JP, Bellerby RGJ, Brewer PG, et al. (2007) Comment on “Modern-age buildup of CO_2 and its effects on seawater acidity and salinity” by Hugo A. Loaiciga. *Geophysical Research Letters* 34: 3.
- Doney SC, Fabry VJ, Feely RA, Kleypas JA (2009) Ocean acidification: the other CO_2 problem. *Annual Review of Marine Science* 1: 169–192.
- Medakovic D (2000) Carbonic anhydrase activity and biomineralization process in embryos, larvae and adult blue mussels *Mytilus edulis* L. *Helgolander Marine Research* 54: 1–6.
- Green MA, Jones ME, Boudreau CL, Moore RL, Westman BA (2004) Dissolution mortality of juvenile bivalves in coastal marine deposits. *Limnology and Oceanography* 49: 727–734.
- Gutiérrez JL, Jones CG, Strayer DL, Iribarne OO (2003) Mollusks as ecosystem engineers: the role of shell production in aquatic habitats. *Oikos* 101: 79–90.
- Norling P, Kautsky N (2007) Structural and functional effects of *Mytilus edulis* on diversity of associated species and ecosystem functioning. *Marine Ecology Progress Series* 351: 163–175.
- Ellis RP, Bersey J, Rundle SD, Hall-Spencer JM, Spicer JJ (2009) Subtle but significant effects of CO_2 acidified seawater on embryos of the intertidal snail, *Littorina obtusata*. *Aquatic Biology* 5: 41–48.
- Gazeau F, Gattuso J-P, Dawber C, Pronker AE, Peene F, et al. (2010) Effect of ocean acidification on the early life stages of the blue mussel *Mytilus edulis*. *Biogeosciences* 7: 2051–2060.
- Kurihara H, Asai T, Kato S, Shimatsu A (2008) Effects of elevated pCO_2 on early development in the mussel *Mytilus galloprovincialis*. *Aquatic Biology* 4: 225–233.
- Kurihara H, Kato S, Shimatsu A (2007) Effects of increased seawater CO_2 on early development of the oyster *Crassostrea gigas*. *Aquatic Biology* 1: 91–98.
- Miller AW, Reynolds AC, Sobrino C, Riedel GF (2009) Shellfish face uncertain future in high CO_2 world: Influence of acidification on oyster larvae calcification and growth in estuaries. *PLoS ONE* 4: e5661.
- Parker LM, Ross PM, O'Connor WA (2009) The effect of ocean acidification and temperature on the fertilization and embryonic development of the Sydney rock oyster *Saccostrea glomerata* (Gould 1850). *Global Change Biology* 15: 2123–2136.
- Talmage SC, Gobler CJ (2009) The effects of elevated carbon dioxide concentrations on the metamorphosis, size, and survival of larval hard clams (*Mercentaria mercenaria*), bay scallops (*Argopecten irradians*), and Eastern oysters (*Crassostrea virginica*). *Limnology and Oceanography* 54: 2072–2080.
- Watson S-A, Southgate PC, Tyler PA, Peck LS (2009) Early larval development of the Sydney Rock oyster *Saccostrea glomerata* under near-future predictions of CO_2 -driven ocean acidification. *Journal of Shellfish Research* 28: 431–437.
- Talmage SC, Gobler CJ (2010) Effects of past, present, and future ocean carbon dioxide concentrations on the growth and survival of larval shellfish. *Proceedings of the National Academy of Sciences* 107: 17246–17251.
- Weiss IM, Tuross N, Addadi L, Weiner S (2002) Mollusc larval shell formation: Amorphous calcium carbonate is a precursor phase for aragonite. *Journal of Experimental Zoology* 293: 478–491.
- Dickson AG, Sabine CL, Christian JR (2007) Guide to best practices for ocean CO_2 measurements.
- Lavigne H, Gattuso J-P (2011) seacarb: seawater carbonate chemistry with R. R package version 2.4.2. The Comprehensive R Archive Network. Available: <http://CRAN.R-project.org/package=seacarb>. Accessed 2011 July 12.

22. His E, Seaman MNL, Beiras R (1997) A simplification of the bivalve embryogenesis and larval development bioassay method for water quality assessment. *Water Research* 31: 351–355.
23. Jury CP, Whitehead RF, Szmant AM (2010) Effects of variations in carbonate chemistry on the calcification rates of *Madracis auretenra* (= *Madracis mirabilis* sensu Wells, 1973): bicarbonate concentrations best predict calcification rates. *Global Change Biology* 16: 1632–1644.
24. Tambutte E, Allemand D, Mueller E, Jaubert J (1996) A compartmental approach to the mechanism of calcification in hermatypic corals. *Journal of Experimental Biology* 199: 1029–1041.
25. Ip YK, Krishnaveni P (1991) Incorporation of strontium ($^{90}\text{Sr}^{2+}$) into the skeleton of the hermatypic coral *Galaxea fascicularis*. *Journal of Experimental Zoology* 258: 273–276.
26. Bayne BL (1976) *Marine mussels: their ecology and physiology*. Cambridge: Cambridge University Press. 506 p.
27. McConnaughey TA, Gillikin DP (2008) Carbon isotopes in mollusk shell carbonates. *Geo-Marine Letters* 28: 287–299.
28. Thomsen J, Gutowska MA, Saphörster J, Heinemann A, Trübenbach K, et al. (2010) Calcifying invertebrates succeed in a naturally CO_2 -rich coastal habitat but are threatened by high levels of future acidification. *Biogeosciences* 7: 3879–3891.

BY CLAUDINE HAURI, NICOLAS GRUBER,
GIAN-KASPER PLATTNER, SIMONE ALIN,
RICHARD A. FEELY, BURKE HALES,
AND PATRICIA A. WHEELER

OCEAN ACIDIFICATION IN THE CALIFORNIA CURRENT SYSTEM

ABSTRACT. Eastern boundary upwelling systems (EBUS) are naturally more acidic than most of the rest of the surface ocean. Observations of EBUS already show pH values and saturation states with regard to the carbonate mineral aragonite that are as low as those expected for most open ocean waters several decades from now. Thus, as atmospheric CO₂ increases further, EBUS are prone to widespread and persistent undersaturation with regard to aragonite, making them especially sensitive to ocean acidification. Here, we describe ocean carbonate chemistry and its short-term-to-seasonal variability in one major EBUS, the California Current System (CCS), based on observations and results from an eddy-resolving regional model. Results reveal high variability in ocean carbonate chemistry, largely driven by seasonal upwelling of waters with low pH and saturation states, and subsequent interactions of transport and biological production. Model simulations confirm that the pH of CCS waters has decreased by about 0.1 pH unit and by 0.5 in saturation state since pre-industrial times. A first assessment of the vulnerability of CCS marine organisms and ecosystems to ocean acidification suggests that there will be winners and losers, likely provoking changes in species composition. Benthic organisms appear to be among those that will be most affected by the continuing acidification of the CCS. More accurate projections require special consideration of the integrated effects of ocean acidification, ocean warming, decreasing oxygen levels, and other processes that are expected with global change.

INTRODUCTION

Oceanic uptake of anthropogenic CO₂ from the atmosphere increases seawater's concentration of CO₂, but lowers its carbonate ion concentration and its pH (Caldeira and Wickett, 2003, 2005; Feely et al., 2004; Orr et al., 2005). Marine organisms, from microbes to large predatory fish and mammals, may be very sensitive to these chemical changes, potentially leading to substantial ecological and biogeochemical shifts (Hare et al., 2007). Of particular concern is the crossing of thresholds, such as when seawater becomes undersaturated with regard to biogenically produced calcium carbonate minerals (i.e., reaches the state where minerals are prone to dissolution; Feely et al., 2004; Kleypas et al., 2006; Fabry et al., 2008; Guinotte and Fabry, 2008; Doney et al., 2009). However, critical thresholds may already have been passed; many organisms, such as corals,

respond negatively to a lowering of the saturation state even though the waters are still supersaturated (Hoegh-Guldberg et al., 2007). Global mean surface pH has already decreased by approximately 0.1 units, from about 8.2 to 8.1, since the pre-industrial period, and, depending on future levels of atmospheric CO₂, pH is expected to decrease by another 0.3–0.4 units by the end of the century (Orr et al., 2005).

To assess the potential vulnerability of marine organisms and biogeochemical processes to these changes, it is not sufficient to determine only global mean changes in pH, carbonate ion concentrations, and carbonate saturation states. Global changes might not adequately reflect regional variability and thus may mask the urgency of the problem and its regional acuteness. Regional variations in ocean acidification are the result of long-term changes in carbonate chemistry

being superimposed on its natural variability, which is significant relative to predicted ocean acidification-driven changes, even in the surface ocean. These variations in natural acidity levels may put some marine organisms in certain regions at greater risk earlier. To date, attention has been focused on surface waters at high latitudes, which have a naturally low pH and low carbonate saturation states because thermodynamic factors support high dissolved inorganic carbon (DIC) concentrations relative to alkalinity for the same atmospheric CO₂ levels (Orr et al., 2005; McNeil et al., 2008; Steinacher et al., 2009). As a result, these regions are expected to become undersaturated with regard to calcium carbonate minerals more quickly than the rest of the ocean. Annually, both the Arctic Ocean and the Southern Ocean may become undersaturated with respect to aragonite (the less-stable form of calcium carbonate) during this century (Orr et al., 2005; Steinacher et al., 2009). Seasonally, this threshold may occur within the next few decades (McNeil et al., 2008). The Arctic surface ocean is projected to become completely undersaturated with respect to aragonite as early as 2040 (Steinacher et al., 2009), with 10% of the area already having become undersaturated at least one month per year during this decade. The carbonate system changes in ocean waters at temperate latitudes have received less attention because these surface waters have a higher pH, on average, and are strongly supersaturated with respect to aragonite and calcite. As a result, it has generally been concluded that critical thresholds will not be crossed until much later in these regions. Here, we demonstrate that eastern

boundary upwelling systems (EBUS), such as the California Current System (CCS), are particularly vulnerable to future ocean acidification. Recent CCS observations show that nearshore regions are currently exposed to waters that exhibit chemical conditions like those predicted for open-ocean surface waters several decades into the future (Feely et al., 2008). These observations also show that the aragonite saturation horizon already reaches the surface in certain regions during strong upwelling events (Figure 1a). With only a little additional CO₂, surface waters in these regions likely will become permanently undersaturated with regard to aragonite. Given the economic and biogeochemical importance of EBUS (e.g., Chavez and Toggweiler, 1995), it is essential to assess the potential impacts of ocean acidification in these regions. We focus here on the CCS, but we expect similar results for other major EBUS, particularly the Humboldt Current System, because they are subject to the same governing processes.

We first characterize CCS chemical conditions in greater detail, and then attempt to assess the vulnerability of CCS organisms and ecosystems to continued ocean acidification. We also account for the fact that ocean acidification does not act in isolation, but that

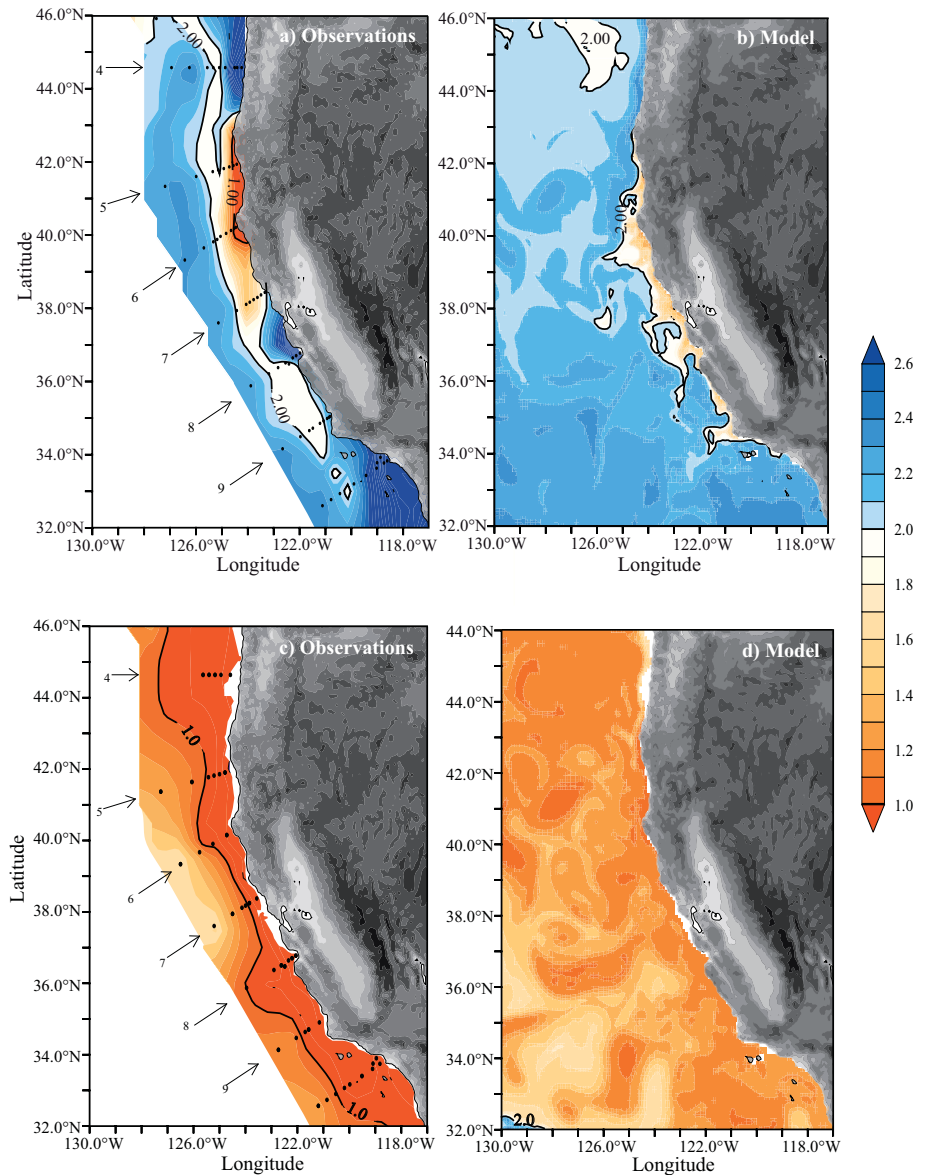


Figure 1. Maps of the aragonite saturation state for the California Current System (CCS) off the US West Coast in mid May. Observations (a, c) and model simulations (b, d) are shown for the surface (a, b) and for 120 m (c, d). Observations are from Feely et al. (2008) and model results are based on ROMS simulations (Gruber et al., 2006)

Claudine Hauri (claudine.hauri@env.ethz.ch) is PhD Candidate, Environmental Physics, Institute of Biogeochemistry and Pollutant Dynamics, ETH Zurich, Zurich, Switzerland. **Nicolas Gruber** is Professor, Environmental Physics, Institute of Biogeochemistry and Pollutant Dynamics, ETH Zurich, Zurich, Switzerland. **Gian-Kasper Plattner** is Research Scientist, Environmental Physics, Institute of Biogeochemistry and Pollutant Dynamics, ETH Zurich, Zurich, Switzerland, and is now Affiliate Scientist at the Climate and Environmental Physics Group, Physics Institute, University of Bern, Bern, Switzerland. **Simone Alin** is Oceanographer, Coastal Carbon Dynamics, Pacific Marine Environmental Laboratory, National Oceanic and Atmospheric Administration (NOAA), Seattle, WA, USA. **Richard A. Feely** is Program Leader, CO₂ Program, Pacific Marine Environmental Laboratory, NOAA, Seattle, WA, USA. **Burke Hales** is Associate Professor, College of Oceanic and Atmospheric Sciences, Oregon State University, Corvallis, OR, USA. **Patricia A. Wheeler** is Distinguished Professor Emeritus, College of Oceanic and Atmospheric Sciences, Oregon State University, Corvallis, OR, USA.

future changes likely will be characterized by warmer and more stratified conditions as well as by more frequent and severe occurrences of low-oxygen waters (hypoxia; e.g., Plattner et al., 2002; Oschlies et al., 2008). Due to the currently very limited understanding of the sensitivity of organisms and ecosystems to ocean acidification, our assessment is by necessity just a first step and remains generally qualitative. Our goal is to identify CCS ecosystem vulnerability in order to provide guidance for future research and management activities.

THE CARBONATE CHEMISTRY OF THE CALIFORNIA CURRENT SYSTEM

The generally low pH and saturation state of nearshore waters in the CCS is a direct consequence of coastal upwelling. Upwelling is driven by the seasonal shift to a southward (alongshore) wind that pushes surface waters offshore from approximately April through October, causing subsurface waters to be pulled to the surface (upwelled) nearshore. These upwelled waters follow long paths on their transit to the CCS, and are isolated from the surface ocean for many years. Along their journey, these waters accumulate the products of organic matter respiration, which rain down from the illuminated surface waters above, resulting in waters that are high in nutrients and dissolved CO_2 , but low in oxygen, pH, and carbonate saturation state. For example, for waters that are upwelled off the Oregon coast, respiration adds more than $200 \mu\text{mol kg}^{-1}$ of DIC to the source waters. This addition results in a pH decrease of over 0.3 units, and an increase in the partial pressure of CO_2 ($p\text{CO}_2$) of over 700 μatm relative

to presumed pre-industrial conditions. During strong upwelling, Feely et al. (2008) observed seawater with pH values as low as 7.75, and undersaturation with respect to aragonite starting at depths ranging from the surface to 120 m along the northern US Pacific coast (Figure 1a, c). Biweekly observations from a time-series site in Santa Monica Bay over more than five years confirm this shallow depth for the saturation horizon, but also show great temporal variability, mostly associated with intermittent upwelling events and passing mesoscale eddies (recent work of the authors; see also Leinweber et al., 2009). The high nutrient content of the upwelled waters makes the CCS a highly productive ocean region, leading to high rates of photosynthetic fixation of the upwelled nutrients and CO_2 . As the upwelled waters are pushed

offshore by a combination of Ekman transport and mesoscale eddies, this photosynthetic removal of CO_2 lowers the surface $p\text{CO}_2$, sometimes even far below atmospheric levels (Hales et al., 2005). This CO_2 drawdown brings a concomitant increase in surface water pH and carbonate mineral saturation state. The highly turbulent nature of the CCS, driven by the instabilities of the California Current and the nearshore undercurrent, causes the various waters to mix in a complex manner, leading to a highly variable mosaic of surface ocean carbonate saturation states and pH values that reflect transport and reaction (Figures 1b and 2).

Coupling the Regional Ocean Modeling System (ROMS) to a simple ecological-biogeochemical model produced the snapshots shown in Figures 1b, d, and 2 (Gruber et al., 2006).

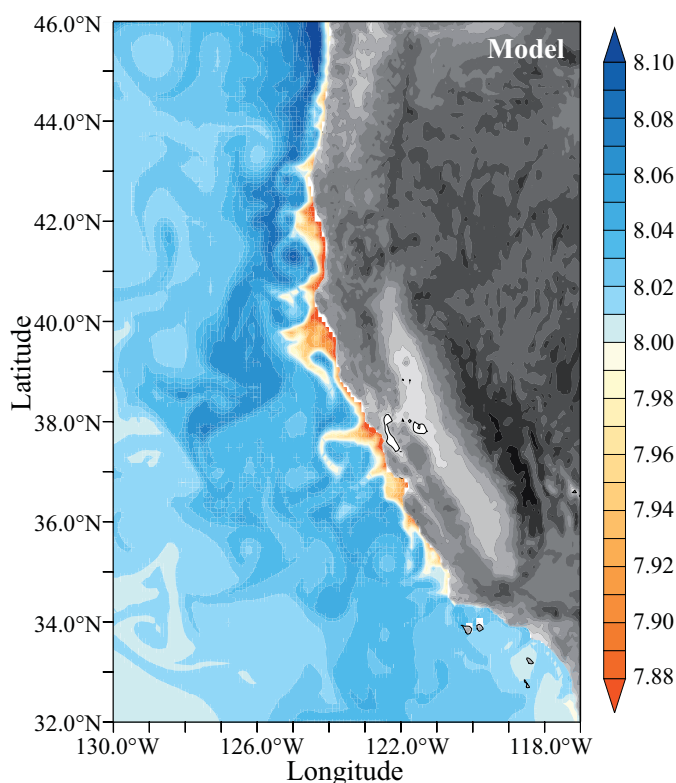


Figure 2. Model-simulated snapshot of surface pH for the month of August. Low-pH waters in nearshore areas are the result of seasonal upwelling in summer, while the elevated pH in offshore waters reflects the photosynthetic removal of CO_2 from the water as it is transported offshore.

The three-dimensional, eddy-resolving model simulates the flow and mixing of ocean waters at a resolution of 5 km. This fine resolution enables representation of the processes of upwelling and subsequent transport and mixing by eddies, which occur at scales of tens of kilometers. Typical global models, with resolutions of 100 km or more, would not capture such processes. ROMS is set up for a domain covering the entire US West Coast from 28°N to 48°N and incorporates the effect of ocean acidification on carbonate chemistry by responding to elevated atmospheric CO₂ levels and elevated DIC concentrations at the lateral boundaries (see Box 1 for details).

We use our model results to put the springtime observations from Feely et al.

(2008) into a seasonal and wider spatial context. Field data (Feely et al., 2008) and model results show similar low levels of aragonite saturation (Ω_{ar}) along the coast, especially near the California-Oregon border (41°N–42°N) (Figure 1). Although Feely et al. (2008) observed surface water to be undersaturated at some locations near the coast (Figure 1a transect line 5), the model snapshot for mid May shows, for surface waters, a minimum Ω_{ar} of 1.2 (Figure 1b). However, the saturation state decreases rapidly with depth (see also Figure 3), so that in the model, waters also become undersaturated with respect to aragonite at depths as shallow as 10 m. At 120-m depth, observations (Figure 1c) show pervasive undersaturation along

a roughly 100-km-wide strip off the US West Coast, with a clear onshore-offshore gradient in saturation state. The model simulates a similar spatial pattern, but it tends to overestimate the aragonite saturation state by about 0.2 units (Figure 1c, d), likely due to potential biases in the saturation state prescribed at the lateral boundaries (see Box 1 for discussion).

Because seasonally resolved, large-scale observations of oceanic pH and carbonate saturation state along the US West Coast are lacking, we use the model to characterize the temporal variability of chemical water properties. We focus here on the region near the California-Oregon border, where the lowest aragonite saturation states were

BOX 1. DESCRIPTION OF MODEL AND SIMULATION SETUP

The Regional Ocean Modeling System (ROMS) is a three-dimensional, eddy-resolving physical circulation model that simulates flow and mixing of ocean waters and is configured at a resolution of 5 km (ROMS ETHZ) for a domain covering the US West Coast (Marchesiello et al., 2003; Shchepetkin and McWilliams, 2005). ROMS is coupled to a nitrogen-based nutrient-phytoplankton-zooplankton-detritus (NPZD) biogeochemical model and includes a representation of the marine carbon cycle (Gruber et al., 2006). The model was forced at surface with monthly climatologies of momentum and density fluxes computed from QuikSCAT and the Comprehensive Ocean-Atmosphere Data Set (COADS) data products, respectively. Initial conditions for temperature and salinity were taken from the World Ocean Atlas 2001 database (http://www.nodc.noaa.gov/OC5/WOA01/pr_woa01.html). Monthly climatological means were also used to prescribe temperature, salinity, and momentum fluxes along the three lateral open

boundaries following a radiative scheme. Initial and boundary conditions for the inorganic carbon system (dissolved inorganic carbon [DIC] and alkalinity) are based on GLObal Ocean Data Analysis Project (GLODAP) data (Key et al., 2004) for pre-industrial and present-day simulations. A seasonal cycle was added to the DIC boundary conditions using the monthly climatology of $p\text{CO}_2$ and assuming constant alkalinity. A limitation of the GLODAP database is that the observations used to create this gridded product do not include the US West Coast, but come from far offshore in the Pacific Ocean. We suspect that extrapolation of these observations toward the shore led to too low DIC concentrations at a given depth at the lateral boundaries of our model (i.e., too high saturation states). This overestimation of the saturation state at the lateral boundaries would then have caused the observed biases of our modeled aragonite saturation states in the nearshore areas (see text).

observed and modeled. Snapshots of vertical sections of modern-day aragonite saturation state for each of the four seasons reveal strong seasonal variations close to the coast (Figure 3). During the winter months (Figure 3a), the water exhibits a uniform horizontal chemical pattern, with the upper 40 m of the water column being supersaturated with an Ω_{ar} range of 1.8 to 2, and with the saturation horizon located at about 300-m depth. During spring, waters with lower aragonite saturation states are upwelled close to the coast, causing a drop of Ω_{ar} to values of less than 2 in the entire water column within 20 km of the coast (Figure 3b). During the summer months, due to upwelling and high remineralization rates, Ω_{ar} drops further to values of

less than 1.3 in the entire water column within 10 km of the coast. The entire water column of the nearshore region within 30 km of the coast has Ω_{ar} values less than 2 (Figure 3c). In close proximity to the coast, the saturation horizon shoals almost to the surface. In fall, nearshore areas still experience saturation states with $\Omega_{ar} < 1.2$, and waters with Ω_{ar} values less than 2 expand to about 100 km offshore (Figure 3d).

These results suggest that organisms living at shallow depths and in close proximity to the coast are not only frequently exposed to low saturation states (and pH) but also to chemical conditions that can change on short time scales. Within 50 km of the coast, the aragonite saturation state of the entire

water column from the surface down to 100 m undergoes large seasonal changes (Figure 4). The percentage of water volume that has a saturation state $\Omega_{ar} > 2$ (blue) decreases from more than 75% in winter to about 35% in summer. This is a substantial decrease, because water with saturation states $\Omega_{ar} < 2$ could cause a threat to some organisms (see below). The water volume that has an $\Omega_{ar} < 1.5$ (orange) increases from less than 5% in winter to 25% in summer and to 40% in fall. The first peak in summer is due to the acidification stemming from remineralization of the organic matter produced by phytoplankton blooms that were triggered by nutrient-rich upwelled water. The second peak in November is likely also caused by acidification from

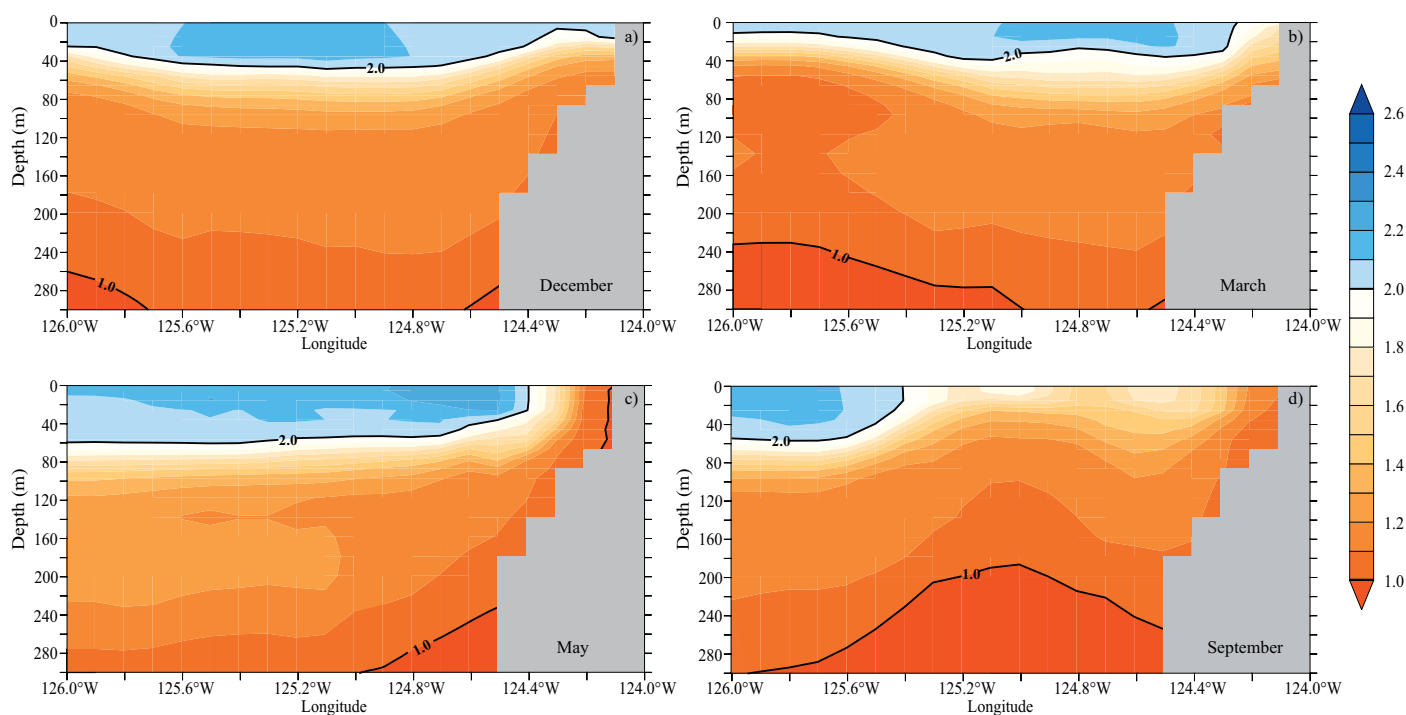


Figure 3. Model-simulated vertical offshore sections of the aragonite saturation state in the northern CCS near Point St. George (41.7°N). Snapshots are for the months of (a) December, (b) March, (c) May, and (d) September.

remineralization of the organic matter. It is now accentuated because the reduced photosynthetic activity in the fall is no longer offsetting this effect as efficiently as during the summer.

Although much of the low pH and saturation state of waters that upwell in the CCS can be attributed to respiration-derived CO_2 , some fraction stems from the oceanic uptake of anthropogenic CO_2 . Upwelled waters were last in contact with the atmosphere only a few decades ago, recently enough for them to have been exposed to elevated atmospheric CO_2 at that time, thereby taking up some of it. For the central CCS, Feely et al. (2008) estimate a transit time of about 40–50 years, resulting in an anthropogenic CO_2 content of about $31 \pm 4 \mu\text{mol kg}^{-1}$. Although this amounts to only about a tenth of the metabolic CO_2 addition, it is sufficient to shoal the saturation horizon with respect to aragonite minerals several tens of meters. The ROMS-based simulations of pre-industrial and current (year 2000) conditions support this conclusion. Results

for the years 1750 and 2000 show that surface pH decreased (from 8.14 to 8.05) and surface ocean saturation state with regard to aragonite decreased (from 2.7 to 2.3) due to the increase in atmospheric CO_2 . The model also indicates that water masses that had an $\Omega_{\text{ar}} > 2.5$ in 1750 have by now been replaced completely by water masses with a saturation state $\Omega_{\text{ar}} < 2.1$, with a growing percentage of water with $\Omega_{\text{ar}} < 1.5$ (Figure 4).

With atmospheric CO_2 bound to increase further (Tans et al., 2009), pH and saturation state in the CCS inevitably will decrease further, possibly causing surface pH to go as low as 7.6 and causing waters to become undersaturated with regard to aragonite along large stretches of the US West Coast in the next few decades. Given this prospect, it is critical to assess which organisms and ecosystems in the CCS are vulnerable to such changes so that appropriate mitigation and adaptation strategies can be developed and implemented.

VULNERABILITY OF ORGANISMS AND INFLUENCE ON FISHERIES

When assessing the potential vulnerability of organisms and ecosystems to ocean acidification in the CCS (see the brief overview in Table 1), it is important to consider that organisms are already frequently exposed to water with low pH and saturation levels, especially during upwelling events and in near-shore regions. As a result, it may be expected that they are well adapted to variable conditions, and therefore more resilient to future changes (see, e.g., Deutsch et al., 2008). But this expectation may be applicable only if future changes do not move the chemical environment substantially outside of its natural envelope of variability. Given current projections of future CO_2 levels, this expectation is feasible in the CCS, despite the large level of variability. Furthermore, the growth and success of an individual species in a changing ocean depends on many environmental factors. In the case of phytoplankton, these factors include nutrients and iron

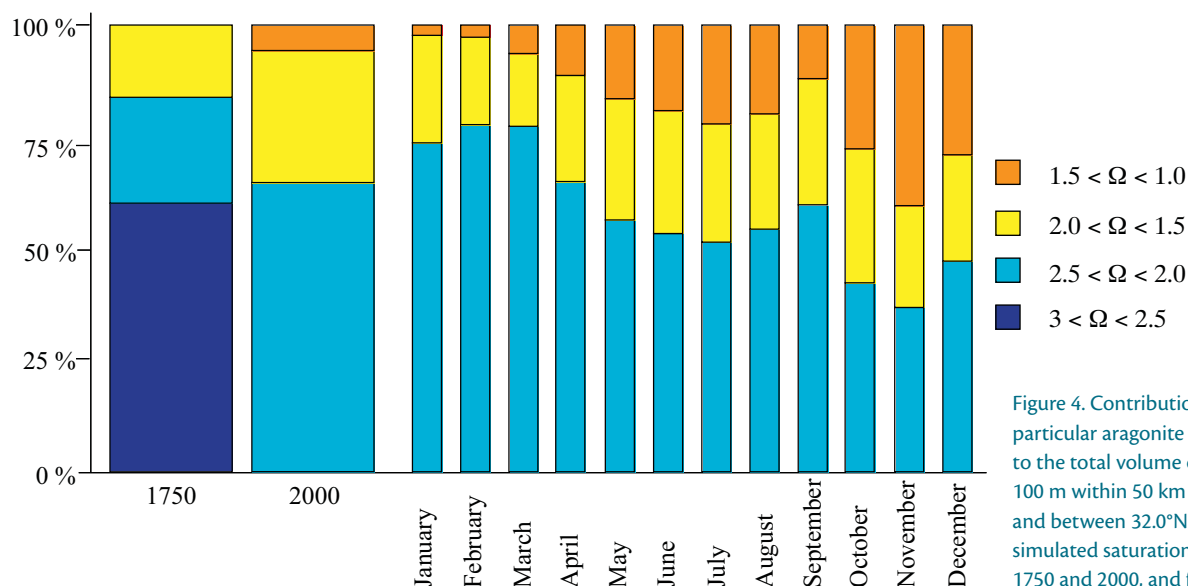


Figure 4. Contribution of waters with a particular aragonite saturation state relative to the total volume of water in the upper 100 m within 50 km of the US West Coast and between 32.0°N and 46.0°N. Model-simulated saturation states are shown for 1750 and 2000, and for each month in 2000.

availability, temperature, light, and predation (Hare et al., 2007; Tortell et al., 1997, 2008). Because many of these factors might change in parallel in the future, and given the lack of experiments that cover a combination of all factors, any conclusions about future phytoplankton compositions in the CCS remain speculative. Nevertheless, our preliminary assessment (Table 1) suggests that ocean acidification in the CCS will cause a species shift in open

ocean phytoplankton, with diatoms possibly profiting at the expense of calcifying phytoplankton.

Similar conclusions can be drawn for nearshore and benthic primary producers. The two dominant species of the giant kelp forest (*Saccharina* and *Nereocystis*) exhibit species-specific adverse responses to low pH and high UVB (Swanson and Fox, 2007), suggesting that any combination of these two global change factors could possibly

lead to a change in species composition and reduced biodiversity.

Secondary producers in the CCS can be affected both directly as a result of a change in seawater chemistry, and also indirectly by changes in food quality, prey disappearance, and altered timing of phytoplankton blooms. Limited experiments available today suggest that the aragonite-shelled pteropods, foraminifera, and planktonic life stages of bivalves and echinoderms are affected

Table 1. Expected vulnerability of marine flora and fauna to ocean acidification. Level of understanding indicates consistency of results and/or possibility that natural system can reach experimental pH. *Adapted from Fabry et al., 2008*

	Vulnerability	Level of Understanding	Comment	References
Diatoms	Low	High	Increased productivity, smaller or larger chain-forming species (?)	Tortell et al., 1997, 2008; Hare et al., 2007
Coccolithophorid	Medium	Low	Species specific response in calcification, increased photosynthesis	Iglesias-Rodriguez et al., 2008; Engel et al., 2005
Kelp	Medium	Medium	Species specific response in photosynthesis	Swanson and Fox, 2007
Copepods	Medium	Low	Shallow water copepods showed less tolerance to high $p\text{CO}_2$ than deep water copepods	Watanabe et al., 2006
Noncalcifying tunicate	Low	Medium	Increased growth, development, and fecundity	Dupont and Thorndyke, 2009
Shelled pteropod	High	Low	Shell dissolution	Orr et al., 2005; Fabry et al., 2008
Foraminifera	High	Medium	8–14% reduction in shell mass	Spero et al., 1997; Bijma et al., 1999, 2002; Moy et al., 2009
Sea urchin	Medium	Medium	Species specific, lack of pH regulation, decreased fertilization success	Burnett et al., 2002; Dupont and Thorndyke, 2008
Mussel	High	High	Decreased calcification in saturated water; dissolution and mortality in undersaturated water	Gazeau et al., 2007
Oyster	Medium	High	Decrease in calcification rate, highly vulnerable larval stage	Gazeau et al., 2007; Lee et al., 2006
Dungeness crab	Low	Low	Capable of pH regulation during 24 h	Pane and Barry, 2007
Cold water corals	High	Low	Experimental results only for warm water corals	Guinotte and Fabry, 2008
Coralline algae	High	Medium	Decrease in calcification rate, net dissolution, disappearance	Martin and Gattuso, 2009

directly by ocean acidification as they experience either rapid shell dissolution and reduced calcification ability or larvae develop with a temporal delay, build abnormal asymmetry, and often die before metamorphosis in aragonite-

for the local industry relying on marine resources. Once the aragonite saturation horizon has permanently reached the surface, organisms sensitive to ocean acidification may vanish, move elsewhere, or develop new physiological

In total, aragonite-calcifying species accounted for 23% of the total US West Coast catch value of about \$384M in 2007 (Figure 5), suggesting that either a loss in quality or a decrease in quantity of this subgroup will impact fisheries income substantially. Additionally, consequences of these species' disappearance could cascade through the food web because aragonite-forming organisms are found at very low or mid-trophic food levels. To what extent this indirect effect of ocean acidification will impact predators and thus the remaining CCS catch will strongly depend on whether other prey are available and whether the predators can switch prey.

The problems associated with ocean acidification provoke discussions and raise questions for the fishing industry (Warren, 2009). Supporting sustainable fish stocks is no longer just a matter of resilient catch quantity but also of maintaining suitable habitat. Ocean acidification is a problem of habitat degradation. Knowledge about the impact of ocean acidification on fish stocks and total financial loss is thus crucial to managing fisheries in a changing ocean and to driving policies that can protect the ocean.

INTEGRATED EFFECTS

Ocean acidification is just one of several stress factors, which include hypoxia, anomalous sea surface temperatures, pollution, and overfishing, that are challenging CCS ecosystems. Although overfishing and marine pollution are two independent problems that are manageable at the local scale, global warming and ocean acidification are directly linked and can only be addressed globally.

In addition, increasing sea surface

OCEAN ACIDIFICATION HAS ALREADY DECREASED MEAN SURFACE WATER pH IN THE CCS TO A LEVEL THAT WAS NOT EXPECTED TO HAPPEN FOR OPEN-OCEAN SURFACE WATERS FOR SEVERAL DECADES.

undersaturated waters (Orr et al., 2005; Fabry et al., 2008; Kurihara et al., 2008; Dupont and Thorndyke, 2009; Lebrato et al., in press). However, Dupont and Thorndyke (2009) point out that such negative responses are species specific, so that the primary effect in a future, more acidic ocean is likely to be a shift in species composition rather than the complete disappearance of an entire class of organisms. Recent abundance observations have not indicated any significant decrease in CCS pteropod population size (Ohman and Lavaniegos, 2008), whereas the Pacific oyster *Crassostrea gigas* exhibited recruitment failure during four consecutive years (2005–2008; Elston et al., 2008). *C. gigas* has an aragonitic larval stage, making it exceptionally vulnerable to decreasing aragonite saturation states (Lee et al., 2006). Whether or not ocean acidification has caused these heavy losses in the backbone of the US West Coast shellfish industry remains unclear.

Overall, ocean acidification in the CCS could become a severe challenge

survival strategies. The aragonite shells of mussels, sea urchins, and gastropods could soon experience dissolution (Burnett et al., 2002; Gazeau et al., 2007; Hall-Spencer et al., 2008; Wootton et al., 2008). However, survival strategies such as the production of a protective outer organic periostracum, developed by the mussel *Bathymodiolus brevior*, may support life in extreme conditions of pH down to 5.4 (Tunnicliffe et al., 2009). Comparing the potential vulnerability of different species and ecosystems, we conclude that benthic organisms will probably be most affected by ocean acidification in the CCS.

They will be exposed to the lowest pH and aragonite saturation states in the nearshore, shallow areas, and many of them appear to be sensitive to ocean acidification. Moreover, their ability to migrate is limited. Given our limited understanding, this conclusion should be viewed as a preliminary assessment rather than a final conclusion.

What could the potential impact of these changes be on fisheries in the CCS?

temperature and stratification tend to enhance low-oxygen conditions in the CCS, adding another stressor, with resultant cascading effects on benthic and pelagic ecosystems (Bograd et al., 2008). A further expansion of low-oxygen conditions could also be driven by ocean acidification. An ocean-acidification-induced reduction in production of mineral ballast by calcifying organisms will result in reduced transport of organic matter to the deeper layers of the ocean, thus leading to enhanced remineralization of organic matter in shallow waters (Balch and Utgoff, 2009). This effect leads to higher oxygen demand in the upper ocean, resulting in a drop in the dissolved oxygen concentration there (Hofmann and Schellnhuber, 2009). Because these waters constitute the source of the upwelling waters in the CCS, such a decrease likely will cause

more frequent low-oxygen events along the US West coast in the future. This ocean deoxygenation could substantially amplify the impact of ocean acidification on marine ecosystems in the CCS (Brewer and Peltzer, 2009).

Such concomitant perturbations also complicate their detection and surveillance. Because it is difficult to link stress signs to particular causes, and well-known stress factors may mask others, management actions could be wrong or late. A decrease in fish stocks could be mistaken to be a result of overfishing although caused in reality by direct or indirect effects of climate change and ocean acidification. The consequences of such a misreading could have large economic and ecological dimensions, as management would focus on fisheries policy improvement instead of supporting actions to mitigate CO₂.

SUMMARY

Ocean acidification has already decreased mean surface water pH in the CCS to a level that was not expected to happen for open-ocean surface waters for several decades. However, present-day surface pH in the CCS exhibits considerable spatial and temporal variability. This variability could provide the basis for a certain degree of adaptability by marine organisms in this region to future ocean acidification, but only as long as future changes do not move substantially out of this natural range—a move that is feasible. If atmospheric CO₂ continues to increase at current rates in the near future, both pH and saturation state will decrease even more, further shoaling the saturation horizon and possibly moving it up into the euphotic zone year round. Responses of marine organisms and ecosystems to

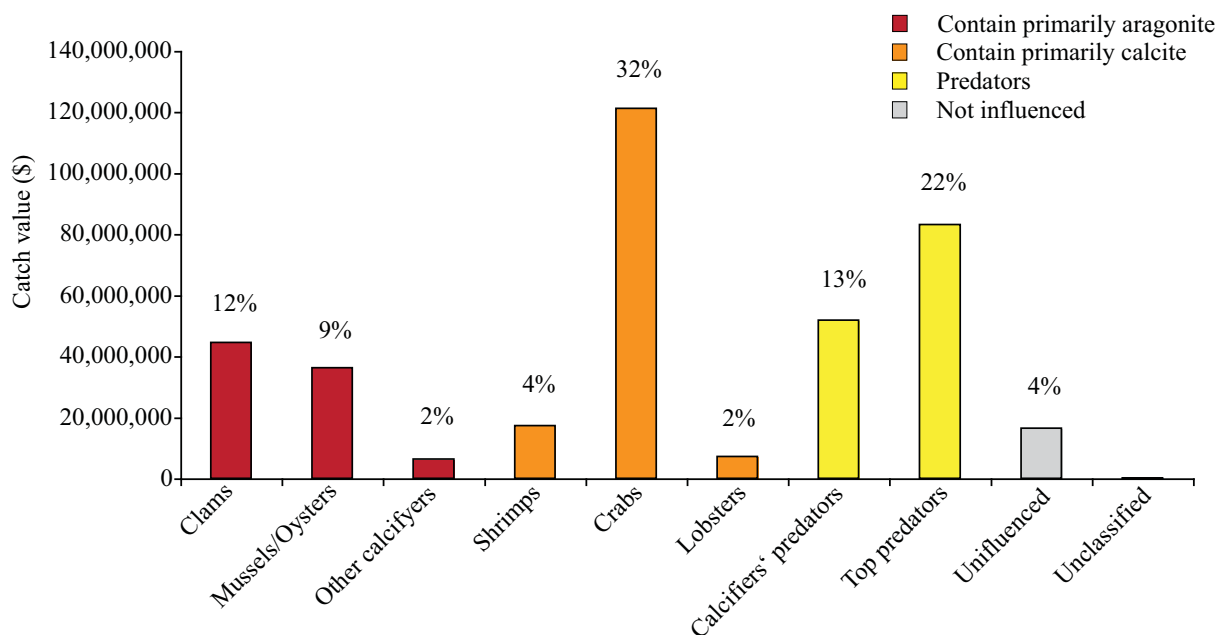



Figure 5. US West Coast commercial fishing ex-vessel revenue (the price paid at the time the fish are delivered by the commercial fisherman to the fish receiver or processor) for 2007 (adapted from Cooley and Doney, 2009, using NOAA National Marine Fisheries Service statistics), including California, Oregon, Washington, and Pacific, and at sea. Colors indicate which form (if any) of calcium carbonate these groups contain. Based on present understanding, organisms containing aragonite are most likely to be affected by ocean acidification.

such permanently low-pH conditions are not yet well investigated. Thus, we must improve our currently insufficient understanding of the consequences of ocean acidification for individual organisms, entire ecosystems, marine biogeochemical cycling, and feedbacks to the climate system in order to inform policymakers and provide a sound science basis for urgent decisions regarding CO₂ mitigation. Meanwhile, it is important to lower the pressure on marine ecosystems from other stressors such as pollution, coastal degradation, and eutrophication to make these systems less vulnerable to the changing marine chemical conditions associated with increasing CO₂.

ACKNOWLEDGEMENTS

We are grateful to Zouhair Lachkar and Damian Loher for providing us with results from their ROMS simulations. Claudine Hauri's work was funded by the European Project on Ocean Acidification (EPOCA), which received funding from the European Community's Seventh Framework Programme (FP7/2007-2013) under grant agreement no. 211384. EPOCA is endorsed by the international programs Integrated Marine Biogeochemistry and Ecosystem Research (IMBER), Land-Ocean Interactions in the Coastal Zone (LOICZ), and Surface Ocean Lower Atmosphere Study (SOLAS). Nicolas Gruber and Gian-Kasper Plattner acknowledge support by ETH Zurich. Richard A. Feely and Simone R. Alin were supported by the NOAA Climate Program under the Office of Climate Observations (Grant No. GC04-314 and the Global Carbon Cycle Program (Grant No. GC05-288). Pacific Marine Environmental Laboratory contribution number 3453. 

REFERENCES

- Balch, W.M., and P.E. Utgoff. 2009. Potential interactions among ocean acidification, coccolithophores, and the optical properties of seawater. *Oceanography* 22(4):146–159.
- Bijma, J., H.J. Spero, and D.W. Lea. 1999. Reassessing foraminiferal stable isotope geochemistry: Impact of the oceanic carbonate systems (experimental results). Pp. 489–512 in *Use of Proxies in Paleoceanography: Examples from the South Atlantic*. G. Fisher and G. Wefer, eds., Springer-Verlag, New York, NY.
- Bijma, J., B. Honisch, and R.E. Zeebe. 2002. Impact of the ocean carbonate chemistry on living foraminiferal shell weight: Comment on “Carbonate ion concentration in glacial-age deepwaters of the Caribbean Sea” by W.S. Broecker and E. Clark. *Geochemistry, Geophysics, Geosystems* 3(1064), doi:10.1029/2002GC000388.
- Bograd, S.J., C.G. Castro, E. Di Lorenzo, D.M. Palacios, H. Bailey, W. Gilly, and F.P. Chavez. 2008. Oxygen declines and the shoaling of the hypoxic boundary in the California Current. *Geophysical Research Letters* 35, doi:10.1029/2008GL034185.
- Brewer, P.G., and E.T. Peltzer. 2009. Oceans: Limits to marine life. *Science* 324:347–348.
- Burnett, L., N. Terwilliger, A. Carroll, D. Jorgensen, and D. Scholnick. 2002. Respiratory and acid-base physiology of the purple sea urchin, *Strongylocentrotus purpuratus*, during air exposure: Presence and function of a facultative lung. *Biological Bulletin* 203:42–50.
- Caldeira, K., and M.E. Wickett. 2003. Oceanography: Anthropogenic carbon and pH. *Nature* 425:365, doi:10.1038/425365a.
- Caldeira, K., and M.E. Wickett. 2005. Ocean model predictions of chemistry changes from carbon dioxide emissions to atmosphere and ocean. *Journal of Geophysical Research* 110, C09S04, doi:10.1029/2004JC002671.
- Chavez, F.P., and J.R. Toggweiler. 1995. Physical estimates of global new production: The upwelling contribution. Pp. 313–320 in *Upwelling in the Ocean: Modern Processes and Ancient Records*. C.P. Summerhayes, K.C. Emeis, M.V. Angel, R.L. Smith, and B. Zeitzschel, eds., J. Wiley & Sons, Chichester, UK.
- Cooley, S.R., and S.C. Doney. 2009. Anticipating ocean acidification's economic consequences for commercial fisheries. *Environmental Research Letters* 4, doi:10.1088/1748-9326/4/2/024007.
- Deutsch, C.A., J.J. Tewksbury, R.B. Huey, K.S. Sheldon, C.K. Ghalambor, D.C. Haak, and P.R. Martin. 2008. Impacts of climate warming on terrestrial ectotherms across latitude. *Proceedings of the National Academy of Sciences of the United States of America* 105(18):6,668–6,672, doi:10.1073/pnas.0709472105.
- Doney, S.C., V.J. Fabry, R.A. Feely, and J.A. Kleypas. 2009. Ocean acidification: The other CO₂ problem. *Annual Review of Marine Science* 1:169–192.
- Dupont, S., and M.C. Thorndyke. 2009. Impact of CO₂-driven ocean acidification on invertebrates' early life-history: What we know, what we need to know and what we can do. *Biogeosciences Discussions* 6:3,109–3,131.
- Dupont, S., and M.C. Thorndyke. 2008. Ocean acidification and its impact on the early life-history stages of marine animals. Pp. 89–97 in *Impacts of Acidification on Biological, Chemical and Physical Systems in the Mediterranean and Black Seas*. CIESM Workshop Monographs, n°36. F. Briand, ed., Monaco, 124 pp.
- Elston, R.A., H. Hasegawa, K.L. Humphrey, I.K. Polyak, C.C. Häse. 2008. Re-emergence of *Vibrio tubiashii* in bivalve shellfish aquaculture: Severity, environmental drivers, geographic extent and management. *Diseases of Aquatic Organisms* 82:119–134, doi:10.3354/dao01982.
- Engel, A., I. Zondervan, K. Aerts, L. Beaufort, A. Benthien, L. Chou, B. Delille, J.-P. Gattuso, J. Harlay, and C. Heemann. 2005. Testing the direct effect of CO₂ concentration on a bloom of the coccolithophorid *Emiliania huxleyi* in mesocosm experiments. *Limnology and Oceanography* 50(2):493–507.
- Fabry, V.J., B.A. Seibel, R.A. Feely, and J.C. Orr. 2008. Impacts of ocean acidification on marine fauna and ecosystem processes. *ICES Journal of Marine Science* 65:414–432.
- Feely, R.A., C.L. Sabine, K. Lee, W. Berelson, J. Kleypas, V.J. Fabry, and F.J. Millero. 2004. Impact of anthropogenic CO₂ on the CaCO₃ system in the oceans. *Science* 305(5682):362–366.
- Feely, R.A., C.L. Sabine, J.M. Hernandez-Ayon, D. Ianson, and B. Hales. 2008. Evidence for upwelling of corrosive “acidified” water onto the continental shelf. *Science* 320(5882):1,490–1,492, doi:10.1126/science.1155676.
- Gazeau, F., C. Quiblier, J.M. Jansen, J.-P. Gattuso, J.J. Middelburg, and C.H.R. Heip. 2007. Impact of elevated CO₂ on shellfish calcification. *Geophysical Research Letters* 34, L07603, doi:10.1029/2006GL028554.
- Gruber, N., H. Frenzel, S.C. Doney, P. Marchesiello, J.C. McWilliams, J.R. Moisan, J. Oram, G.-K. Plattner, and K.D. Stolzenbach. 2006. Eddy-resolving simulation of plankton ecosystem dynamics in the California Current System. *Deep-Sea Research Part I* 53:1,483–1,516, doi:10.1016/j.dsr.2006.06.005.
- Guinotte, J.M., and V.J. Fabry. 2008. Ocean acidification and its potential effects on marine ecosystems. *Annals of the New York Academy of Sciences* 1134:320–342, doi:10.1196/annals.1439.013.
- Hales, B., T. Takahashi, and L. Bandstra. 2005. Atmospheric CO₂ uptake by a coastal upwelling system. *Global Biogeochemical Cycles* 19, GB1009, doi:10.1029/2004GB002295.
- Hall-Spencer, J.M., R. Rodolfo-Metalpa, S. Martin, E. Ransome, M. Fine, S.M. Turner, S.J. Rowley, D. Tedesco, and M.C. Buia. 2008. Volcanic carbon

- dioxide vents show ecosystem effects of ocean acidification. *Nature* 454(7200):96–99, doi:10.1038/nature07051.
- Hare, C.E., K. Leblanc, G.R. Ditullio, R.M. Kudela, Y. Zhang, P.A. Lee, S. Riseman, and D.A. Hutchins. 2007. Consequences of increased temperature and CO₂ for phytoplankton community structure in the Bering Sea. *Marine Ecology Progress Series* 352:9–16, doi:10.3354/meps07182.
- Hoegh-Guldberg, O., P.J. Mumby, A.J. Hooten, R.S. Steneck, P. Greenfield, E. Gomez, C.D. Harvell, P.F. Sale, A.J. Edwards, K. Caldeira, and others. 2007. Coral reefs under rapid climate change and ocean acidification. *Science* 318(5857):1,737–1,742, doi:10.1126/science.1152509.
- Hofmann, M., and H.J. Schellnhuber. 2009. Oceanic acidification affects marine carbon pump and triggers extended marine oxygen holes. *Proceedings of the National Academy of Sciences of the United States of America* 106(9):3,017–3,022. doi:10.1073/pnas.0813384106.
- Iglesias-Rodriguez, M.D., P.R. Halloran, R.E.M. Rickaby, I.R. Hall, E. Colmenero-Hidalgo, J.R. Gittins, D.R.H. Green, T. Tyrrell, S.J. Gibbs, P. von Dassow, and others. 2008. Phytoplankton calcification in a high-CO₂ world. *Science* 320(5874):336–340, doi:10.1126/science.1154122.
- Kleypas, J.A., R.A. Feely, V.J. Fabry, C. Langdon, C.L. Sabine, and L.L. Robbins. 2006. *Impacts of Ocean Acidification on Coral Reefs and Other Marine Calcifiers: A Guide for Future Research*. Report of a workshop held 18–20 April 2005, St. Petersburg, FL, sponsored by NSF, NOAA, and the US Geological Survey, 88 pp.
- Kurihara, H. 2008. Effects of CO₂-driven ocean acidification on the early developmental stages of invertebrates. *Marine Ecology Progress Series* 373:275–284.
- Lee, S.W., S.M. Hong, and C.S. Choi. 2006. Characteristics of calcification processes in embryos and larvae of the Pacific oyster, *Crassostrea gigas*. *Bulletin of Marine Science* 78(2):309–317.
- Lebrato, M., D. Iglesias-Rodríguez, R.A. Feely, D. Greeley, D.O.B. Jones, N. Suarez-Bosche, R.S. Lampitt, J.E. Cartes, D.R.H. Green, and B. Alker. In press. Global contribution of echinoderms to the marine carbon cycle. *Ecological Monographs*.
- Leinweber, A., N. Gruber, H. Frenzel, G.E. Friederich, and F.P. Chavez. 2009. Diurnal carbon cycling in the surface ocean and lower atmosphere of Santa Monica Bay, California. *Geophysical Research Letters* 36, L08601, doi:10.1029/2008GL037018.
- Martin, S., and J.-P. Gattuso. 2009. Response of Mediterranean coralline algae to ocean acidification and elevated temperature. *Global Change Biology* 15:2,089–2,100, doi:10.1111/j.1365-2486.2009.01874.x.
- McNeil, B.I., and R.J. Matear. 2008. Southern Ocean acidification: A tipping point at 450-ppm atmospheric CO₂. *Proceedings of the National Academy of Sciences of the United States of America* 105(48), doi:10.1073/pnas.0806318105.
- Moy, A.D., W.R. Howard, S.G. Bray, and T.W. Trull. 2009. Reduced calcification in modern Southern Ocean planktonic foraminifera. *Nature Geoscience* 2:276–280, doi:10.1038/NGEO460.
- Ohmann, M.D., and B.E. Lavanegos. 2008. Multi-decadal variations in calcareous holo-zooplankton in the California Current System: Thecosome pteropods and foraminifera from CalCOFI. Paper OS31A-1238 presented at the American Geophysical Union Fall Meeting, San Francisco, 2008.
- Orr, J.C., V.J. Fabry, O. Aumont, L. Bopp, S.C. Doney, R.A. Feely, A. Gnanadesikan, N. Gruber, A. Ishida, F. Joos, and others. 2005. Anthropogenic ocean acidification over the twenty-first century and its impact on calcifying organisms. *Nature* 437(7059), doi:10.1038/nature04095.
- Oschlies, A., K.G. Schulz, U. Riebesell, and A. Schmittner. 2008. Simulated 21st century's increase in oceanic suboxia by CO₂-enhanced biotic carbon export. *Global Biogeochemical Cycles* 22, GB4008, doi:10.1029/2007GB003147.
- Pane, E.F., and J.P. Barry. 2007. Extracellular acid-base regulation during short-term hypercapnia is effective in a shallow-water crab, but ineffective in a deep-sea crab. *Marine Ecology Progress Series* 334:1–9.
- Plattner, G.-K., F. Joos, and T.F. Stocker. 2002. Revision of the global carbon budget due to changing air-sea oxygen fluxes. *Global Biogeochemical Cycles* 16(4), doi:10.1029/2001gb001746.
- Spero, H.J., J. Bijma, D.W. Lea, and B.E. Bemis. 1997. Effect of seawater carbonate concentration on foraminiferal carbon and oxygen isotopes. *Nature* 390(6659):497–500.
- Steinacher, M., F. Joos, T.L. Frolicher, G.K. Plattner, and S.C. Doney. 2009. Imminent ocean acidification in the Arctic projected with the NCAR global coupled carbon cycle-climate model. *Biogeosciences* 6(4):515–533.
- Swanson, A.K., and C.H. Fox. 2007. Altered kelp (Laminariales) phlorotannins and growth under elevated carbon dioxide and ultraviolet-B treatments can influence associated intertidal food webs. *Global Change Biology* 13(8):1,696–1,709, doi:10.1111/j.1365-2486.2007.01384.x.
- Tans, P. 2009. An accounting of the observed increase in oceanic and atmospheric CO₂ and an outlook for the future. *Oceanography* 22(4):26–35.
- Tortell, P.D., J.R. Reinfelder, and F.M.M. Morel. 1997. Active uptake of bicarbonate by diatoms. *Nature* 390(6657):243–244.
- Tortell, P.D., C.D. Payne, Y.Y. Li, S. Trimbora, B. Rost, W.O. Smith, C. Riesselman, R.B. Dunbar, P. Sedwick, and G.R. DiTullio. 2008. CO₂ sensitivity of Southern Ocean phytoplankton. *Geophysical Research Letters* 35(4), L04605, doi:10.1029/2007gl032583.
- Tunnicliffe, V., K.T.A. Davies, D.A. Butterfield, R.W. Embley, J.M. Rose, and W.W. Chadwick Jr. 2009. Survival of mussels in extremely acidic waters on a submarine volcano. *Nature Geoscience*, doi:10.1038/NGEO500.
- Warren, B. 2009. The big seven: Acidification risks and opportunities for the seafood industry. *Current: The Journal of Marine Education* 25(1):22–26.
- Watanabe, Y., A. Yamaguchi, H. Ishida, T. Harimoto, S. Suzuki, Y. Sekido, T. Ikeda, Y. Shirayama, M.M. Takahashi, T. Ohsumi, and J. Ishizaka. 2006. Lethality of increasing CO₂ levels on deep-sea copepods in the western North Pacific. *Journal of Oceanography* 62:185–196.
- Wootton J.T., C.A. Pfister, and J.D. Forester. 2008. Dynamic patterns and ecological impacts of declining ocean pH in a high-resolution multi-year dataset. *Proceedings of the National Academy of Sciences of the United States of America* 105(48): 18,848–18,853, doi:10.1073/pnas.0810079105.



The Geological Record of Ocean Acidification

Bärbel Hönisch, *et al.*

Science **335**, 1058 (2012);

DOI: 10.1126/science.1208277

This copy is for your personal, non-commercial use only.

If you wish to distribute this article to others, you can order high-quality copies for your colleagues, clients, or customers by [clicking here](#).

Permission to republish or repurpose articles or portions of articles can be obtained by following the guidelines [here](#).

The following resources related to this article are available online at www.sciencemag.org (this information is current as of March 1, 2012):

Updated information and services, including high-resolution figures, can be found in the online version of this article at:

<http://www.sciencemag.org/content/335/6072/1058.full.html>

Supporting Online Material can be found at:

<http://www.sciencemag.org/content/suppl/2012/03/01/335.6072.1058.DC2.html>

<http://www.sciencemag.org/content/suppl/2012/02/29/335.6072.1058.DC1.html>

This article **cites 193 articles**, 62 of which can be accessed free:

<http://www.sciencemag.org/content/335/6072/1058.full.html#ref-list-1>

This article appears in the following **subject collections**:

Geochemistry, Geophysics

http://www.sciencemag.org/cgi/collection/geochem_phys

The Geological Record of Ocean Acidification

Bärbel Hönisch,^{1*} Andy Ridgwell,² Daniela N. Schmidt,³ Ellen Thomas,^{4,5} Samantha J. Gibbs,⁶ Appy Sluijs,⁷ Richard Zeebe,⁸ Lee Kump,⁹ Rowan C. Martindale,¹⁰ Sarah E. Greene,^{2,10} Wolfgang Kiessling,¹¹ Justin Ries,¹² James C. Zachos,¹³ Dana L. Royer,⁵ Stephen Barker,¹⁴ Thomas M. Marchitto Jr.,¹⁵ Ryan Moyer,¹⁶ Carles Pelejero,¹⁷ Patrizia Ziveri,^{18,19} Gavin L. Foster,⁶ Branwen Williams²⁰

Ocean acidification may have severe consequences for marine ecosystems; however, assessing its future impact is difficult because laboratory experiments and field observations are limited by their reduced ecologic complexity and sample period, respectively. In contrast, the geological record contains long-term evidence for a variety of global environmental perturbations, including ocean acidification plus their associated biotic responses. We review events exhibiting evidence for elevated atmospheric CO₂, global warming, and ocean acidification over the past ~300 million years of Earth's history, some with contemporaneous extinction or evolutionary turnover among marine calcifiers. Although similarities exist, no past event perfectly parallels future projections in terms of disrupting the balance of ocean carbonate chemistry—a consequence of the unprecedented rapidity of CO₂ release currently taking place.

The geological record is imprinted with numerous examples of biotic responses to natural perturbations in global carbon cycling and climate change (Fig. 1), some of which could have been caused by large-scale ocean acidification. By reconstructing past changes in marine environmental conditions, we can test hypotheses for the causes and effects of future-

relevant stressors such as ocean acidification on ecosystems (1). However, for the fossil record to be of direct utility in assessing future ecosystem impacts, the occurrence and extent of past ocean

acidification must be unambiguously identified. In recent years, a variety of trace-element and isotopic tools have become available that can be applied to infer past seawater carbonate chemistry. For instance, the boron isotopic composition ($\delta^{11}\text{B}$) of marine carbonates reflects changes in seawater pH, the trace element (such as B, U, and Zn)-to-calcium ratio of benthic and planktic foraminifer shells records ambient $[\text{CO}_3^{2-}]$, and the stable carbon isotopic composition ($\delta^{13}\text{C}$) of organic molecules (alkenones) can be used to estimate surface ocean aqueous $[\text{CO}_2]$ (2).

Because direct ocean geochemical proxy observations are still relatively scarce, past ocean acidification is often inferred from a decrease in the accumulation and preservation of CaCO₃ in marine sediments, potentially indicated by an increased degree of fragmentation of foraminiferal shells (3). However, it is difficult to distinguish between the original calcification responses to chemical changes in the surface ocean and post-mortem conditions at the sea floor. For instance, planktic calcifiers may secrete heavier or lighter shells (4), but that signal may be modified at the sea floor through dissolution or overgrowth after deposition (5, 6). This duality can introduce controversy over the identification of causes and effects, the drivers of biological change, and

¹Lamont-Doherty Earth Observatory of Columbia University, Palisades, NY 10964, USA. ²School of Geographical Sciences, University of Bristol, Bristol BS8 1SS, UK. ³School of Earth Sciences, University of Bristol, Bristol, BS8 1RJ, UK. ⁴Department of Geology and Geophysics, Yale University, New Haven, CT 06520, USA. ⁵Department of Earth and Environmental Sciences, Wesleyan University, Middletown, CT 06459, USA. ⁶Ocean and Earth Science, National Oceanography Centre Southampton, University of Southampton, Southampton SO14 3ZH, UK. ⁷Department of Earth Sciences, Utrecht University, 3584 CD Utrecht, Netherlands. ⁸School of Ocean and Earth Science and Technology, Department of Oceanography, University of Hawaii at Manoa, Honolulu, HI 96822, USA. ⁹Department of Geosciences, Pennsylvania State University, University Park, PA 16802, USA. ¹⁰Department of Earth Sciences, University of Southern California (USC), Los Angeles, CA 90089, USA. ¹¹Museum für Naturkunde at Humboldt University, 10115 Berlin, Germany. ¹²Department of Marine Sciences, University of North Carolina—Chapel Hill, NC 27599, USA. ¹³Earth and Planetary Sciences Department, University of California Santa Cruz, CA 95064, USA. ¹⁴School of Earth and Ocean Sciences, Cardiff University, Cardiff CF10 3AT, UK. ¹⁵Department of Geological Sciences and Institute of Arctic and Alpine Research, University of Colorado, Boulder, CO 80309, USA. ¹⁶University of South Florida St. Petersburg, Department of Environmental Science, Policy, and Geography, St. Petersburg, FL 33701, USA. ¹⁷Institució Catalana de Recerca i Estudis Avançats and Department of Marine Biology and Oceanography, Consejo Superior de Investigaciones Científicas, 08003 Barcelona, Catalonia, Spain. ¹⁸Institute of Environmental Science and Technology, Universitat Autònoma de Barcelona, 01893 Barcelona, Spain. ¹⁹Department of Earth Sciences, Vrije Universiteit, 1081HV Amsterdam, Netherlands. ²⁰W. M. Keck Science Department of Claremont McKenna College, Pitzer College, and Scripps College, Claremont, CA 91711, USA.

*To whom correspondence should be addressed. E-mail: hoenisch@ldeo.columbia.edu

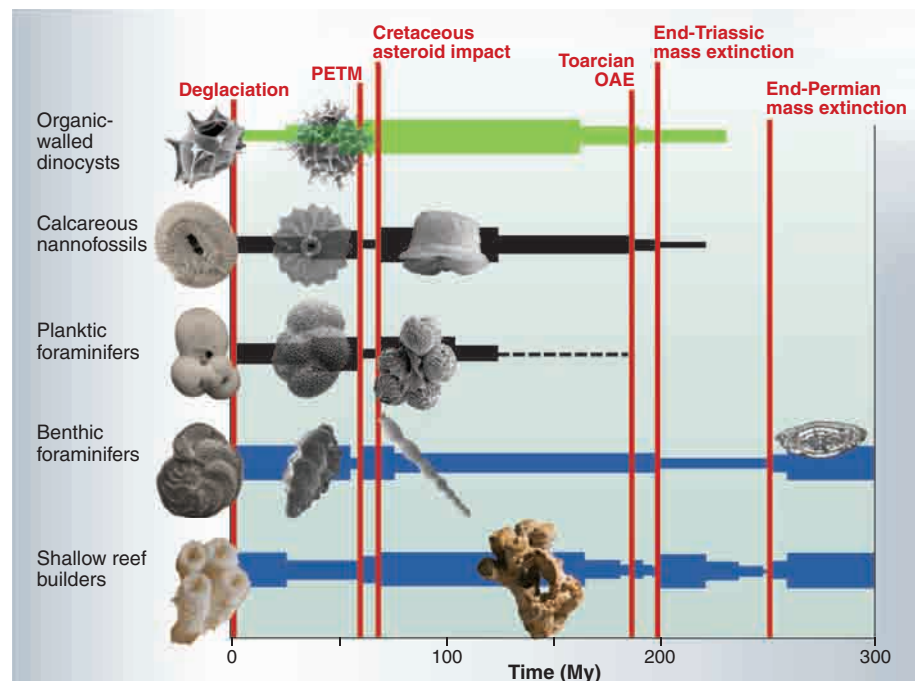


Fig. 1. Idealized diversity trajectories of the calcareous and organic fossil lineages discussed in the text. Extinction and radiation suggest events of major environmental change throughout the past 300 My. Calcareous plankton is shown in black, calcareous benthos in blue, and organic fossils in green, and the line thickness indicates relative and smoothed species richness. Highlighted events (vertical red lines) have been associated with potential ocean acidification events (Fig. 4). Calcareous organisms were not uniformly affected at all times, suggesting the importance of synergistic environmental factors to extinction, adaptation, and evolution as well as different sensitivity due to physiological factors. Identification of a paleo-ocean acidification event therefore requires independent geochemical evidence for ocean chemistry changes. Images of organisms are exemplary. References and further information on the displayed organisms are available in the supporting online material.

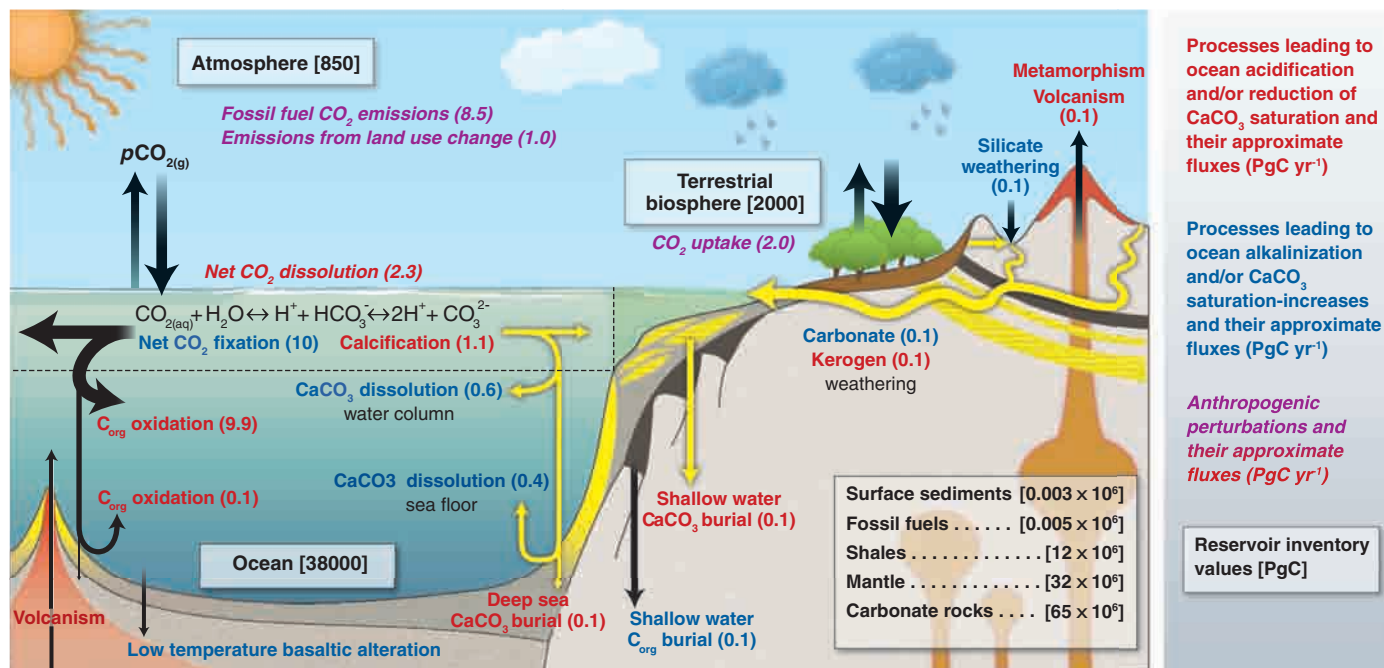


Fig. 2. When CO₂ dissolves in seawater, it reacts with water to form carbonic acid, which then dissociates to bicarbonate, carbonate, and hydrogen ions. The higher concentration of hydrogen ions makes seawater acidic, but this process is buffered on long time scales by the interplay of seawater, seafloor carbonate sediments, and weathering on land. Shown are the major pathways of reduced carbon (black) and of alkalinity (yellow). Processes leading to ocean acidification and/or reduction of CaCO₃ saturation are indicated in red, and pro-

cesses leading to ocean alkalization and/or CaCO₃ saturation increases are indicated in blue. Anthropogenic perturbations are marked in italics. Approximate fluxes are printed in parentheses [PgC year⁻¹], whereas reservoir inventory values are shown in brackets [PgC]. Natural carbon cycle fluxes are from (70); anthropogenic fluxes for 2008 are from (57), which for the land sink is significantly above its 1990–2000 average of 2.6 PgC year⁻¹ due to the 2008 La Niña state (8).

whether past intervals of ocean acidification are characterized by environmental conditions relevant for the near future. Coeval changes in ocean circulation will also introduce regional biases in proxy records and hence affect global interpretations.

Here, we review the factors controlling ocean acidification, describe evidence for the occurrence of ocean acidification events in the past, and discuss the potential as well as weaknesses of the geological record in helping us predict future ecosystem changes.

Is Ocean Acidification Primarily a pH-Decline Phenomenon?

The current rate of anthropogenic CO₂ release leads to a surface ocean environment characterized not only by elevated dissolved CO₂ and decreased pH (7) but, critically, decreased saturation with respect to calcium carbonate (CaCO₃), a compound widely used by marine organisms for the construction of their shells and skeletons (8). In contrast, slower rates of CO₂ release lead to a different balance of carbonate chemistry changes and a smaller seawater CaCO₃ saturation response, which may induce differential biotic response or even no response at all, invalidating a direct analog. The reason for a smaller saturation response to slow CO₂ release is that the alkalinity released by rock weathering on land must ultimately be balanced by the preservation and burial of CaCO₃ in marine sediments (Fig. 2), which

itself is controlled by the calcium carbonate saturation state of the ocean (9). Hence, CaCO₃ saturation is ultimately regulated primarily by weathering on long time scales, not atmospheric partial pressure of CO₂ (Pco₂). While weathering itself is related to atmospheric Pco₂ (10), it is related much more weakly than ocean pH, which allows pH and CaCO₃ saturation to be almost completely decoupled for slowly increasing atmospheric Pco₂.

Using a global carbon cycle model (2), we show the progressive coupling between CaCO₃ saturation and pH as the rate of CO₂ emissions increases and sources (weathering) and sinks (CaCO₃ burial) of alkalinity are no longer balanced. For rapid century-scale and thus future-relevant increases in atmospheric Pco₂, both surface ocean pH and saturation state decline in tandem (Fig. 3). The projected decrease in ocean surface saturation state—here, with respect to aragonite (Ω_{aragonite})—is an order of magnitude larger for a rapid CO₂ increase than for a slow [100 thousand years (ky)] CO₂ increase. Ultimately, saturation recovers while the pH remains suppressed, reflecting how changes in the oceanic concentrations of dissolved inorganic carbon (DIC) and alkalinity make it possible to have simultaneously both high CO₂ and high carbonate ion concentration saturation ([CO₃²⁻], which controls saturation), but with the relatively greater increase in [CO₂] causing lower pH. The key to unlocking the geological record of ocean acid-

ification is hence to distinguish between long-term steady states and transient changes. We use the term “ocean acidification event” for time intervals in Earth’s history that involve both a reduction in ocean pH and a substantial lowering of CaCO₃ saturation, implying a time scale on the order of 10,000 years and shorter (Fig. 3).

Indications of Paleo-Ocean Acidification

With these criteria in mind, we review (in reverse chronological order) the intervals in Earth’s history for which ocean acidification has been hypothesized, along with the evidence for independent geochemical and biotic changes. We confine this review to the past ~300 million years (My) because the earlier Phanerozoic (and beyond) lacks the pelagic calcifiers that not only provide key proxy information but also create the strong deep-sea carbonate (and hence atmospheric Pco₂) buffer that characterizes the modern Earth system (9). Our criteria for identifying potentially future-relevant past ocean acidification are (i) massive CO₂ release, (ii) pH decline, and (iii) saturation decline. We also discuss evidence for the time scale of CO₂ release, as well as for global warming. Events are given a similarity index that is based on available geochemical data (table S1) and are indicated in Fig. 4A.

Late Pleistocene deglacial transitions. The last deglaciation is the best documented past event associated with a substantive (30%) CO₂ rise: 189 to 265 μatm between 17.8 to 11.6 ky before

the present (B.P.) (11). Boron isotope estimates from planktic foraminifers show a 0.15 ± 0.05 unit decrease in sea surface pH (12) across the deglacial transition—an average rate of decline of ~ 0.002 units per 100 years compared with the current rate of more than 0.1 units per 100 years (table S1). Planktic foraminiferal shell weights decreased by 40 to 50% (4), and coccolith mass decreased by $\sim 25\%$ (13). In the deep ocean, changes in carbonate preservation (14), pH [from foraminiferal $\delta^{11}\text{B}$ (15)] and $[\text{CO}_3^{2-}]$ [from foraminiferal B/Ca and Zn/Ca (16, 17)] differed between ocean basins, reflecting covarying changes in deep-water circulation and an internal carbon shift within the ocean. The regional nature of these variations highlights the general need for careful evaluation of regional versus global effects in paleo-studies.

Oligocene–Pliocene. The climate of the Oligocene to Pliocene [34 to 2.6 million years ago (Ma)] contains intervals of elevated temperature and modest deviations of atmospheric P_{CO_2} from modern values (Fig. 4). Of particular interest has been the Pliocene warm period [3.29 to 2.97 Ma (18, 19)], which is characterized by global surface temperatures estimated to be $\sim 2.5^\circ\text{C}$ higher than today (19), atmospheric P_{CO_2} between 330 to 400 μatm (Fig. 4C) (18, 20), and sea surface $\text{pH}_{\text{sws}} \sim 0.06$ to 0.11 units lower (18) than the preindustrial. Ecological responses to the warming include migration of tropical foraminifer species toward the poles (21), but there are no documented calcification responses or increased nannoplankton extinction rates (22). The early to middle Miocene (23 to 11 Ma) and Oligocene (34 to 23 Ma) were also characterized periods of elevated temperatures and slightly higher P_{CO_2} compared with preindustrial values (Fig. 4C) but, because of their long duration, were not associated with changes in CaCO_3 saturation (Fig. 3C).

Paleocene–Eocene. Evidence for rapid carbon injection associated with the Paleocene–Eocene Thermal Maximum (PETM, 56 Ma) as well as a number of smaller transient global warming events (hyperthermals) during the late Paleocene and early Eocene (58 to 51 Ma) comes primarily from observations of large [up to -4

per mil (‰)] negative $\delta^{13}\text{C}$ excursions (23) associated with pronounced decreases in calcium carbonate preservation (24). Depending on the assumed source, rate, and magnitude of CO_2 release (25), a 0.25 to 0.45 unit decline in surface seawater pH is possible, with a reduction in mean surface ocean aragonite saturation from $\Omega = 3$ down to 1.5 to 2 (1). The calcite compensation depth (CCD) (8) rose by ~ 2 km to shallower than

1.5 km in places (24) (compared with >4 km today). Although a pH decrease or P_{CO_2} increase remains to be confirmed by geochemical proxies for any of the hyperthermal events, the amount of carbon injected can be modeled on the basis of consistent carbonate $\delta^{13}\text{C}$ and CCD changes, yielding between ~ 2000 and 6000 PgC for the onset of the PETM (26, 27). However, as with the last glacial transition, deep sea geochemistry appears strongly modulated by regional ocean circulation changes (28), which adds an additional layer of complexity to global extrapolation and highlights the importance of adequate spatial coverage of the data.

PETM sediments record the largest extinction among deep-sea benthic foraminifers of the past 75 My (29), and a major change in trace fossils indicates a disruption of the macrobenthic community (30). However, the covariation of ocean acidification, warming, and corresponding oxygen depletion (fig. S2) (23) precludes the attribution of this extinction to a single cause (1, 29). In shallow water environments, a gradual shift from calcareous red algae and corals to larger benthic foraminifers as dominant calcifiers started in the Paleocene and was completed at the PETM with the collapse of coral reefs and larger benthic foraminiferal turnover (31). This event is recognized as one of the four major metazoan reef crises of the past 300 My (Fig. 1) (32). In marginal marine settings, coccolithophore (33) and dinoflagellate cyst (34) assemblages display changes in species composition, but these are interpreted to reflect sensitivity to temperature, salinity stratification, and/or nutrient availability (34, 35), not necessarily acidification (fig. S2). In the open ocean, the occurrence of deformities in some species of calcareous nannoplankton has been described (36), but despite a strong change in assemblages, there is no bias in extinction or diversification in favor of or against less or more calcified planktic species (37).

Cretaceous and Cretaceous–Paleogene. The well-known mass extinction at 65 Ma is generally accepted to have been triggered by a large asteroid impact (38). In addition to potential terrestrial biomass or fossil carbon burning, the impact may have caused the emission of SO_2 from vaporized gypsum deposits at the impact site and/or nitric acid aerosols produced by shock heating of the atmosphere, which could have led to acid rain and hence potentially to rapid acidification of the surface ocean (38). Although planktic calcifiers exhibited elevated rates of extinction and reduced production (22, 39), reef corals did not experience a major extinction (32), and benthic foraminifers were not affected in either shallow or deep waters (29). Because multiple environmental changes covaried and proxy data for marine carbonate chemistry are not yet available, unambiguous attribution of the planktic extinctions to any one driver such as ocean acidification is currently not possible.

The earlier Cretaceous (K) (Fig. 4A) is generally a time of massive chalk deposition (mainly

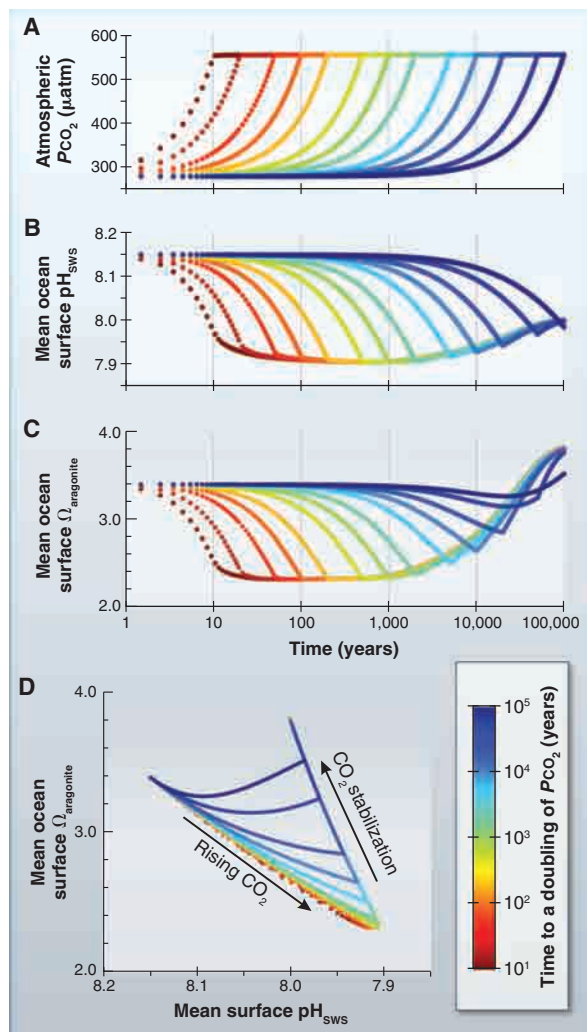


Fig. 3. The trajectories of mean ocean surface pH and aragonite saturation ($\Omega_{\text{aragonite}}$) become progressively decoupled as the rate of atmospheric P_{CO_2} change increases. The four panels show the results of a series of experiments in an Earth system model (2). (A) Prescribed linear increases of atmospheric P_{CO_2} (on a \log_{10} scale) from $\times 1$ to $\times 2$ preindustrial CO_2 , with the different model experiments spanning a range of time scales (but experiencing the same ultimate CO_2 change). (B) Evolution of mean surface pH in response to rising CO_2 . (C) Evolution of mean surface $\Omega_{\text{aragonite}}$. (D) A cross-plot illustrating how $\Omega_{\text{aragonite}}$ is progressively decoupled from pH as the rate of P_{CO_2} increase slows, with future-relevant rate of P_{CO_2} increase showing a diagonal trajectory from top left to bottom right, whereas slow P_{CO_2} increases result in an almost horizontal trajectory toward lower pH with very little saturation change. All plots are color-coded from red ("fast") to blue ("slow"). These model results include both climate and long-term (silicate) weathering feedback. See (2) and fig. S1 for the role of these and other feedbacks.

in the form of nannofossil calcite), as well as one of elevated P_{CO_2} (Fig. 4B) and lower pH (Fig. 4D). This association can be misconceived as evidence that marine calcification will not be impaired under conditions of low pH in the future. However, this reasoning is invalid because extended periods of high P_{CO_2} (Fig. 4B) do not necessarily result in a suppressed seawater calcite saturation state (Fig. 3) (1, 40), which exerts an important control on organisms' calcification (41).

Cretaceous and Jurassic oceanic anoxic events. The Mesozoic oceanic anoxic events (OAEs) (in particular, OAE 2 ~93 Ma, OAE1a ~120 Ma, and Toarcian OAE ~183 Ma) were intervals during which the ocean's oxygen minimum and deep anoxic zones expanded markedly (42). The onsets of these OAEs have been linked to the emplacement of large igneous provinces, degassing large amounts of CO_2 and associated environmental consequences of warming, lower oxygen solubility, and possibly ocean acidification (42). Some of the Cretaceous OAEs were associated with turnover in plankton communities (43). Deformities and some minor size reduction in coccoliths, as well as a massive increase in the abundance of heavily calcified nannoconids, have been observed (44, 45). However, similar to more recent events, there is difficulty in unequivocally attributing observations to surface water acidification given the covariation of environmental changes (46).

Because most old sea floor (~180 Ma or older) is subducted, the sedimentary record of the Toarcian OAE is now restricted to former continental margins. Sedimentary organic and inorganic carbon deposits display initially negative, followed by positive $\delta^{13}\text{C}$ excursions, which is consistent with an influx of CO_2 into the atmosphere followed by organic carbon burial (42). The negative isotopic transition occurs in distinct negative $\delta^{13}\text{C}$ shifts, each estimated to occur in less than 20 ky (47) and possibly in as little as 650 years (48). The Toarcian OAE is associated with a reef crisis that was particularly selective against corals and hypercalcifying sponges (animals with a large skeletal-to-organic biomass ratio) (Fig. 4B) (32) and with a decrease in nannoplankton flux (49). Again, these observations could have been a response to any one or combination of a number of different contemporaneous environmental changes.

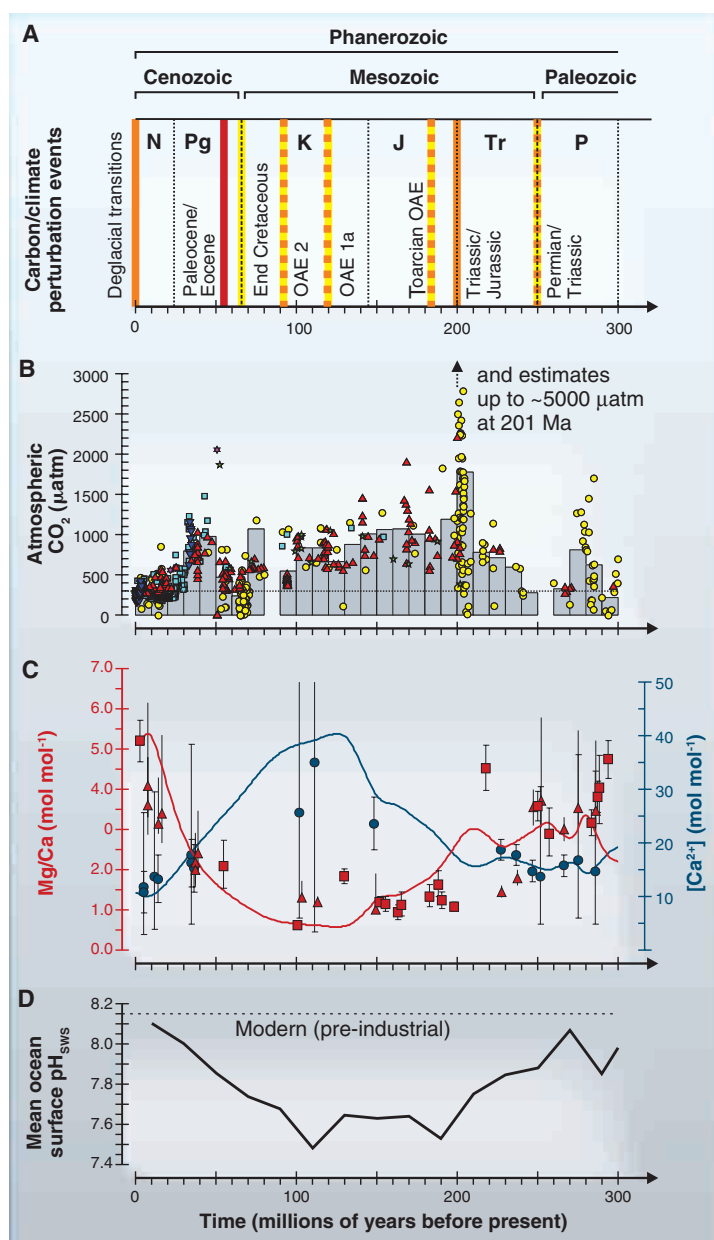


Fig. 4. Compilation of data-based [(B) and (C)] and model-reconstructed [(C) and (D)] indicators of global carbon cycle evolution over the past 300 My together with candidate ocean acidification events (A). (A) Summarization of the degree to which events (table S1) have some similarity to modern ocean acidification. The similarity index (table S1) is color-coded, where red indicates 3/most similar, orange indicates 2/partly similar, and yellow indicates 1/unlike. (B) Proxy-reconstructed atmospheric P_{CO_2} (2) grouped by proxy: yellow circles indicate paleosol $\delta^{13}\text{C}$, light blue squares indicate marine phytoplankton $\delta^{13}\text{C}$, red triangles indicate stomatal indices/ratios, dark blue inverted triangles indicate planktic foraminiferal $\delta^{13}\text{B}$, green five-pointed stars indicate liverwort $\delta^{13}\text{C}$, purple six-pointed stars indicate sodium carbonates, with 10-My averages shown by gray bars. For plotting convenience, estimates exceeding 3000 μatm are not shown [primarily paleosol $\delta^{13}\text{C}$ from the uppermost Triassic/lowermost Jurassic (2)]. (C) Ocean Mg/Ca ratios (red triangles, left axis), reconstructed from fluid inclusions (2) and echinoderm fossil carbonate [red squares (71)] together with the Phanerozoic seawater model of (72) (red line). Also shown (blue circles, right axis) is $[\text{Ca}^{2+}]$ from fluid inclusions (2) and models [blue line (72)]. (D) Model-reconstructed changes in mean ocean surface pH at 20-My intervals [black line (73)].

Triassic–Jurassic. The Triassic–Jurassic (T/J) mass extinction is linked to the coeval emplacement of the Central Atlantic Magmatic Province (50). Proxy records across the T/J boundary (~200 Ma) suggest a doubling of atmospheric P_{CO_2} over as little as 20 ky (51, 52), although the absolute P_{CO_2} estimates differ greatly between proxies, with leaf stomata suggesting an increase from 700 to 2000 μatm, whereas pedogenic carbonates indicate an increase from 2000 to 4400 μatm (Fig. 4C) (2). Decreased carbonate saturation is inferred from reduced pelagic carbonate accumulation in shelf sediments (53), although shallow water carbonate deposition can vary in response to many parameters, not only acidification. A calcification crisis amongst hypercalcifying taxa is inferred for this period (Fig. 4B), with reefs and scleractinian corals experiencing a near-

total collapse (32). However, the observation that tropical species were more affected than extratropical species suggests that global warming may have been an important contributor or even dominant cause of this extinction (32).

Permian–Triassic. The Permo–Triassic (P/T) mass extinction (252.3 Ma) was the most severe of the Phanerozoic Era and coincided, at least in part, with one of the largest known continental eruptions, the Siberian trap basalts. Recent estimates for the total CO_2 release put it at ~13,000 to 43,000 PgC in 20 to 400 ky (54–56)—an annual carbon release of ~0.1 to 1 PgC [compared with 9.9 PgC in 2008 (57)]. There is some observational evidence for carbonate dissolution in shelf settings (54), but its interpretation is again debated (58). There is abundant evidence for ocean anoxia, photic zone euxinia (enrichment in

hydrogen sulfide) (59), and strong warming (54), but no direct proxy evidence for pH or carbonate ion changes. Knoll *et al.* (59) inferred the preferential survival of taxa with anatomical and physiological features that should confer resilience to reduced carbonate saturation state and hypercapnia (high CO₂ in blood) and preferential extinction of taxa that lacked these traits, such as reef builders (32).

Is There a Geologic Analog for the Future?

A number of past ocean carbon-cycle perturbation events share many of the characteristics of anthropogenic ocean acidification (Fig. 4 and table S1), with the notable exception of the estimated rates of CO₂ release. In the general absence of direct proxy evidence for lower pH and reduced saturation before the Pliocene, global carbon cycle models can be used to infer the magnitude of carbon release by fitting observed changes in the $\delta^{13}\text{C}$ of calcium carbonates and organic remnants (60). However, as well as needing information on the source and isotopic composition of the added carbon, the time scale of $\delta^{13}\text{C}$ change is critically important to the estimation of CO₂ fluxes (25). Because of the lack of open-ocean sediments and increasingly poor temporal and spatial resolution of the geological record further back in time, it is difficult to place adequate constraints on the duration and rate of CO₂ release. Radiometric dating techniques are not accurate enough to identify Mesozoic intervals of 10-ky duration, although orbital spectral analysis of highly resolved isotope and/or sedimentological records can help to partly overcome this—for example, if a $\delta^{13}\text{C}$ excursion is shorter or longer than one precession cycle [21 ky (51)]. Even for the well-studied PETM, the duration of the main phase of this carbon injection is still debated (35, 61), and model-inferred peak rates of ≤ 1 PgC per year (26, 61) could potentially be an underestimate.

Additional complications arise because carbon may not have been released at a uniform rate and, in the extreme, may have occurred in the form of rapid pulses. In such cases, the assumption of an average emissions rate throughout the entire duration of the pulsed release will fail to capture the potential for episodes of intense acidification. For instance, although the total duration of the CO₂ release from the T/J-age Central Atlantic Magmatic Province was estimated to be ~600 ky, pulses as short as ~20 ky have been suggested (51, 62). Similarly, the main phase of OAE1a (excluding the recovery interval) was ~150 ky (45) and hence too slow for carbonate saturation to be significantly affected (Fig. 3), but major volcanic eruptions and thus rapid CO₂ release could potentially have produced future-relevant perturbations in the carbon cycle. Substantially improved chronologies and higher-resolution records are needed to refine estimates of rate.

Given current knowledge of the past 300 My of Earth's history (Fig. 4 and table S1), the PETM and associated hyperthermal events, the T/J, and

potentially the P/T all stand out as having excellent potential as analog events, although the T/J and P/T are much more poorly constrained because of the absence of deep-sea carbonate deposits. OAEs may also be relevant but were associated with less severe volcanism (CO₂ release) than were the older events (P/T and T/J). The last deglacial transition, although characterized by temperature and CO₂-increase, is two orders of magnitude slower than current anthropogenic change. It is also thought to largely represent a redistribution of carbon within the ocean and to the atmosphere and terrestrial biosphere and hence did not have as potent and globally uniform an acidification effect as an input from geological reserves. Because of the decoupling between pH and saturation on long time scales (Fig. 3), extended intervals of elevated P_{CO_2} such as the middle Miocene, Oligocene, and Cretaceous can be firmly ruled out as future-relevant analogs.

What Are the Perspectives for Using the Geological Record to Project Global Change?

Only rapid or pulsed CO₂ release events can provide direct future-relevant information. Assessment of such events critically depends on independent geochemical quantification of the associated changes in the carbonate system, specifically seawater-pH and CaCO₃ saturation. Geochemical proxy estimates are not yet available for the Cretaceous and beyond and need to be obtained to verify whether ocean acidification did indeed happen. This is challenging, because in addition to the potential for increasing post-depositional alteration and reduced stratigraphic exposure, uncertainty over the chemical and isotopic composition of seawater increases and limits our interpretation of these proxies (63, 64). Future studies will have to improve and expand geochemical estimates and their uncertainties of surface and deep-ocean carbonate chemistry associated with carbonate dissolution and ecological changes. This includes finding new archives to study the secular evolution of seawater chemistry but also the laboratory study of living proxy carriers under conditions mimicking past seawater chemistry. An unfortunate aspect of the geological record, however, is the lack of deep-sea carbonates in the Early Jurassic and beyond, which further reduces our ability to reconstruct the carbonate chemistry of those older events.

The sensitivity of ocean chemistry to CO₂ release, and the relationship between induced pH and P_{CO_2} changes, vary through time and further complicate the picture. For instance, seawater calcium and magnesium ion concentrations were different in the past (Fig. 4C). This alters the ocean's carbonate ion buffering capacity and hence sensitivity of the Earth system to carbon perturbation (65) because all other things being equal, higher ambient Ca²⁺ concentrations means that a lower carbonate ion concentration is required to achieve the same saturation and hence balance weathering. Varying seawater Mg/Ca ratios may potentially also affect the mineralogy of marine calcifiers,

where the more soluble high-Mg calcite predominated Neogene reefs and reefs during the Permian through Early Jurassic, and more resistant low-Mg calcite predominated during the Late Jurassic through Paleogene (66). Thus, on this mineralogical basis the response of marine calcifiers to ocean acidification and seawater geochemistry during the P/T and T/J would arguably be closer to the modern than, for example, during the PETM (67). Improved estimates of past seawater-Mg/Ca composition are necessary to better evaluate all of this.

Although we have concentrated on the prospects for extracting information from the geological record concerning the impact of ocean acidification, we must question whether it really is necessary to isolate its effect on marine organisms from other covarying factors (68). In particular, consequences of increasing atmospheric CO₂ will also be associated with warming in the surface ocean and a decrease in dissolved oxygen concentration (69). Massive carbon release, whether future or past, will hence share the same combination and sign of environmental changes. The strength of the geological record therefore lies in revealing past coupled warming and ocean acidification (and deoxygenation) events as an “integrated” analog, with future and past events sharing the same combination and sign of environmental changes. However, in additionally driving a strong decline in calcium carbonate saturation alongside pH, the current rate of (mainly fossil fuel) CO₂ release stands out as capable of driving a combination and magnitude of ocean geochemical changes potentially unparalleled in at least the last ~300 My of Earth history, raising the possibility that we are entering an unknown territory of marine ecosystem change.

References and Notes

1. A. Ridgwell, D. N. Schmidt, *Nat. Geosci.* **3**, 196 (2010).
2. Materials and methods are available as supporting material on Science Online.
3. W. H. Berger, *Deep-Sea Res.* **15**, 31 (1968).
4. S. Barker, H. Elderfield, *Science* **297**, 833 (2002).
5. S. Barker *et al.*, *Paleoceanography* **19**, PA3008 (2004).
6. S. J. Gibbs, H. M. Stoll, P. R. Bown, T. J. Bralower, *Earth Planet. Sci. Lett.* **295**, 583 (2010).
7. K. Caldeira, M. E. Wickett, *Nature* **425**, 365 (2003).
8. An online associated carbonate chemistry tutorial is available as supporting material on Science Online.
9. A. Ridgwell, R. E. Zeebe, *Earth Planet. Sci. Lett.* **234**, 299 (2005).
10. D. Archer, H. Kheshgi, E. Maier-Reimer, *Geophys. Res. Lett.* **24**, 405 (1997).
11. E. Monnin *et al.*, *Science* **291**, 112 (2001).
12. B. Hönisch, N. G. Hemming, *Earth Planet. Sci. Lett.* **236**, 305 (2005).
13. L. Beaufort *et al.*, *Nature* **476**, 80 (2011).
14. J. W. Farrell, W. Prell, *Paleoceanography* **4**, 447 (1989).
15. B. Hönisch, T. Bickert, N. G. Hemming, *Earth Planet. Sci. Lett.* **272**, 309 (2008).
16. J. Yu *et al.*, *Science* **330**, 1084 (2010).
17. T. M. Marchitto, J. Lynch-Stieglitz, S. R. Hemming, *Earth Planet. Sci. Lett.* **231**, 317 (2005).
18. O. Seki *et al.*, *Earth Planet. Sci. Lett.* **292**, 201 (2010).
19. A. M. Haywood *et al.*, *Global Planet. Change* **66**, 208 (2009).
20. M. Pagani, Z. Liu, J. LaRiviere, A. C. Ravelo, *Nat. Geosci.* **3**, 27 (2010).

21. H. J. Dowsett, M. M. Robinson, *Micropaleontology* **53**, 105 (2007).
22. P. R. Bown *et al.*, in *Coccolithophores—From Molecular Processes to Global Impacts*, H. R. Thierstein, J. R. Young, Eds. (Springer, Berlin, 2004), pp. 481–508.
23. J. P. Kennett, L. D. Stott, *Nature* **353**, 225 (1991).
24. J. C. Zachos *et al.*, *Science* **308**, 1611 (2005).
25. J. C. Zachos, H. McCarren, B. Murphy, U. Röhl, T. Westerhold, *Earth Planet. Sci. Lett.* **299**, 242 (2010).
26. R. E. Zeebe, J. C. Zachos, G. R. Dickens, *Nat. Geosci.* **2**, 576 (2009).
27. K. Panchuk, A. Ridgwell, L. R. Kump, *Geology* **36**, 315 (2008).
28. R. E. Zeebe, J. C. Zachos, *Paleoceanography* **22**, PA3201 (2007).
29. E. Thomas, in *Geological Society of America Special Paper*, S. Monechi, R. Coccioni, M. R. Rampino, Eds. (Geological Society of America, Boulder, CO, 2007), pp. 1–23.
30. F. J. Rodríguez-Tovar, A. Uchman, L. Alegret, E. Molina, *Mar. Geol.* **282**, 178 (2011).
31. C. Scheibner, R. P. Speijer, *Earth Sci. Rev.* **90**, 71 (2008).
32. W. Kiessling, C. Simpson, *Glob. Change Biol.* **17**, 56 (2011).
33. S. J. Gibbs, T. J. Bralower, P. R. Bown, J. C. Zachos, L. M. Bybell, *Geology* **34**, 233 (2006).
34. A. Sluijs, H. Brinkhuis, *Biogeosciences* **6**, 1755 (2009).
35. A. Sluijs *et al.*, *Nat. Geosci.* **2**, 777 (2009).
36. I. Raffi, B. De Bernardi, *Mar. Micropaleontol.* **69**, 119 (2008).
37. S. J. Gibbs, P. R. Bown, J. A. Sessa, T. J. Bralower, P. A. Wilson, *Science* **314**, 1770 (2006).
38. P. Schulte *et al.*, *Science* **327**, 1214 (2010).
39. S. D'Hondt, M. E. Q. Pilson, H. Sigurdsson, A. K. Hanson Jr., S. Carey, *Geology* **22**, 983 (1994).
40. R. E. Zeebe, P. Westbroek, *Geochem. Geophys. Geosyst.* **4**, 1104 (2003).
41. C. Langdon *et al.*, *Global Biogeochem. Cycles* **14**, 639 (2000).
42. H. C. Jenkyns, *Geochem. Geophys. Geosyst.* **11**, Q03004 (2010).
43. R. M. Leckie *et al.*, *Paleoceanography* **17**, 1041 (2002).
44. E. Erba, F. Tremolada, *Paleoceanography* **19**, PA1008 (2004).
45. E. Erba, C. Bottini, H. J. Weissert, C. E. Keller, *Science* **329**, 428 (2010).
46. S. J. Gibbs, S. A. Robinson, P. R. Bown, T. D. Jones, J. Henderiks, *Science* **332**, 175; author reply, 175 (2011).
47. G. Suan *et al.*, *Earth Planet. Sci. Lett.* **267**, 666 (2008).
48. A. S. Cohen, A. L. Coe, D. B. Kemp, *J. Geol. Soc. London* **164**, 1093 (2007).
49. E. Mattioli, B. Pittet, L. Petitpierre, S. Mailliot, *Global Planet. Change* **65**, 134 (2009).
50. J. H. Whiteside, P. E. Olsen, D. V. Kent, S. J. Fowell, M. Et-Touhami, *Palaeogeogr. Palaeoclimatol. Palaeoecol.* **244**, 345 (2007).
51. D. B. Kemp, A. L. Coe, A. S. Cohen, L. Schwark, *Nature* **437**, 396 (2005).
52. M. Ruhl, N. R. Bonis, G. J. Reichart, J. S. Sinninghe Damsté, W. M. Kürschner, *Science* **333**, 430 (2011).
53. A. E. Crne, H. Weissert, S. Gorican, S. M. Bernasconi, *Geol. Soc. Am. Bull.* **123**, 40 (2011).
54. J. L. Payne *et al.*, *Proc. Natl. Acad. Sci. U.S.A.* **107**, 8543 (2010).
55. S. V. Sobolev *et al.*, *Nature* **477**, 312 (2011).
56. S. Z. Shen *et al.*, *Science* **334**, 1367 (2011).
57. C. Le Quéré *et al.*, *Nat. Geosci.* **2**, 831 (2009).
58. P. B. Wignall, S. Kershaw, P.-Y. Collin, S. Crasquin-Soleau, *Geol. Soc. Am. Bull.* **121**, 954 (2009).
59. A. H. Knoll, R. K. Bambach, J. L. Payne, S. Pruss, W. W. Fischer, *Earth Planet. Sci. Lett.* **256**, 295 (2007).
60. J. Zachos, M. Pagani, L. Sloan, E. Thomas, K. Billups, *Science* **292**, 686 (2001).
61. Y. Cui *et al.*, *Nat. Geosci.* **4**, 481 (2011).
62. M. Ruhl *et al.*, *Earth Planet. Sci. Lett.* **295**, 262 (2010).
63. D. Lemarchand, J. Gaillardet, E. Lewin, C. J. Allègre, *Nature* **408**, 951 (2000).
64. R. M. Coggon, D. A. Teagle, C. E. Smith-Duque, J. C. Alt, M. J. Cooper, *Science* **327**, 1114 (2010).
65. R. E. Zeebe, A. Ridgwell, in *Ocean Acidification*, J.-P. Gattuso, L. Hansson, Eds. (Oxford Univ. Press, Oxford, 2011), pp. 21–40.
66. S. M. Stanley, L. A. Hardie, *Palaeogeogr. Palaeoclimatol. Palaeoecol.* **144**, 3 (1998).
67. J. B. Ries, *Biogeosciences* **7**, 2795 (2010).
68. C. Turley *et al.*, *Mar. Pollut. Bull.* **60**, 787 (2010).
69. N. Gruber, *Philos. Trans. R. Soc. A-Math. Phys. Eng. Sci.* **369**, 1980 (2011).
70. E. T. Sundquist, K. Visser, Elsevier, in *Treatise on Geochemistry: Biogeochemistry*, W. H. Schlesinger, Ed. (Elsevier, Pergamon, Oxford, 2004), chap. 9.
71. J. A. D. Dickson, *Science* **298**, 1222 (2002).
72. R. V. Demicco, T. K. Lowenstein, L. A. Hardie, R. J. Spencer, *Geology* **33**, 877 (2005).
73. A. Ridgwell, *Mar. Geol.* **217**, 339 (2005).

Acknowledgments: Funding for the “Workshop on Paleocene Acidification and Carbon Cycle Perturbation Events” was provided by NSF OCE 10-32374 and Past Global Changes (PAGES). We thank the workshop participants for stimulating discussions and contributions to this manuscript, and the USC Wrigley Institute on Catalina Island for hosting the workshop. Particular thanks are owed to Thorsten Kiefer of PAGES, who initiated the workshop and supported it at all stages. This work is a contribution to the “European Project on Ocean Acidification” (EPOCA). Data presented in Fig. 4 are presented in tables S2 and S3 (2).

Supporting Online Material

www.sciencemag.org/cgi/content/full/335/6072/1058/DC1
SOM Text
Figs. S1 to S3
Tables S1 to S3
References (74–217)

10.1126/science.1208277

A novel method for determination of aragonite saturation state on the continental shelf of central Oregon using multi-parameter relationships with hydrographic data

L. W. Juranek,¹ R. A. Feely,¹ W. T. Peterson,² S. R. Alin,¹ B. Hales,³ K. Lee,⁴
C. L. Sabine,¹ and J. Peterson⁵

Received 3 September 2009; revised 10 November 2009; accepted 23 November 2009; published 31 December 2009.

[1] We developed a multiple linear regression model to robustly determine aragonite saturation state (Ω_{arag}) from observations of temperature and oxygen ($R^2 = 0.987$, RMS error 0.053), using data collected in the Pacific Northwest region in late May 2007. The seasonal evolution of Ω_{arag} near central Oregon was evaluated by applying the regression model to a monthly (winter)/bi-weekly (summer) water-column hydrographic time-series collected over the shelf and slope in 2007. The Ω_{arag} predicted by the regression model was less than 1, the thermodynamic calcification/dissolution threshold, over shelf/slope bottom waters throughout the entire 2007 upwelling season (May–November), with the $\Omega_{arag} = 1$ horizon shoaling to 30 m by late summer. The persistence of water with $\Omega_{arag} < 1$ on the continental shelf has not been previously noted and could have notable ecological consequences for benthic and pelagic calcifying organisms such as mussels, oysters, abalone, echinoderms, and pteropods. **Citation:** Juranek, L. W., R. A. Feely, W. T. Peterson, S. R. Alin, B. Hales, K. Lee, C. L. Sabine, and J. Peterson (2009), A novel method for determination of aragonite saturation state on the continental shelf of central Oregon using multi-parameter relationships with hydrographic data, *Geophys. Res. Lett.*, 36, L24601, doi:10.1029/2009GL040778.

1. Introduction

[2] Since the preindustrial, atmospheric loading of CO_2 from fossil fuel combustion and land use changes has driven an anthropogenic ocean uptake of 146 ± 20 Pg C (updated from Sabine and Feely [2007]) and a corresponding average surface water pH change of 0.1 units [Feely et al., 2004]. Accelerating emission rates and reduced buffering capacity will decrease pH by as much as 0.3–0.4 units by the end of this century under business-as-usual scenarios [Orr et al., 2005]. Effects of these “ocean acidification” changes on marine organisms are still under intense study [Kleypas et al., 2006; Fabry et al., 2008; Doney et al., 2009], but increased ocean CO_2 content will result in a reduced

saturation state for calcium carbonate minerals and potentially deleterious impacts for organisms that form $CaCO_3$ shells, including corals, pteropods, foraminifera, and commercially important shellfish and their larvae.

[3] The saturation state (Ω) of $CaCO_3$ minerals is determined by the relationship:

$$\Omega = [Ca^{2+}][CO_3^{2-}]/K'_{sp}, \quad (1)$$

where K'_{sp} , the stoichiometric solubility product, is a function of temperature, salinity, pressure, and the particular mineral phase (aragonite or calcite). In a thermodynamic sense, $\Omega > 1$ indicates mineral precipitation is favored and $\Omega < 1$ indicates dissolution is favored, although biogenic calcification is subject to “vital effects” such as organic shell coatings and species-specific calcification mechanisms, and calcification/dissolution can occur when ambient-water Ω values indicate opposing thermodynamic effects [Langdon et al., 2003; Tunnicliffe et al., 2009]. However, recent experiments indicate that $\Omega < 1$ adversely impacts some organisms; Fabry et al. [2008] reported net dissolution in live pteropods within 48 hours of exposure to undersaturated water. Because aragonitic $CaCO_3$ has a metastable crystalline structure and is $\approx 50\%$ more soluble than calcite [Mucci, 1983], organisms that form aragonitic shells will likely be affected first, and perhaps most severely, by ocean acidification.

[4] Transient episodes of reduced aragonite Ω (Ω_{arag}) have already been noted in productive eastern boundary upwelling systems such as the California current system [Feely et al., 2008a]. Understanding the duration, intensity, and overall ecological impact of these events is a key need in economically and socially important coastal fisheries regions. Here we present an approach, updated from Feely et al. [2008b], to determine Ω_{arag} from temperature and O_2 , using data collected on a 2007 survey of North American Pacific coastal waters. We justify the approach with a statistical evaluation, and apply it to a hydrographic time-series from the central Oregon coast to evaluate seasonal changes in Ω_{arag} .

2. Algorithm Development

[5] Ω_{arag} is a function of temperature (T), salinity (S), pressure (P), and the $[Ca^{2+}]$ and $[CO_3^{2-}]$ of seawater (equation (1)). Because $[Ca^{2+}]$ changes are proportionally small in seawater, variations in Ω_{arag} are largely determined by changes in $[CO_3^{2-}]$, which can be predicted from observations of dissolved inorganic carbon (DIC) and total

¹Pacific Marine Environmental Laboratory, NOAA, Seattle, Washington, USA.

²Northwest Fisheries Science Center, NMFS, Newport, Oregon, USA.

³College of Oceanic and Atmospheric Sciences, Oregon State University, Corvallis, Oregon, USA.

⁴School of Environmental Science and Engineering, Pohang University of Science and Technology, Pohang, South Korea.

⁵Cooperative Institute for Marine Resources Studies, Oregon State University, Newport, Oregon, USA.

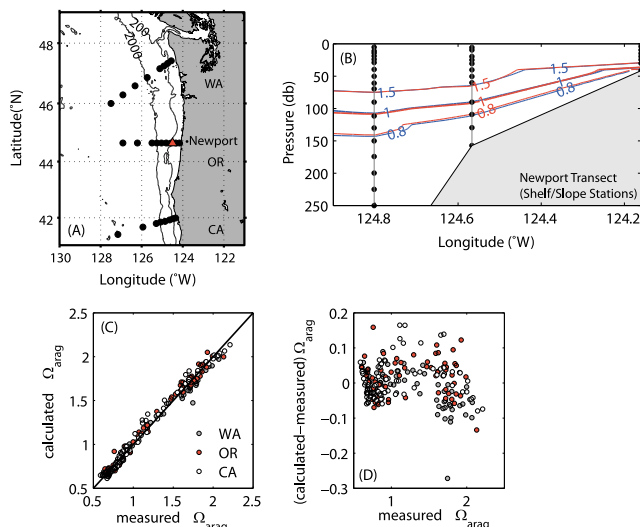


Figure 1. (a) Region map showing location of three coastal transects used in developing the algorithm and location of NDBC buoy 46050 (red triangle). Sampling locations for the Newport time-series shown in Figure 2 are similar to those shown here, but with higher resolution over shelf/slope areas and a reduced seaward extent. (b) Ω_{arag}^e (blue) and Ω_{arag} (red) contours for transect collected near Newport, Oregon in late May 2007, with profiles (vertical lines) and sampling depths indicated. (c) Measured Ω_{arag} and calculated Ω_{arag}^e , color coded by transect location. Lack of geographic bias in residuals indicates that the algorithm applies for WA, OR, and N. CA coastal areas. (d) Residual ($\Omega_{arag}^e - \Omega_{arag}$) versus Ω_{arag} for PNW data, color coded as in C. All Ω_{arag}^e values were determined using the regression model described by equation (3).

alkalinity (TA). DIC concentrations are governed by physics (solubility, surface gas exchange) and biology (photosynthesis/respiration) and therefore should be a function of T , S , and either O_2 or NO_3^- [Anderson and Sarmiento, 1994; Lee *et al.*, 2000]. TA can also be modeled as a function of T and S [Lee *et al.*, 2006]. We would therefore expect a predictive relationship for Ω_{arag} as a function of T , S , P , O_2 , NO_3^- , or a subset of these parameters.

[6] A hydrographic survey of the U.S. west coast in 2007 [Feely *et al.*, 2008a] allowed an opportunity to develop predictive relationships for Ω_{arag} based on contemporaneous T , S , P , O_2 , and NO_3^- measurements. We first evaluated a linear additive model of the following form:

$$\Omega_{arag}^e = \beta_0 + \beta_1 T + \beta_2 S + \beta_3 P + \beta_4 O_2 + \beta_5 NO_3^-, \quad (2)$$

where Ω_{arag}^e is the empirically predicted aragonite saturation state, and the coefficients β_i are empirical constants. We determined coefficients for equation (2) using an ordinary least-squares regression of Ω_{arag} observations collected in the Pacific Northwest (PNW) region (transects of Washington, Oregon, and N. California coastal waters, Figure 1a), using only data in the 30–300 m depth range to minimize localized effects of surface warming, gas exchange and riverine inputs and to include only relevant source water masses for the shelf/slope region. Although all resulting regression coefficients

were significant, tests of collinearity among the independent variables (via pair wise regression and the variance inflation factor test, see Table 1) indicated that S , O_2 , and NO_3^- were too closely related, leading to potential errors in least-squares regression coefficients [Kutner *et al.*, 2004]. Stepwise regression and regression statistics (R^2 , RMS error) subsequently identified O_2 as the most robust predictor of the three collinear variables.

[7] A multiple linear regression of T , P , and O_2 yielded significant regression coefficients and reasonable regression statistics (Table 1). However, residuals for this relationship showed a strong bias, i.e., overestimation of Ω_{arag}^e at minimum and maximum T and O_2 (see Figure S1 of the auxiliary material).¹ This bias is likely the result of the non-linear dependence of CO_3^{2-} on TA and DIC, which arises in coastal waters with high pCO_2 and significant contributions to TA from non-carbon species. We examined several possible non-linear terms and found that the bias could be minimized through the addition of an interaction term between T and O_2 (Figure S1); when this term is added, P and T are no longer significant as predictor variables. To reduce large magnitudes of the product of $T \cdot O_2$ and subsequent errors in the least-squares regression analysis (Table 1) [Kutner *et al.*, 2004], we normalized each term by subtracting a reference value for each variable, i.e.,

$$\Omega_{arag}^e = \alpha_0 + \alpha_1 (O_2 - O_{2,r}) + \alpha_2 (T - T_r) \cdot (O_2 - O_{2,r}). \quad (3)$$

Where α 's indicate regression coefficients and T_r and $O_{2,r}$ are values representative of upwelling source water in the PNW region ($T_r = 8^\circ\text{C}$ and $O_{2,r} = 140 \mu\text{mol/kg}$, see Figure 2 and Table 1). The resulting model had improved regression statistics (Table 1) and resulted in Ω_{arag}^e predictions that correctly reproduce both the magnitude and depth-distribution of Ω_{arag} observations for the effective range experienced over the shelf/slope areas (≈ 0.6 to 2.2) of the PNW region (Figure 1).

3. Model Evaluation and Caveats

[8] We evaluated the skill of the model described by equation (3) by comparison of the unexplained error in Ω_{arag}^e and the ability to constrain Ω_{arag} given analytical uncertainties in DIC and TA (2 and $3 \mu\text{mol/kg}$, respectively [Feely *et al.*, 2008a]). Uncertainty in Ω_{arag} was determined by a Monte Carlo approach, in which DIC and TA inputs into the Matlab[®] program CO2SYS [van Heuven *et al.*, 2009] were varied randomly about chosen values for the PNW data, with standard deviations equal to analytical uncertainties. The 1σ values of 1000 individually calculated Ω_{arag} determinations, $0.017/0.034$ for minimum/maximum Ω_{arag} values in the PNW data ($0.61/2.22$, respectively), represent the theoretical lower limit for unexplained random error, ε , in any model used to predict Ω_{arag}^e . The RMS error determined for the equation (3) model is close to, but still slightly higher than, the limit calculated for analytical uncertainties alone (ε). Although adding new terms to the regression model causes the RMS error to approach ε , the contribution of these additional terms to the explained

¹Auxiliary materials are available in the HTML. doi:10.1029/2009GL040778.

Table 1. Summary of Model Parameters, Coefficients, and Indicators Used in Model Selection^a

Parameters	VIF ^b	R ²	RMS Error	Coefficients \pm STD Error ^c	Comments
T, S, P, O_2, NO_3^-	3.9, 24, 2.9, 35, 9.3	0.966	0.090	$\beta_0 = 6.3 \pm 1.7$ $\beta_1 = 9.5 \cdot 10^{-2} \pm 1.0 \cdot 10^{-2}$ $\beta_2 = -1.94 \cdot 10^{-1} \pm 5.0 \cdot 10^{-2}$ $\beta_3 = 8.6 \cdot 10^{-4} \pm 1.5 \cdot 10^{-4}$ $\beta_4 = 2.82 \cdot 10^{-3} \pm 4.5 \cdot 10^{-4}$ $\beta_5 = -3.7 \cdot 10^{-3} \pm 1.7 \cdot 10^{-3}$	$O_2, S,$ and NO_3^- collinear (VIF > 5)
T, O_2, P	2.8, 3.8, 3.0	0.965	0.084	$\beta_0 = -0.521 \pm 7.0 \cdot 10^{-2}$ $\beta_1 = 7.74 \cdot 10^{-2} \pm 8.3 \cdot 10^{-3}$ $\beta_2 = 5.18 \cdot 10^{-3} \pm 1.3 \cdot 10^{-4}$ $\beta_3 = 1.16 \cdot 10^{-3} \pm 1.3 \cdot 10^{-4}$	Residuals show bias at high/low O_2 and T (see Figure S1)
O_2	N/A	0.946	0.088	$\beta_0 = 1.145 \pm 6 \cdot 10^{-3}$ $\beta_1 = 4.99 \cdot 10^{-3} \pm 7 \cdot 10^{-5}$	Residuals show bias, as above
$(O_2 - O_{2,r}),$ $(T - T_r)(O_2 - O_{2,r})$	1.5, 1.5	0.987	0.053	$\alpha_0 = 9.242 \cdot 10^{-1} \pm 4.4 \cdot 10^{-3}$ $\alpha_1 = 4.492 \cdot 10^{-3} \pm 5.0 \cdot 10^{-5}$ $\alpha_2 = 9.40 \cdot 10^{-4} \pm 3.4 \cdot 10^{-5}$	$T_r = 8^\circ\text{C};$ $O_{2,r} = 140 \mu\text{mol/kg};$
$(T - T_r),$ $(O_2 - O_{2,r}),$ $(T - T_r)(O_2 - O_{2,r}),$ $(S - S_r)(O_2 - O_{2,r}),$ $(P - P_r)(O_2 - O_{2,r})$	9, 33, 7, 23, 19	0.990	0.043	$\alpha_0 = 9.079 \cdot 10^{-1} \pm 4.6 \cdot 10^{-3}$ $\alpha_1 = 3.37 \cdot 10^{-2} \pm 7.0 \cdot 10^{-3}$ $\alpha_2 = 3.4710^{-3} \pm 1.8 \cdot 10^{-4}$ $\alpha_3 = 7.49 \cdot 10^{-4} \pm 5.9 \cdot 10^{-5}$ $\alpha_4 = -1.32 \cdot 10^{-3} \pm 1.3 \cdot 10^{-4}$ $\alpha_5 = 5.8 \cdot 10^{-6} \pm 1.2 \cdot 10^{-6}$	$T_r = 8^\circ\text{C};$ $O_{2,r} = 140 \mu\text{mol/kg};$ $P_r = 200 \text{ dbar } S_r = 34$

^aBold denotes selected model. 227 observations used in each model.

^bVIF: Variance inflation factor. See *Kutner et al.* [2004] for a full description, but briefly, the VIF is an objective measure of the inflation in coefficient uncertainty from poorly scaled or singular matrices (e.g., due to rounding errors during matrix inversion). The VIF is calculated as $(1 - R^2)^{-1}$ for the regression of each variable versus the remaining independent variables; values given in the order parameters are listed. Values >5 indicate potential collinearity among predictor variables.

^cCoefficients with standard error estimates for robust-fit multiple linear regression, which reduces the weight of outliers in the regression analysis. Coefficients correspond to order in which parameters appear. Following equations (2) and (3) in text, β and α values are coefficients for regressions without/with a reference value subtracted.

variance is marginal (Table 1). To avoid overfitting, we rejected these models. A simple model based only on O_2 , which was the strongest predictor variable of Ω_{arag}^e ($R^2 = 0.946$, RMS error 0.088; Table 1) was also considered. However, the O_2 model had a higher RMS error and a strong bias in residuals similar to that observed for the multiple linear regression of T, P , and O_2 (Figure S1). Based on these observations, we chose the equation (3) model.

[9] Because the only Ω_{arag} data available for algorithm development in this region are from late May 2007, we note there may be important caveats to a seasonal application of equation (3). However, three lines of evidence indicate seasonal application is justified. First, biologically-driven changes in Ω_{arag} for the 30–300 m depth range (i.e., due to remineralization of organic matter over the productive summer months) are to a first order driven by changes in DIC rather than TA, since diatoms typically dominate coastal upwelling systems [*Lassiter et al.*, 2006]. DIC and O_2 changes are expected to be proportional in remineralization zones that are not anoxic [*Hales et al.*, 2005; *Anderson and Sarmiento*, 1994], and therefore changes in DIC should be inherently captured in an algorithm involving O_2 . Second, the T - S (and T - O_2) range experienced spatially in the PNW data is similar to the range observed seasonally near Newport (see Figure S2), suggesting that the water masses present in the seasonal data are present in the regional PNW data. Finally, algorithm developments for the Southern California Bight region suggest no significant bias of algorithm development using only late May data (i.e., difference of measured and predicted values for August 2008 was 0.075 (S. Alin, unpublished data, 2009)). As more Ω_{arag} data become available, the algorithm for this region

can be tested and refined. Nevertheless, these arguments point toward the ability to model the seasonal Ω_{arag} dynamics near Newport with the data in hand.

[10] One potential time frame when algorithm predictions could deviate from observations is between February and May. PNW coastal waters experience intense river inputs during the rainy winter months, and the TA:DIC signature of these freshwaters is often different than in the open ocean [*Park et al.*, 1969]. Proportionality of $[Ca^{2+}]$ to salinity, an assumption used in calculating Ω_{arag} , may also change during these months. Consequently, we do not present predictions for this time period.

4. Seasonal Evolution of Ω_{arag}^e on the Oregon Coast

[11] We calculated the seasonal evolution of Ω_{arag}^e on the shelf and slope near Newport, Oregon with the model described by equation (3) and a time-series of T and O_2 data (described by *Peterson and Keister* [2003]) collected on biweekly to monthly intervals in 2007. The central Oregon coast is located in the northern end of the California Current system and experiences seasonal upwelling during spring and summer months. The region has been well-studied with regard to the physical forcing driving seasonal and interannual variability in water properties (cf. the 2006 *Geophysical Research Letters* special issue devoted to this region). Selected sections of Ω_{arag}^e (Figure 2) show a distinct seasonal cycle that is tightly coupled to upwelling dynamics near Newport. In January, the $\Omega_{arag}^e = 1$ saturation horizon sits near the shelf break (≈ 125 m), roughly at the depth horizon of the $140 \mu\text{mol/kg } O_2$ contour and the

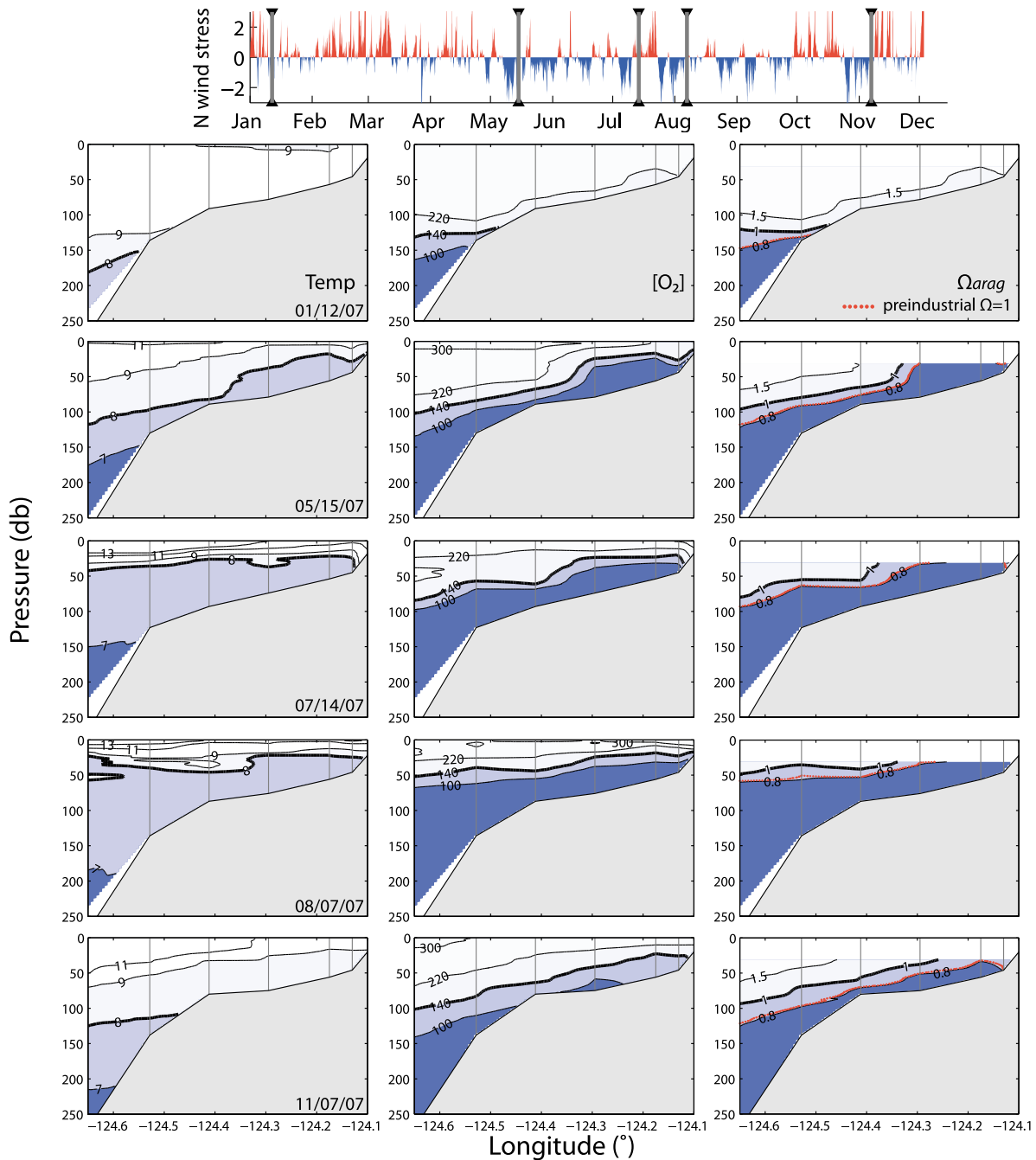


Figure 2. (bottom) Selected sections of T ($^{\circ}\text{C}$, left), $[\text{O}_2]$ ($\mu\text{mol/kg}$, center), and Ω_{arag}^e (right), for January to November 2007. Ω_{arag}^e was calculated from T and O_2 data (averaged in 1 db bins) using the regression model described by equation (3). Also shown is an estimated preindustrial $\Omega_{\text{arag}}^e = 1$ line. Locations of profiles indicated by vertical lines. Note that Ω_{arag}^e are only shown for depths greater than 30 m (see text for explanation). Propagated uncertainty in Ω_{arag}^e , based on uncertainties of T and O_2 data (0.003°C and $0.45 \mu\text{mol/kg}$, respectively) is 0.002 . (top) Northward wind stress (dynes cm^{-2}) from NDBC buoy 46050 (see Figure 1 for location), with upwelling-favorable winds (southward winds, negative wind stress) denoted in blue and downwelling-favorable winds (northward winds, positive wind stress) denoted in red. Dates of sections are designated by grey bars.

9°C isotherm. The $1.5 \Omega_{\text{arag}}^e$ horizon is 25 m shallower, at ≈ 100 m. The onset of upwelling season begins in early May with the physical spring transition [Huyer *et al.*, 1979], during which wind forcing becomes predominantly equatorward, and offshore transport becomes positive. The offshore transport is compensated by the upwelling of cold, dense waters that are rich in DIC and nutrients, and poor in

O_2 . The strong upwelling event in mid-May (strongly negative N wind stress, blue lines in Figure 2 (top)) results in sharply up-warped iso-surfaces, and the outcropping of the $0.8 \Omega_{\text{arag}}^e$ horizon to the upper 30 m from the mid-shelf (80 m isobath) to the coast. After the spring transition, persistent upwelling-favorable winds pull the $1.0 \Omega_{\text{arag}}^e$ and the $140 \mu\text{mol/kg}$ O_2 contour onto the shelf where they

remain through mid-November (Figure 2). Occasional poleward wind stress events (Figure 2, top) result in relaxation from upwelling, but the source water remains over shelf/slope regions. The late May transect used to formulate the algorithm (Figure 1b) occurred during one of these relaxation events.

[12] Throughout the remainder of the season Ω_{arag}^e and O_2 distribution show depletion on similar hydrographic surfaces, presumably as a result of biological activity (e.g., 1.0/1.5 Ω_{arag}^e and 140/220 $\mu\text{mol/kg}$ O_2 contours retain similar behavior). Between May and November the 1.0 Ω_{arag}^e contour reaches 30 m near-continuously over the inner shelf (i.e., from the 80 m isobath shoreward), with the exception of early October, when a strong downwelling event confines the low- Ω_{arag}^e water to the shelf-bottom (not shown). Over the outer shelf and slope, the 1.5 Ω_{arag}^e horizon shoals to less than 30 m by mid-July and the 1.0 horizon shoals to 50 m by mid-August (Figure 2). After the onset of persistent downwelling-favorable winds in mid-November the 1.0 Ω_{arag}^e and 140 $\mu\text{mol/kg}$ contours retreat back to the shelf-break/slope region, similar to conditions predicted for January 2007.

[13] The coupling of low Ω_{arag} state and physically-driven upwelling dynamics would be expected, given the high DIC (low pH) signature associated with upwelling source waters [Hales et al., 2005]. The absolute magnitude of Ω_{arag} over the coastal shelf regions, however, is largely unknown, due to a lack of depth-resolved DIC and TA measurements. This model therefore provides previously unattainable insight into both the magnitude of Ω_{arag} and how it relates to seasonal hydrography changes on the central Oregon shelf. The range in Ω_{arag}^e experienced seasonally over the shelf (e.g., 0.5–1.4 and 0.8–1.8 for the mid-shelf at 80 and 30 m, respectively) is also much greater than the uncertainty in model predictions (0.053). This favorable signal to noise ratio makes the region particularly amenable to this approach, compared to open ocean subtropical regions where the seasonal range is considerably less [Doney et al., 2009].

[14] An obvious question to ask is: What is the anthropogenic contribution to Ω_{arag} on the central Oregon shelf? We used the density-anthropogenic CO_2 relationship presented by Feely et al. [2008a, supplement] to correct observed DIC in PNW waters for anthropogenic CO_2 input (20–40 $\mu\text{mol/kg}$) and calculated a “preindustrial” Ω_{arag}^e for our data. A parallel algorithm with the same form as equation (3) was fitted to the data ($R^2 = 0.989$) and used to predict the preindustrial $\Omega_{arag}^e = 1$ horizon for the time-series data (Figure 2). This preindustrial $\Omega_{arag}^e = 1$ threshold very closely follows the 2007 Ω_{arag}^e 0.8 isoline. Therefore, within the ability to estimate anthropogenic CO_2 content in coastal waters ($\pm 50\%$ [Feely et al., 2008a]), undersaturation over shelf/slope bottom waters is likely a natural phenomena, but an anthropogenic reduction in Ω_{arag} by 0.2 units has caused a shoaling of the 1.0 horizon by $\approx 25\text{m}$ (shelf/slope) to $\approx 40\text{m}$ (offshore). Exposure of pelagic communities to undersaturated water may therefore be lengthened or intensified by anthropogenic CO_2 input.

5. Implications

[15] The persistence of water with $\Omega_{arag} < 1$ over the shelf throughout the May–November upwelling season has

not been previously noted. Although it is unclear how organisms on the central Oregon coast are directly affected by these conditions, laboratory experiments have indicated potentially deleterious impacts for organisms exposed to waters with $\Omega_{arag} < 1$ [Kleypas et al., 2006; Fabry et al., 2008; Doney et al., 2009]. A clear application of the regression model presented here is to explore effects of low Ω_{arag} on shelf communities when DIC and TA data are unavailable. Preliminary examination of historical pteropod abundance data from the Oregon coast from the last 20 years (B. Peterson, unpublished data, 2009) indicates that pteropods are generally found where upwelling water is not; their abundances are maximum in offshore waters outside of the upwelling region and peak over the shelf only during winter or El Niño events, when upwelling is suppressed. In-depth examination of these data and other historical records may provide insight into adaptations organisms use to cope with low Ω_{arag} conditions.

[16] Bakun [1990] and Snyder et al. [2003] have suggested that upwelling intensity is likely to increase under future warming climate scenarios. Because the transit time of upwelling source waters from last atmospheric exposure to the sites of local upwelling are on the order of decades [Feely et al., 2008a], additional anthropogenic CO_2 is already “in the pipeline” in the ocean interior, and will continue to decrease coastal Ω_{arag} well into this century, regardless of atmospheric CO_2 rise scenarios. Impacts of these changes will be better understood as studies of the seasonality in Ω_{arag} and effects on coastal organisms emerge. The Ω_{arag}^e relationship presented here (equation (3)) will need to be adjusted on 5–10 year intervals to account for the additional anthropogenic CO_2 input.

[17] A key advantage of the ability to estimate Ω_{arag} using commonly available hydrographic parameters (T , O_2) is the capability to hindcast Ω_{arag} from historical datasets to explore relationships with previously documented ecological/physical observations, provided corrections for reduced anthropogenic CO_2 in prior data, if significant, can be taken into account. For example, regression model development efforts by T. Kim et al. (Prediction of East/Japan Sea acidification over the past 40 years using a multiple-parameter regression model, submitted to *Global Biogeochemical Cycles*, 2009) highlight the importance of ventilation events for determining subsurface (50–500 m) Ω_{arag} in a 50-year hydrographic time-series in the East/Japan Sea. Continued refinement of Ω_{arag}^e regression models for the PNW and other coastal regions (Kim et al., submitted manuscript, 2009; S. R. Alin et al., manuscript in preparation, 2009) as more Ω_{arag} data become available will significantly enhance our understanding of the sensitivity of coastal regions to future CO_2 -chemistry changes and warming.

[18] **Acknowledgments.** Financial support for this work was provided by NOAA Global Carbon Cycle Program Grant GC05288 to RAF, CLS, and BH. LWJ was supported by a NRC Postdoctoral Fellowship. Partial support for KL was made possible by the NRL program of KOSEF. This is NOAA/PMEL contribution 3418.

References

Anderson, L. A., and J. L. Sarmiento (1994), Redfield ratios of remineralization determined by nutrient data analysis, *Global Biogeochem. Cycles*, 8, 65–80, doi:10.1029/93GB03318.

- Bakun, A. (1990), Global climate change and intensification of coastal ocean upwelling, *Science*, 247, 198–201, doi:10.1126/science.247.4939.198.
- Doney, S. C., et al. (2009), Ocean acidification: The other CO₂ problem, *Annu. Rev. Mar. Sci.*, 1, 169–192, doi:10.1146/annurev.marine.010908.163834.
- Fabry, V. J., et al. (2008), Impacts of ocean acidification on marine fauna and ecosystem processes, *ICES J. Mar. Sci.*, 65, 414–432, doi:10.1093/icesjms/fsn048.
- Feely, R. A., et al. (2004), Impact of anthropogenic CO₂ on the CaCO₃ system in the oceans, *Science*, 305, 362–366, doi:10.1126/science.1097329.
- Feely, R. A., et al. (2008a), Evidence for upwelling of corrosive “acidified” water onto the continental shelf, *Science*, 320, 1490–1492, doi:10.1126/science.1155676.
- Feely, R. A., et al. (2008b), A new proxy method for estimating the aragonite saturation state of coastal waters using chemical and hydrographic Data, *Eos Trans. AGU*, 89(53), Fall Meet. Suppl., Abstract OS33E-03.
- Hales, B., T. Takahashi, and L. Bandstra (2005), Atmospheric CO₂ uptake by a coastal upwelling system, *Global Biogeochem. Cycles*, 19, GB1009, doi:10.1029/2004GB002295.
- Huyer, A., E. J. C. Sobey, and R. L. Smith (1979), The spring transition in currents over the Oregon continental shelf, *J. Geophys. Res.*, 84, 6995–7011, doi:10.1029/JC084iC11p06995.
- Kleypas, J. A., et al. (2006), Impacts of ocean acidification on coral reefs and other marine calcifiers: A guide to future research, 88 pp., Univ. Corp. of Atmos. Res., Boulder, Colo., (Available at http://www.ucar.edu/communications/Final_acidification.pdf)
- Kutner, M., et al. (2004), *Applied Linear Regression Models*, McGraw-Hill, Boston, Mass.
- Langdon, C., et al. (2003), Effect of elevated CO₂ on the community metabolism of an experimental coral reef, *Global Biogeochem. Cycles*, 17(1), 1011, doi:10.1029/2002GB001941.
- Lassiter, A. M., et al. (2006), Phytoplankton assemblages in the CoOP-WEST coastal upwelling area, *Deep Sea Res., Part II*, 53, 3063–3077, doi:10.1016/j.dsr2.2006.07.013.
- Lee, K., et al. (2000), Global relationships of total inorganic carbon with temperature and nitrate in surface seawater, *Global Biogeochem. Cycles*, 14, 979–994, doi:10.1029/1998GB001087.
- Lee, K., et al. (2006), Global relationships of total alkalinity with salinity and temperature in surface waters of the world’s oceans, *Geophys. Res. Lett.*, 33, L19605, doi:10.1029/2006GL027207.
- Mucci, A. (1983), The solubility of calcite and aragonite in seawater at various salinities, temperatures, and one atmosphere total pressure, *Am. J. Sci.*, 283, 780–799.
- Orr, J. C., et al. (2005), Anthropogenic ocean acidification over the twenty-first century and its impact on calcifying organisms, *Nature*, 437, 681–686, doi:10.1038/nature04095.
- Park, P. K., et al. (1969), Alkalinity budget of the Columbia River, *Limnol. Oceanogr.*, 14, 559–567.
- Peterson, W. T., and J. E. Keister (2003), Interannual variability in copepod community composition at a coastal station in the northern California Current: A multivariate approach, *Deep Sea Res., Part II*, 50, 2499–2517, doi:10.1016/S0967-0645(03)00130-9.
- Sabine, C. L., and R. A. Feely (2007), The oceanic sink for carbon dioxide, in *Greenhouse Gas Sinks*, edited by D. Reay et al., pp. 31–49, CABI, Oxfordshire, U. K.
- Snyder, M. A., et al. (2003), Future climate change and upwelling in the California Current, *Geophys. Res. Lett.*, 30(15), 1823, doi:10.1029/2003GL017647.
- Tunnicliffe, V., et al. (2009), Survival of mussels in extremely acidic waters on a submarine volcano, *Nat. Geosci.*, 2, 344–348, doi:10.1038/ngeo500.
- van Heuven, S., et al. (2009), MATLAB Program Developed for CO₂ System Calculations, *Rep. ORNL/CDIAC-105b*, U.S. Dep. of Energy, Oak Ridge, Tenn.

S. R. Alin, R. A. Feely, L. W. Juraneck, and C. L. Sabine, Pacific Marine Environmental Laboratory, NOAA, 7600 Sand Point Way NE, Seattle, WA 98115, USA.

B. Hales, College of Oceanic and Atmospheric Sciences, Oregon State University, 104 Ocean Administration Bldg., Corvallis, OR 97331, USA.

K. Lee, School of Environmental Science and Engineering, Pohang University of Science and Technology, San 31, Hyoja-dong, Nam-gu, Pohang 790-784, South Korea.

J. Peterson, Cooperative Institute for Marine Resources Studies, Oregon State University, 2030 Marine Science Dr., Newport, OR 97365, USA.

W. T. Peterson, Northwest Fisheries Science Center, NMFS, 2030 S. Marine Science Dr., Newport, OR 97365, USA.

[Home](#)
[Blog](#)
[News](#)
[About](#)
[Sightline](#)

Coming to a Shore Near You

Acidified water has shown up sooner than we thought.

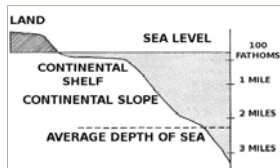
Jennifer Langston on May 26, 2011 at 10:30 am



This post is part of the research project: [Northwest Ocean Acidification](#)

Five years ago, many scientists probably thought they'd never see large pools of corrosive water near the ocean's surface in their lifetimes.

Basic chemistry told them that as the [oceans absorbed more carbon dioxide pollution](#) from cars and smokestacks and industrial processes, seawater would become more acidic. Eventually, the oceans could become corrosive enough to kill vulnerable forms of sea life like corals and shellfish and plankton.



But scientists believed the effects of this chemical process—called [ocean acidification](#)—would be confined to deep offshore ocean waters for some time. [Models projected it would take decades](#) before corrosive waters reached the shallow continental shelf off the Pacific Coast, where an abundance of sea life lives.

Until a group of oceanographers started hunting for it.

"What we found, of course, was that it was [everywhere we looked](#)," said Richard Feely, an oceanographer at the National Oceanic and Atmospheric Administration's [Pacific Marine Environmental Laboratory](#) in Seattle, who was one of the first to recognize the trouble ahead.

The [researchers found surprisingly acidic water](#)—corrosive enough to begin dissolving the shells and skeletal structures of some marine creatures—at relatively shallow depths all along the West Coast, from British Columbia to the tip of Baja California. Researchers [hadn't expected to see that extent of ocean](#) acidification until the middle to the end of this century. But in a seasonal process called "upwelling," summertime winds pushed surface waters offshore and pulled deeper, more acidic water towards the continental shelf, shorelines, and beaches.

Or, as one Oregon State University marine ecologist put it: ["The future of ocean acidification is already here off the Oregon Coast."](#)

[OPB Share](#)



Subscribe

Stay up to date on the Northwest's most important sustainability issues.

Sightline Daily is made possible by the generosity of people like you!

[Donate Today](#)

Thanks to:

Jill Andrews
for supporting a sustainable Northwest.

Stay Connected



Popular Posts

The YMCA Should Not Need a Guide-Outfitter Permit, a Special Use Permit, a National Environmental Policy Act Assessment, and a Business Plan to Take Poor Kids into National Forests

Making Sustainability Legal

Legalize Personal Car-Sharing

Talking Climate Change

Why You Can't Stop the White Pages

Recent Comments

S Hobbs on Why You Can't Stop the White Pages

The Real Reason Cities Don't Work For Families With Children | citytank on Crosscut's Flawed Take On Families in Seattle

Clyde on Talking Climate Change

Alan Durning on Safety in Numbers

Albert Kaufman on Why You Can't Stop the White Pages

Blog Topics

Series

Best of Sightline's blog

Oregon Field Guide: Ocean Acidification

The ocean is more acidic as CO₂ emissions rise and shellfish are struggling to survive.

Acidifying water poses a threat to marine animals, especially ones that need calcium carbonate to build shells and skeletons. In the Northwest, that includes everything from [geoducks](#), a giant clam that supports one of the region's most valuable commercial fisheries, to [krill](#), the tiny shrimplike creatures that [give salmon flesh its distinctive pink color](#) and feed rockfish, seals, and whales.

Other effects of low pH water on marine creatures range from lethal to bizarre to beneficial. In laboratory studies, clownfish exposed to more acidic seawater have [lost their sense of smell](#) and ability to find habitat, Antarctic krill embryos [failed to hatch](#), northern abalone larvae [from British Columbia died](#), squid [didn't want to move](#), and some eelgrass [grew more abundantly](#).



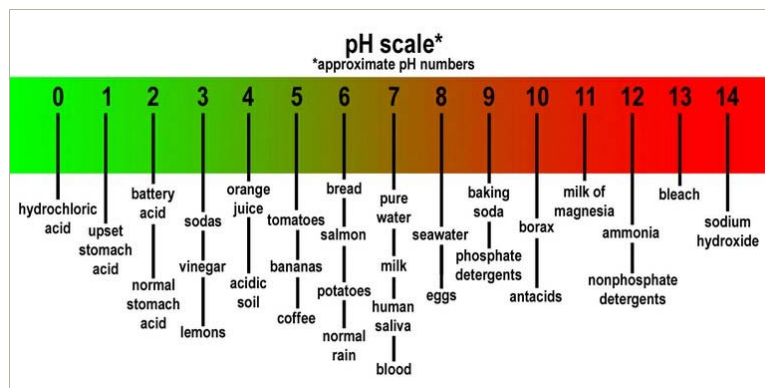
Then, the oceanographers announced [another startling discovery last summer](#). On the surface of Puget Sound, they found waters with a pH of 7.7, roughly on par with the most acidified waters found in the earlier study along the West Coast. In the deeper waters of southern Hood Canal, the acidity level was even higher—the pH plummeted to 7.4.

It was some of the most corrosive seawater recorded anywhere on Earth.

Are you enjoying this article? [Please consider making a gift to support our work.](#)

Hotspots of acidification

To put those numbers in context, the [pH scale](#) runs from 0 to 14, with pure distilled water a perfectly neutral 7. Anything below 7 – battery acid, coffee and orange juice – is acidic, and anything above 7 – eggs, toothpaste, and bleach – is basic, or alkaline.



Seawater is not an acid, because it measures above 7 on the scale. But as the world's oceans have absorbed more carbon dioxide pollution, those waters have moved towards the acidic end of that scale. Since the Industrial Revolution, the average pH of surface seawater around the globe [has dropped from 8.2 to 8.1](#).

That small numerical change may not seem like a big deal, until you realize that the pH scale is logarithmic. Each whole number represents a tenfold increase in acidity or alkalinity. For example, a lime with a pH value of 2 is 100 times more acidic than a tomato with a pH of 4.

So the world's oceans on average have already grown [30 percent more acidic](#) since we began

Dude, Where Are My Cars?
Sustainababy: Born to be Green
The Reluctant Cyclist

[View all series »](#)

Current Work

Making Sustainability Legal
Northwest Ocean Acidification
Storwater Solutions: Curbing Toxic Runoff
The Dirt on Coal
Word on the Street

[View older work »](#)

Issue Areas

Climate & Energy
Economy & Jobs
Environment
Food & Sustainable Living
Land Use & Transportation

Regions

British Columbia
Oregon
Washington

burning fossil fuels in abundance. But there are also geographic hotspots for ocean acidification, where currents and chemistry combine to make the problem worse. For example, the 7.7 pH level already found at the surface of Puget Sound (and near the surface along the West Coast) is roughly 100 percent more acidic than the current worldwide average.

The 7.4 pH water found deeper in Hood Canal is 340 percent more acidic.

Not just a coral reef problem



[Summertime conditions in Hood Canal](#) routinely kill fish, octopus, crabs, shrimp and other creatures by the hundreds or thousands. Water becomes more acidic, and oxygen levels drop so low that [fish cluster near the surface and eels visibly pant](#).

The corrosive waters lurking in Hood Canal aren't the result of ocean acidification alone. Natural processes and other forms of pollution also

contribute to low pH values there. For instance, Hood Canal is naturally rich in phytoplankton. When it dies and decomposes, it sinks and releases carbon dioxide. That process lowers the pH and also robs the water of oxygen that everything from fish to spot prawns to eels need to survive. As with many estuaries, [nutrient-rich pollution](#) from lawns, septic tanks and farm fields makes the problem worse.

So how much of the low pH conditions in Hood Canal can be attributed to ocean acidification versus other processes? Researchers estimate acidification is to blame for [24 to 49 percent of the drop in pH](#) in the deep waters of Hood Canal, compared to pre-industrial levels.

If carbon dioxide pollution continues, they expect ocean acidification to become an even more powerful factor, accounting for 49 to 82 percent of the pH decrease in Puget Sound waters. That means the manmade carbon dioxide emissions from cars and smokestacks will have a growing influence on how acidic that water becomes in the future.

Already, seawater corrosive enough to dissolve shellfish larvae is showing up within spitting distance of beaches and commercial hatcheries. As NOAA oceanographer Feely puts it:

Our decision to work in Puget Sound was to say 'Don't think of ocean acidification as an open ocean problem or a coral reef problem.'

Start thinking about it as a multi-stressor problem in estuaries where you have combined effects of increased nutrients and increased carbon dioxide.

And do the low pH levels found in Puget Sound mean that animals there have grown accustomed to more acidic waters and are possibly better prepared to adapt to the changes ahead? Or that creatures in this low-pH environment are already so stressed that they'll be among the first to wink out?

This is the big question we as scientists have to address. We don't know.

In our next post, we'll visit a lab where local scientists are working to figure that out.

Photos courtesy of the following flickr users under a Creative Commons license: [sunset Hood Canal](#) photo from MiK and [sea star photo](#) by zlatkarp. The [pH scale](#) is from [abcteach.com](#) and [continental shelf graphic](#) from [wpclipart.com](#).

We can't do this work without you!

[Please make a donation today and help keep us running.](#)

Read more in [Climate & Energy, Environment](#)

Share: [f](#) [t](#) [e](#)

Comments

Rian says:

May 26, 2011 at 12:39 pm

Has there been any study down on the effect of Fourth of July weekend on Hood Canal. I grew-up spending summers on the Canal and amount and scale of commercial grade fireworks has grown massively over the years. When I was a kid it was upsetting to see all the debris float about the next day, but as an adult I'm more concerned about what I cannot see—all the chemicals are launched into the water annually over this holiday weekend.

[Reply](#)

Collen Marquist says:

May 27, 2011 at 9:04 am

Here's a great page from Back Country Attitude that I am going to post to my Facebook page:

http://www.backcountryattitude.com/toxic_fireworks.html

Thanks for asking!!

[Reply](#)

Leave a Comment

Your email address will not be published.

Name

Email

Your website (optional)

Comment

You may use these HTML tags and attributes: <abbr title=""> <acronym title=""> <blockquote cite=""> <cite> <code> <del datetime=""> <i> <q cite=""> <strike>

[Contact](#) [Privacy Policy](#) [Free Use Policy](#) [RSS](#)

Sightline Daily brought to you by Sightline Institute.

1402 Third Avenue, Suite 500 | Seattle, Washington 98101 | tel: +1.206.447.1880 | fax: +1.206.447.2270

Home Blog News About Sightline

Trouble on the Half Shell

Baby oysters and carbon dioxide don't mix.

Jennifer Langston on June 22, 2011 at 3:00 pm



This post is part of the research project: [Northwest Ocean Acidification](#)



gautsch.net, flickr

Four summers ago, Sue Cudd couldn't keep a baby oyster alive.

She'd start with hundreds of millions of oyster larvae in the tanks at the Whiskey Creek Shellfish Hatchery in Netarts, Oregon. Only a handful would make it.

Sometimes, they'd swim for a couple of weeks. But they'd stop developing before they grew a critical shell structure, or maybe the foot or

eyespot. They'd feed poorly. One day, the larvae would simply die. A hatchery that has supplied seafood businesses for three decades had virtually nothing to sell for months, said Cudd, who owns the hatchery.

They would just sort of fade away...It was really devastating. We're kind of the independent growers' hatchery, and we had always been reliable up until that point. People were just shocked. I heard a lot of times how it was ruining people's businesses.

It's tough to say with scientific certainty that ocean acidification is the sole cause of the [die-offs that have plagued two of the Northwest's three major oyster hatcheries](#) in the last few years.

But this much seems clear: young oysters have a hard time surviving in conditions that will only become more widespread as carbon dioxide from cars, coal plants and other industries cause the fundamental chemistry of the ocean to become more acidic. (For more on that process, see our earlier posts [here](#), [here](#) and [here](#)).

Are you enjoying this article? [Please consider making a gift to support our work.](#)

Scientists have linked the mass mortalities at Whiskey Creek with seasonal "upwelling" events drawing acidic and corrosive seawater that normally lurks down deep towards our beaches and shorelines. And that kind of water is likely to surface more often along the Pacific Coast as more carbon dioxide is pumped into the atmosphere.

Put simply, carbon dioxide causes seawater to shift towards the acidic end of the pH scale. Calcium carbonate—a basic building block for shells and skeletons—becomes unavailable to creatures like oysters and abalone and sea urchins that need it. And if waters become corrosive enough, those shells simply start to dissolve.

Along with the hatchery problems, wild oysters for the last six years [have failed to spawn in Washington's Willapa Bay](#), one of the few places where Pacific oysters used to reproduce naturally.

Margaret Barrette, executive director of the [Pacific Coast Shellfish Growers Association](#), said nearly everyone in the industry, whether they grow oysters, geoducks, mussels, or clams, is

Subscribe

Stay up to date on the Northwest's most important sustainability issues.

Sightline Daily is made possible by the generosity of people like you!

[Donate Today](#)

Thanks to:

Marvin & Jean Durning
for supporting a sustainable
Northwest.

Stay Connected



Popular Posts

The YMCA Should Not Need a Guide-Outfitter Permit, a Special Use Permit, a National Environmental Policy Act Assessment, and a Business Plan to Take Poor Kids into National Forests

Making Sustainability Legal

Legalize Personal Car-Sharing

Talking Climate Change

Why You Can't Stop the White Pages

Recent Comments

S Hobbs on [Why You Can't Stop the White Pages](#)

The Real Reason Cities Don't Work For Families With Children | [citytank](#) on [Crosscut's Flawed Take On Families in Seattle](#)

Clyde on [Talking Climate Change](#)

Alan Durning on [Safety in Numbers](#)

Albert Kaufman on [Why You Can't Stop the White Pages](#)

Blog Topics

Series

[Best of Sightline's blog](#)

paying attention to ocean acidification. No one knows how other species may be affected down the road, and the vulnerable oyster crop supports the region's shellfish infrastructure.

Says Barrette:

It's in their face now—they have no reason to turn a shoulder to it because it's directly affecting them...These are people's jobs. Rural economies are fueled by these shellfish farms and without the larvae being successful, nothing can happen. It's right at the top of our list of things to worry about.

What scientists don't yet know is just what makes the upwelled water so lethal to baby oysters. Is it the elevated carbon dioxide, the low pH, the lack of calcium carbonate to build shells, some kind of algae or trace metals or bacteria that exist in upwelled water, or some combination of all of the above? Oregon State University researchers are [designing laboratory experiments right now](#) to tease apart exactly what is causing the problems. As OSU oceanographer Burke Hales puts it:

I think it's absolutely clear that high carbon dioxide and baby oysters don't go well together...But it's really hard to do experiments when you're seeing these natural fluctuations and say "yes, this in fact is the thing that's causing the problem," as opposed to something else that might happen to correlate with carbon dioxide.

No seeds, no oysters



cswtwo, flickr

In the Northwest, everyone from waterfront homeowners with shellfish gardens to mom and pop oyster growers to multi-million dollar commercial farms rely on oyster hatcheries.

The Pacific Oyster favored by commercial growers is native to Japan and is loathe to spawn in our cooler waters. So most West Coast farms buy tiny oyster "seed"—or larvae—from hatcheries and grow them out to maturity on shellfish beds or in bags or racks.

When the hatcheries have problems, the effects ripple across the \$72 million West Coast oyster industry, which pumps more money into the regional economy than farmed clams, mussels, geoduck, and other forms of shellfish combined. It would be like a tomato farmer plowing the ground in spring and getting all ready to plant, only to find he couldn't get his hands on any tomato seeds.

Eighty percent of those oyster sales are in Washington state, 17 percent in California, and the rest in Oregon and Alaska, [according to the Pacific Coast Shellfish Growers Association](#). Because oysters take several years to grow and harvest, it's not yet clear how much the recent seed shortages will cost the regional economy. But from 2005 to 2009, West Coast oyster production dropped from 94 million pounds to 73 million pounds, resulting in an \$11 million loss in sales.

A [recent paper on the potential impact of ocean acidification on fisheries](#) did the math this way: In lab experiments, growth rates for oysters and mussels decrease by about 10 percent and 25 percent in ocean conditions that might be reached by 2060 if we do nothing to control carbon dioxide. If comparable losses occur in nature, the decrease in 2006 shellfish and crustacean harvests across the US would have racked up \$200 to \$500 million in losses.

In the Northwest, those kind of losses would hit rural counties the hardest. In particular, coastal communities in places like Pacific, Gray's Harbor, or Mason counties in Washington State are highly dependent on the health of the shellfish industry, Barrette says:

In the economic downturn we've experienced as a country, some of these communities have managed to stay pretty solid because these farms are providing family wage jobs and they're contributing to the economic base of that community. And that's huge right now, especially where timber

Dude, Where Are My Cars?
Sustainababy: Born to be Green
The Reluctant Cyclist

[View all series »](#)

Current Work

Making Sustainability Legal
Northwest Ocean Acidification
Storwater Solutions: Curbing Toxic Runoff
The Dirt on Coal
Word on the Street

[View older work »](#)

Issue Areas

Climate & Energy
Economy & Jobs
Environment
Food & Sustainable Living
Land Use & Transportation

Regions

British Columbia
Oregon
Washington

production has gone down.

Estimating potential losses for the broader seafood industry is nearly impossible, since it's not yet clear how many species will be affected by ocean acidification. But just about every ocean creature that might wind up on your dinner plate—from salmon to halibut to scallops to shrimp—either uses calcium carbonate that is vulnerable to more acidic seas or eats something that does.



willapalens, flickr

'A ticking time bomb'

In 2008 and 2009, the largest US producer of farmed shellfish had its own oyster debacle. Taylor Shellfish Farms relies on its hatchery on Dabob Bay, a finger of Hood Canal, to supply much of the company's oyster seed. Production plummeted by 60 and 80 percent during those two years, no matter what they tried, said chief hatchery scientist Benoit Eudeline.

It was pretty much massive mortalities in the tanks. You'd do your thing and feed them and grow them and suddenly at a certain stage they'd just die. Like pretty much the whole group. Over and over again.

Then, things turned around. In 2010, and so far this summer, the hatchery has had some of its best years for oyster larvae ever. But that's largely due to better monitoring equipment and lucky weather.

Federal funding allowed the company to install equipment that allows hatchery operators to monitor the chemistry of the seawater which they use to grow oysters and mussels and geoducks.

In Dabob Bay, there's a layer of "good" water for rearing oysters that rests near the surface and "bad" water down deeper that's high in carbon dioxide and low in pH. Some summers, strong winds hopelessly mix the two. But for the last two years, the weather has cooperated and the corrosive water has stayed down deep. The hatchery has been able to avoid the "bad" acidic seawater by only using an intake pipe near the surface.

But running a hatchery is never as easy as following a cookbook, and the information they're gathering changes all the time, Eudeline said. When he's tried to grow oyster larvae in the deep corrosive water, for instance, the results have been inconsistent, he says:

I still think we're sitting on a ticking time bomb...My gut feeling is that if there was an upwelling event right now, we'd see larvae slowing down or dying. But it's not something I'm eager to find out.

New monitoring systems also alert hatchery operators at Whiskey Creek to high carbon dioxide conditions. They adjust their spawning times to try to avoid it, but the business still isn't where it used to be. They've also had some luck with manipulating the water chemistry once it gets into their tanks, but it's unclear how economical and practical that will be in the long run. Researchers are also racing to find out if certain families or strains of oysters are less vulnerable.

But as frustrating as her hatchery problems have been, Cudd is even more worried about wild creatures that will have to fend for themselves in more acidic seas. In normal years, they have to clear out barnacles and mussels from their intake pipes every three months. They haven't seen any of that growth in a while, she says:

That was the thing that was even more surprising. I think the really bigger issue is what's happening to the natural species in these conditions—stuff we can't control. I just don't know what's going to happen.

In our next post, we'll talk to others in the seafood industry about what the future may hold.

We can't do this work without you!

[Please make a donation today and help keep us running.](#)

Read more in [Climate & Energy](#), [Economy & Jobs](#), [Environment](#), [Food & Sustainable](#) Share: [!\[\]\(dfbd6b3763a6d1d9afaa974f64e2e4b5_img.jpg\)](#) [!\[\]\(b89ecf30df3dbaee65fa9f1829524a6e_img.jpg\)](#) [!\[\]\(12caa8c16ee33cc266cee3a47dfba46b_img.jpg\)](#)

[Living](#)

Leave a Comment

Your email address will not be published.

Name

Email

Your website (optional)

Comment

You may use these HTML tags and attributes: `` `<abbr title="">` `<acronym title="">` `` `<blockquote cite="">` `<cite>` `<code>` `<del datetime="">` `` `<i>` `<q cite="">` `<strike>` ``

[Post Comment](#)

[Contact](#) [Privacy Policy](#) [Free Use Policy](#) [RSS](#)

Sightline Daily brought to you by Sightline Institute.

1402 Third Avenue, Suite 500 | Seattle, Washington 98101 | tel: +1.206.447.1880 | fax: +1.206.447.2270

Shellfish Face Uncertain Future in High CO₂ World: Influence of Acidification on Oyster Larvae Calcification and Growth in Estuaries

A. Whitman Miller^{1*}, Amanda C. Reynolds¹, Cristina Sobrino², Gerhard F. Riedel¹

¹ Smithsonian Environmental Research Center, Edgewater, Maryland, United States of America, ² Universidad de Vigo, Vigo, Pontevedra, Spain

Abstract

Background: Human activities have increased atmospheric concentrations of carbon dioxide by 36% during the past 200 years. One third of all anthropogenic CO₂ has been absorbed by the oceans, reducing pH by about 0.1 of a unit and significantly altering their carbonate chemistry. There is widespread concern that these changes are altering marine habitats severely, but little or no attention has been given to the biota of estuarine and coastal settings, ecosystems that are less pH buffered because of naturally reduced alkalinity.

Methodology/Principal Findings: To address CO₂-induced changes to estuarine calcification, veliger larvae of two oyster species, the Eastern oyster (*Crassostrea virginica*), and the Suminoe oyster (*Crassostrea ariakensis*) were grown in estuarine water under four pCO₂ regimes, 280, 380, 560 and 800 µatm, to simulate atmospheric conditions in the pre-industrial era, present, and projected future concentrations in 50 and 100 years respectively. CO₂ manipulations were made using an automated negative feedback control system that allowed continuous and precise control over the pCO₂ in experimental aquaria. Larval growth was measured using image analysis, and calcification was measured by chemical analysis of calcium in their shells. *C. virginica* experienced a 16% decrease in shell area and a 42% reduction in calcium content when pre-industrial and end of 21st century pCO₂ treatments were compared. *C. ariakensis* showed no change to either growth or calcification. Both species demonstrated net calcification and growth, even when aragonite was undersaturated, a result that runs counter to previous expectations for invertebrate larvae that produce aragonite shells.

Conclusions and Significance: Our results suggest that temperate estuarine and coastal ecosystems are vulnerable to the expected changes in water chemistry due to elevated atmospheric CO₂ and that biological responses to acidification, especially calcifying biota, will be species-specific and therefore much more variable and complex than reported previously.

Citation: Miller AW, Reynolds AC, Sobrino C, Riedel GF (2009) Shellfish Face Uncertain Future in High CO₂ World: Influence of Acidification on Oyster Larvae Calcification and Growth in Estuaries. PLoS ONE 4(5): e5661. doi:10.1371/journal.pone.0005661

Editor: Zoe Finkel, Mt. Alison University, Canada

Received: February 4, 2009; **Accepted:** April 27, 2009; **Published:** May 27, 2009

Copyright: © 2009 Miller et al. This is an open-access article distributed under the terms of the Creative Commons Attribution License, which permits unrestricted use, distribution, and reproduction in any medium, provided the original author and source are credited.

Funding: Funding for this research was provided by the Seward Johnson Endowment provided through the Smithsonian Marine Science Network as well as federal appropriations made to the Smithsonian Institution.

Competing Interests: The authors have declared that no competing interests exist.

* E-mail: millerw@si.edu

Introduction

During the past 200 years the combustion of fossil fuels, deforestation, and land development have increased atmospheric concentrations of carbon dioxide by 36% and the rate of CO₂ emission is expected to increase during the coming century [1–3]. Approximately one third of all anthropogenic CO₂ has been absorbed by Earth's oceans [4–5]. Although the ocean has partially absorbed recently liberated anthropogenic atmospheric CO₂, this has come at the expense of significantly reduced pH (acidification) and altered carbonate chemistry in the ocean's surface waters. Since ca. 1760, the pH of the ocean's surface (the upper 200 m of the water column) has decreased by approximately 0.1 of a unit, and further reductions of 0.1 to 0.5 units are expected during the next 100 years [6–8]. There is widespread concern that these changes will produce irreversible ecological regime shifts in marine habitats, such as massive reductions in

coral reef habitats and their associated biodiversity as well as reduced availability of carbonate ions for calcifying biota [9–11].

To date most research has focused on CO₂-induced acidification in fully marine waters, while little attention has been devoted to lower salinity estuaries and temperate nearshore ecosystems. But coastal and estuarine biomes are among the most biologically productive and maintain some of the most extensive and measurable ecosystem services (e.g., commercial and recreational fisheries, fish and invertebrate nursery grounds, water purification, flood and storm surge protection, human recreation). Because they are shallower, less saline, and have lower alkalinity [12], estuaries and coastal marine habitats are more susceptible to changes in pH than the open ocean. Estuaries are also susceptible to substantial enrichment in CO₂, produced by the respiration of both natural and anthropogenic carbon. While many estuaries already have high and variable pCO₂ [13], atmospheric CO₂ enrichment will shift the baseline toward even higher values. For these reasons,

these ecosystems will likely experience more acute impacts from elevated CO₂ in coming decades.

A direct consequence of CO₂-induced acidification is the reduction of carbonate ion concentration [CO₃²⁻] in the water column. Of special concern in marine and estuarine systems is the effect of rising CO₂ on the saturation state of water with respect to calcium carbonate (Ω), where

$$\Omega = \frac{[\text{Ca}^{2+}][\text{CO}_3^{2-}]}{K'_{\text{sp}}}$$

and K'_{sp} is the apparent solubility product [14–15]:

$$K'_{\text{sp}} = [\text{Ca}^{2+}_{(\text{aq})}][\text{CO}_3^{2-}_{(\text{aq})}]$$

Ω is therefore a proxy for the ease with which organisms can produce calcium carbonate (CaCO₃). The water's saturation states with respect to aragonite and calcite, the two most commonly biomineralized forms of CaCO₃, are diminished with increased partial pressures of CO₂ ($p\text{CO}_2$) [15].

In estuaries, Ω naturally decreases with decreasing salinity due to gradients in pH, Ca²⁺ and CO₃²⁻ produced by the dilution of seawater with river water (see Cai and Wang [13]). A recent study by Salisbury et al. [16] indicates that seasonal discharges of acidic riverine water will further exacerbate acidification in estuaries, suggesting the possibility of negative impacts to shell fisheries.

In Chesapeake Bay, Wong [12] showed that water from the James River and ocean mix conservatively and that salinity and

total alkalinity (TA) are linearly related from approximately 5 psu to 32 psu. At ~18 psu, TA in the Bay is ~1250 $\mu\text{mol/kg-SW}$. If conservative mixing of water and equilibrium with current atmospheric CO₂ (380 μatm) are assumed, the aragonite compensation point (i.e., $\Omega_{\text{arag}} = 1.0$) at summer temperatures should lie near the 18 psu isopleth. As atmospheric CO₂ increases, assuming Ca²⁺ and alkalinity remain at present levels, the aragonite compensation point in estuaries will shift seaward toward higher salinities. We contend that the aragonite compensation point has already shifted significantly toward the Bay's mouth since the beginning of the industrial era (Fig. 1). The compensation point for calcite, which is approximately 1.5 times less soluble than aragonite [14] occurs at lower salinities and will shift seaward in a similar way. In reality, estuaries are frequently not in equilibrium with the atmosphere, however, a change in atmospheric $p\text{CO}_2$ will shift the baseline equilibrium to which estuaries tend, and result in wider spread elevated $p\text{CO}_2$.

We expect bivalve larvae to be more vulnerable than adults to increased CO₂ because larvae biomineralize aragonite, the more soluble form of CaCO₃, rather than calcite, the predominant material used in adult shell. Weiss et al. [17] further indicate that during biomineralization some bivalve larvae, (e.g., *Crassostrea gigas* and *Mercenaria mercenaria*) generate an even more soluble amorphous CaCO₃ as an ephemeral precursor to crystalline aragonite, and because larvae are generally less robust than adults to a variety of stresses. If larvae are indeed more susceptible to acidification, it may lead to their reduced performance, or even failure, ultimately leading to negative effects on oysters and other shellfish populations. Kurihara et al. observed at very high $p\text{CO}_2$

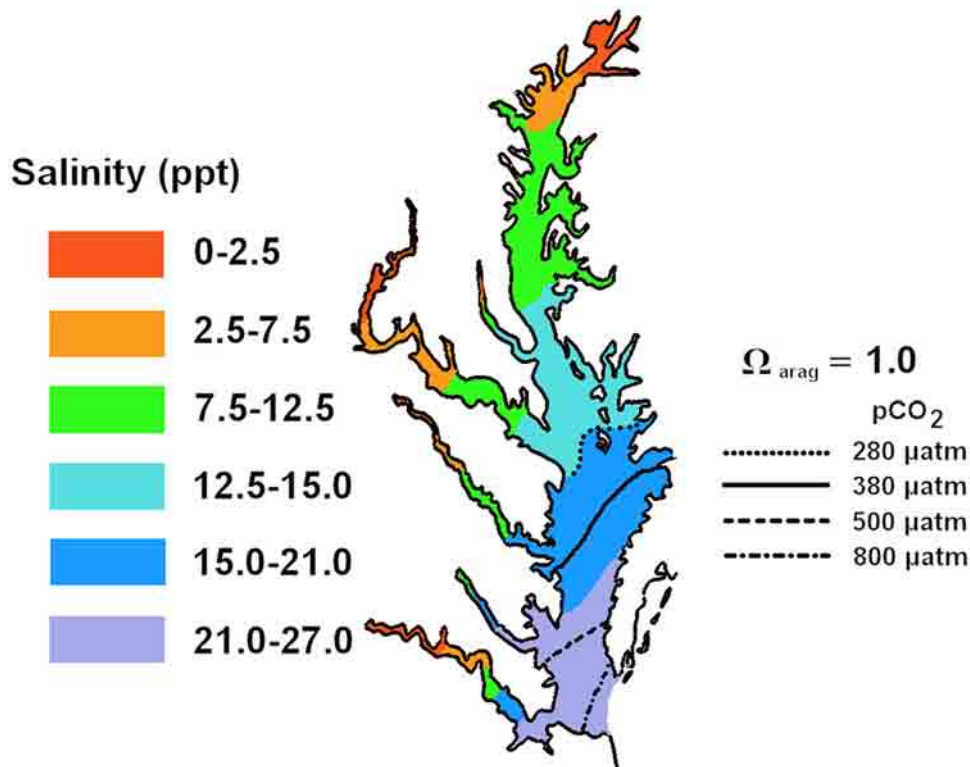


Figure 1. Projected mean summer positions of aragonite compensation points ($\Omega_{\text{arag}} = 1.0$) for Chesapeake Bay. Theoretical aragonite compensation positions were plotted under past, present and predicted atmospheric CO₂. Aragonite saturation was calculated using the program CO₂SYS.XLS from alkalinity and atmospheric $p\text{CO}_2$ at 25°C and 0 mbar pressure, assuming conservative mixing of Atlantic and the Susquehanna River alkalinities, and mean summer salinities (1985–2006 – data from Chesapeake Bay Program [47]). Aragonite is supersaturated seaward of compensation lines.

doi:10.1371/journal.pone.0005661.g001

(2268 μatm) that embryonic development and shell formation in *Crassostrea gigas* was inhibited during the initial 48 h following fertilization [18]. How shifting carbonate chemistry will alter the ecological structure and function in benthic communities remains a critical gap in our knowledge [1–2].

We conducted experiments on the veliger larvae of two closely related euryhaline oyster species, the Eastern oyster (*Crassostrea virginica* [Gmelin 1791]) and the Suminoe oyster (*Crassostrea ariakensis* [Fujita 1913]), under conditions of continuously controlled pH/pCO₂ for up to 28 days. *C. virginica* is native to the Western Atlantic, but the recent landings are just 1% of their historical maximum in Chesapeake Bay, due in large measure to overfishing and disease [19–20]. The introduction of *C. ariakensis* to Chesapeake Bay has been considered in the hopes of restoring the oyster fishery and important ecosystem functions, such as water filtration and reduction of nutrients and sediment in the water column [21]. We hypothesize that (a) oyster larvae will exhibit reduced growth and calcification at elevated pCO₂ and (b) larval development will be adversely and measurably affected when $\Omega_{\text{arag}} < 1.0$. By extension, oyster fisheries, other shellfish, and calcifying benthic fauna are expected to be negatively influenced by acidification.

Materials and Methods

All oyster larvae tested were obtained from the Virginia Institute for Marine Science's Eastern Shore Laboratory, Wachapreague, VA, where *C. virginica* and *C. ariakensis* were spawned in

quarantined facilities. Experiment *Ca* 1 larvae were derived from *C. ariakensis* stocks originating in the Ariake Sea of Japan but accidentally transferred to the west coast of the US with shipments of *C. gigas* in the 1970s [22]. *Cv* 1 were derived from Wachapreague seaside *C. virginica* stocks. Table 1 summarizes all experimental parameters for experiments *Cv* 1 and *Ca* 1. At 72 hours post fertilization, D-stage larvae were transferred from Wachapreague to a quarantined laboratory at the Smithsonian Environmental Research Center in Edgewater, MD, and placed into culture. To test the effects of elevated pCO₂, reduced pH, and aragonite saturation state on larval growth and calcification, we cultured oyster larvae under controlled conditions that simulated a typical summer estuarine environment in upper mesohaline reaches of the Chesapeake Bay: salinity = 18 psu, temperature = 25°C, day/night cycle = 14:10 hrs. Experimental treatments were blocked across two incubators (Percival I-36 Controlled Environment Chambers with Philips 700 series 32 W fluorescent bulbs) and individual aquaria randomly positioned within each incubator. Incubator A contained 280 μatm and 380 μatm pCO₂ treatments and incubator B contained 560 μatm and 800 μatm for all experiments. Prior to experiments, the PAR irradiance was measured inside each incubator and shown to be similar ($A = 167.7 \pm 5.3 \mu\text{E m}^{-2} \text{s}^{-1}$ compared with $B = 169.2 \pm 7.3 \mu\text{E m}^{-2} \text{s}^{-1}$ (mean \pm SEM).

Natural sea water was collected from Sinepuxent Bay, MD (~28 psu) and Delaware Bay, DE (~24 psu) and filtered through a 0.2 μm filter and diluted with deionized water to 18 psu. An open cell, two-point titration [23] determined the TA of the water

Table 1. Carbonate chemistry parameter values/sources and culture conditions for Eastern oyster (*Crassostrea virginica*) and Suminoe oyster (*C. ariakensis*) larvae experiments.

Parameter	<i>C. virginica</i> (<i>Cv</i> 1)				<i>C. ariakensis</i> (<i>Ca</i> 1)				Parameter Source
Simulation date	Pre-IR	2008	2050	2100	Pre-IR	2008	2050	2100	
Target pCO ₂ (μatm)	280	380	560	800	280	380	560	800	
Mean pCO ₂ (μatm)	284	389	572	840	291	386	581	823	CO ₂ SYS calc.
SEM	4.8	7.9	10.8	17.4	3.8	6.7	13.6	11.8	
Mean hourly pH	8.16	8.06	7.91	7.76	8.17	8.08	7.92	7.79	Direct Measure
SEM	0.002	0.005	0.005	0.006	0.004	0.006	0.008	0.006	
Mean TA ($\mu\text{mol/kg}$)	1229	1268	1283	1289	1297	1324	1357	1360	CO ₂ SYS calc.
SEM	15.7	18.4	17.2	15.7	16.6	15.5	23.9	16.4	
Mean TDIC ($\mu\text{mol/kg}$)	1126	1188	1232	1265	1187	1237	1301	1331	Direct Measure
SEM	15.1	17.8	16.9	15.7	15.3	14.6	23	15.8	
Mean [CO ₂] ($\mu\text{mol/kg}$)	8.8	12	17.7	25.9	9	11.9	18	25.4	CO ₂ SYS calc.
SEM	0.15	0.24	0.33	0.54	0.12	0.21	0.42	0.36	
Mean [HCO ₃ ⁻] ($\mu\text{mol/kg}$)	1045	1116	1169	1206	1100	1159	1234	1269	CO ₂ SYS calc.
SEM	14.1	16.8	16	14.9	13.9	13.6	21.7	15	
Mean [CO ₃ ⁻] ($\mu\text{mol/kg}$)	72.4	60.4	45.1	32.7	78.3	65.7	49.6	36.9	CO ₂ SYS calc.
SEM	0.8	1	0.7	0.6	1.4	1.3	1.4	0.8	
Mean Ω_{arag}	1.2	1	0.8	0.6	1.3	1.1	0.8	0.6	CO ₂ SYS calc.
SEM	0.01	0.02	0.01	0.01	0.02	0.02	0.02	0.01	
Salinity (psu)	18.2	18.2	18.2	18.2	18.2	18.2	18.2	18.2	Direct Measure
SEM	0.04	0.04	0.04	0.04	0.03	0.03	0.03	0.03	
Duration (d)	26	26	26	26	28	28	28	28	

Larvae were grown under four pCO₂ conditions (280, 380, 560, 800 μatm), simulating equilibration with atmospheric CO₂ in the preindustrial era, present (2008), 2050 and 2100 CE. All experiments were conducted at 25°C and under a 14 h:10 h light:dark cycle, simulating summer growing conditions in Chesapeake Bay. TA = Total Alkalinity, TDIC = Total Dissolved Inorganic Carbon.

doi:10.1371/journal.pone.0005661.t001

just prior to the onset of each experiment. Total alkalinity and $p\text{CO}_2$ targets for pre-industrial ($p\text{CO}_2 = 280 \mu\text{atm}$), present day ($p\text{CO}_2 = 380 \mu\text{atm}$), year 2050 ($p\text{CO}_2 = 560 \mu\text{atm}$) and year 2100 ($p\text{CO}_2 = 800 \mu\text{atm}$) settings, as projected by the IS92a “business as usual” scenario [24] were then entered into the computer program CO₂SYS.XLS [25]. The program was parameterized specifically with the two dissociation constants K_1 and K_2 for carbonic acid in estuarine waters of Cai and Wang [13] to determine corresponding experimental pH levels.

Larvae were grown in 4-L polycarbonate aquaria, under four $p\text{CO}_2$ treatments, and each treatment included three replicate aquaria that were independently controlled for $p\text{CO}_2/\text{pH}$ ($n = 12$). Filtered water samples ($0.2 \mu\text{m}$) were collected from each aquarium every few days throughout the experiments for total dissolved inorganic carbon (TDIC) analysis. (To maintain water quality, water was changed in all aquaria every two days. TDIC samples were taken 24–48 hours after a water change.) Water samples were capped without head space and analyzed immediately, or stored at 4°C and analyzed within 48 hrs. TDIC was measured using a total organic carbon analyzer, outfitted with a phosphoric acid inorganic carbon reagent reaction chamber and non-dispersive infrared detector (Schimadzu TOC-V with IC reactor kit). TDIC was then partitioned into $p\text{CO}_2$, bicarbonate, and carbonate and TA calculated with CO₂SYS.XLS [25] (Table 1.) Experiments were ended when larvae of the largest size classes achieved competence as indicated by the presence of eye spots.

Experiments *Cv* 1 (*Crassostrea virginica*) and *Ca* 1 (*C. ariakensis*) were inoculated with 15,000 four day-old D-stage larvae respectively, and were grown for up to 28 days. Aquaria received controlled quantities of the microalgae *Isochrysis galbana* (Prymnesiophyceae) as food. Microalgae were grown in semi-continuous cultures using f/2-Guillard medium. Equal quantities of microalgae were pipetted daily from cultures of known density into each aquarium, with daily doses increasing as larvae grew larger. Target inoculation densities in each aquarium increased from $1.5 \cdot 10^4 \text{ cells} \cdot \text{ml}^{-1}$ at the beginning of an experiment to $1.0 \cdot 10^5 \text{ cells} \cdot \text{ml}^{-1}$ during the final days, when larvae were larger and ingesting more food.

The $p\text{CO}_2$ in each aquarium was sustained by intermittent bubbling with CO₂-enriched air (commercially available, certified 1.0% CO₂) and continuous aeration with CO₂-stripped air. Soda-lime filters were used to strip CO₂. Continuous aeration with CO₂-stripped air oxygenated and mixed the water, while simultaneously driving CO₂ out of the water and pushing pH upward. Each aquarium was continuously monitored with a pH probe (NBS scale) and control system. Once a target pH set point was exceeded, an automated controller opened a solenoid and delivered the 1% CO₂ air mixture to an aquarium, thereby driving pH downward. The flow of CO₂ was automatically stopped when the pH set point was reached. Based on hourly pH measurements, the negative feedback control system was shown to maintain pH (and $p\text{CO}_2$) at near constant levels for up to 4 weeks. The four pH set points used corresponded to desired target $p\text{CO}_2$ treatments for water of known total alkalinity. Probes were calibrated prior to the experiment using NIST traceable buffers (pH = 4.00 and 7.00), recalibrated at least one time during the experiment, and again at the conclusion of the experiment to ensure proper operation.

At the end of each experiment, larvae from each aquarium were collected and fixed in 95% ethanol. Random samples were taken from each replicate and photographed at $20\times$ magnification; ($n = 205 \pm 6.4$ shells per replicate (mean \pm SEM)). Larval shells were positioned on their sides and photographed in silhouette. Outer shell areas were measured using digital image analysis [26] (Scion

Image, ver. 4.0.3.2). All areas are reported as total outer surface areas (i.e., $2\times$ photographed area = total surface area of both valves). The same samples were rinsed with deionized water to remove sea salts and ethanol, and the shells dissolved in trace metal grade HCl, and diluted to a known volume. Inductively coupled plasma/optical emission spectroscopy (ICP/OES) was used to measure the mean calcium content per shell from each replicate sample across treatments.

For each experimental treatment, the mean mass of CaCO₃ per unit area ($\mu\text{g}/\mu\text{m}^2$) was determined by dividing the mean CaCO₃ content of shells by the mean shell area. These values were then divided by the density of crystalline aragonite ($2.93 \text{ g}/\text{cm}^3$) [27] to estimate the mean apparent aragonite thickness of larval shells. However, this uniformly overestimates shell thickness slightly, because image analysis calculated shell area in silhouette, thereby underestimating the true three-dimensional shell surface. This bias should not affect comparisons with treatments for the same organism.

Results

Larval Development

Larval development proceeded from 96 h post fertilization to the eyed veliger and pediveliger stages (i.e., achieved competence) among the largest size classes in all treatments and across all experiments. Experiments *Cv* 1 and *Ca* 1 ran to larval ages of 30 d and 32 d, respectively.

Shell Area

Crassostrea virginica grew more slowly at elevated $p\text{CO}_2$ than at either 280 or 380 μatm treatments, as indicated by analysis of variance (*Cv* 1: $F_{3,8} = 6.605$, $n = 12$, $P = 0.015$, Fig. 2a). No significant differences in shell growth were observed across $p\text{CO}_2$ treatments for *C. ariakensis* (*Ca* 1: $F_{3,8} = 0.024$, $n = 12$, $P = 0.995$, Fig. 2b). Cumulative shell size frequencies for each species and treatment reveal: (1) that ninety percent of *C. virginica* shells exceeded the median size class of *C. ariakensis* and (2) clear treatment effects in *C. virginica* growth but none in *C. ariakensis* (Fig. 3).

Calcification

The amount of CaCO₃ biomineralized by *Crassostrea virginica* larvae decreased as $p\text{CO}_2$ increased (Fig. 2c). Analysis of variance confirmed significant differences among $p\text{CO}_2$ treatments (*Cv* 1: $F_{3,8} = 11.8026$, $n = 12$, $P = 0.0026$). By contrast, no clear trends or differences in biomineralization were apparent for *C. ariakensis* (*Ca* 1: $F_{3,7} = 0.6451$, $n = 11$, $P = 0.6103$, Fig. 2d).

Aragonite Saturation

In each experiment, aragonite conditions ranged from super-saturating ($\Omega_{\text{arag}} = 1.2–1.3$) to undersaturating ($\Omega_{\text{arag}} = 0.6$). *C. ariakensis* was unaffected by differences in aragonite saturation, but growth and calcification in *C. virginica* were significantly curtailed when $p\text{CO}_2$ was high and $\Omega_{\text{arag}} < 1.0$ (Fig. 2). Importantly, both species achieved net growth even when the saturation state of aragonite was well below 1.0.

Shell Thickness

Although cross sectional measurements of larval shells were not performed directly, we derived an estimate of average shell thickness that is theoretically attributable to aragonite volume. For each experimental treatment, the mean CaCO₃ content per shell was divided by the corresponding mean shell area ($\mu\text{g}/\mu\text{m}^2$). This value was then divided by the density of crystalline aragonite

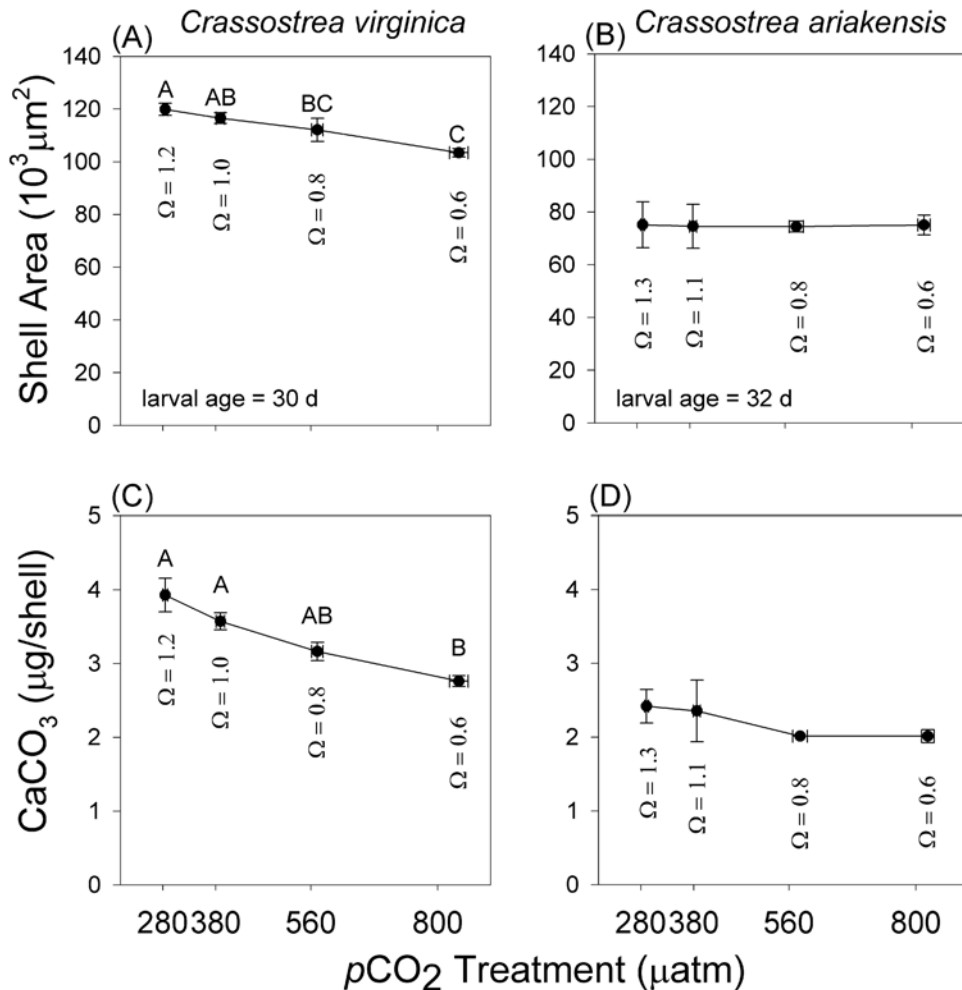


Figure 2. Effects of pCO₂ treatment on larval shell growth and calcification. Mean shell areas ± SEM (μm²) (panels A and B) and mean shell CaCO₃ content ± SEM (μg/shell) (panels C and D) reported by pCO₂ treatment ± SEM (μatm) for two oyster species. Corresponding aragonite saturation states (Ω_{arag}) are indicated for each treatment. Statistical differences determined by ANOVA and Tukey HSD tests. *C. virginica* grew more quickly than *C. ariakensis* under all treatments but experienced reduced growth at high pCO₂. The growth of *C. ariakensis* was not noticeably affected by elevated pCO₂ or aragonite saturation. *C. virginica* calcified less at elevated pCO₂ and Ω_{arag} < 1.0 (panel C), whereas calcification of *C. ariakensis* was not significantly influenced by elevated pCO₂ or aragonite saturation (panel D). doi:10.1371/journal.pone.0005661.g002

(2.93 × 10⁻⁶ μg/μm³), leaving the mean apparent aragonite thickness in μm. The mean apparent aragonite thickness was strikingly similar across treatments and experiments (ranging from 9 to 11 μm) regardless of species or larval age (Fig. 4).

A second pair of similar experiments was conducted using a modified design (i.e., fed with a two algal species diet, use of a different strain of *C. ariakensis*, and a greater starting larval density). Because of ciliate contamination in one of the *C. virginica* treatments, the experiments had to be prematurely terminated. Nevertheless, at larval ages of 14 d, results were similar to those reported above, indicating significantly reduced shell area and calcium content for *C. virginica* at elevated pCO₂, but no significant pCO₂ effects for *C. ariakensis*.

Discussion

Most ocean acidification studies have focused on either warm water corals or pelagic biota [1–2], [28]. In general, marine fauna exhibit reductions in calcification at elevated pCO₂ (e.g., scleratinian corals, Gattuso et al. [29], Langdon [9]; pteropods,

Feely et al. [15], Orr et al. [8]; foraminifera, Bijima et al. [30]; see Fabry et al. [28] for review of marine faunal responses to elevated pCO₂). As a group, coccolithophores react more variably, appearing to show species-specific responses to elevated CO₂ [31], with Iglesias-Rodriguez et al. [32] reporting increased calcification in *Emiliania huxleyi* at pCO₂ at 750 μatm. Experiments to date have largely simulated elevated atmospheric CO₂ in fully marine settings (i.e., high salinity), meaning that water was supersaturated for CaCO₃ under all challenge treatments due the relatively high total alkalinity of the seawater.

In cases where marine mollusks have been subjected to aragonite undersaturation, the results have generally been deleterious. For example, Kurihara et al. [18] observed that calcification and shell formation was inhibited during early development of *Crassostrea gigas* larvae when seawater was undersaturated with respect to aragonite (Ω_{arag} = 0.68). When adult pteropods (*Clio pyramidata*) were exposed to seawater that was undersaturated for aragonite, their shells began to dissolve within 48 hours [8], [15], [28]. Green et al. [33] showed that newly set juvenile hard shell clams (*Mercenaria mercenaria*, <2.0 mm) grown in

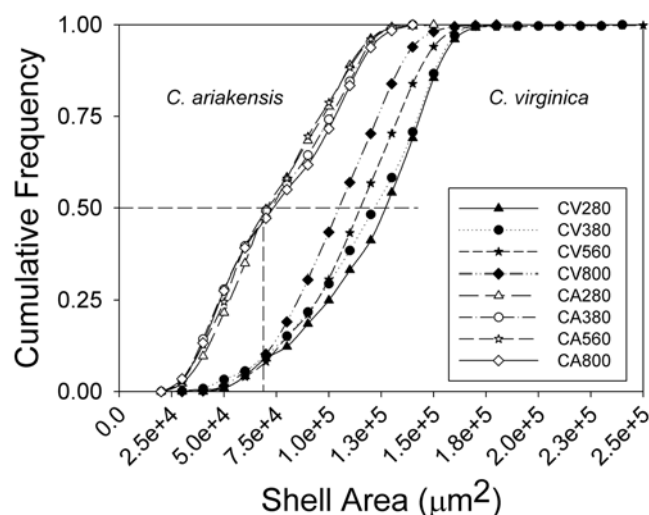


Figure 3. Effects of $p\text{CO}_2$ treatment on cumulative size frequency of larval shells ($\mu\text{m}^2/\text{shell}$) for two oyster species. Black symbols and curves on right show results from *Crassostrea virginica*, experiment Cv 1, age=30 d. Open symbols and left curves plot *C. ariakensis* results (experiment Ca 1, age=32 d). $p\text{CO}_2$ treatments=280, 380, 560, 800 μatm . Number of shells per treatment=615 \pm 26.7 (mean \pm SEM). *C. virginica* grew to markedly larger sizes than *C. ariakensis*. Ninety percent of *C. virginica* shells were as large as or larger than the median *C. ariakensis* size class (dashed line). Growth of *C. virginica* was influenced by $p\text{CO}_2$ treatment and *C. ariakensis* was unaffected.
doi:10.1371/journal.pone.0005661.g003

benthic sediments with porewater undersaturated for CaCO_3 showed signs of corrosion and significantly increased mortality. Hall-Spencer et al. [34] have observed that the shells of adult gastropods living in ultra high $p\text{CO}_2$ habitats associated with natural underwater volcanic CO_2 vents in the Mediterranean also dissolve when $\Omega < 1.0$.

In contrast, when *C. virginica* and *C. ariakensis* larvae were cultured continuously from 96 h post fertilization (D-stage) to ~30 d in typical estuarine conditions (salinity = 18 psu, TA \approx 1225 $\mu\text{mol/kg}$) and exposed to elevated $p\text{CO}_2$ levels, both species appeared to grow, calcify and develop normally with no obvious morphological deformities, despite conditions of significant aragonite undersaturation ($\Omega_{\text{arag}} = 0.6\text{--}0.7$). These findings demonstrate the physiological capacity of oyster larvae to withstand prolonged exposure (up to 28 days) to high $p\text{CO}_2$ and aragonite undersaturation, and run counter to expectations that aragonite shelled larvae should be especially prone to dissolution at high $p\text{CO}_2$ [28]. It should not be surprising that some mollusks can grow in undersaturated conditions; most fresh water mollusks are clearly well adapted to such conditions. Nevertheless, as atmospheric CO_2 continues to rise, all calcifying organisms will be encountering conditions that they have not experienced in recent geologic history.

When Carrier and Palmer [35] studied the normal growth and development of *C. virginica* larval shells using scanning electron microscopy, they found uniform, extremely thin shells, 4–6 μm across a range of larvae 100–350 μm in length. The thinness of the shells for their area, ca. 2–4% of the total length, is likely an adaptation to planktonic living. In our study, both oyster species generated larval shells that were of similar mean thickness, regardless of $p\text{CO}_2$, Ω_{arag} , or shell area. We interpret the pattern of similar shell thickness as further evidence of normal larval shell development.

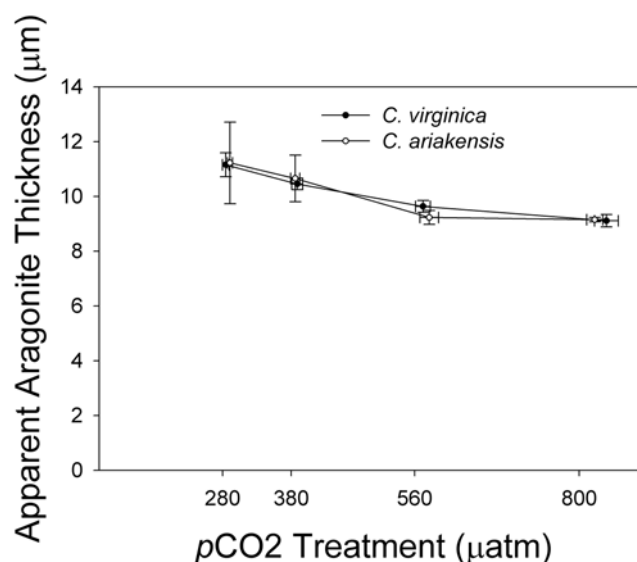


Figure 4. Effects of $p\text{CO}_2$ treatment on apparent aragonite shell thickness for two oyster species. Apparent aragonite thickness (μm) of larval shells = mean CaCO_3 content (μg)/mean shell area (μm^2)/aragonite density ($2.93 \times 10^{-6} \mu\text{g}/\mu\text{m}^3$). Aragonite thickness was similar across species and varied little across $p\text{CO}_2$ treatments.
doi:10.1371/journal.pone.0005661.g004

Regardless of their shared physiological tolerance to undersaturated aragonite, *C. virginica* and *C. ariakensis* have divergent responses to elevated $p\text{CO}_2$. *C. virginica* demonstrates consistently reduced growth and calcification at high $p\text{CO}_2$. Conversely, *C. ariakensis* larvae are not differentially affected by $p\text{CO}_2$, but do grow and calcify more slowly than *C. virginica* under all $p\text{CO}_2$ treatments. These differences suggest that CO_2 -induced acidification is species-specific and will have unpredictable consequences in estuaries and nearshore ecosystems, even in closely related species.

From strictly thermodynamic considerations, the process of calcification in undersaturated environments ($\Omega_{\text{arag}} < 1.0$) must require the input of exogenous energy to go forward. Weiner and Dove [36] describe two predominant processes of biomineralization widely used by marine and estuarine invertebrates. Extracellular mineralization is used by mollusks, scleratinian corals, bryozoans and some foraminifera and requires active pumping of ions or secretion and active transport of vesicles containing aqueous solutions of high ionic concentrations across cell membranes to produce conditions favorable for calcification. Coccolithophores, echinoderms, and other foraminifera use intracellular biomineralization, whereby nucleation of mineral structures occurs directly inside vesicles using similar active transport systems. The resulting carbonate structures are then secreted across the cell membrane (Weiner and Dove [36] and references therein). As aragonite becomes less saturated, the energetic costs for biomineralization should become progressively more expensive.

We do not perceive aragonite undersaturation as a “formal” barrier to calcification by marine or estuarine organisms in general. Aragonite saturation state is rather a convenient index to the ease with which biomineralization can be carried out. The higher the saturation state, the greater the relative availability of both Ca^{2+} and CO_3^{2-} , and the lower the energy requirement for biochemical pumping to generate local supersaturation used when producing shell material. Just as species differ according to many environmental requirements, they likely differ in their ability or efficiency to supply energy for calcification. Marine taxa such as

corals and pteropods, which are well adapted to marine conditions where both Ca²⁺ and CO₃²⁻ have been abundant and relatively constant for millions of years, may have problems calcifying as CO₃²⁻ declines due to anthropogenic CO₂ enrichment, even though their water remains above saturation for both aragonite and calcite. In contrast, larvae of the euryhaline oysters *C. virginica* and *C. ariakensis*, cultured in mesohaline conditions with lower Ca²⁺ and CO₃²⁻ are able to generate and maintain aragonite shells when aragonite is somewhat below saturation. Although calcification is suppressed in lower saturation states for *C. virginica*, *C. ariakensis* is less affected by these conditions. Estuaries and open oceans differ substantially in their physical and chemical characteristics and dynamics, as do the evolutionary histories of their biota. For these reasons, expectations about the biological response to increasing atmospheric CO₂ and acidification ought to be different as well.

Because of extreme spatial and temporal heterogeneity in estuaries and coastal systems, uniform equilibrium with atmospheric CO₂ is neither expected nor achieved [37–38]. Estuarine habitats where shellfish settle and live often experience localized high pCO₂, up to as much as 6000 µatm, due to benthic respiration [39]. Our results suggest that for one key species, *C. virginica*, growth and calcification are diminished at relatively low enhancements of pCO₂, conditions that fall within the bounds of variation that currently exist in its native habitat. When combined with existing natural forcing, future increases to pCO₂ may influence significantly the success of larvae, and ultimately the success and distribution of these oysters in Chesapeake Bay and similar systems.

We predict that as atmospheric CO₂ concentrations increase, conditions in estuaries will be less favorable for calcification in all salinity zones and will pose new environmental stresses on their inhabitants. For some calcifying species, the added energetic burden of producing shell under less favorable conditions may restrict growth. Our results suggest that this will be the case for *C. virginica*, but not necessarily for *C. ariakensis*. As energy costs mount, calcifying biota may be faced with a trade-off, either to allocate more energy to calcification at the cost of growth and stored energy reserves, or to accept a lesser degree of calcification in exchange for greater growth and more stored energy.

When invertebrate larvae become physiologically stressed from chemical and physical factors encountered in their environment, they sometimes delay settlement and metamorphosis. Pechenik [40] lists temperature, salinity, nutrition, low dissolved oxygen, pollution, and ultraviolet radiation as possible stressors that may induce delayed metamorphosis, and further indicates that larvae are more sensitive than adults to such stressors (Pechenik [41] and references therein). High pCO₂ and reduced CaCO₃ saturation may produce similar effects. For planktotrophic larvae, even minor increases in energy expenditure for shell production may reduce energy reserves that are critical for larval growth and survival. Metamorphosis is energetically demanding and relies entirely on energy stores accumulated during the larval stage [41–42]. If larval growth and calcification are adversely affected by CO₂-induced acidification, larvae may well be energetically disadvantaged as they attempt metamorphosis, thereby suffering reduced survivorship and fitness. Furthermore, Pechenik [41] indicates that latent larval effects (i.e., impacts to post-metamorphic growth and mortality due to larval experience) may be common and species-specific among marine organisms.

Our findings suggest that as atmospheric CO₂ rises in coming decades, the larvae of *C. virginica*, and perhaps other estuarine species, will grow and calcify more slowly than today. Unless larvae can achieve settling/metamorphic competence more

efficiently in the future, slowed growth and calcification will lead to prolonged times in the water column, a situation that can result in higher pre-settlement larval mortality. Mortality from predation and disease increases the longer the larvae remain in the water column [43–44]. To illustrate the impact of relatively small changes in water column residence and mortality on recruitment, Kennedy [45] modeled the theoretical fate of *C. virginica* larval offspring from a single female, using natural daily mortality data from a variety of investigators. An 89% reduction in successful recruitment was postulated when metamorphosis was delayed five days (from 20 d to 25 d) and daily mortality rate increased from 20% to 25%. If higher water column mortality rates are coupled with lower larval quality at settlement (i.e., larvae settling with fewer energy reserves), then rates of recruitment could be expected to decrease in the future.

Whether or not prolonged time in the plankton and increased energy expenditures during larval growth and development from elevated CO₂ adversely affect later life stages and, ultimately, the population dynamics and ecology of *C. virginica* or other species is unknown. Clearly, the larvae of both *Crassostrea* species that we studied have the physiological capacity to grow and calcify in undersaturated conditions, but if and how increasing pCO₂ at all points in their habitat will adversely affect survivorship in the plankton as well as metamorphic success and recruitments dynamics remains to be tested.

On the Pacific coast of the United States, commercial oyster hatcheries are experiencing alarming and widespread difficulties keeping Pacific oyster (*C. gigas*) larvae alive in culture, with two of the largest hatcheries reporting production rates down by as much as 80%. Moreover, there has been little or no “natural” recruitment for several years in areas where *C. gigas* have previously established naturalized populations. (R. Downey, Pacific Coast Shellfish Growers Association, pers. comm.). In regions of upwelling along the continental shelf of western North America, Feely et al. [46] have determined that the pH and Ω_{arag} of surface waters are more acidic and have less aragonite saturation than expected. At water depths of 40–120 m in many locations along the coast, but at 0 m in the region near the California/Oregon border, pH was reported to be ~7.75 and Ω_{arag} < 1.0. Whether recent recruitment and aquaculture failures are linked to changes in carbonate chemistry are unknown, but should be investigated.

The natural spatial and temporal heterogeneity in salinity, alkalinity, pH, and pCO₂ in estuaries impose more complex environmental stresses on calcifying biota than in the open ocean where the environment is far less variable. As atmospheric CO₂ concentrations increase, the proportion of estuarine habitat undersaturated for aragonite will increase. In a high CO₂ world, we predict that the aragonite compensation point in estuaries (salinity isopleth where Ω_{arag} = 1.0) will shift seaward toward higher salinities. Because estuarine species have evolved in such variable environments, they may possess greater physiological capacity to respond to CO₂-induced acidification than fully marine taxa. Nevertheless, adaptive physiological tolerance of larvae may not be sufficient to sustain populations of calcifying benthic species, including widespread economically important fisheries, in the face of changing atmospheric CO₂.

Acknowledgments

We thank J.P. Megonigal, E. Jewett, P. Neale, and R. Osman for their consultation and technical advice. We thank S. Bonniwell and M. Luckenbach for supplying oyster larvae and culturing advice, as well as K. Erasmus, R. Lowenthal, and K. Stull, G. Riedel, D. Butera, S. Santagata, K. Klug, M. Hagan, and G.M. Ruiz for their contributions to these experiments and manuscript.

Author Contributions

Conceived and designed the experiments: AWM CS GFR. Performed the experiments: AWM ACR GFR. Analyzed the data: AWM ACR CS GFR.

References

- Royal Society (2005) Ocean acidification due to increasing carbon dioxide. Policy document 12/05 The Royal Society. 60 p.
- Kleypas JA, Feely RA, Fabry VJ, Langdon C, Sabine CL, et al. (2006) Impacts of Ocean Acidification on Coral Reefs and Other Marine Calcifiers: A guide for Future Research, report of a workshop held 18–20 April 2005, St. Petersburg, FL, sponsored by NSF, NOAA, and the U.S. Geological Survey. 88 p.
- Turley C, Blackford J, Widdicombe S, Lowe D, Nightingale PD, et al. (2006) Reviewing the impact of increased atmospheric CO₂ on oceanic pH and the marine ecosystem, In Schellnhuber HJ, Cramer W, Nakicenovic N, Wigley T, Yohe G, eds. Avoiding Dangerous Climate Change, Cambridge University Press, 8. pp 65–70.
- Sabine CL, Feely RA, Gruber N, Key RM, Lee K, et al. (2004) The Oceanic Sink for Anthropogenic CO₂. Science 305: 367–371.
- Canadell JG, Le Que re C, Raupach MR, Field CB, Buitenhuis ET, et al. (2007) Contributions to accelerating atmospheric CO₂ growth from economic activity, carbon intensity, and efficiency of natural sinks. Proc Nat Acad Sci USA 104(47): 18866–18870.
- Caldeira K, Wickett ME (2003) Anthropogenic carbon and ocean pH. Nature 425: 365.
- Caldeira K, Wickett ME (2005) Ocean model predictions of chemistry changes from carbon dioxide emissions to the atmosphere and ocean, J Geophys Res Oceans 110(C9), C09504: doi:10.1029/2004JC002671.
- Orr JC, Fabry VJ, Aumont O, Bopp L, Doney SC, et al. (2005) Anthropogenic ocean acidification over the twenty-first century and its impact on calcifying organisms. Nature 437(7059): 681–686.
- Langdon C (2002) Review of experimental evidence for effects of CO₂ on calcification of reef builders. Proceedings of the 9th International Coral Reef Symposium 2: 1091–1098.
- Gazeau F, Quiblier C, Jansen JM, Gattuso J-P, Middelburg JJ, et al. (2007) Impact of elevated CO₂ on shellfish calcification. Geophys Res Lett 34: L07603. doi:10.1029/2006GL028354.
- Carpenter KE, Abrar M, Aeby G, Aronson RB, Banks S, et al. (2008) One-third of reef-building corals face elevated extinction risk from climate change and local impacts. Science 321: 560–563.
- Wong GT (1979) Alkalinity and pH in the southern Chesapeake Bay and the James River estuary. Limnol Oceanogr 24: 970–977.
- Cai W-J, Wang Y (1998) The chemistry, fluxes, and sources of carbon dioxide in the estuarine waters of the Satilla and Altamaha Rivers, Georgia. Limnol Oceanogr 43: 657–668.
- Doney SC, Fabry VJ, Feely RA, Kleypas JA (2009) Ocean acidification: the other CO₂ problem. Annu Rev Mar Sci 1: 169–192.
- Feely RA, Sabine CL, Lee K, Berelson W, Kleypas J, et al. (2004) Impact of anthropogenic CO₂ on the CaCO₃ system in the oceans. Science 305: 362–366.
- Salisbury J, Green M, Hunt C, Campbell J (2008) Coastal acidification by rivers: A new threat to shellfish? EOS Trans AGU 89: 513.
- Weiss IM, Tuross N, Addadi L, Weiner S (2002) Mollusc larval shell formation: amorphous calcium carbonate is the precursor phase for aragonite. J Exp Biol 293: 478–491.
- Kurihara H, Kato S, Ishimatsu A (2007) Effect of increased seawater pCO₂ on early development of the oyster *Crassostrea gigas*. Aquat Biol 1: 91–98.
- Kirby MX (2004) Fishing down the coast: Historical expansion and collapse of oyster fisheries along continental margins. Proc Acad Nat Sci U S A 101: 13096–13099.
- Breitburg DL, Riedel GF (2005) Multiple Stressors in Marine Systems. In: EA Norse and LB Crowder editors, Marine Conservation Biology: The Science of Maintaining the Sea's Biodiversity (MCB), Island Press, Washington, D.C. pp 167–182.
- OSB (2004) Nonnative Oysters in Chesapeake Bay. Ocean Studies Board, Division on Earth and Life Studies, National Research Council of the National Academies, The National Academies Press, Washington, D.C., 325 p.
- Breese WP, Malouf RE (1977) Hatchery rearing techniques for *Crassostrea rivularis*. Aquaculture 12: 123–126.
- Edmond JM (1970) High precision determination of titration alkalinity and total carbon dioxide content of sea water by potentiometric titration. Deep Sea Res 17: 737–750.
- Leggett J, Pepper WJ, Swart RJ (1992) Emissions Scenarios for the IPCC: An Update. In: J. T. Houghton, B. A. Callander, S. K. Varney editors. Climate Change 1992: The Supplementary Report to the IPCC Scientific Assessment, Cambridge University Press, Cambridge. pp 69–95.
- Pelletier G, Lewis E, Wallace D (2007) CO₂sys.xls: a calculator for the CO₂ system in seawater for Microsoft Excel/VBA, Washington State Department of Ecology/Brookhaven National Laboratory, Olympia, WA/Upton, NY, USA.
- Scion Image for Windows. Release alpha 4.0.3.2, © 2000–2001, Scion Corporation, www.scioncorp.com.
- Lide DR (2007) CRC Handbook of Chemistry and Physics, 88th Edition (Crc Handbook of Chemistry and Physics). CRC.
- Fabry VJ, Seibel BA, Feely RA, Orr JC (2008) Impacts of ocean acidification on marine fauna and ecosystem processes. ICES J Mar Sci 65: 414–432.
- Gattuso JP, Frankignoulle M, Bourge I, Romaine S, Buddemeir RW (1998) Effect of calcium carbonate saturation of seawater on coral calcification. Global Planet Change 18: 37–46.
- Bijma J, Honisch B, Zeebe RE (2002) Impact of the ocean carbonate chemistry on living foraminifera shell weight: comment on “Carbonate ion concentration in glacial-age deepwaters of the Caribbean Sea” by WS Broecker and E Clark. Geochim. Geophys. Geosyst 3: 1064. doi:10.1029/2002GC000388.
- Fabry VJ (2008) Marine calcifiers in a high-CO₂ ocean. Science 320: 120–122.
- Iglesias-Rodriguez MD, Halloran PR, Rickaby REM, Hall IR, Colmenero-Hidalgo E, et al. (2008) Phytoplankton calcification in a high-CO₂ world. Science 320: 336–340.
- Green MA, Jones ME, Boudreau CL, Moore RL, Westman BA (2004) Dissolution mortality of juvenile bivalves in coastal marine deposits. Limnol Oceanogr 49(3): 727–734.
- Hall-Spencer JM, Rodolfo-Metalpa M, Martin S, Ransome E, Fine M, et al. (2008) Volcanic carbon dioxide vents show ecosystem effects of ocean acidification. Nature-online; doi:10.1038/nature07051.
- Carriker MR, Palmer RE (1979) Ultrastructural morphogenesis of prodissoconch and early dissoconch valves of the oyster *Crassostrea virginica*. Proc Natl Shellfish. Assoc 69: 102–128.
- Weiner S, Dove PM (2003) An overview of biomineralization processes and the problem of the vital effect. In Dove PM, DeYoreo JJ, Weiner S, editors. Biomineralization, Reviews in Mineralogy & Geochemistry 54. pp 1–29.
- Smith SV, Hollibaugh JT (1997) Annual cycle and interannual variability of ecosystem metabolism in a temperate climate embayment. Ecol Monogr 67: 509–533.
- Frankignoulle M, Abril G, Borges A, Bourge I, Canon C, et al. (1998) Carbon dioxide emission from European estuaries. Science 282: 434–436.
- Cai W-J, Pomeroy LR, Moran MA, Wang Y (1999) Oxygen and carbon dioxide mass balance for the estuarine-intertidal marsh complex of five rivers in the southeastern U.S. Limnol. Oceanogr 44: 639–649.
- Pechenik JA (1999) On the advantages and disadvantages of larval stages in benthic marine invertebrate life cycles. Mar Ecol Prog Ser 177: 269–297.
- Pechenik JA (2006) Larval experience and latent effects—metamorphosis is not a new beginning. Integr Comp Biol 46: 323–333.
- Burke K, Battler E, Miron G, Ouellette M, Tremblay R (2008) Larval quality of a nonnative bivalve species (European oyster, *Ostrea edulis*) off the east Canadian coast. J Shellfish Res 27(4): 701–710.
- Morgan SG (1996) Life and death in the plankton: larval mortality and adaptation. In: L. McEdward, editor. Ecology of Marine Invertebrate Larvae, CRC Press, New York, NY. pp 279–321.
- Underwood AJ, Fairweather PG (1989) Supply-side ecology and benthic marine assemblages. Trends Ecol Evol 4: 16–20.
- Kennedy VS (1996) Biology of larvae and spat. In: VS Kennedy, RIE Newell and AF Eble, editors. The eastern oyster, *Crassostrea virginica*, Maryland Sea Grant, College Park, MD. pp 371–441.
- Feely RA, Sabine CL, Hernandez-Ayon JM, Ianson D, Hales B (2008) Evidence for upwelling of corrosive acidified water onto the continental shelf. Science 320(5882): 1490–1492.
- Chesapeake Bay Program. Chesapeake Bay Program Water Quality Database 1984–present. Accessed October 20, 2008, from <http://www.chesapeakebay.net/wquality.htm>.



June 14, 2011

Dennis McLerran, Regional Administrator
EPA - Region 10
1200 6th Ave., Suite 900
Seattle, WA. 98101
McLerran.Dennis@epa.gov

Lisa Jackson, Administrator
United States Environmental Protection Agency
Ariel Rios Building
1200 Pennsylvania Ave., NW
Washington, DC 20460
jackson.lisa@epa.gov

Re: Ocean Acidification and Oregon State's 2008-2010 List of Impaired Waterbodies Under Clean Water Act Section 303(d)

On behalf of the Center for Biological Diversity ("Center"), I am writing to urge the United States Environmental Protection Agency ("EPA") to partially disapprove Oregon's list of impaired waterbodies and add ocean segments threatened or impaired by ocean acidification. Specifically, EPA has the authority and duty under the Clean Water Act section 303(d) to add ocean waters that are not attaining Oregon's water quality standards. The Center for Biological Diversity submitted ample information and data concerning ocean acidification to Oregon to warrant this action, and those letters and supporting documents are incorporated herein by reference.

First, in making its determination under section 303(d) of the Clean Water Act, Oregon failed to evaluate all water quality criteria, not solely pH criteria. EPA must include all water bodies that fail to meet "any water quality standard," including numeric criteria, narrative criteria, water body uses, and antidegradation requirements. 40 C.F.R. § 130.7 (b)(1),(3), & (d)(2). As described in the Center's letters and scientific information submitted to the state of Oregon, ocean acidification is harming aquatic life causing non-attainment of one or more of Oregon's water quality standards. Clearly, aquatic life criteria are not being met because, inter alia, the collapse of oyster recruitment.

EPA has a duty to identify its coastal waters as impaired for ocean acidification

because the water quality standards protecting Oregon's designated uses are not being attained or are threatened with non-attainment within the foreseeable future. Ocean acidification interferes with the state's designated uses for marine waters. Oregon's coastal water segments are contained within three designated basins: the North Coast basin, Mid Coast basin, and South Coast basin. In all three basins, the beneficial uses for coastal waters include fish and aquatic life, fishing and recreation. O.A.R. 340-41-0230 tbl.230A; O.A.R. 340-41-0220 tbl.220A; O.A.R. 340-41-0300 tbl.300A. The narrative water quality criteria include maintenance of water quality at its highest possible level and, minimization of, among other things, "dissolved chemical substances" and "other deleterious factors." O.A.R. 340-041-0007(1). Furthermore, the narrative criteria prohibit "[t]he creation of tastes or odors or toxic or other conditions that are deleterious to fish or other aquatic life." O.A.R. 340-041-0007(11). The Oregon standard for dissolved gases, OAR 340-041-0031, states:

(1) Waters will be free from dissolved gases, such as carbon dioxide, hydrogen sulfide, or other gases, in sufficient quantities to cause objectionable odors or to be deleterious to fish or other aquatic life, navigation, recreation, or other reasonable uses made of such water.

Additionally, Oregon's antidegradation policy is contravened by increasingly acidifying waters.

Because Oregon's water quality standard for marine pH is inadequate, impacts of ocean acidification must be measured against the state's beneficial uses and narrative water quality criteria. Present standards state that marine waters must have a pH between 7.0 and 8.5, and estuarine waters between 6.5 and 8.5 units. OAR 340-041-0021. There is an abundance of new scientific data available that points to the continuing threat of ocean acidification and its deleterious effects on fisheries and marine ecosystems, even at pH levels within the range set by Oregon's water quality standards. Accordingly, EPA should require Oregon to revise its marine pH standard and should add other standards based on the best scientific knowledge available on ocean acidification.

Second, contrary to its response to comments, the Center supplied information and data specific to Oregon. Feely et al., Hauri et al., and Byrne et al. discuss the existence of ocean acidification affecting Pacific Ocean waters that are directly applicable to Oregon's coast (Feely et al. 2008; Hauri et al. 2009; Byrne et al. 2010). Feely et al. reported that a survey cruise found corrosive waters affected by ocean acidification upwelling onto the continental shelf along the entire coast of California (Feely et al. 2008). Notably, the waters were last at the surface over 50 years ago, meaning that there is additional acidification already in the pipeline. (*Id.*) Feely et al. (2008) highlight that ocean acidification is impacting the continental shelf of western North America much earlier than predicted. They note that the occurrence at the surface of open-ocean water undersaturated in aragonite was not predicted to occur until 2050 (under a IS92a business-as-usual emissions scenario where atmospheric CO₂ concentration reached 550 ppmv) and only in the Southern Ocean—not along the west coast of North America (Feely et al. 2008). Secondly, the

researchers calculated that *without the anthropogenic signal of CO₂*, the equilibrium aragonite saturation level would be deeper by about 50 m across the shelf and no undersaturated waters would reach the surface. The aragonite and calcite saturation depths in the North Pacific are already among the shallowest in the global ocean (Feely et al. 2004: Figure 2). The uptake of anthropogenic CO₂ has caused aragonite saturation depths in the North Pacific to migrate upwards by 50-100 m since pre-industrial times, with current upward migration occurring at a rate of 1-2 meters per year, while calcite saturation depths have moved upwards by 40-100 m since pre-industrial times (Feely et al. 2004, Fabry et al. 2008, Feely et al. 2008). Seasonal upwelling is enhancing the advancement of the corrosive deep water into broad regions of the California Current System with large predicted impacts on marine species (Feely et al. 2008).

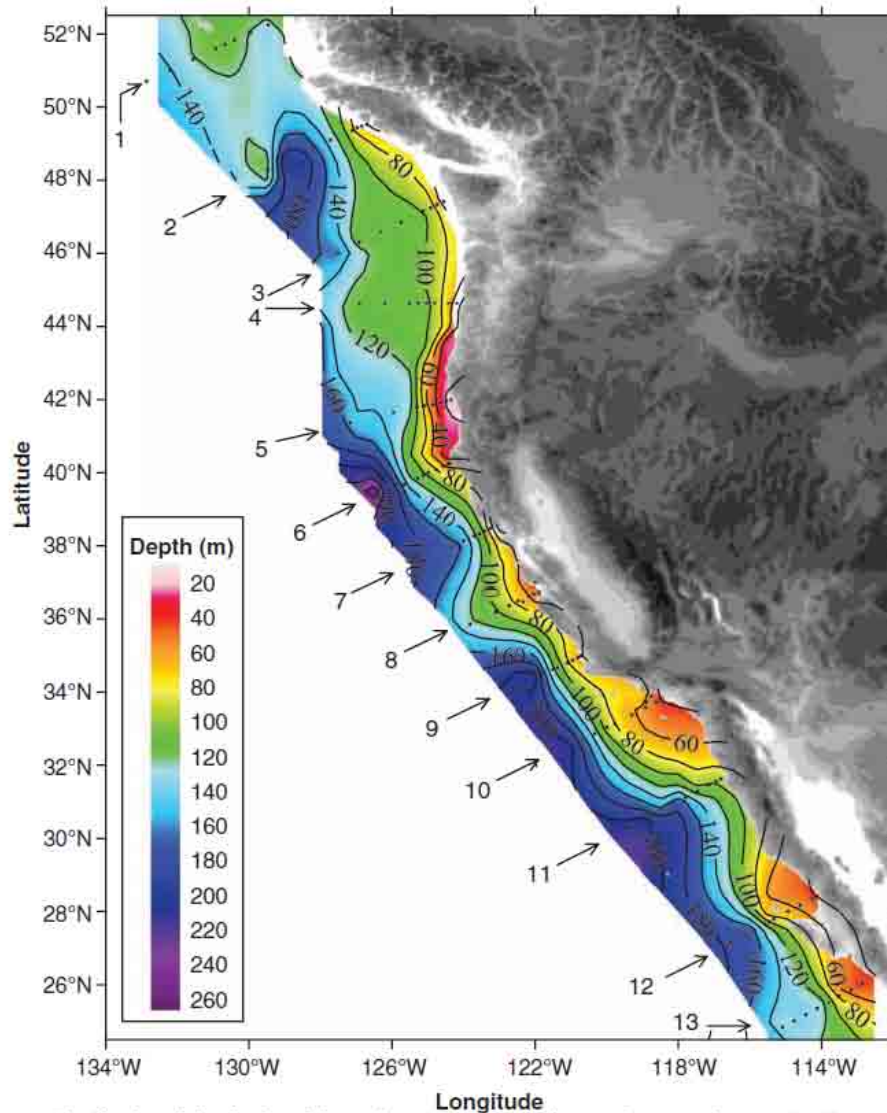


Fig. 1. Distribution of the depths of the undersaturated water (aragonite saturation < 1.0 ; $\text{pH} < 7.75$) on the continental shelf of western North America from Queen Charlotte Sound, Canada, to San Gregorio Baja California Sur, Mexico. On transect line 5, the corrosive water reaches all the way to the surface in the inshore waters near the coast. The black dots represent station locations.

(Source: Feely et al. 2008).

Hauri et al. explained that the California Current System is particularly sensitive to ocean acidification with the pH of surface waters comparatively low and change in pH for a given uptake of anthropogenic CO_2 is particularly high (Hauri et al. 2009). Already the aragonite saturation horizon has shoaled by ~ 100 m and now reaches the euphotic zone in a few eddies and in near-shore environments during upwelling along the Pacific Coast (Hauri et al. 2009). Additionally, modeling specific to the California Current System predicts rapid changes in pH and aragonite saturation (Hauri et al. 2009). Recently, another survey in the Pacific revealed that ocean acidification from anthropogenic sources is already significantly affecting surface waters and is accelerating (Byrne et al. 2009). Juranek et al. (2009) studied the

upwelling in the central coast of Oregon and found that the persistence of water with undersaturated with respect to aragonite on the continental shelf has not been previously noted and could have notable ecological consequences for benthic and pelagic calcifying organisms such as mussels, oysters, abalone, echinoderms, and pteropods (Juranek et al. 2009).

Most importantly, the consequences of ocean acidification described above are already adversely impacting aquatic life on the Oregon Coast (Bonfils 2010; Welch 2009). Most strikingly, oysters in the Pacific Northwest have failed to reproduce for the past six years (Southern California Coastal Water Research Project 2010). Pacific Coast oyster hatcheries are already experiencing difficulties associated with increasing ocean acidification. Two of the largest hatcheries, including one in Oregon, report production rates down by as much as 80% (Miller et al. 2009). The oyster failures in recent years may foreshadow the widespread effects that increasingly acidic waters will have on the shellfishing and fishing industry. Assuming business as usual projections for carbon emissions and a corresponding decline in ocean pH and mollusk harvests, ocean acidification's broader economic losses for the United States would range from \$1.5–6.4 billion through 2060 (Cooley et al. 2009).

Specifically, Whiskey Creek Shellfish Hatchery has experienced problems that correspond to measurements of low pH and consistent with upwelling of acidified waters (Barton, Cudd, and Weigardt 2009). Barton et al. reported a huge mortality event in 2008 for oysters that resulted in the loss of several billion bivalve larvae at Whiskey Creek. The hatchery gets its seawater from coastal Oregon waters at Netarts Bay. Research revealed that during upwelling, which would bring corrosive waters to the surface, oyster larvae died. Shellfish larvae are particularly vulnerable to increased acidification because their shells are composed of readily dissolvable species of calcium carbonate (Barton et al. 2009). Adult oysters form their shells from calcite, which is more difficult to dissolve than aragonite, which oyster larvae use to form their shells. Very small oyster larvae are the most susceptible: their shells contain amorphous calcium carbonate, which is extremely easy to dissolve (Barton et al. 2009). Thus, in acidic conditions, juvenile species must expend more of their available energy reserves on shell-building (Miller et al. 2009). The increased energy expenditures results in stunted growth and reduced fitness, further increasing mortality rate. Scientists predict an 89% reduction in successful recruitment and 5% increase in daily mortality rate in oyster larval offspring from a single female (Miller et al. 2009).

Third, information and data that is not specific to Oregon's waters, or does not otherwise conform to Oregon's methods, must still be considered when determining whether waters are threatened or impaired. The regulations governing implementation of the Clean Water Act's section 303(d) *require* that states "evaluate all existing and readily available water quality-related data and information to develop the list." 40 C.F.R. § 130.7(b)(5); *see also Sierra Club v. Leavitt*, 488 F.3d 904 (11th Cir. 2007)

The scientific data and information on ocean acidification that were submitted to Oregon are of high quality and credibility using methods and parameters to control for errors. Moreover, EPA's guidance states that the "[l]ack of a State-approved QAPP should not, however, be used as the basis for summarily rejecting data and information submitted by such organizations, or assuming it is of low quality, regardless of the actual QA/QC protocols employed during the gathering, storage, and analysis of these data" (EPA, Guidance for 2006 Assessment, Listing and Reporting Requirements Pursuant to Sections 303(d), 305(b) and 314 of the Clean Water Act at 33 (2005) ("EPA 2006"))(EPA advised states to prepare their 2010 303(d) lists consistent with the 2006 Guidance).

EPA's guidance for listing of impaired waters emphasizes that states should evaluate all data, and that listings may be based on small data sets, data other than site specific monitoring, and data from the public (EPA 2006 Guidance). With regard to 303(d) listing, the absence of site specific monitoring should not obviate the need to list ocean waters as threatened or impaired, rather it demonstrates a need for additional coastal monitoring. Recognizing the limited monitoring data available, states must consider a more expansive versus cautious approach to monitoring data (EPA 2006 Guidance). Site-specific monitoring data is not required for impaired water listing. EPA regulations require that "reports from dilution calculations and predictive modeling" be included in the data and information that a state considers in its assessment process for section 303(d) listing purposes. 40 CFR 130.7(b)(5)(ii)). EPA guides states to consider even very small sample sets to ascertain the attainment status of waters. Moreover, states should use information about observed effects, predictive modeling, and knowledge about pollutant sources and loadings when making its listing determinations (EPA 2006 Guidance).

Oregon, therefore, should have but failed to take into account not only site-specific monitoring, but also studies of offshore monitoring, predictive modeling, knowledge about atmospheric carbon dioxide levels and rates of increase, as well as laboratory studies on the impacts of ocean acidification on organisms to identify threatened and impaired waters. "EPA also supports the use of predictive modeling and other non-site-specific data such as remote sensing data, land use analysis, and knowledge about pollutant sources and loadings to make assessment decisions"(Environmental Protection Agency, 2010: 7). Additionally, Oregon can make a presumption that a pollutant source from atmospheric deposition is uniformly affecting water segments in large geographic areas (Environmental Protection Agency 2010). The best available scientific information on ocean acidification can and must inform the development of 303(d) lists, even if site-specific measurements are not available. There is a significant body of science confirming that ocean acidification is occurring which must be fully considered in the 303(d) listing process. Additionally, the synergistic effects of global warming, pollution, with ocean acidification should be considered.

Due to the unique nature of ocean acidification, lack of site specific monitoring does not diminish the severity of the problem or the need to list waters as impaired. Accordingly, Oregon may not dismiss any of the information and data previously submitted concerning ocean acidification—whether or not it contains site-specific measurements in Oregon coastal waters.

Fourth, EPA affirmed that states must consider ocean acidification when developing their section 303(d) lists under the Clean Water Act. In a memorandum dated November 15, 2010, EPA affirmed that Oregon has the authority and duty to identify waters threatened or impaired by acidification under section 303(d) of the Clean Water Act (Environmental Protection Agency 2010). “EPA has concluded that States should list waters not meeting water quality standards...waters should be listed for [ocean acidification] when data are available” (Environmental Protection Agency, 2010: 4). EPA also recommended that states focus on vulnerable waters that are at risk from ocean acidification affecting fisheries and shellfish resources. Furthermore, the memorandum provided recommendations for how states conduct assessments and monitoring, and it provided sources for more information on ocean acidification and assessment. EPA also stressed that if a designated use is not supported and the segment is impaired or threatened, even if the specific pollutant is not known, it must be identified as a part of the section 303(d) list.

In sum, Oregon’s failure to include its coastal waters on its section 303(d) list as threatened or impaired due to ocean acidification is in violation of the Clean Water Act. EPA must act now to correct this problem by partially disapproving Oregon’s 303(d) list and adding ocean waters as threatened or impaired water bodies.

Sincerely,

/s/ Miyoko Sakashita

Miyoko Sakashita

Miyoko@biologicaldiversity.org

References

- Barton, Alan, Sue Cudd, and Mark Weigardt. 2009. *Update on Hatchery Research and Use of State Funds to improve Larval Performance at Whiskey Creek Shellfish Hatchery Impacts of upwelling on shellfish larvae.*
- Bonfils, Darcy. 2010. Ocean acidification hits Northwest oyster farms. *abcNews*, April 22.
- Byrne, R.H., Sabine Mecking, R.A. Feely, and Xuewu Liu. 2010. Direct observations of basin-wide acidification of the North Pacific Ocean. *Geophysical Research Letters* 37, no. 2 (January 20): L02601. doi:10.1029/2009GL040999.

- Environmental Protection Agency. 2010. Memo: Integrated reporting and listing decisions related to ocean acidification.
- Feely, R.A., CL Sabine, J.M. Hernandez-Ayon, Debby Ianson, and Burke Hales. 2008. Evidence for upwelling of corrosive “acidified” water onto the continental shelf. *Science* 320, no. 5882 (June 13): 1490. doi:10.1126/science.1155676.
- Hauri, C., N. Gruber, G.K. Plattner, S. Alin, R.A. Feely, B. Hales, and P.A. Wheeler. 2009. Ocean acidification in the California current system. *Oceanography* 22, no. 4: 60–71.
- Juranek, Lw, Ra Freely, W Peterson, Sr Alin, B. Hales, K. Lee, C Sabine, and J Peterson. 2009. A novel method for determination of aragonite saturation state on the continental shelf of central Oregon using multi-parameter relationships with hydrographic data. *Geophysical Research Letters* 36, no. 24 (December 31): 1-6. doi:10.1029/2009GL040778.
- Miller, A.W., A.C. Reynolds, Cristina Sobrino, and G.F. Riedel. 2009. Shellfish face uncertain future in high CO₂ world: influence of acidification on oyster larvae calcification and growth in estuaries. *PLoS One* 4, no. 5 (January): e5661. doi:10.1371/journal.pone.0005661.
- Southern California Coastal Water Research Project. 2010. Ocean acidification effects on shellfish workshop: Findings and recommendations. In *Ocean acidification effects on shellfish workshop*.
- Welch, Craig. 2009. Oysters in deep trouble: Is Pacific Ocean's chemistry killing sea life ? *Seattle Times*, June 15.